UNIVERSITY OF CALIFORNIA
RIVERSIDE

Synthetic Agonists of Abscisic Acid Receptors and Their Metabolomic Effects on Plants

A Dissertation submitted in partial satisfaction
of the requirements for the degree of

Doctor of Philosophy

in

Plant Biology

by

Jonathan Dean Helander

June 2017

Dissertation Committee:
Dr. Sean Cutler, Chairperson
Dr. Julia Bailey-Serres
Dr. Ryan Julian

The Dissertation of Jonathan Dean Helander is approved:

Committee Chairperson

University of California,
Riverside

Acknowledgments

Professor Sean Cutler has been an excellent, challenging, and rewarding mentor and his contributions to my work as a student and scientist and are extensive and have always been extremely appreciated.

My dissertation committee members, Julia Bailey-Serres and Ryan Julian have provided great insights and perspectives in my work and I am thankful they agreed to be on my committee and further challenge my work here in a beneficial manner.

The many lab mates I've come to know have given me so much helpful advice from all aspects of graduate student life and scientific inquiry.

Appreciation is given to the NSF and Syngenta for their funding of our lab and my work.

Finally my family members, who have all been overly supportive and pushed me to continue this work and advancement of my research through tough times.

Dedication

To my mother and father, Brenda Lindstedt and Randall Helander

ABSTRACT OF THE DISSERTATION

Synthetic Agonists of Abscisic Acid Receptors and Their Metabolomic Effects on Plants

by

Jonathan Dean Helander

Doctor of Philosophy, Graduate Program in Plant Biology
University of California, Riverside, June 2017
Dr. Sean Cutler, Chairperson

Abstract

Land plants respond to multiple abiotic stresses, including drought, through the signaling cascade induced by the phytohormone abscisic acid (ABA). Endogenous production, or externally applied ABA has a major function of eliciting guard cell closure, ultimately lowering transpiration and increasing drought tolerance in plants. Accordingly, the mechanisms of action in which ABA facilitates this response have been popular targets for agricultural research and applications. However, ABA has a multitude of responses aside from stomatal closure that are important for plant's survival to abiotic stress. In response to limited water availability, the phytohormone is known to maintain primary root growth while decreasing shoot growth, increase osmolyte accumulation, inhibit seed germination, and is involved in substantial crosstalk with other phytohormones. These responses are dependent on a core ABA signaling pathway comprised of three components: the ABA receptors known as the *PYRABACTIN RESISTANT*/*PYRABACTIN RESISTANT-LIKE*/*REGULATORY COMPONENT OF ABA RECEPTOR*s (PYR/PYL/RCARs), the clade A protein phosphatase 2Cs (PP2Cs), and the sucrose nonfermenting related subfamily 2 (SnRK2s).

The ABA receptors are the first interactors with ABA within the pathway, and cluster into three clades (I, II, III) based on sequence identity. Additionally, these clades

can be further grouped based on oligomeric preference; clades I and II are preferentially monomeric, while clade III is preferentially dimeric. While some research has been done on non-redundant functions of the PYL proteins, many of the ABA responses remain uncharacterized with respect to the differential contributions of the different receptors. Additionally, most of the published ABA-receptor agonists are either direct ABA analogs displaying pan-agonist activity, or are primarily active only on the dimeric subgroup of the receptors. It would thus be potentially beneficial to develop agonists that show preferential activation of the monomeric receptors, allowing for temporal activation and subsequent analysis of their biological relevance.

In order to identify compounds with novel selectivities, preferably on the monomeric receptors, I used high-throughput virtual screening to evaluate compounds unbiased to previous, active scaffolds. This resulted in a series of chemically similar hits which showed potent activity on the monomeric receptors, and translated to some *in vivo* responses. This potent, monomeric-specific scaffold was optimized using structure-aided design, improving the *in vivo* responses. Using this probe molecule I provide data that suggest that monomeric and dimeric ABA receptors may differentially control metabolomic and transcriptional responses, but are adequate in seed germination inhibition and primary root elongation.

TABLE OF CONTENTS

Contents

List of Figures

Introduction

Chapter 1

Chapter 2

List of Tables

Chapter 1 Virtual Screening

Chapter 2 Metabolomics

Introduction

Plants are sessile organisms and must adapt to their immediate environment in order to survive. Global temperatures and drought occurrences are expected to rise and this puts pressure on agriculture to produce food for a growing population (1). Critical to a plant's survival is the availability of water, a universal requirement for life on Earth. However, there is a critical trade-off between the growth of plants and water loss due to evapotranspiration. This tradeoff is centralized on the fact that for carbon-sequestration to occur, carbon dioxide must access the photosynthetic machinery through open stomata of the leaves, however these open pores present a mechanism in which water loss through evaporation can occur. When evapotranspiration is high, although land plants can minimize water loss by closing the stomata, this necessarily results in decreased carbon assimilation. While this trade-off seems insurmountable, there are many factors involved, from genetics and agrochemical controls, to infrastructure changes such as drip irrigation (2).

Plants have multiple mechanisms for surviving through periods of low water, however these are not always the most beneficial to agriculture. As stated above, the stomata are a major leverage point for plants to limit water loss by decreasing stomatal aperture. Closing of the stomata limits immediate water loss, but prolonged periods of drought often require plants to change metabolic flux (3, 4). In general, these large shifts direct metabolism from growth and development to carbon and nitrogen storage. The nutrient and metabolome profile of plants under varying degrees of drought can be observed to dramatically shift. Here, I will discuss aspects of metabolic shifts in drought responses in plants, and their alignment with the ABA signaling cascade.

Plant Mechanisms for Drought Response

The responses plants employ to drought is complex and dependent on the severity, duration, and the existence of any of other concurrent stresses. While stomatal conductance is one of the most important physiological responses plants have to drought, closing of the stomata can coincide with an inhibitory effect on photosynthesis and the subsequent overproduction of reactive oxygen species (ROS). ROS accumulation, if severe enough in duration or intensity, can result in oxidative damage to essential components of the cell. To remedy this, plants up-regulate ROS-scavenging systems as well as the biosynthesis of osmo-compatible solutes (osmolytes, compatible solutes) when ROS concentrations are high (5). If the accumulation of ROS species is not dealt with, significant damage can occur to proteins, DNA, and membranes (6–8).

ROS is an umbrella term for higher-energy forms of oxygen such as singlet oxygen, superoxides, hydrogen peroxide, or the hydroxyl radical (9, 10). Under normal conditions in plants, the levels of ROS are in an equilibrium of constant production and elimination (scavenging) by various mechanisms (11). Interestingly, ROS have a valuable role in the plant, acting as mobile signaling molecules to induce transcriptional and metabolic changes to deal with the origin of the stress signal (12, 13). For instance, ROS are observed to function in the control of stomatal aperture participating as downstream signaling effectors from ABA signaling cascade. Additionally, stomata are responsive to exogenous treatments of the ROS hydrogen peroxide, which result in stomatal closure (14). H_2O_2 is a widely accepted primary signaling molecule that is accumulated in response to multiple stresses and is a central component to cross-tolerance stress

signaling (15). Still, sustained high levels of ROS are subtractive to plant health. One such mechanism plants employ to sequester ROS damage and accumulation is by producing osmolytes and antioxidants.

Osmolytes have been extensively studied in microbes and plants and many display ROS-scavenging capabilities, protection of native-protein folding, and water retention, all of which have a beneficial effect on the organism's survival in low-water potential, high osmolarity, or oxidative stress conditions (16–19). Osmolytes include polyols, amino acids and their derivatives, tertiary sulfonium compounds, polyamines, and zwitterionic quaternary ammonium compounds. Reflecting their diverse structures, their mechanisms for producing stress-alleviating effects can be varied and, in many cases, is not fully understood.

Perhaps one of the most ubiquitous and broadly studied osmolytes is proline, which accumulates to high levels in response to osmotic stress in both plants and microbes (20, 21). The conservation of the metabolic regulation of proline levels in response to osmotic stress is highly conserved in land plants, as evident with its presence in the ancestral moss *Physcomitrella patens* (*P. patens*) (22). While the exact role and mechanisms of proline are not fully understood in the context of drought- or osmotic stress-induced accumulation, it has been shown that it promotes beneficial effects primarily by stabilizing protein structural integrity, protein complexes, detoxification of ROS, and stabilizing $NADP^+$/NADPH ratios (23–25). A review of proline's scavenging reactions with various ROS indicated that proline's ability to react with singlet oxygen is due to its cyclic secondary-amine structure (26), and that although the aromatic amino acids have favorable scavenging properties similar or superior to proline, their lowered solubility in aqueous solutions likely limits their effectiveness in this regard.

One of the reasons why proline has been a focus in the field of osmolyte research is that concentrations can increase over 100-fold in response to various stresses, indicating extensive molecular machinery dedicated to its accumulation further supporting the idea of its key role in stress-mitigation (27, 28).

Proline is the only non-aromatic cyclic amino acid and is primarily produced from the substrate glutamate, but a minor secondary pathway exists from ornithine. Glutamate is converted into proline in two enzymatic steps, with the first being conversion of glutamate to glutamate-semialdehyde by the bifunctional enzyme Δ^1-Pyrroline-5-Carboxylate (P5CS), which is also the rate limiting step in proline biosynthesis (29). Glutamate-semialdehyde is able to spontaneously cyclize to Δ1-pyrroline-5-carboxylate (P5C), but this step is in an equilibrium. Finally, an NADPH-dependent enzyme, P5C reductase (P5CR), catalyzes the last step, reducing P5C to proline.

It has been reasoned that due to proline's beneficial effects and intense accumulation upon drought and in other stresses, plants producing synthetically high concentrations of proline may display potential benefits in the agricultural setting. Therefore, genetic means to increase basal proline levels or proline accumulation in response to stresses have been logical targets of agricultural research to benefit crop yields and plant survival in the face of drought and osmotic stressors. Since P5CS catalyzes the rate limiting step, efforts to overexpress P5CS in both *Arabidopsis* and *Nicotiana* have been attempted and resulted in increased proline accumulation (30–32). While over-expressing P5CS in tobacco was reported to increase growth substantially when subjected to soil drying and salinity stress in comparison to WT, the role of proline played in these results has been contested (33, 34). While it is clear that proline levels do correlate with drought stress and have been shown to protect cellular membranes and

protein folding, the exact mechanisms in which it promotes plant's survival and growth in drought stress still requires more research.

Abscisic Acid as a Signaling Molecule

The signals that initiate the above mentioned representative responses to drought stress, including stomatal conductance and subsequent whole-organismal shifts in metabolism are more correlated with the root environment than leaf water status, which supports the idea of a mobile, long-distance root-to-shoot signal (35, 36). Plant hormones, or phytohormones, are a group of well-studied, mobile small-molecules that regulate major physiological changes in the plant largely through signal cascades. The plant hormone abscisic acid (ABA) is the major mobile regulator of abiotic stress responses such as drought. Discovered in the late 1960's, abscisic acid's name was attributed to its apparent function in abscission (37, 38), however this later turned out to be only a minor, indirect role.

The bonafide roles of ABA are controlling of seed dormancy (39), stomatal conductance (40, 41), root architecture (42–44), plant growth (45–47), seed and fruit set (48, 49), as well as other abiotic stress responses and hormonal crosstalk (50–52). When roots experience mild drought, ABA synthesis largely takes place within the root. The produced ABA requires transportation to the leaf in order for perception of the hormonal signal to occur in the guard cells. ABA can be catabolically inactivated esterification into the glucosyl ester (ABA-GE), which may play a minor role in supplementing the pool of ABA in response to drought by hydrolysis, however there is substantial evidence that ABA-GE only plays a minor role as an activatable storage product of ABA (53).

ABA is observed to be transported in both the xylem and phloem, with the concentration of ABA in the xylem being highly correlated with stomatal conductance (54, 55). Interestingly, the concentration of ABA in the xylem is not only a result of root biosynthesis, but also redistribution from the leaves to the root and back into the xylem (56). Additionally, while free ABA is present in the xylem and correlated with root-to-shoot signaling, ABA-GE is also known to be a mobile transporter of the signal (57), but the proportion of its effect relative to free-ABA is not clear (53).

Under longer durations and more severe drought stress where leaf turgor pressure approaches zero, biosynthesis of ABA in the leaf can increase dramatically (54). However this finding has led to an unclear differentiation between root-to-shoot signaling and leaf biosynthesis as the major contributors to the ABA response. Regardless, it is likely that ABA biosynthesis in plastids of both the leaf and the root contributes to the overall intensity of the hormone's signal.

Abscisic Acid Biosynthesis Pathway

ABA is a C_{15}-sesquiterpenoid (Figure 1A) and a biosynthetic product of the carotenoid pathway, a downstream branch of the mevalonate pathway. The abundance of free ABA is reflective of the net change produced by biosynthesis and removed by inactivation through conjugation or metabolism. The majority of the carotenoid pathway takes place in the plastid organelle, with β-carotene being the first cyclized carotenoid (58). β-carotene is the direct precursor to zeaxanthin, which is the first carotenoid containing a polar cyclohexenol head-group. Zeaxanthin can be further oxidized into violaxanthin by ABA1 and then *trans*-neoxanthin by ABA4 (59, 60).

Zeaxanthin, violaxanthin, and neoxanthin belong to a chemical group known as the xanthophylls. The carotenoids, and specifically xanthophylls, are known to be protective for photo-oxidative stress (61). *Trans*-neoxanthin and *trans*-violaxanthin can isomerize into their respective 9-*cis*-epoxycarotenoids and be cleaved by a 9-*cis*-epoxycarotenoid dioxygenase (NCED) to yield the C_{15} xanthoxin. Cleavage of the xanthophylls by NCED is the rate limiting step of ABA biosynthesis and also the last step which occurs exclusively in the plastid. There are five characterized and active NCEDs in *Arabidopsis* that have different binding and localization preferences within the plastids (62). The two remaining steps are oxidation of xanthoxin by ABA2, affording abscisic aldehyde, and finally oxidation of the aldehyde by abscisic aldehyde oxidase (AAO) to produce 2-*cis*,4-*trans*-*S*-(+)-ABA as the single, naturally-occurring enantiomer (63).

While *S*-(+)-ABA is most abundantly present as the 2-*cis*, 4-*trans* conformation, it can be reversibly isomerized to the biologically inactive form 2-*trans*, 4-*trans* with UV radiation (64). The *R*-(−)-ABA enantiomer is active in seed germination inhibition but it is unable to mimic stomatal closure control observed with the *S*-(+) natural isomer (65). Interestingly, there seems to be an uptake mechanism that favors the natural *S*-(+)-ABA isomer, when plants are treated with media containing a racemic mixture (66).

Because of the NCEDs essential role in ABA biosynthesis, they have been the target for selective, chemical inhibitors which could be useful for understanding biological roles of ABA as well as in agronomical applications. The similarity between the reaction mechanisms of NCED and lignostilbene-*α*,*β*-dioxygenase (LSD), a designed inhibitor of LSD (nordihydroguaiaretic acid, NDGA) was modified with the intent to produce a selective NCED inhibitor. A slight modification of NDGA was able to produce a successful candidate

that acted on the NCEDs, termed Abamine (67). Abamine was able to lower the mannitol-induced biosynthetic accumulation of ABA by a maximum of 50%. Abamine was further modified using structure-activity relationship (SAR) analyses to produce a more potent version and was termed AbamineSG (68). Plants grown on 0.4 M mannitol had a 77% reduction in ABA accumulation when treated with AbamineSG, compared to only 35% with Abamine.

There is currently one crystal structure of the NCEDs, produced from the maize protein Viviporous14 (VP14, PDB ID:3NPE). VP14 is a β-propeller type structure containing seven blades and four α-helical inserts that produce an α-helical domain. In the catalytic region, four His residues coordinate an Fe^{2+}, which is proximal to a water molecule and an O_2. Additional to the crystal structure, Messing et al., propose a possible mechanism for the cleavage of 9-*cis*-violaxanthin into xanthoxin by VP14 (69).

One step downstream from the NCEDs in the ABA biosynthesis pathway is ABA2, which is the first step that occurs outside of the plastids. ABA2 is responsible for the conversion of xanthoxin to abscisic aldehyde, the first cyclohexenone containing metabolite of the pathway. In *Arabidopsis*, the *aba2* mutant is one of the stronger ABA-deficient mutant lines with a severe wilty phenotype and low basal levels of ABA. In treatment to drought stress, *aba2* mutants are unable to produce an effective ABA-induced response. While wild-type plants can increase endogenous ABA levels 25 to hundreds of fold compared to basal, well-watered conditions, the biosynthetic mutant has little change in ABA levels and is hypersensitive to osmotic stress (70). The *aba2* mutant lines have largely been isolated from screens for early germination, and germination on salt and osmotic stress-inducing media such as mannitol (71, 72). It is interesting to note that although the *aba2* mutant is essentially devoid of any accumulation of ABA in osmotic

stress, it does have ~20% of the basal ABA levels compared to WT, indicating a minor alternative pathway to ABA (73).

Both NCEDs and ABA2 are good targets for inhibitors of ABA biosynthesis. While NCED has had some success, a selective and potent ABA2 inhibitor is yet to be produced. While the majority of this work will focus on the ABA-signaling pathway far downstream of biosynthesis, efforts for chemical manipulators of all stages of ABA effects in plants would likely be beneficial in agricultural settings. In a parallel manner, many of the methodologies proposed here to identify synthetic agonists of the ABA receptors could be used for searching the chemical space to discover ABA-biosynthesis inhibitors through ABA2 or NCED proteins.

The Conservation of ABA in Land Plants and Agricultural Applications

ABA is found in many organisms and is in all kingdoms of life aside from Archaea. It can be found at low levels in cyanobacteria, algae, and bryophytes and is ubiquitous in cormophytes through higher plants (74). Although present in low levels in cyanobacteria, and cyanophytes, no physiological function is known in these organisms. Oddly, in cyanobacteria that produce elevated levels of ABA in response to salt stress, this ABA was observed to be released into the extracellular space (75, 76). Building on these findings, ABA has been highlighted to have an evolutionarily dynamic regulatory role in physiological control. In early land plants, such as the model fern *Ceratopteris richardii*, the ABA signal cascade has been determined to have a role in sex determination (77, 78). Later, the emergence of angiosperms gave rise to ABA's role in seed dormancy (79).

ABA's control in root architecture, shoot growth inhibition, and stomatal conductance have a broad effect of promoting drought tolerance. In general, ABA inhibits shoot growth but requires higher concentrations to inhibit lateral and primary root growth (42, 80, 81). Maintaining primary root growth in low water conditions can be advantageous, analogous to increasing the length of the rope in a drying well (82, 83). It has been well established that primary root growth can be even be enhanced by ABA, indicating a true hormetic effect (45, 46, 84, 85). This has been hypothesized to support the idea that low-intensity drought conditions will result in increased primary root growth, but high intensity drought inhibits most plant growth to preserve resources (86, 87).

These advantageous features of ABA in the context of crop yield and survival have led to extensive biotechnological and agrichemical efforts to improve crop yields during conditions of drought that utilize the hormone's signaling pathway. Using ABA itself in the field is limited due to its photoinstability, however the plant hormone has shown some beneficial effects in commercial crops. Most of these research efforts in field applications have been in the context of fruit appearance and morphological traits. Some representative examples produced by exogenous ABA application are the promotion of fruit ripening in strawberries and bananas, control of anthocyanin production in grape, and protection against chilling injury in cotton, maize and melon (88–96).

While the benefits of ABA to plant survival are evident and extensive, field applications utilizing ABA are difficult to implement due to the ABA response having complex and contrasting effects, which are highly dependent on the plant's current abiotic conditions (97). For example, ABA's stomatal conductance control can be inhibited by ABA's own induction of aquaporin accumulation when drought stress is high (98–100). Cross-talk with the other major hormones of auxin, cytokinin, ethylene, gibberellin, and

jasmonic acid contribute to the complexity of ABAs' physiological responses (101–104). The difficulty that these complex and contrasting regulations present for agricultural applications is compounded by the undesirable qualities of ABA itself, such as its instability in UV irradiation, general rapid *in vivo* catabolization, and moderate structure complexity (105–108). Further complicating the matter, the core signaling pathway of ABA involves multiple redundant and semi-redundant members with unknown unique or contributory functions with regards to these complex responses within the plants. It should be beneficial to establish the function of each component of the core signaling pathway to elucidate points where undesirable regulation from an agricultural standpoint can be minimized.

Abscisic Acid Core Signaling Pathway

The ABA core pathway (Figure 1B) references a three-component module represented by 1; ABA PYR/PYL/RCAR receptors (hereafter PYLs), 2; the clade A protein phosphatase 2Cs (PP2Cs), and 3; the small family of the sucrose non-fermenting related subfamily 2 kinases (SnRK2) (109). The signal of ABA is initiated upon binding of ABA by the PYL receptors, which causes a conformational change in which ABA becomes "enclosed" within the binding pocket of the PYLs (110, 111). This conformational change is able to stably interact with and deactivate the PP2Cs. Once the PP2Cs are inactivated, their phosphatase targets, the SnRK2s, are able to autophosphorylate, and accumulate as an active state. If active, the SnRK2s are able to phosphorylate downstream effectors of the ABA response, including ABA-responsive element-binding proteins/ABRE-binding factors/ABA-insensitive 5 (AREB/ABF/ABI5) basic/region leucine zipper (bZIP)

transcription factors, ion channels, and NADPH oxidases to provide the ABA-induced whole-organismal responses.

The first component of ABA perception, the PYL receptor family, is part of the BetV I-like superfamiliy which contain hydrophobic-binding properties (112). While the large size of the PYL receptor family is rare for hormone receptors, the size is evolutionarily conserved in many land plants (113), likely indicating selective pressure to retain this characteristic. In *Arabidopsis*, the PYL family consists of 14 members, which is divided into three subfamilies based on sequence identity (114). The subfamilies also dictate oligomeric preference; subfamily I and II are monomeric, while PYR1, PYL1 and PYL2 of subfamily III are dimeric - PYL3 shows an equilibrium between monomer-dimer states (115–117). Some members of the monomers, such as PYL10 and PYL13 display some ABA-independent inhibition of the PP2Cs (117, 118), however for PYL10 this has been described at least partially as an artifact of BSA-dependent activation of the receptor (119). The monomeric type receptors generally have a higher affinity for ABA than that of the dimeric in vitro (116).

The ability for binding ABA by the PYR/PYL/RCARs is the result of a hydrophobic cavity near the center of the protein created by two α-helical and seven β-sheet domains. In solution, and in the absence of high concentrations of ABA, the receptors are in an open conformation, with direct solvent access to the pocket (117, 120). Upon perception of ABA, the pocket closes around ABA by a “gate-latch” mechanism produced by a flexible loop termed CL2 (117, 120, and 121). Once bound, the closed conformation of the ABA receptors forms a surface on the receptor that can accommodate interactions with the PP2C proteins.

The clade A PP2Cs, are the second critical component of the core signaling pathway and act as negative regulators to ABA signaling. All clades of the PP2Cs are monomeric members of the protein phosphatases M (PPM) superfamily and are differentiated from the PPP superfamily (groups PP1, PP2A, PP2B), due to sequence differences in the catalytic region (122). Additionally, the PP2C catalytic action requires Mg^{2+} or Mn^{2+}, while PP2A require Ca^{2+}. The PP2C catalytic domain is divergent enough such that they are generally insensitive to PP2A or PP1 inhibitors (123). The PP2Cs comprise the largest family of the protein phosphatases in plants, with 76 members that are divided into 10 subfamilies, designated with clades A-J (124, 125). There are 11 subdomains shared between the PP2Cs within the catalytic region, which is preferentially positioned at the C- or N-termini (126).

In Eukaryotes, a common role of the PP2Cs is to reverse stress-induced kinase signal cascades by dephosphorylating mitogen-activated protein kinases (MAPKs), MAPKKs, MAPKKKs, and receptor-like kinases (RLKs). They also play important roles in cell cycle regulation (125, 127, and 128). Their original role in ABA signaling was revealed by screening for mutants that were able to germinate on ABA concentrations that would normally inhibit wild-type (WT) *Arabidopsis* plants (129). Two strong mutants were termed *abi1* and *abi2*. After positional-mapping and cloning, both were identified as PP2Cs with high homology to one another, and a unique N-terminal extension (130–134). Both mutations in *abi1-1* and *abi2-1* confer a dominant, single residue change of Gly-Asp. Interestingly at the time, no recessive alleles could be identified in either loci which was attributed to functional redundancy, and described as a dominant loss-of-function mutation (133). However, it was shown that the *abi1-1* mutant could still inhibit SnRK2s via phosphatase activity (135). Together, the dominant phenotype trait caused confusion,

because of the proposed loss-of-function phenotype would require a hypermorphic protein. It was not until the identification of the PYL proteins that the double-negative regulation of the PYL-PP2C-SnRK2 core pathway indicated that the *abi1-1* (and similarly *abi2-1*) mutation blocked PYR1s ability to bind, and inhibit, the PP2C (110).

The interaction between the PYL receptors and the PP2Cs is mediated by a conserved tryptophan in all of the PP2Cs except AHG1 (HAB1 W385, designated the Trp-lock) that forms a hydrogen bond with a water molecule that directly interacts with ABA's cyclohexenone oxygen (120, 136). There are nine clade A PP2Cs (125, 137) in *Arabidopsis*, all of which (except AHG1) have been shown to interact on some level with the PYL receptors (138). The group consists of ABA-INSENSITIVE 1 (ABI1), ABI2, ABA HYPERSENSITIVE GERMINATION 1 (AHG1), PP2CA/AHG3, HYPERSENSITIVE TO ABA 1 (HAB1), HAB2, HIGHLY ABA-INDUCED 1 (HAI1), AKT1-Interacting PP2C1/HAI2, and HAI3. With respect to sequence analysis on the catalytic phosphatase domain, these PP2Cs are split into two groups; one consisting of HAB1, HAB2, ABI1, and ABI2, and a second one consisting of PP2CA/AHG3, AHG1, HAI1, HAI2, and HAI3 (125). Interestingly the mutant *abi1-1* (and *abi2-1*) shows dominant segregation and is insensitive to ABA, which is paradoxical in light of the WT protein acting as a negative regulator to ABA signaling. This was later explained after discovery of the receptors elucidated that the *abi1-1* mutant protein is unable to bind to PYR1, but can still inactivate the SnRK2 proteins (110). Although redundancy does exist in the clade A PP2C family single mutants in multiple PP2Cs can give hypersensitive responses to ABA, and in most cases is how they were discovered in screening efforts (135).

The SnRK2s are the third component of the conserved ABA signaling core pathway in land plants, and act as phosphatase targets for the clade A PP2Cs. They are

related to the animal AMP-dependent protein kinases (AMPK), a kinase superfamily which is important for energy signaling through their involvement in ATP consumption and production (139, 140). Their identification in the ABA pathway was resultant on the observation of the highly phosphorylated status of late embryogenesis abundant (LEA) proteins, such as RAB-17. Since LEA proteins accumulate in desiccating seeds and drying seedlings, and because of the high phosphorylation state, their respective kinases have been hypothesized to be involved in drought stress responses in plants (141–143).

One of the first efforts to reveal any drought-responsive or ABA-induced kinases in plants identified protein kinase responsive to ABA 1 (PKABA1), which was discovered from a seedling cDNA library, cloned in wheat, and exhibited a 49% sequence identity with the carbon- and energy-source sensitive kinase from yeast, sucrose non-fermenting 1 (SNF1) (144, 145). Later it was shown that ABA-responsive K^+ ion channels in stomata were sensitive to kinase inhibitors, further supporting the idea that a kinase signal cascade was incorporated in the downstream ABA responses (146, 147). Within the guard cells of fava bean, an ABA-activated and Ca^{2+}-independent serine/threonine kinase (AAPK) was discovered that could undergo autophosphorylation(148). These two discoveries eventually lead to the identification of the ortholog open stomata 1 (OST1/SnRK2.6) in *Arabidopsis*. The single mutant of *At*SnRK2.6 showed a moderate ABA-insensitivity and plant growth similar to WT, but did have increased water loss (149). Sequence analysis and screening for other drought- or ABA-responsive kinases eventually lead to the discovery of nine SnRK2s in Arabidopsis (150) of which three, SnRK2.2, 2.3 and 2.6 (SnRK2.2/2.3/2.6) are critical for the ABA downstream-signal cascade. The triple mutant *snrk2.2/snrk2.3/snrk2.6* has an extreme wilty phenotype, and can germinate on 50 μM of ABA, a concentration 50 times higher than that which can inhibit WT *Arabidopsis thaliana*

(81, 151, and 152). The single mutant in SnRK2.6 displays a moderate wilty phenotype, but SnRK2.2 and SnRK2.3 are redundant requiring the *snrk2.2/snrk2.3* double mutant to display ABA-insensitivity and enhanced water loss.

Finally, the inclusion of the SnRK2's into the ABA core signaling pathway was revealed shortly after the discovery of the PYL proteins and characterized in a yeast two-hybrid assay indicating that the ABA-responsive PP2Cs physically interacted with SnRK2.2/2.3/2.6 (153). The SnRK2s contain a conserved, highly acidic, region termed the ABA-box that pertains to a region near OST1's Ser-332 and is required for the PP2C interaction (154). Interestingly, SnRK2.4, which has not been included in the ABA-signaling pathway, inhibits the core PP2Cs PP2CA and ABI1 in an ABA-independent manner, however the mechanism is not completely understood (155).

Downstream substrates of ABA-dependent SnRK2 phosphorylation include the bZIP ABA-Responsive Element Binding (AREB) transcription factors, the Slow Anion Channel-associated 1 (SLAC1) ion channel proteins, the K^+ channel in *Arabidopsis thaliana* (KAT1), and the Respiratory Burst Oxidase Homolog F (RBOHF), and more recently SnRK2-substrate 1 (SNS1) (139). While not formally included in the three-component module of the core signaling pathway, an additional major branch of the downstream effectors from SnRK2s, include the MAPK/MAPKK/MAPKKK cascade.

The crucial role played by the SnRK2s is evident by phenotypes observed in the *snrk2.2/2.2/2.6* triple mutant, which is significantly hindered in germination inhibition and stomatal closure by endogenous ABA, and largely unresponsive to exogenous treatment as well (151, 152, 156). Although phosphoproteomic assays have shown dramatically altered ABA-dependent phosphorylation in the triple mutant, some ABA-dependent

phosphorylation still existed, indicating other interactors of the core pathway that are not yet fully characterized (139).

Basal, ABA-independent phosphorylation is present in the three SnRK2s, the result of autophosphorylation, which is highest (5-10 fold higher) in SnRK2.6 as compared to SnRK2.2/2.3. Mutational analyses indicated that phosphorylation of Ser175 in the activation loop of SnRK2.6 (and homologous positions in SnRK2.2/2.3) is required for full activity of these kinases, and the S175A mutation knocks out ~98% of SnRK2.6's activity to ABF2 (157). Evidence for both intra- and inter-molecular phosphorylation is strongly supported between the three SnRK2s, as mutations inhibiting *cis*-phosphorylation for SnRK2.6 still leads to phosphorylation when the mutant SnRK2.6 is incubated with WT SnRK2.6 protein *in vitro (157)*.

The mechanism in which the PP2Cs inactivate the SnRK2s is proposed to be the combination of two steps, as observed from the HAB1-SnRK2.6 crystal structure and supported by mutational analyses. The first step is by dephosphorylation of the crucial S175 residue, which removes the majority of kinase activity. The second inactivating step is the production of a physically hindered conformation by PP2C:SnRK2 binding, creating a barrier to the catalytic site of the kinase (158). Both disruption of the catalytic site as well as physical hindrance of the ABA-box are are required for full PP2C-induced inhibition; single mutants in residues that partake in either mechanism result in slightly weakened PP2C inhibition. Interestingly, the PP2C:SnRK2 binding is similar to the gate-latch-lock mechanism of PYL:PP2C binding, which was likely important for PP2C specificity for the SnRK2s and producing the ABA core signaling pathway (158).

As with the presence of ABA itself, this three-component core pathway is highly conserved and has likely existed since the first land plants due to the sudden high selective

pressure for tolerance to limited and sporadic availability of water (113). Evidence for a functioning core signaling pathway is present in the moss *P. patens* by the existence of ABA-responsive stomata (113) and by the presence of bonafide ABA-receptor PYL-orthologs along with ABA-inhibited PP2Cs existant in *Marchantia polymorpha* (liverwort, MpPYRL1), one of the earliest diverging land-plants (113, 159, 160). With respect to SnRK2s, they are present in the moss *P*. *patens* possibly indicating a fully functional core-signaling pathway mimicking that of angiosperms. The presence of SnRK2 homologs has also been identified in the algae *Chlamydomonas* but was labelled as divergent from land plants, and likely nonfunctional in the same context (161). The further downstream transcription factors orthologous to the Arabidopsis ABF/AREB/ABI5 were found in some mosses, but not in non-land plants (113). Together, these indicate that the core pathway likely evolved with plant's colonization of land, and has maintained a highly conserved three-component module.

The nomenclature of some members of the ABA signaling pathway are the result of forward genetic screens. There have been multiple mutants that display ABA-insensitivities in a variety of contexts, and despite their differential biological roles. For clarity, ABI1 and ABI2 encode PP2Cs, but ABI3, ABI4, and ABI5 are transcription factors downstream of the core pathway. All have been identified by mutagenesis screens for similar early germination or ABA-insensitive germination phenotypes (162, 163).

These ABA-insensitive phenotypes were discovered multiple times, and helped give some elucidation to some of the members in the ABA signaling pathway. However, these genetic screens were unfruitful for many decades in attempting to identify the receptors of ABA, indicating a level of complexity or redundancy that was able to hide single-order receptor mutants. It was not until the utilization of a synthetic seed-

germination inhibitor, pyrabactin (Figure 1A), was used in forward chemical genetic screens that gave resistance to the chemical that these receptors were finally revealed. Ultimately this led to the identification of a mutation in PYR1 (110) which was enough to cause pyrabactin insensitivity due to its low potency on only a small subset of the receptor family. In parallel to this forward genetic screen, another group was able to identify interactors of the PP2Cs *via* a yeast-hybrid screen, further solidifying the evidence that this 14-member family in *Arabidopsis* acted as the ABA receptors (111).

Retrospectively, the number of members within the family easily explained the difficulty in identifying the receptors from forward chemical genetic screens aimed to enrich for ABA-insensitive phenotypes. The redundancy of the PYL receptor family is extensive, requiring higher-order mutants to produce any ABA-insensitive genotypes. Further, functional redundancy exists in all three modules of the core pathway. Thus it has been difficult to study the pathway using solely genetic techniques.

Synthetic ABA-receptor Agonists

Partially due to the genetic redundancy observed in the core signaling pathway, much research has been done to characterize the structure-activity relationship of ABA and its respective receptors, with one major benefit being the synthesis of a multitude of ABA scaffold analogs (164). Part of this work has been to develop analogs with agricultural benefits such as increased potency and longevity of the ABA-response due to modifications that inhibit endogenous catabolism. Other modifications have been helpful in explaining the importance of functional groups on the ABA backbone. For instance, the necessity of the cyclohexenone oxygen in the ABA headgroup has been supported

highlighted in studies where this oxygen is removed, producing 4′-deoxo-ABA **(4)** (Figure 2) (165), which had greatly reduced biological activity. This ketone oxygen is seen in many of the available crystal structures to hydrogen-bond to a conserved “gate-latch” water, which helps stabilize the interaction of the ABA-PYL-PP2C complex (115, 120, 121, 136, and 161). Quinabactin (Figure 1A), which was identified in a small-molecule screen and bares little chemical similarity to ABA, also contains an oxygen moiety which is observed to hydrogen bond to this water (166).

Chemical modifications to the hydrophobic portions of ABA have been pursued. Replacement of the 7′-methyl group with an H **(5)** reduces activity, indicative of a loss in hydrophobic interactions with the gate-latch area of the protein (167). Modifications of the 8′-methyl group with di- and tri-fluoro **(6)** substitutions resulted in analogs that increased the *in vivo* response, due to a decreased hydroxyl-metabolism at this position (168). Similarly, 8′- **(7)** and 9′-acetylene substitutions increase *in vivo* activity, as they act as suicide substrates for the CYP707A, the major 8′- and 9′-hydroxylation enzyme (107, 108, 169, and 170). These acetylene and fluoro-substitutions indicated that an increases in electron-withdrawing or hydrophobic bulk near the gate-latch region on the 8′- and 9′-carbons is tolerated by the pocket residues. However, a bulkier 8′-cyclopropyl analog **(8)** displayed reduced activity, highlighting a relative limited volume for the hydrophobic substitution size that can be tolerated (171).

Another important region of the binding pocket, termed the C6-cleft, has been elucidated by the subsequent loss of activity when replacing ABA’s 6-methyl group with an H, producing 6-nor-ABA **(9)** (167). This loss of activity is also seen when through SAR studies with the quinabactin scaffold. The 4-methyl benzyl group of quinabactin overlaps nearly perfectly in the space of ABA’s C6-methyl group, and an analog of quinabactin

lacking this methyl group **(10)** has substantially reduced potency (172, 173). Other unpublished data has indicated that 4-cyclopropyl analogs of quinabactin are inactive, which likely indicates an inability for the C6-cleft to accommodate this bulkier substitution.

Bicyclic analogs of ABA, termed tetralone ABAs **(11-13)**, where the 3', 4', and 7'-carbons are incorporated into a phenyl ring, have similar or even increased potency to that of ABA on the receptors (174–176). Interestingly, some of these were developed before the bicyclic synthetic agonists pyrabactin and quinabactin were characterized as ABA receptor ligands. The activity of the tetralone-ABA compounds, along with pyrabactin and quinabactin, indicate that there is some flexibility for the gate-latch region to accommodate hydrophobic bulk near. Similarly to **(7)**, these tetralone analogs were also modified to have acetylene constituents substituted on the positions homologous to the 8'- and 9'-methyl groups **(13)** which would likely inhibit the respective 9'- or 10'-hydroxylation by CYP707A. Indeed these acetylene suicide-substrates had increased and prolonged activity *in vivo (174)*.

Results from a virtual screening effort that sought to identify pyrabactin-analogs produced multiple active agonists that closely resemble pyrabactin (figure 1.2) (177). The compound **(16)** is the result of the replacement of pyrabactin's methylamino linked pyridyl moiety with a methionine derivative. From the same screen, the naptholactam compounds **(17)**-**(19)** gave moderate activity in a phosphatase inhibition assay. In a significantly larger screen, utilizing the natural product library RIKEN (178, 179), over 20,000 compounds were assayed for their ability to inhibit ABI1 when co-incubated with PYR1 (180). Multiple agonists and antagonists were identified and characterized, with the two strongest antagonists displaying highly decorated tetrahydropyrans.

Quinabactin has a novel interaction with the receptors not seen with the previously reported structures containing ABA or pyrabactin. The *N*-propyl chain from quinabactin's lactam moiety forms hydrophobic interactions with a gate-latch region known as the 3'-tunnel (181, 182). In some structures, this tunnel is evident with ABA-binding, although with ABA binding it exists unoccupied. It was reasoned that a sufficiently long alkyl substitution at the 3'-position of ABA could mimic the *N*-propyl chain of quinabactin. This led to the design of a series of analogs that had 3'-thioether substitutions on the ABA scaffold **(14-15)**, predicted to interact with this tunnel in a favorable manner (181). The analogs produced varied in chain length, and subsequently were observed to produce a gradient of activity from agonist to antagonistic effects, with longer alkyl lengths favoring the latter. AS2 **(14)** displayed active vegetative responses similar to ABA and quinabactin while AS6 **(15)**, a 3'-hexylsulfanyl ABA analog, showed extensive antagonism for all the receptors tests. It's hypothesized that the antagonism resultant from the longer alkyl chains is due to the protrusion through this tunnel and beyond the receptor surface, ultimately disrupting favorable interactions that would otherwise take place between the conformation of the bound-receptor and the PP2Cs.

This alkyl-chain modification was applied to the tetralone analogs as well, producing *O*-alkyl substituted tetralone ABA compounds termed PAO_n which also showed a gradient effect of agonism to antagonism based on the linker length (183). PAO_4 **(12)** showed increased biological activity compared to ABA, indicating that the additional hydrophobic interactions near the gate-latch interface were additive to the binding activity, and likely stabilized the closed conformation of the gate-latch.

The above briefly summarizes the existence of many agonists and antagonists on most of the receptors. However, while the tetralone and 3'-thioester

derivatives of ABA have both potent agonist and antagonist effects, they lack selectivity for the receptors, masking any non-redundant functions without analysis on an extensive number of higher-order mutants. Also, while both pyrabactin and quinabactin show some potency and selectivity, their selectivity largely overlaps, leaving potent, selective activation of the monomeric subset of receptors unprobed.

Summary of Research Herein

ABA is an important plant hormone for agriculture as it is a key regulator in drought response. Transcriptomic, proteomic, and metabolomic responses have been fairly well studied in the context of drought or exogenously applied ABA. However, many of these responses have not be fully characterized at the individual receptor-level, or even with respect to receptor-subset activation. Part of this lack of understanding and research in this area is partially due to the observed high level of redundancy in all modules of the core pathway, while another reason is a lack of differentially selective yet potent agonists for the PYL receptors. It would be beneficial to have such selective agonists to elucidate any non-redundant, or only semi-redundant roles for that may influence important aspects of drought response such as root growth, metabolite regulation, or water use efficiency.

Pyrabactin was a valuable tool in shedding light onto the core signaling pathway, however it has little effect in vegetative, adult plants. As such, similar efforts have been used to screen for compounds that produced a more robust or similar response to that of ABA. These efforts eventually led to the discovery the other small sulfonamide, quinabactin (also termed AM1) (166, 172). While quinabactin's response in adult plants is

similar, if not more potent than ABA, its selectivity for the receptors overlaps with pyrabactin and leaves multiple receptors unactivated.

In an attempt to identify new agonists that may help in understanding the roles of the other receptors, I have developed an *in silico* screening method meant to identify novel ligands for the receptors in an unbiased manner. This required a pre-screening effort to identify a crystal structure model that showed a high enrichment for preferentially docking known true-positives. A proportion of the best scoring hits were purchased and an *in vitro* assay was developed to identify the potency and selectivity for these ligands in a relatively high-throughput manner. This resulted in multiple positive hits *in-vitro* were able to produce an ABA response *in vivo* as well. Following identification of these agonists, structure-aided design was used to chemically optimize some of these compounds and lead to increased potency both *in vitro* and *in vivo*.

While multiple assays have been developed to assess the biological activity of these agonists *in vivo*, additional research is warranted in the quantification of metabolic changes that could result from small differences in potency or selectivity between agonists. Thus this method could produce a new screening platform for identifying ABA agonists, based on metabolic regulation, but additionally, deconvolute differential regulation based on receptor specificity of agonists being analyzed. These findings could benefit agriculture with respect to both direct metabolic regulation, such that wanted or unwanted metabolites can be differentially regulated by receptor specificity. Additionally, general identification of differential regulation of osmolytes through receptor specificity, could prove beneficial to plant WUE.

My research has thus been aimed at identifying novel ligands for the ABA receptors that may show unique receptor selectivity and producing a method to quantify the plants' responses by measuring metabolic regulation.

Chapter one focuses on the discovery and optimization of new ABA receptor agonists using virtual screening and describes a potent agonist that selectively and potently activates monomeric ABA receptors. Using this probe *in vivo*, I present data suggesting differential control of ABA transcriptional responses by monomeric and dimeric receptors. Chapter two focuses on characterizing metabolomic changes induced by ABA and using these as markers to dissect the contributions of different receptor classes to the control of metabolomic ABA responses. This work demonstrates that dimeric ABA receptors play a major role in regulating metabolomic responses to ABA.

References

1. Battisti DS, Naylor RL (2009) Historical warnings of future food insecurity with unprecedented seasonal heat. *Science* 323(5911):240–244.

2. Blum A (2005) Drought resistance, water-use efficiency, and yield potential—are they compatible, dissonant, or mutually exclusive? *Aust J Agric Res* 56(11):1159–1168.

3. Nelson DE, Shen B, Bohnert HJ (1998) Salinity Tolerance — Mechanisms, Models and the Metabolic Engineering of Complex Traits. *Genetic Engineering*, Genetic Engineering., ed Setlow JK (Springer US), pp 153–176.

4. Ingram J, Bartels D (1996) THE MOLECULAR BASIS OF DEHYDRATION TOLERANCE IN PLANTS. *Annu Rev Plant Physiol Plant Mol Biol* 47:377–403.

5. Bohnert HJ, Sheveleva E (1998) Plant stress adaptations--making metabolism move. *Curr Opin Plant Biol* 1(3):267–274.

6. Cruz de Carvalho MH (2008) Drought stress and reactive oxygen species: Production, scavenging and signaling. *Plant Signal Behav* 3(3):156–165.

7. Girotti AW (2001) Photosensitized oxidation of membrane lipids: reaction pathways, cytotoxic effects, and cytoprotective mechanisms. *J Photochem Photobiol B* 63(1-3):103–113.

8. Rebeiz CA, et al. (1988) Photodynamic herbicides. Recent developments and molecular basis of selectivity. *CRC Crit Rev Plant Sci* 6(4):385–436.

9. Apel K, Hirt H (2004) Reactive oxygen species: metabolism, oxidative stress, and signal transduction. *Annu Rev Plant Biol* 55:373–399.

10. Klotz L-O (2002) Oxidant-induced signaling: effects of peroxynitrite and singlet oxygen. *Biol Chem* 383(3-4):443–456.

11. Alscher RG, Donahue JL, Cramer CL (1997) Reactive oxygen species and antioxidants: Relationships in green cells. *Physiol Plant* 100(2):224–233.

12. Jonak C, Okrész L, Bögre L, Hirt H (2002) Complexity, cross talk and integration of plant MAP kinase signalling. *Curr Opin Plant Biol* 5(5):415–424.

13. Kovtun Y, Chiu WL, Tena G, Sheen J (2000) Functional analysis of oxidative stress-activated mitogen-activated protein kinase cascade in plants. *Proc Natl Acad Sci U S A* 97(6):2940–2945.

14. McAinsh MR, Clayton H, Mansfield TA, Hetherington AM (1996) Changes in

Stomatal Behavior and Guard Cell Cytosolic Free Calcium in Response to Oxidative Stress. *Plant Physiol* 111(4):1031–1042.

15. Pastori GM, Foyer CH (2002) Common Components, Networks, and Pathways of Cross-Tolerance to Stress. The Central Role of “Redox” and Abscisic Acid-Mediated Controls. *Plant Physiol* 129(2):460–468.

16. Bashir A, et al. (2014) Plant-derived compatible solutes proline betaine and betonicine confer enhanced osmotic and temperature stress tolerance to Bacillus subtilis. *Microbiology* 160(Pt 10):2283–2294.

17. Street TO, Bolen DW, Rose GD (2006) A molecular mechanism for osmolyte-induced protein stability. *Proc Natl Acad Sci U S A* 103(38):13997–14002.

18. Kempf B, Bremer E (1998) Uptake and synthesis of compatible solutes as microbial stress responses to high-osmolality environments. *Arch Microbiol* 170(5):319–330.

19. Smirnoff N, Cumbes QJ (1989) Hydroxyl radical scavenging activity of compatible solutes. *Phytochemistry* 28(4):1057–1060.

20. Delauney AJ, Verma DPS (1993) Proline biosynthesis and osmoregulation in plants. *Plant J* 4(2):215–223.

21. Hayat S, et al. (2012) Role of proline under changing environments: a review. *Plant Signal Behav* 7(11):1456–1466.

22. Erxleben A, Gessler A, Vervliet-Scheebaum M, Reski R (2012) Metabolite profiling of the moss Physcomitrella patens reveals evolutionary conservation of osmoprotective substances. *Plant Cell Rep* 31(2):427–436.

23. Szabados L, Savouré A (2010) Proline: a multifunctional amino acid. *Trends Plant Sci* 15(2):89–97.

24. Ashraf M, Foolad MR (2007/3) Roles of glycine betaine and proline in improving plant abiotic stress resistance. *Environ Exp Bot* 59(2):206–216.

25. Hare PD, Cress WA (1997) Metabolic implications of stress-induced proline accumulation in plants. *Plant Growth Regul* 21(2):79–102.

26. Matysik J, Bhalu B, Mohanty P, Others (2002) Molecular mechanisms of quenching of reactive oxygen species by proline under stress in plants. *Curr Sci* 82(5):525–532.

27. Verbruggen N, Hermans C (2008) Proline accumulation in plants: a review. *Amino Acids* 35(4):753–759.

28. Handa S, Bressan RA, Handa AK, Carpita NC, Hasegawa PM (1983) Solutes contributing to osmotic adjustment in cultured plant cells adapted to water stress. *Plant Physiol* 73(3):834–843.

29. Liang X, Zhang L, Natarajan SK, Becker DF (2013) Proline mechanisms of stress survival. *Antioxid Redox Signal* 19(9):998–1011.

30. Hare PD, Cress WA, van Staden J (1999) Proline synthesis and degradation: a model system for elucidating stress-related signal transduction. *J Exp Bot* 50(333):413–434.

31. Hong Z, Lakkineni K, Zhang Z, Verma DP (2000) Removal of feedback inhibition of delta(1)-pyrroline-5-carboxylate synthetase results in increased proline accumulation and protection of plants from osmotic stress. *Plant Physiol* 122(4):1129–1136.

32. Savouré A, et al. (1995) Isolation, characterization, and chromosomal location of a gene encoding the delta 1-pyrroline-5-carboxylate synthetase in Arabidopsis thaliana. *FEBS Lett* 372(1):13–19.

33. Kishor P, Hong Z, Miao GH, Hu C, Verma D (1995) Overexpression of [delta]-Pyrroline-5-Carboxylate Synthetase Increases Proline Production and Confers Osmotolerance in Transgenic Plants. *Plant Physiol* 108(4):1387–1394.

34. Blum A, et al. (1996) Genetically Engineered Plants Resistant to Soil Drying and Salt Stress: How to Interpret Osmotic Relations? *Plant Physiol* 110(4):1051–1053.

35. Gowing DJG, Davies WJ, Jones HG (1990) A Positive Root-sourced Signal as an Indicator of Soil Drying in Apple, Malus x domestica Borkh. *J Exp Bot* 41(12):1535–1540.

36. Davies WJ, Zhang J (1991) Root Signals and the Regulation of Growth and Development of Plants in Drying Soil. *Annu Rev Plant Physiol Plant Mol Biol* 42(1):55–76.

37. Cracker LE, Abeles FB (1969) Abscission: role of abscisic Acid. *Plant Physiol* 44(8):1144–1149.

38. F T Addicott, Lyon JL (1969) Physiology of Abscisic Acid and Related Substances. *Annu Rev Plant Physiol* 20(1):139–164.

39. Hilhorst HWM, Karssen CM (1992) Seed dormancy and germination: the role of abscisic acid and gibberellins and the importance of hormone mutants. *Plant Growth Regul* 11(3):225–238.

40. Melotto M, Underwood W, Koczan J, Nomura K, He SY (2006) Plant stomata function in innate immunity against bacterial invasion. *Cell* 126(5):969–980.

41. McAinsh MR, Brownlee C, Hetherington AM, Others (1990) Abscisic acid-induced elevation of guard cell cytosolic Ca2+ precedes stomatal closure. *Nature* 343(6254):186–188.

42. De Smet I, Signora L, Beeckman T, Inzé D (2003) An abscisic acid- sensitive checkpoint in lateral root development of Arabidopsis. *The Plant*. Available at:

http://onlinelibrary.wiley.com/doi/10.1046/j.1365-313X.2003.01652.x/full.

43. De Smet I, Zhang H, Inzé D, Beeckman T (2006) A novel role for abscisic acid emerges from underground. *Trends Plant Sci* 11(9):434–439.

44. Zhao Y, et al. (2014) The ABA receptor PYL8 promotes lateral root growth by enhancing MYB77-dependent transcription of auxin-responsive genes. *Sci Signal* 7(328):ra53.

45. Watts S, Rodriguez JL, Evans SE, Davies WJ (1981) Root and Shoot Growth of Plants Treated with Abscisic Acid. *Ann Bot* 47(5):595–602.

46. Creelman RA, Mason HS, Bensen RJ, Boyer JS (1990) Water deficit and abscisic acid cause differential inhibition of shoot versus root growth in soybean seedlings analysis of growth, sugar accumulation, and gene …. *Plant*. Available at: http://www.plantphysiol.org/content/92/1/205.short.

47. Saab IN, Sharp RE, Pritchard J, Voetberg GS (1990) Increased endogenous abscisic Acid maintains primary root growth and inhibits shoot growth of maize seedlings at low water potentials. *Plant Physiol* 93(4):1329–1336.

48. Debeaujon I, Koornneef M (2000) Gibberellin requirement for Arabidopsis seed germination is determined both by testa characteristics and embryonic abscisic acid. *Plant Physiol* 122(2):415–424.

49. Stephenson AG (1981) Flower and Fruit Abortion: Proximate Causes and Ultimate Functions. *Annu Rev Ecol Syst* 12:253–279.

50. Anderson JP, et al. (2004) Antagonistic interaction between abscisic acid and jasmonate-ethylene signaling pathways modulates defense gene expression and disease resistance in Arabidopsis. *Plant Cell* 16(12):3460–3479.

51. Chiwocha SDS, et al. (2005) The etr1-2 mutation in Arabidopsis thaliana affects the abscisic acid, auxin, cytokinin and gibberellin metabolic pathways during maintenance of seed dormancy, moist-chilling and germination. *Plant J* 42(1):35–48.

52. Fedoroff NV (2002) Cross-talk in abscisic acid signaling. *Sci STKE* 2002(140):re10.

53. Piotrowska A, Bajguz A (2011) Conjugates of abscisic acid, brassinosteroids, ethylene, gibberellins, and jasmonates. *Phytochemistry* 72(17):2097–2112.

54. Jiang F, Hartung W (2008) Long-distance signalling of abscisic acid (ABA): the factors regulating the intensity of the ABA signal. *J Exp Bot* 59(1):37–43.

55. Sauter A, Davies WJ, Hartung W (2001) The long-distance abscisic acid signal in the droughted plant: the fate of the hormone on its way from root to shoot. *J Exp Bot* 52(363):1991–1997.

56. Burla B, et al. (2013) Vacuolar transport of abscisic acid glucosyl ester is mediated

by ATP-binding cassette and proton-antiport mechanisms in Arabidopsis. *Plant Physiol* 163(3):1446–1458.

57. Sauter A, Dietz K-J, Hartung W (2002) A possible stress physiological role of abscisic acid conjugates in root-to-shoot signalling. *Plant Cell Environ* 25(2):223–228.

58. Ruiz-Sola MÁ, Rodríguez-Concepción M (2012) Carotenoid biosynthesis in Arabidopsis: a colorful pathway. *Arabidopsis Book* 10:e0158.

59. North HM, et al. (2007) The Arabidopsis ABA-deficient mutant aba4 demonstrates that the major route for stress-induced ABA accumulation is via neoxanthin isomers. *Plant J* 50(5):810–824.

60. Rock CD, Zeevaart JA (1991) The aba mutant of Arabidopsis thaliana is impaired in epoxy-carotenoid biosynthesis. *Proc Natl Acad Sci U S A* 88(17):7496–7499.

61. Demmig-Adams B Carotenoids and photoprotection in plants: A role for the xanthophyll zeaxanthin - ScienceDirect. Available at: http://www.sciencedirect.com/science/article/pii/000527289090088L [Accessed January 20, 2017].

62. Tan B-C, et al. (2003) Molecular characterization of the Arabidopsis 9-cis epoxycarotenoid dioxygenase gene family. *Plant J* 35(1):44–56.

63. González-Guzmán M, et al. (2002) The short-chain alcohol dehydrogenase ABA2 catalyzes the conversion of xanthoxin to abscisic aldehyde. *Plant Cell* 14(8):1833–1846.

64. Rock CD, Heath TG, Zeevaart JAD (1992) 2-Trans-Abscisic Acid Biosynthesis and Metabolism of ABA-Aldehyde and Xanthoxin in Wild Type and the aba Mutant of Arabidopsis thaliana. *J Exp Bot* 43(2):249–256.

65. Milborrow BV (1974) The Chemistry and Physiology of Abscisic Acid. *Annu Rev Plant Physiol* 25(1):259–307.

66. Abrams SR, et al. (1989) Ratio of (S)- to (R)-abscisic acid from plant cell cultures supplied with racemic aba. *Phytochemistry* 28(11):2885–2889.

67. Han S-Y, et al. (2004) A novel inhibitor of 9-cis-epoxycarotenoid dioxygenase in abscisic acid biosynthesis in higher plants. *Plant Physiol* 135(3):1574–1582.

68. Kitahata N, et al. (2006) A 9-cis-epoxycarotenoid dioxygenase inhibitor for use in the elucidation of abscisic acid action mechanisms. *Bioorg Med Chem* 14(16):5555–5561.

69. Messing SAJ, et al. Structural Insights into Maize Viviparous14, a Key Enzyme in the Biosynthesis of the Phytohormone Abscisic Acid. doi:10.1105/tpc.110.074815.

70. Christmann A, Hoffmann T, Teplova I, Grill E, Müller A (2005) Generation of active

pools of abscisic acid revealed by in vivo imaging of water-stressed Arabidopsis. *Plant Physiol* 137(1):209–219.

71. Quesada V, Ponce MR, Micol JL (2000) Genetic analysis of salt-tolerant mutants in Arabidopsis thaliana. *Genetics* 154(1):421–436.

72. León P, Sheen J (2003) Sugar and hormone connections. *Trends Plant Sci* 8(3):110–116.

73. Cheng W-H, et al. (2002) A Unique Short-Chain Dehydrogenase/Reductase in Arabidopsis Glucose Signaling and Abscisic Acid Biosynthesis and Functions. *Plant Cell* 14(11):2723–2743.

74. Hartung W (2010) The evolution of abscisic acid (ABA) and ABA function in lower plants, fungi and lichen. *Funct Plant Biol* 37(9):806–812.

75. Zahradníčková H, Maršálek B, Polišenská M (1991) High-performance thin-layer chromatographic and high-performance liquid chromatographic determination of abscisic acid produced by cyanobacteria. *J Chromatogr A* 555(1):239–245.

76. Maršálek B, Zahradníčková H, Hronková M (1992) Extracellular Abscisic Acid Produced by Cyanobacteria under Salt Stress. *J Plant Physiol* 139(4):506–508.

77. Banks JA, Hickok L, Webb MA (1993) The Programming of Sexual Phenotype in the Homosporous Fern Ceratopteris richardii. *Int J Plant Sci* 154(4):522–534.

78. Hickok LG (1983) Abscisic acid blocks antheridiogen-induced antheridium formation in gametophytes of the fern Ceratopteris. *Can J Bot* 61(3):888–892.

79. McAdam SAM, et al. (2016) Abscisic acid controlled sex before transpiration in vascular plants. *Proc Natl Acad Sci U S A*. doi:10.1073/pnas.1606614113.

80. Duan L, et al. (2013) Endodermal ABA signaling promotes lateral root quiescence during salt stress in Arabidopsis seedlings. *Plant Cell* 25(1):324–341.

81. Fujii H, Zhu J-K (2009) Arabidopsis mutant deficient in 3 abscisic acid-activated protein kinases reveals critical roles in growth, reproduction, and stress. *Proc Natl Acad Sci U S A* 106(20):8380–8385.

82. Spollen WG, Sharp RE, Saab IN, Wu Y (1993) Regulation of cell expansion in roots and shoots at low water potentials. *Water deficits: plant responses from cell to community*:37–52.

83. Sharp RE, Davies WJ (1989) A restricted supply of water. *Plants under stress: biochemistry, physiology and ecology and their application to plant improvement* 39:71.

84. Geng Y, et al. (2013) A spatio-temporal understanding of growth regulation during the salt stress response in Arabidopsis. *Plant Cell* 25(6):2132–2154.

85. Sharp RE, et al. (2004) Root growth maintenance during water deficits: physiology to functional genomics. *J Exp Bot* 55(407):2343–2351.

86. Spollen WG, LeNoble ME, Samuels TD, Bernstein N, Sharp RE (2000) Abscisic acid accumulation maintains maize primary root elongation at low water potentials by restricting ethylene production. *Plant Physiol* 122(3):967–976.

87. Sharp RE, Wu Y, Voetberg GS, Saab IN, LeNoble ME (1994) Confirmation that abscisic acid accumulation is required for maize primary root elongation at low water potentials. *J Exp Bot* 45(Special_Issue):1743–1751.

88. Jia H-F, et al. (2011) Abscisic acid plays an important role in the regulation of strawberry fruit ripening. *Plant Physiol* 157(1):188–199.

89. Jiang Y, Joyce DC, Macnish AJ (2014) Effect of Abscisic Acid on Banana Fruit Ripening in Relation to the Role of Ethylene. *J Plant Growth Regul* 19(1):106–111.

90. Ban T, Ishimaru M, Kobayashi S, Goto-Yamamoto N, Horiuchi S (2003) Abscisic acid and 2,4-dichlorophenoxyacetic acid affect the expression of anthocyanin biosynthetic pathway genes in “Kyoho” grape berries. *J Hortic Sci Biotechnol* 78(4):586–589.

91. Peppi MC, Fidelibus MW, Dokoozlian N (2006) Abscisic Acid Application Timing and Concentration Affect Firmness, Pigmentation, and Color of `Flame Seedless’ Grapes. *HortScience* 41(6):1440–1445.

92. Prasad TK, Anderson MD, Stewart CR (1994) Acclimation, Hydrogen Peroxide, and Abscisic Acid Protect Mitochondria against Irreversible Chilling Injury in Maize Seedlings. *Plant Physiol* 105(2):619–627.

93. Rikin A, Blumenfeld A, Richmond AE (1976) Chilling Resistance as Affected by Stressing Environments and Abscisic Acid. *Bot Gaz* 137(4):307–312.

94. Flores A, Grau A, Laurich F, Dörffling K (1988/4) Effect of New Terpenoid Analogues of Abscisic Acid on Chilling and Freezing Resistance. *J Plant Physiol* 132(3):362–369.

95. Kim Y-H, Choi K-I, Khan AL, Waqas M, Lee I-J (2016) Exogenous application of abscisic acid regulates endogenous gibberellins homeostasis and enhances resistance of oriental melon (Cucumis melo var. L.) against low temperature. *Sci Hortic* 207:41–47.

96. Rikin A, Atsmon D, Gitler C Chilling injury in cotton (Gossypium hirsutum L. Prevention by abscisic acid. Available at: http://oup.silverchair-cdn.com/oup/backfile/Content_public/Journal/pcp/20/8/10.1093/oxfordjournals.pcp.a075956/2/20-8-1537.pdf?Expires=1485050391&Signature=EN8ZE-FWivEddp99Stvybq3q2TI3WM2MecTYsl-EXHLYe-~~5uponIUCEd4SywJ4Al9j15d4BXwephdlRdNRQJHHcIKEiNx~pk~DmYBLcdQcn2BIGxNHWo7F594bSQQYRvUtxdgzGTlQzkkhXKaRcHwIrK3eTTXHG3I~SMr-

UE3d8Wjd5w0QbC1FC3r0mpd2aDtMS5Zkz6-KbAT0QK8naLYnQSotNJD7iorlPSEI5Lvra9Q1UHhdKC3EHGLGpdTJQUvWwff3Lb0iMfdqLEQtcr98oDgibZJvsboQohL-AEKHedqpjirMrSz~4CN1gOuiriPoJ4kpRqvwhBarZYMGnA__&Key-Pair-Id=APKAIUCZBIA4LVPAVW3Q.

97. Sharp RE (2002) Interaction with ethylene: changing views on the role of abscisic acid in root and shoot growth responses to water stress. *Plant Cell Environ* 25(2):211–222.

98. Kudoyarova G, et al. (2011) Involvement of root ABA and hydraulic conductivity in the control of water relations in wheat plants exposed to increased evaporative demand. *Planta* 233(1):87–94.

99. Wilkinson S, Kudoyarova GR, Veselov DS, Arkhipova TN, Davies WJ (2012) Plant hormone interactions: innovative targets for crop breeding and management. *J Exp Bot* 63(9):3499–3509.

100. Tardieu F, Parent B, Simonneau T (2010) Control of leaf growth by abscisic acid: hydraulic or non-hydraulic processes? *Plant Cell Environ* 33(4):636–647.

101. Davies WJ, Kudoyarova G, Hartung W (2005) Long-distance ABA Signaling and Its Relation to Other Signaling Pathways in the Detection of Soil Drying and the Mediation of the Plant's Response to Drought. *J Plant Growth Regul* 24(4):285.

102. Wilkinson S, Davies WJ (2010) Drought, ozone, ABA and ethylene: new insights from cell to plant to community. *Plant Cell Environ* 33(4):510–525.

103. Lackman P, et al. (2011) Jasmonate signaling involves the abscisic acid receptor PYL4 to regulate metabolic reprogramming in Arabidopsis and tobacco. *Proc Natl Acad Sci U S A* 108(14):5891–5896.

104. Riemann M, et al. (2015) Exploring Jasmonates in the Hormonal Network of Drought and Salinity Responses. *Front Plant Sci* 6:1077.

105. Todoroki Y, Tanaka T, Kisamori M, Hirai N (2001) 3′-Azidoabscisic acid as a photoaffinity reagent for abscisic acid binding proteins. *Bioorg Med Chem Lett* 11(17):2381–2384.

106. Wenjian L, et al. (2013) Synthesis, photostability and bioactivity of 2,3-cyclopropanated abscisic acid. *Phytochemistry* 96:72–80.

107. Abrams SR, et al. (1997) 8[prime]-Methylene Abscisic Acid (An Effective and Persistent Analog of Abscisic Acid). *Plant Physiol* 114(1):89–97.

108. Kushiro T, et al. (2004) The Arabidopsis cytochrome P450 CYP707A encodes ABA 8'-hydroxylases: key enzymes in ABA catabolism. *EMBO J* 23(7):1647–1656.

109. Cutler SR, Rodriguez PL, Finkelstein RR, Abrams SR (2010) Abscisic acid: emergence of a core signaling network. *Annu Rev Plant Biol* 61:651–679.

110. Park S-Y, et al. (2009) Abscisic acid inhibits type 2C protein phosphatases via the PYR/PYL family of START proteins. *Science* 324(5930):1068–1071.

111. Ma Y, et al. (2009) Regulators of PP2C phosphatase activity function as abscisic acid sensors. *Science* 324(5930):1064–1068.

112. Radauer C, Lackner P, Breiteneder H (2008) The Bet v 1 fold: an ancient, versatile scaffold for binding of large, hydrophobic ligands. *BMC Evol Biol* 8:286.

113. Hauser F, Waadt R, Schroeder JI (2011) Evolution of abscisic acid synthesis and signaling mechanisms. *Curr Biol* 21(9):R346–55.

114. Raghavendra AS, Gonugunta VK, Christmann A, Grill E (2010) ABA perception and signalling. *Trends Plant Sci* 15(7):395–401.

115. Nishimura N, et al. (2009) Structural mechanism of abscisic acid binding and signaling by dimeric PYR1. *Science* 326(5958):1373–1379.

116. Dupeux F, et al. (2011) A thermodynamic switch modulates abscisic acid receptor sensitivity. *EMBO J* 30(20):4171–4184.

117. Hao Q, et al. (2011) The molecular basis of ABA-independent inhibition of PP2Cs by a subclass of PYL proteins. *Mol Cell* 42(5):662–672.

118. Li W, et al. (2013) Molecular basis for the selective and ABA-independent inhibition of PP2CA by PYL13. *Cell Res* 23(12):1369–1379.

119. Li J, et al. (2015) The HAB1 PP2C is inhibited by ABA-dependent PYL10 interaction. *Sci Rep* 5:10890.

120. Yin P, et al. (2009) Structural insights into the mechanism of abscisic acid signaling by PYL proteins. *Nat Struct Mol Biol* 16(12):1230–1236.

121. Melcher K, et al. (2009) A gate-latch-lock mechanism for hormone signalling by abscisic acid receptors. *Nature* 462(7273):602–608.

122. Cohen P, Cohen PT (1989) Protein phosphatases come of age. *J Biol Chem* 264(36):21435–21438.

123. Cohen P (1989) The Structure and Regulation of Protein Phosphatases. *Annu Rev Biochem* 58(1):453–508.

124. Kerk D, et al. (2002) The complement of protein phosphatase catalytic subunits encoded in the genome of Arabidopsis. *Plant Physiol* 129(2):908–925.

125. Schweighofer A, Hirt H, Meskiene I (2004) Plant PP2C phosphatases: emerging functions in stress signaling. *Trends Plant Sci* 9(5):236–243.

126. Bork P, Brown NP, Hegyi H, Schultz J (1996) The protein phosphatase 2C (PP2C) superfamily: detection of bacterial homologues. *Protein Sci* 5(7):1421–1425.

127. Ofek P, Ben-Meir D, Kariv-Inbal Z, Oren M, Lavi S (2003) Cell Cycle Regulation and p53 Activation by Protein Phosphatase 2Cα. *J Biol Chem* 278(16):14299–14305.

128. Menges M, Hennig L, Gruissem W, Murray JAH (2002) Cell Cycle-regulated Gene Expression inArabidopsis. *J Biol Chem* 277(44):41987–42002.

129. Koornneef M, Reuling G, Karssen CM (1984) The isolation and characterization of abscisic acid-insensitive mutants of Arabidopsis thaliana. *Physiol Plant* 61(3):377–383.

130. Leung J, et al. (1994) Arabidopsis ABA response gene ABI1: features of a calcium-modulated protein phosphatase. *Science* 264(5164):1448–1452.

131. Leung J, Merlot S, Giraudat J (1997) The Arabidopsis ABSCISIC ACID-INSENSITIVE2 (ABI2) and ABI1 genes encode homologous protein phosphatases 2C involved in abscisic acid signal transduction. *Plant Cell* 9(5):759–771.

132. Meyer K, Leube MP, Grill E (1994) A protein phosphatase 2C involved in ABA signal transduction in Arabidopsis thaliana. *Science* 264(5164):1452–1455.

133. Rodriguez PL, Benning G, Grill E (1998) ABI2, a second protein phosphatase 2C involved in abscisic acid signal transduction in Arabidopsis. *FEBS Lett* 421(3):185–190.

134. Rodriguez PL (1998) Protein phosphatase 2C (PP2C) function in higher plants. *Plant Mol Biol* 38(6):919–927.

135. Gosti F, et al. (1999) ABI1 protein phosphatase 2C is a negative regulator of abscisic acid signaling. *Plant Cell* 11(10):1897–1910.

136. Miyazono K-I, et al. (2009) Structural basis of abscisic acid signalling. *Nature* 462(7273):609–614.

137. Xue T, et al. (2008) Genome-wide and expression analysis of protein phosphatase 2C in rice and Arabidopsis. *BMC Genomics* 9:550.

138. Bhaskara GB, Nguyen TT, Verslues PE (2012) Unique drought resistance functions of the highly ABA-induced clade A protein phosphatase 2Cs. *Plant Physiol* 160(1):379–395.

139. Wang P, et al. (2013) Quantitative phosphoproteomics identifies SnRK2 protein kinase substrates and reveals the effectors of abscisic acid action. *Proc Natl Acad Sci U S A* 110(27):11205–11210.

140. Hardie DG (2007) AMP-activated/SNF1 protein kinases: conserved guardians of cellular energy. *Nat Rev Mol Cell Biol* 8(10):774–785.

141. Hanks SK, Quinn AM (1991) [2] Protein kinase catalytic domain sequence database: Identification of conserved features of primary structure and classification

of family members. *Methods in Enzymology* (Academic Press), pp 38–62.

142. Hanks SK, Quinn AM, Hunter T (1988) The protein kinase family: conserved features and deduced phylogeny of the catalytic domains. *Science* 241(4861):42–52.

143. Hong-Bo S, Zong-Suo L, Ming-An S (2005) LEA proteins in higher plants: structure, function, gene expression and regulation. *Colloids Surf B Biointerfaces* 45(3-4):131–135.

144. Anderberg RJ, Walker-Simmons MK (1992) Isolation of a wheat cDNA clone for an abscisic acid-inducible transcript with homology to protein kinases. *Proc Natl Acad Sci U S A* 89(21):10183–10187.

145. Hedbacker K, Carlson M (2008) SNF1/AMPK pathways in yeast. *Front Biosci* 13:2408–2420.

146. Armstrong F, et al. (1995) Sensitivity to abscisic acid of guard-cell K+ channels is suppressed by abi1-1, a mutant Arabidopsis gene encoding a putative protein phosphatase. *Proc Natl Acad Sci U S A* 92(21):9520–9524.

147. Schmidt C, Schelle I, Liao YJ, Schroeder JI (1995) Strong regulation of slow anion channels and abscisic acid signaling in guard cells by phosphorylation and dephosphorylation events. *Proc Natl Acad Sci U S A* 92(21):9535–9539.

148. Li J, Assmann SM (1996) An Abscisic Acid-Activated and Calcium-Independent Protein Kinase from Guard Cells of Fava Bean. *Plant Cell* 8(12):2359–2368.

149. Mustilli A-C, Merlot S, Vavasseur A, Fenzi F, Giraudat J (2002) Arabidopsis OST1 protein kinase mediates the regulation of stomatal aperture by abscisic acid and acts upstream of reactive oxygen species production. *Plant Cell* 14(12):3089–3099.

150. Harmon AC (2003) Calcium-regulated protein kinases of plants. *Gravit Space Biol Bull* 16(2):83–90.

151. Nakashima K, et al. (2009) Three Arabidopsis SnRK2 protein kinases, SRK2D/SnRK2.2, SRK2E/SnRK2.6/OST1 and SRK2I/SnRK2.3, involved in ABA signaling are essential for the control of seed development and dormancy. *Plant Cell Physiol* 50(7):1345–1363.

152. Fujita Y, et al. (2009) Three SnRK2 protein kinases are the main positive regulators of abscisic acid signaling in response to water stress in Arabidopsis. *Plant Cell Physiol* 50(12):2123–2132.

153. Umezawa T, et al. (2009) Type 2C protein phosphatases directly regulate abscisic acid-activated protein kinases in Arabidopsis. *Proc Natl Acad Sci U S A* 106(41):17588–17593.

154. Belin C, et al. (2006) Identification of features regulating OST1 kinase activity

and OST1 function in guard cells. *Plant Physiol* 141(4):1316–1327.

155. Krzywińska E, et al. (2016) Protein phosphatase type 2C PP2CA together with ABI1 inhibits SnRK2.4 activity and regulates plant responses to salinity. *Plant Signal Behav*:0.

156. Yoshida R, et al. (2006) The regulatory domain of SRK2E/OST1/SnRK2.6 interacts with ABI1 and integrates abscisic acid (ABA) and osmotic stress signals controlling stomatal closure in Arabidopsis. *J Biol Chem* 281(8):5310–5318.

157. Ng L-M, et al. (2011) Structural basis for basal activity and autoactivation of abscisic acid (ABA) signaling SnRK2 kinases. *Proc Natl Acad Sci U S A* 108(52):21259–21264.

158. Soon F-F, et al. (2012) Molecular mimicry regulates ABA signaling by SnRK2 kinases and PP2C phosphatases. *Science* 335(6064):85–88.

159. Hartung W (2010) The evolution of abscisic acid (ABA) and ABA function in lower plants, fungi and lichen. *Funct Plant Biol* 37(9):806–812.

160. Tougane K, et al. (2010) Evolutionarily conserved regulatory mechanisms of abscisic acid signaling in land plants: characterization of ABSCISIC ACID INSENSITIVE1-like type 2C protein phosphatase in the liverwort Marchantia polymorpha. *Plant Physiol* 152(3):1529–1543.

161. Umezawa T, et al. (2010) Molecular basis of the core regulatory network in ABA responses: sensing, signaling and transport. *Plant Cell Physiol* 51(11):1821–1839.

162. Bonetta D, McCourt P (1998) Genetic analysis of ABA signal transduction pathways. *Trends Plant Sci* 3(6):231–235.

163. Finkelstein RR (1994) Mutations at two new Arabidopsis ABA response loci are similar to the abi3 mutations. *Plant J* 5(6):765–771.

164. Helander JDM, Vaidya AS, Cutler SR (2016) Chemical manipulation of plant water use. *Bioorg Med Chem* 24(3):493–500.

165. Takahashi S, Oritani T, Yamashita K (1986) Synthesis and Biological Activities of (±)-Deoxy-abscisic Acid Isomers. *Agric Biol Chem* 50(12):3205–3206.

166. Okamoto M, et al. (2013) Activation of dimeric ABA receptors elicits guard cell closure, ABA-regulated gene expression, and drought tolerance. *Proc Natl Acad Sci U S A* 110(29):12132–12137.

167. Takeuchi J, Ohnishi T, Okamoto M, Todoroki Y (2015) The selectivity of 6-nor-ABA and 7'-nor-ABA for abscisic acid receptor subtypes. *Bioorg Med Chem Lett* 25(17):3507–3510.

168. Todoroki Y, Hirai N, Koshimizu K (1995) 8′,8′-Difluoro- and 8′,8′,8′-trifluoroabscisic acids as highly potent, long-lasting analogues of abscisic acid.

Phytochemistry 38(3):561–568.

169. Okamoto M, et al. (2011) ABA 9’-hydroxylation is catalyzed by CYP707A in Arabidopsis. *Phytochemistry* 72(8):717–722.

170. Rose PA, et al. (1997) 8’-Acetylene ABA: an irreversible inhibitor of ABA 8'-hydroxylase. *Bioorg Med Chem Lett* 7(19):2543–2546.

171. Benson CL, et al. (2015) Abscisic acid analogs as chemical probes for dissection of abscisic acid responses in Arabidopsis thaliana. *Phytochemistry* 113:96–107.

172. Cao M, et al. (2013) An ABA-mimicking ligand that reduces water loss and promotes drought resistance in plants. *Cell Res* 23(8):1043–1054.

173. Cutler SR, Okamoto M (2016) Synthetic compounds for vegetative ABA responses. *US Patent*. Available at: https://www.google.com/patents/US9345245 [Accessed February 25, 2017].

174. Nyangulu JM, et al. (2006) Synthesis and biological activity of tetralone abscisic acid analogues. *Org Biomol Chem* 4(7):1400–1412.

175. Kepka M, et al. (2011) Action of natural abscisic acid precursors and catabolites on abscisic acid receptor complexes. *Plant Physiol* 157(4):2108–2119.

176. Han X, et al. (2015) Synthesis and bioactivity of 2′,3′-benzoabscisic acid analogs. *Bioorg Med Chem Lett* 25(11):2438–2441.

177. Melcher K, et al. (2010) Identification and mechanism of ABA receptor antagonism. *Nat Struct Mol Biol* 17(9):1102–1108.

178. Kato N, Takahashi S, Nogawa T, Saito T, Osada H (2012) Construction of a microbial natural product library for chemical biology studies. *Curr Opin Chem Biol* 16(1-2):101–108.

179. Tomiki T, et al. (2006) [Special Issue: Fact Databases and Freewares] RIKEN Natural Products Encyclopedia (RIKEN NPEdia),a Chemical Database of RIKEN Natural Products Depository (RIKEN NPDepo). *Journal of Computer Aided Chemistry* 7:157–162.

180. Ito T, et al. (2015) Novel Abscisic Acid Antagonists Identified with Chemical Array Screening. *Chembiochem* 16(17):2471–2478.

181. Takeuchi J, et al. (2014) Designed abscisic acid analogs as antagonists of PYL-PP2C receptor interactions. *Nat Chem Biol* 10(6):477–482.

182. Hayashi K-I, Kinoshita T (2014) Plant signaling: abscisic acid receptor hole-in-one. *Nat Chem Biol* 10(6):414–415.

183. Takeuchi J, Ohnishi T, Okamoto M, Todoroki Y (2015) Conformationally restricted 3′-modified ABA analogs for controlling ABA receptors. *Org Biomol Chem*

13(14):4278–4288.

Figures and Tables

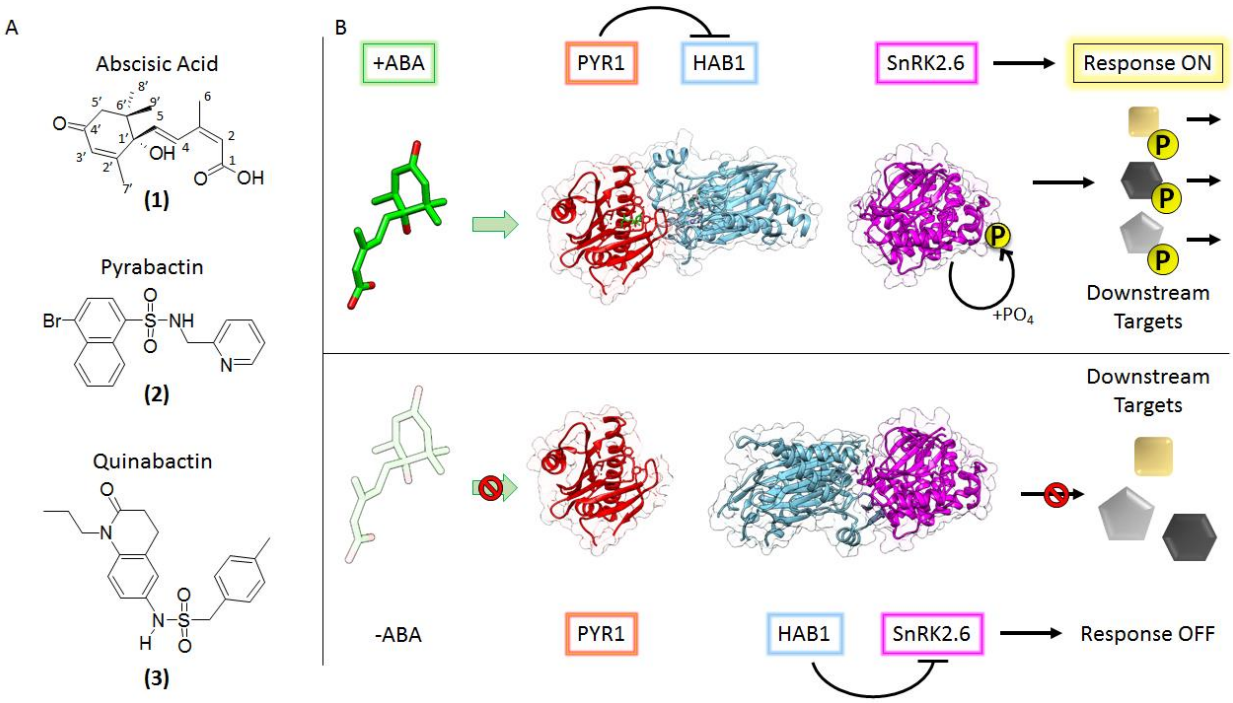

0.1

Figure 1.1 Panel A) Abscisic acid **(1)** shown with corresponding numbering of carbon atoms, the two ABA-receptor agonist sulfonamides pyrabactin **(2)** and quinabactin **(3)**. B) The core ABA signaling pathway. ABA is shown in green, PYL receptor (PYR1, PDB 3QN1) in red, PP2C (HAB1, 3QN1/3UJG) in blue, the SnRK2 kinase (SnRK2.6, PDB 3UJG) in pink, and downstream effectors. Phosphorylation state is positively indicated by the yellow circle labeled “P”. In the presence of ABA (TOP), the PYL receptor binds ABA and can bind to a PP2C, inhibiting it, allowing the SnRK2 to autophosphorylate and phosphorylate downstream effectors, turning the ABA-response on. In the absence of ABA (bottom), the PYL proteins do not bind to the PP2Cs, and the PP2Cs are free to inhibit the kinase activity of the SnRK2s, turning off downstream responses.

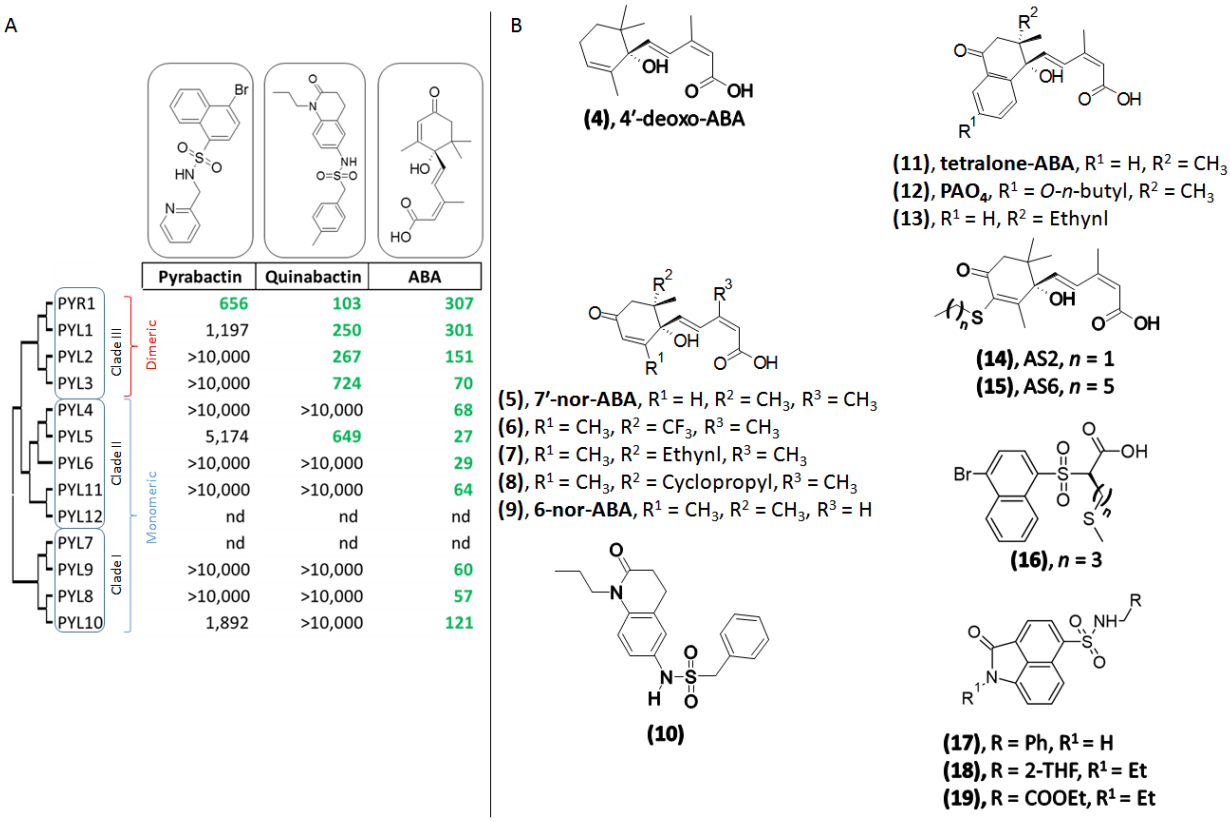

Figure 1.2. Panel A) A phylogenetic tree of the PYL receptors, separated by clade and oligomeric preference. The IC_{50} values in nM are depicted for the three agonists pyrabactin, quinabactin, and ABA with their structures above. Green is highlighted for IC_{50} values under 1,000 nM. nd = not determined. Panel B) Chemical structures of representative agonists and analogs produced with affinity for the ABA receptor family. Given names are in bold.

Chapter One: Identification of a Monomeric-Specific Abscisic Acid Receptor Agonist with a Novel Scaffold Revealing Differential Regulation Between Monomeric and Dimeric Receptor Function

Abstract

The rational control of transpiration using synthetic chemicals may provide new tools with which to limit the effects of drought in rainfed environments and to discover new probes for dissecting plant water relations. As one approach to developing new anti-transpirants, I have focused on discovering compounds that mimic action of the plant hormone abscisic acid (ABA), which regulates guard cell aperture and transpiration. Suitable targets are the ABA-receptor family collectively known as the Pyrabactin Resistance 1/PYR1-Like/Regulatory Component of ABA Receptors (PYR/PYL/RCARs). This family is large in most land plants, often containing over 10 members and displays significant genetic redundancy and functional overlap. As such, the functions of each receptor are not fully understood and may differentially contribute to different ABA responses. Thus, new probes may be beneficial in both agricultural and research contexts. Here, I describe new ABA-receptor agonists discovered using virtual screening and validated using *in-vitro* receptor-mediated phosphatase inhibition assays and *in vivo* bioassays. Structure-aided improvement was pursued on promising lead compounds, which resulted in enhanced potency for one analog (141B) that was selective for monomeric ABA receptors. Characterization of 141B's activity shows that monomeric receptors may play a relatively minor role in mediating ABA's transcriptional effects, but

consistent with other studies, they contribute to seed and root ABA responses. Thus, my virtual screening defined a new non-sulfonamide agonist scaffold with excellent *in vivo* activity and led to a new probe with which to dissect the functions of monomeric receptors.

Introduction

Climatic changes are projected to become more dynamic in the future, with droughts becoming more frequent and more severe, possessing a great risk to producing reliable crop yields to a growing population (1, 2). In an effort to limit the effects of drought on agriculture, biochemical and genetic methods have been extensively studied to maximize crop water use efficiency and tolerance or resistance to drought. A critical discovery to leverage the study of these prospective applications in the field was the identification of the abscisic acid (ABA) receptors and signalling pathway (3, 4).

ABA is a phytohormone that mitigates abiotic stress responses and is a key upstream regulator of stomatal aperture. The downstream signaling of ABA is accomplished through a direct binding of the hormone to the Pyrabactin Resistance 1/PYR1-Like/Regulatory Component of ABA Receptor (PYR/PYL/RCAR) proteins (3, 4). The binding of ABA initiates a conformational change of the receptor that allows for an interaction with - and inhibition of - the Type II C Clade A Protein Phosphatases (PP2Cs) (5–7). If uninhibited, the PP2Cs can inactivate the SNF1-Related Protein Kinases Subfamily 2 (SnRK2s) by dephosphorylation (3, 8). However, inhibition of the PP2Cs allows for SnRK2 autophosphorylation and subsequent activation, leading to a signal cascade involving multiple transcription factors and ion channels (9–12). These changes can lead to the increase of compatible solutes (13, 14), regulation of root architecture (15–

17), and control of stomatal aperture (18, 19) as representative examples, which are all proposed to benefit the plant in periods of drought stress.

Multiple research groups have identified PYL agonists, but most are either direct analogs of ABA or are of a sulfonamide scaffold similar to that of quinabactin and pyrabactin (3, 20). The direct ABA analogs generally mimic the pan-agonist activity of ABA, while quinabactin and pyrabactin are largely dimeric specific. Agonists selective for the monomeric receptors have not yet been reported, and thus without extensive higher-order genetic knock lines, selective activation of these receptors is difficult. Given my interest in differentiating receptor function *in vivo*, it would be beneficial to identify a variety of agonists that display divergent selectivities on the PYL receptors, thus allowing their functions to be probed temporally with agrichemical application. While medicinal chemistry approaches and structure-activity relationships (SAR) on the ABA, pyrabactin, or quinabactin scaffolds could potentially result in desirable agonist traits, a higher throughput methodology that remains unbiased to previous agonist scaffolds would be more likely to produce agonists with novel structures and potentially novel selectivites.

To explore the possibility of novel scaffolds unbiased to previous agonists, virtual screening can be employed to filter through digital libraries of millions of diverse compounds and enrich for chemicals that are likely to bind a protein of interest (21). The benefits of virtual screening are the reduced time and cost compared to *in vitro* screening a similar number of compounds. However, due to the positive correlation of computational cost with relative docking accuracy, the exactness of docking scores to that of actual binding affinities suffer in any higher-throughput virtual screening, leading to false positives and false negatives (22).

In light of these limitations, it is common practice in virtual screening to conduct a preliminary screen to identify a suitable receptor structure to use as a docking target. To quantify the quality of a docking target, a protocol designed to measure the 'enrichment' of true positives within a set of similar "decoy" compounds can be employed, ultimately ranking receptor targets based on enrichment factors (23). This enrichment analysis allows for screening against multiple conformations of a single receptor, or, in the case of the PYL proteins, multiple highly-homologous members of a receptor family to identify the best conformation for the primary screening effort. Standard enrichment protocols rank protein targets by the amount of known actives that score within the top percentiles of docking hits (e.g., 0.1%, 0.5%, 1.0% etc…) (equation 1, methods). Generally, enrichment factors above 10 indicate a strong preference of the protocol for true positives (24). Structures or conformations with the highest amount of true positives within the top proportion of docking scores are then preferred as the suitable target.

After the identification of the most ideal structure to dock against, the chemical library with which to screen must be decided. Ideally, virtual screening is done on as large a chemical space as possible, allowing for the greatest coverage of ligands and chemistry. The largest chemical datasets generally are developed from chemical enumeration libraries which are built from combinations of C, N, and O that are deemed to be chemically synthetically feasible, however these criteria are often difficult to enact in practice. Enumeration libraries can contain hundreds of millions of compounds, but many of which may have never existed, and certainly some that may never exist (25). Screening a rule-based chemical enumeration library of this size can produce valuable leads and insight, however the computational costs can be prohibitive and high-scoring compounds may in fact turn out to be impossible to practically synthesize or purchase. To avoid these issues,

libraries that are curated for compounds not only synthetically feasible, but commercially available do exist. On such library, Zinc Is Not Commercial (ZINC, http://zinc.docking.org/), is a freely accessible chemical database that currently has over 15 million “drug-like” compounds that can be further filtered for commercial availability (26). The ‘drug-likeness’ of compounds is evaluated using Lipinski’s rule of five which states that drug-like compounds have the following characteristics: a molecular weight <500, log*P* < 5, hydrogen donators < 5, hydrogen acceptors < 10 (27, 28). This is only a general rule but was derived from analysis of the chemical space produced by clinically approved drugs.

To facilitate the identification of novel scaffolds that could preferentially activate the monomeric receptors, virtual screening is a high-throughput method that is unbiased to previous agonist chemical structures, and by utilizing the ZINC drug-like library, enriches for compounds that display inherent protein-binding properties. Since the structures are unbiased, the potential for novel scaffolds, and thus, resulting novel selectivities is increased. Here, I report success in using the ZINC drug-like library in virtual screening and lead-hit optimization to produce novel ligands for multiple ABA receptors. Some of these most potent compounds contain new scaffolds, dock with a comparable pose to ABA, and have sub-micromolar IC_{50} values for the receptors. One scaffold which is focused on within this paper, has a specificity for the monomeric-type receptors in *Arabidopsis thaliana* and mimic ABA in seed-germination inhibition and root-growth assays. Structure-activity relationships allowed for the optimization of these compounds, leading to a simple chemical modification that increased potency on the monomeric receptors which translated to an increased *in vivo* responses as well.

Methods

Chemicals

Unless stated otherwise, all reactions were carried out under an atmosphere of argon or nitrogen in dried glassware. Reaction temperatures refer to those of the oil bath and room temperature (rt) is 23 °C. Solvents were anhydrous and purchased from Aldrich Chemical Co. and used as received. For NMR, purified reaction products were dried under high vacuum. Starting materials and reagents were purchased from TCI, Sigma Aldrich, Combiblocks, Fisher Scientific, and AK Scientific and were used as received. Thin layer chromatography (TLC) was performed on silica plates (60 Å, 250 μm, selectscientific.com/au). TLC fluorescence was visualized with a 254 nm UV lamp. ^{1}H NMR spectra were recorded on an Inova 400 MHz spectrometer using DMSO-d_6. Chemical shifts are reported in ppm with the solvent resonance as internal standard (DMSO-d_6 2.5 ppm). Data are reported as: chemical shift, multiplicity (s= singlet, d = doublet, dd = doublet of doublet, t = triplet, q = quartet, br = broad, m = multiplet), number of protons, and coupling constants.

For chemical stocks of the purchased library, fresh DMSO was added to each well to reach a final concentration of 10 mM and were kept at -20° C until in use. Stock plates were aliquoted to 96-well round-bottom plates (https://www.grainger.com/) for a working concentration of 2.5 mM by dilution with fresh DMSO, and also kept at -20° C unless in use. When required for use, plates were allowed to equilibrate to room temperature overnight to reduce the chance of hygroscopic effects.

Enrichment Factors

For calculating enrichment factors, an in-house library of quinabactin and pyrabactin analogs as well as other published ABA-receptor agonists with known IC_{50} values totaling 173 “positive controls” were used. For the decoy set (29) the 50,000-compound library from ChemBridge Diversity Library Premium Set was utilized (http://www.chembridge.com downloaded 6-3-2014). The diversity library was prepared in Maestro using LigPrep, and allowed to produce multiple isomers from each parent compound, which multiplied the total decoy compounds attributed to the diversity set to 131,900. The sum of the diversity library and the 173 positive controls were docked against prepared X-ray crystal structures from PDB (30) (www.rcsb.org). PDB IDs: 3NMN (31), holo-3K3K and apo-3K3K (32), 3RT2 (33), 3W9R (34), 4N0G (35), 3NS2 (36), 4LA7 (20), 3OJI and 4DSC (37), and two induced-fit models from 3W9R.

The equation for enrichment factors was calculated using the equation (1):

$$E_F = \frac{\frac{Known{-}Active\ Hits}{Total\ Hits}}{\frac{Total\ Known{-}Actives}{Total\ Ligands}}$$

The $E_F$was calculated from the top 1% of hits for each receptor, and the receptor with the highest E_F from both the dimeric and monomeric class were chosen to dock against in further analyses.

Virtual Screening & Docking Figures

All crystal structures were prepared using Protein Preparation Wizard (38) (Schrödinger Release 2015-1: Schrödinger Suite 2015-1 Protein Preparation Wizard; Epik

version 3.1, Schrödinger, LLC, New York, NY, 2015; Impact version 6.6, Schrödinger, LLC, New York, NY, 2015; Prime version 3.9, Schrödinger, LLC, New York, NY, 2015.) using default settings and only the conserved gate-latch water was retained. We used ZINC version 12 (39) and downloaded the standard drug-like subset of 17,900,742 molecules dated 11-24-2014. These ligands were then prepared using default settings included in Epik (40) for Schrödinger's Ligand Preparation module, and filtered to remove reactive functional groups (default definition). The glide settings (41) (Small-Molecule Drug Discovery Suite 2015-1: Glide, version 6.6, Schrödinger, LLC, New York, NY, 2015.) were used as default except "Enhance planarity of conjugated pi groups" was checked.

From the first iteration of virtual screening, only the top 0.1% were retained based on docking score. The resulting compounds were filtered further by a re-docking assessment that required an H-bond to PYR1 K59. The compounds remaining had duplicate molecules removed, and were grouped by chemical supplier. One of the suppliers with the largest amount of compounds within this final set were then chosen for purchasing, after removing the largest and smallest compounds that, upon manual inspection, were unlikely to fit into the pocket, or too small to produce good contacts for ligand potency.

Docking poses were created using the UCSF Chimera package (42). Chimera is developed by the Resource for Biocomputing, Visualization, and Informatics at the University of California, San Francisco (supported by NIGMS P41-GM103311). Hydrophobic/hydrophilic (HHP) mesh maps were created using Schrödinger's Maestro with default settings, images of the HHP surface were taken using Maestro.

Agonist/receptor-mediated PP2C inhibition Assays

The PP2C screening assays were carried out using a fluorogenic phosphatase substrate (4-methylumbelliferyl phosphate). Tecan Infinite F200 Pro plate reader (http://lifesciences.tecan.com/). From the working concentration plates, 1 µL was added to the screening plates (96-well, clear, flat-bottom, grainger.com) in duplicate. Each screening plate additionally had, in duplicate, ABA, quinabactin, and three in-house agonists (unpublished data) that were selective for either PYL1, PYL2, or PYL8. Once the chemicals have been aliquoted to each well, there was added a 40.09 uL of assay buffer (23.71 µL of water, 16 µL of phosphatase buffer solution (500 mM Tris-Cl pH 7.9, 500 mM NaCl, 15 mg/mL of bovine-serum albumin, 0.1% v/v β-mercaptoethanol), 1 µL of $MnCl_2$, and a combination of the receptors (.025 µL of PYR1 (1 mg/mL), 0.29 µL of PYL1 (1 mg/mL), 0.25 µL of PYL2 (1 mg/mL), 2 µL of PYL4 (1 mg/mL), 0.5 µL of PYL5 (1 mg/mL), 1.04 µL of PYL6 (1 mg/mL), 2-2.25 µL of PYL8 (1 mg/mL, depending on activity), 3 µL of PYL9 (1 mg/mL), 3 µL of PYL11 (1 mg/mL), and/or 2.50 µL of PYLe (1 mg/mL)), 0.19 µL HAB1, and remaining volume of water for a total of 80 µL. This was allowed to sit at room temperature for 20 minutes to allow any slow-binding ligands to successfully bind. After this incubation period, 20 µL of phosphatase buffer containing 4 mM 4-methylumbelliferyl phosphate was added quickly, and the plate was shaken by hand gently for approximately five seconds and read by the Tecan fluorimeter (Tecan Infinite F200 Pro, http://lifesciences.tecan.com/).

The Tecan settings for the fluorescent assay were: Shaking for 10 seconds, linear mode, 6 mm amplitude. There were 8 kinetic cycles for each well, defined by an excitation of 360 nm, emission of 465 nm, and included 3 flashes. Settle time: 0 ms, read from bottom, and gain was calculated from a negative control (DMSO) well at 30% RFU with gain regulation. There was a total of 20 µs integration time with no lag-time. The data was

exported to excel including raw data measurements and “Percent Activity” which was calculated by each well, divided by the average from all the blank reads, multiplied by 100%; units were read in mean slope RFU/min.

Agonist IC_{50} Measurements

IC_{50} values were quantified using a similar assay to screening above. Purified proteins were pre-incubated in 160 µl assay buffer containing 2 µL ligand for 20 minutes at room temperature. 40 µL of a reaction solution containing 250 mM 4-Nitrophenyl phosphate in assay buffer was quickly injected to each well. After gentle shaking, absorbance measurements were collected using 405 nm wavelength on Tecan Infinite F200 pro as above. Reactions contained 50 nM PP2C and 100-1000 nM PYR/PYL proteins dependent on activity. Ligand concentration of 10000, 1000, 333, 111, 37, 12.33, and 4.11 nM were used to measure PP2C activity. The dose response data was fitted to a log (inhibitor) vs response-(variable slope) model using non-linear regression to infer the IC_{50} values, using GraphPad Prism 6.0

PYL Protein Expression

Recombinant receptor fusion proteins for assays were produced with previously described expression constructs (20, 43). Nine of the 14 Arabidopsis ABA receptors were expressed with 6x-His tags in pET28 (PYR1, PYL1 - PYL6, PYL8 and PYL10). PYL9 and PYL11 were expressed as MBP fusion proteins in the vector pMAL-c. HAB1 was expressed as 6x-His tag in a truncated form (HAB-Δ179) in pETM-11. Expression of proteins was done using BL21(DE3)pLysS host cells. Transformed cells were pre-cultured overnight, transferred to terrific broth (TB) medium, and cultured with shaking at 30 °C to

an A600 of .055-0.60, and the temperature lowered to 18° C and 0.5 mM of isopropyl β-D-1 thiogalactopyranoside (IPTG) was added. In the case of HAB1, 1.0 mM MnCl2 was also added as it was seen to improve stability. Cells were harvested and lysed using two freeze-thaw cycles between -78° C and RT, followed by sonication. pET28-derived proteins were purified on His60 Ni Superflow containing columns and MBP-PYL fusion proteins were purified using amylose resin (New England Biolabs).

Luciferase-based ABA-reporter Gene Induction Assays

The MAPKKK18 gene is highly induced by ABA and a convenient reporter of ABA effects *in vivo*. A pMAPKKK18::LUC+ reporter lines was produced by a postdoctoral scholar in the Cutler lab named Jorge Lozano-Juste as follows: using the MAPKKK18 (At1g05100) promoter (~2 Kb upstream from ATG start codon) and amplified using the forward primer (5'-CACCATAGTAGGTGTTGGTAAAC-3') and reverse primer (5'-TTGGAGAATGATACTAAAAAAG-3') as previously described (20). This PCR product was cloned using the pENTR/D-TOPO vector (Invitrogen). Valid plasmid sequences were recombined into the binary vector pFlash (courtesy of Maria Angeles Nohales and Steve Kay) using LR clonase II (Invitrogen) to produce the pMAPKKK18::LUC+ phusion. The plasmid was infiltrated into the GV3101 strain og *Agrobacterium tumefaciens* and this was introduced into our *Arabidopsis thaliana* (Col-0) plants using the floral dip method. Seeds were selected from plants able to germinate on media containing gentamycin. To analyze expression, single insertion homozygous T3 plants were used. MAPKKK18 promoter::LUC+ activity was measured with 7-d-old seedlings that had been grown on 0.5% agar containing ½ Murashige and Skoog (MS) medium and 0.5% Sucrose under 16 hour light and 8 hour dark condition. At seven days, seedlings were transferred to liquid

plant growth media having ½ MS, 0.5% sucrose, 100M luciferin, and test chemical or DMSO at described concentrations. Luciferase assay image were taken every 30 min during 16 hours in total dark by camera (SONY a7s) with FE1.8/55 lense (FE 55 mm F1.8 ZA; SEL55F18Z) at 12800 ISO. The average luminescent intensity was quantified using Image J with intensities reported as the average for duplicates.

Germination Assays

To 2.5 mL, 24-well plates, there was added 10 µL of chemical dissolved in DMSO, or DMSO control. 990 µL of an agar solution containing 0.5% sucrose, 0.5% agar (gelzan, SigmaAldrich), and ½ MS (2.15 g/L) media was added to each well. Seeds were sterilized by immersion in 1% bleach solution containing .005% tween for 12 minutes, followed by 7 minutes in 70% ethanol. The seeds were washed with DI water two times and suspended in a 0.15% solution of gelzan agar and approximately 5 µL aliquoted to each well. Plates were stratified at 4° C for 48 hours and moved to a dark growth chamber. They were grown for 48 hours to observe hypocotyl elongation and moved to the light to induce chloroplast genesis. Pictures were taken with a Leica MZ12 microscope (leica-camera.com), mounted with a SPOT RT3 camera (spotimaging.com), and illuminated with a Fiber-Lite MI-150 (dolan-jenner.com). In some cases the brightness was adjusted manually using imaging processing software to keep leaves/seeds easily visible.

Root Growth Assays

Sterilized seeds were stratified for 3 days and allowed to grow for 48 hours post-germination in long-day light chambers, then transferred to agar media containing the indicated concentration of chemical or vehicle control. Seedlings were allowed to grow for

approximately 36 hours, and imaged using a scanner. The original root length at transfer and the total root length after 36 hours were measured for each seedling and the ratio of new growth divided by original length was recorded and normalized to that of the control.

General procedure for amidification

To a solution of the carboxylic acid (1 equiv) in anhydrous DCM was added a catalytic amount of DMF and oxalyl chloride (4-6 equiv) was added dropwise to prevent excessive effervescents and the solution was stirred for 1.5 hours at room temperature, which usually resulted in solutions gaining an orange coloration. The solvent was removed in vacuo and the crude acid chloride kept under argon and at -20° C until used for the next step without further purification. The crude acid chloride was then dissolved in anhydrous DCM and excess triethylamine added followed by the alkyl amino acid methyl ester (1.5 eq). Reaction proceeds nearly instantaneously and develops a dark coloration. After 15 minutes, the solution is concentrated under reduced pressure, diluted with DI water which is then acidified to pH ~3 with 2M HCl and extracted 4x with ethyl acetate. The organic layers are washed once with DI water followed by brine and dried over sodium sulfate. The methyl ester is purified by silica gel flash chromatography from hexanes/ethyl acetate 0-60% gradient to yield white crystalline powders with 40-60% yields.

1-[3-(4-cyanophenyl)propanamido]cyclohexane-1-carboxamide (5-43a)

In a similar manner as above, the acid chloride of **3-43a** is prepared. The crude, dried acid chloride is cooled to 0° C and an excess of 15% NH_4OH cooled to 0° C is added. This is allowed to warm to RT over 90 minutes. The resulting solution is acidified to a pH of 4 using dilute HCl and extracted 4x with EtOAc. The organic layers are combined and

washed with 2x DI water followed by brine and then dried over sodium sulfate. The organic layers are concentrated under vacuum and the product purified by silica gel flash chromatography as above to give white crystalline powder in 50% yields.

General procedure for hydrolysis of methyl esters

To a solution of 1:1 methanol/water, the methyl ester (1 equiv) is added followed by lithium hydroxide (3 equiv). The resulting opaque solution is stirred overnight at room temperature or until it becomes clear. The solution is then slowly acidified with 2M HCl to pH of ~2 and cooled at -20° C. The resulting crystals are filtered off and give the final free acid generally in good purity with 40-70% yields.

NMR and Mass Spectrometry Characterization

(145A) $C_{16}H_{18}N_2O_3$ ^{1}H NMR (400 MHz, DMSO-d_6) δ ppm 1.18 (m, 2 H) 1.42 (m, 4 H) 1.59 (m, 2 H) 1.92 (m, 2 H) 3.49 (s, 2 H) 7.30 (d, J=2 Hz, 2 H), 7.75 (d, J=2 Hz, 2 H). $[M+H]^+$ calc. 287.1390 found 287.1396. $[M+Na]^+$ calc. 309.1210, found 309.1249 (figure 2.16)

(141B) $C_{16}H_{18}N_2O_4$ ^{1}H NMR (400 MHz, DMSO-d_6) δ ppm 1.14-1.96 (m, 10 H), 4.64 (s, 2 H), 7.05 (d, 2 H), 7.725 (d, 2H), 8.02 (s, 1 H), 12.21 (s, 1H). $[M+H]^+$ calc. 287.1390 found 287.1396. $[M+Na]^+$ calc. 309.1210, found 309.1249. $[M+H]^+$ calc. 303.1339, found 303.1354. $[M+Na]^+$ calc. 325.1159, found 325.1164. $[M\text{-}CO\text{-}_2\text{-}H\text{--}_2+H]^+$ calc. 257.1285, found 257.1289. (figure 2.15)

(3-43A) $C_{17}H_{20}N_2O_3$ ^{1}H NMR (400 MHz, DMSO-d_6) δ ppm 1.15-1.85 (m, 10 H), 2.43 (t, 2H), 2.85 (t, 2H), 7.39 (d, 2H), 7.69 (d, 2H), 7.75 (s, 1H), 12.01 (s, 1H). [M+H]+ calc. 301.1547, found 301.1566. [M+Na]+ calc. 323.1366, found 323.1370. $[M\text{-}CO\text{-}_2\text{-}H\text{--}_2+H]^+$ calc. 255.1492, found 255.1496. (figure 2.14)

(5-43A) $C_{17}H_{21}N_3O_2$ ^{1}H NMR (400 MHz, DMSO-d_6) δ ppm 1.07-1.94 (m, 10 H), 2.50 (t, 2H), 2.86 (t, 2H), 6.67-6.82 (d, 2H), 7.39 (d, 2H), 7.56 (s, 1H), 7.71 (d, 2H) $[M+H]^+$ calc. 300.1707, found 300.1718. $[M+Na]^+$ calc. 322.1526, found 322.1531. $[M-NH_3+H]^+$ calc. 283.1441, found 283.1447.

$[M-HCONH_2+H]^+$ calc. 255.1492, found 255.1495. (Figure 2.13)

Results

Screening Enrichments

Prior to initiating my virtual screening campaign, I ran control docking experiments using known agonists and decoy ligands against available receptor crystal structures. To assess the optimal structure from the available crystal structures representative of the PYL proteins for use as targets in the high-throughput virtual screening assay, 12 different target proteins were screened computationally against a decoy set of ligands spiked with known active compounds (see methods). Prior to docking against the 3D coordinates of protein crystal structures, it is common practice to address issues such as missing hydrogen atoms, unspecified protonation states, and orientations of water molecules that facilitate their correct hydrogen bonding (38). 10 of the structures used default settings in the protein preparation wizard of Schrödinger from the available pdb file obtained from the Protein Database (www.rcsb.org/). The additional two were modified from the PYL9 3W9R structure which were included due to an inability for the original 3W9R structure to dock favorably with some bona fide PYL9-agonists. These compounds were significantly bulkier than ABA, and were predicted to require a large conformational change of the binding

pocket in comparison to that observed in the ABA-bound 3W9R PYL9 crystal structure. To account for a possible conformation that would allow for these bulkier ligands to favorably dock to PYL9, I created 'induced-fit' docking poses that modify the receptor binding pocket by allowing some proximal residues to become flexible, thus allowing the accommodation of ligands that may require flexibility in the pocket when docked to the unmodified available crystal structures. The addition of these two modified induced-fit receptors was an attempt to incorporate hits that may mimic these bulkier, yet still active, scaffolds. The incorporation of PYL9 was also important, given it is the only holo-protein structure available of the monomeric receptor subtype.

A standard enrichment procedure was outlined to identify the optimal structure(s) to dock against. The protocol involved a 50,000-compound decoy set from the 'Diversity Library' available through ChemBridge. This library was further prepared using the LigPrep module of the Schrödinger software by enumerating all possible enantiomers given the parent structure, ultimately resulting in 131,900 decoys to which I added 173 known agonists of the PYL receptors (using data from prior in-house assays). These were docked using the high throughput virtual screening (HTVS) mode in Schrödinger's Glide module, which filters compounds through an increasingly more stringent and thorough 3-step scoring cutoff. Enrichments were calculated using equation 1 for the top 1% of hits on each individual receptor.

Of the 12 targets, the holo-3K3K PYR1 (chain B) structure resulted in the highest enrichment, with an E_f of 14.6, while the second highest score was with 3NMN PYL1 (Table 2.1). The 3K3K PYR1 structure was selected for the docking campaign to represent the dimeric class receptors. In order to capture the diversity of ABA-binding pocket

structures, we selected a monomeric receptor for virtual screening, selecting the PYL9 3W9R structure, which has the highest E_f (10.0) for the monomeric subtype of receptors.

High-throughput Virtual Screening

Utilizing the prepared structures of PYR1 and PYL9, the ZINC 'drug-like' chemical library was screened against, which contained approximately 16 million compounds. This number was reduced by removing chemicals with reactive functional groups, and, after scoring cutoffs, the docking eventually resulted 14,000 hits. However, many of the highest scoring hits had docking poses that were dramatically different than that observed with any of the known agonists observed in the crystal structures. For instance, ABA, pyrabactin, and in one case quinabactin, hydrogen bond with a conserved lysine within the PYL pockets (homologous to $PYR1^{K59}$) (32, 44, 45), but this interaction was absent in most of the top scoring hits. The conserved lysine is important for a water-mediated hydrogen-bond network deep that is evident within the pocket as observed with multiple ABA-bound crystal structures and mutations at this position dramatically decrease ABA affinity (46, 47). Their docking poses were also often occupying spaces in the pocket which are normally hydrated with water molecules, an outcome obviously resulting from removing these from the crystal structures prior to docking. Ultimately, these poses were deemed unlikely to be reflective of active conformations. To alleviate this, I re-docked the resulting 14,000 hits by requiring an H-bond to $PYR1^{K59}$ (Figure 2.1A).

The addition of this constraint was conducted to filter out compounds unable to either directly, or through water-mediated H-bonding, interact with this conserved lysine residue. It should be noted that quinabactin, a potent agonist on PYR1, in one instance is not observed to form a hydrogen bond with homologous residue of $PYR1^{K59}$ in PYL2 (K64)

(20), accordingly while this restraint may enrich for compounds similar with respects to the ABA and pyrabactin binding conformation that accommodate interactions with the conserved lysine, it could also filter out other ligands that don't necessarily require this interaction. Given that this constraint only incorporates PYR1, the resulting hits from this redocking procedure are biased to conformations that favorably interact with PYR1, or both PYR1 *and* PYL9. Thus, this step may have biased against monomeric-specific agonists in the final set of candidate ligands.

This constraint ended up removing ~4,000 compounds equating to a final set of ~10,000 hits. Visual analysis of the top scoring hits indicated many marked similarities in structures, however there was no further filtering done for this aspect. It was proposed that small differences in ligands could result in large changes in affinities, therefore filtering based on chemical similarity, may result in a loss of SAR from the library. After deciding on a specific supplier to purchase the set of compounds for testing, both the largest and smallest molecules were removed to produce a final set of 1,724 compounds to screen from Enamine (Figure 1A). Thus, the docking campaign provided a set of 1,724 potential ABA receptor agonists that I subsequently tested directly for agonist activity using multiple ABA receptors.

Development of a pooled receptor agonist assay

To test whether these virtual screening hits were active on the PYL receptors *in vitro*, a pooled receptor-mediated phosphatase inhibition assay was developed utilizing an enzyme inhibited by the bound conformation of the PYL-receptors. Homolog of ABI1 (HAB1) was used as the phosphatase target, as it is a direct interactor of the PYL receptors, and involved in the ABA core signaling pathway (3, 4). To increase throughput

of the *in vitro* screening, we combined multiple PYL proteins together into a single assay well; if any single receptor is activated by a screening compound, the co-incubated PP2C will be inhibited.

To evaluate active compounds without screening the entire family of ABA receptors, representative PYLs were chosen. While the virtual screen targeted PYR1, PYL1 has a high similarity with respect to the binding pocket, and is expressed better than PYR1. Small changes in ligand substitutions have shown dramatic differences in PYL1:PYL2 selectivity, and given the relevance of PYL1 and PYL2 in a biological context, we decided to include both (20, 36). Lack of any agonists on the PYL4 receptors, or the *Zea maize* receptor *Zm*PYLe spurred the inclusion of these receptors into the assay as well. Finally, PYL8 is a physiologically important receptor, represents the monomeric subtype, has high similarity to the binding pocket to PYL9, but is more stably expressed (48–50). Thus the final pooled receptor assays contained the receptors *At*PYL1, *At*PYL2, *At*PYL4, *At*PYL8, and *Zm*PYLe.

A series of control experiments were conducted to validate and optimize the use of pooled receptors as a screening technique using compounds with relevant selectivities. With respect to the receptors used, the pan agonist ABA, the PYL1-specific pyrabactin, the PYL1/PYL2-specific quinabactin, the PYL2-specific quinabactin analog 49D3, and the PYL8-specific hexabactin were screened in duplicate. Each compound alone was able to inhibit the phosphatase by at least 80% (figure 2.18A, B) and the duplicate wells showed good reproducibility (figure 2.18B), verifying that this assay can correctly screen for potential agonists that may only be active on a single receptor within the pool.

Identification of a new ABA agonist scaffold

The 1,724 chemicals were assayed against this receptor pool for their ability to inhibit the phosphatase activity of the co-incubated HAB1. To select compounds for further evaluation, a cut-off of 50% phosphatase inhibition at ≤ 25 µM agonist concentration was used. This led to the identification of 22 (1.28%) agonist hits fitting this criteria (Figure 2.1C). To deconvolute the selectivity of each compound's activity on the individual receptors, each of the five receptors used in the pooled assays was tested against the 22 hits at 25 µM. 11 of the initial 22 hits were able to inhibit HAB1 activity >50% on any of the individual receptors tested, representing approximately 0.75% of the total chemicals screened (Figure 2.3). It is likely that some compounds possessed weakly activity against multiple receptors, which yielded an additive effect of PP2C inhibition in the pooled receptor assays, but failed to produce an IC_{50} <25 µM on any single receptor. Thus, nine of the 22 initial hits not evaluated further due to weak activity. An additional one of the 11 strong hits was not characterized (**20A10**) due to a structure nearly identical to compounds previously characterized (data not shown).

The top 10 hits contain a general scaffold of two hydrophobic cyclic moieties connected by a polar linking group. This is hydrophobe-hydrophile-hydrophobe structure is similar to what is seen with both quinabactin and pyrabactin (Figure 2.4A-C). Further, four chemicals, **1G8**, **3B4**, **6E5**, and **3E8**, all contained an even more closely related chemical backbone to each other, which was composed of a cycloalkyl amino-acid linked to a hydrophobic aromatic group. These four compounds had similar activities and within the receptor pool from screening, had the greatest potency on PYL8, with little to no activity on the dimeric receptors. This selectivity was desirable given the lack of monomeric-specific agonists in the literature, and prompted the characterization of these compounds on all the *Arabidopsis* receptors that can be efficiently expressed in *E. coli*. Analysis on

ten of the 14 *At*PYLs indicated a strong monomeric preference of these four hits, with the receptors PYL5, 6, 8, 9, 10, and 11 all displaying nanomolar IC_{50} values for at least one of the compounds (Table 2.2).

Perhaps the most striking difference between the IC_{50} values of these four small acids of is seen in PYL5 and PYL6; while **3B4**, **3E8**, and **6E5** all display nanomolar activity, **1G8** displays only micromolar activity. This difference is likely due to the increased hydrophobic bulk of the dichloro-benzyl headgroup of **1G8** which presumably is proximal to the space where the cyclohexenone headgroup of ABA normally occupies upon binding. If both headgroups of ABA and **1G8** are overlaid, it becomes apparent that these two chloro-substituents of **1G8** could mimic ABA's C7'-9' methyl groups, supported by the fact that methyl/chloride substitutions are common in medicinal chemistry (51). **3B4** and **3E8** differ only by position of a fluoride substitution on the phenyl ring (figure 2.4B) and their activity is largely comparable with the exception of PYL11, where **3B4** has an activity greater than five times that of **3E8**. Lastly, **6E5** is slightly weaker on PYL5 and PYL6 compared to **3B4** and **3E8**, but does show superior activity on PYL10 and PYL8.

Assuming these small-acids adopt a conformation similar to that observed of the bound ABA, the receptors do not tolerate the increased hydrophobic bulk proximal to the gate-latch interface (with the exception of PYL10), as evident by the decreased activity of **1G8** compared to the other three. Overlapping the docked conformation of **3B4** in PYR1 with that of the crystal structure conformation of ABA in PYR1 showed a high similarity between the two docking poses (Figure 2.4D). Not surprisingly, the even when docked without this specific constraint, the conformation of **3B4** indicated that the carboxylic acid group was hydrogen-bonding with the conserved lysine ($PYR1^{K59}$) deep in the pocket. Additionally, as discussed with **1G8**, the hydrophobic aromatic group was observed to be

mimicking that of the ring of the cyclohexenone group of ABA, revealing a very similar binding orientation to that of the endogenous hormone.

Rational improvement of hit potency by increasing probable Trp-lock interactions

The similarity in conformational docking space of these small acids in comparison to ABA lead us to evaluate possible structure-based optimization changes that could improve activity. Both quinabactin and ABA have hydrophilic, hydrogen-bond acceptors which are seen to interact with a conserved “trp-lock” water molecule near the gate-latch interface (Figure 2.5A) (5–7). The capability of a hydrogen bond to this gate-latch water is beneficial to improving affinity, supported by the observation that the ABA analog that lacks ABA’s cyclohexenone-oxygen (4’-deoxo-ABA) has significantly less activity in comparison to that of ABA (52). Pyrabactin, which has no hydrogen-bonding capabilities to the gate-latch water, has significantly weaker activity when compared to quinabactin and ABA, which can partially be explained by this lack of interaction (3, 20, 44, and 53).

If the docked conformation is reflective of the actual pose, this indicates **3B4** (and the other small acids) lack a hydrogen bond acceptor proximal to this conserved trp-lock water. This lack of the hydrogen-bond acceptor of **3B4** is further illustrated when comparing hydrophilic regions of the other two ligands (Figure 2.5B). Clearly 3B4 lacks the hydrophilicty and hydrogen bond capabilities that may prove beneficial to docking, given the importance of this interaction with the conserved water molecule. This observation provided an obvious opportunity to improve potency on the receptors by the addition of a hydrogen-bond acceptor in the region proximal to the gate-latch water (figure 2.5C). We reasoned that the replacement of the para-fluoro group of **3B4** with a para-

cyano group to the phenyl ring could fulfill a hydrogen-bond capability with the “Trp-lock”. The single p-Fluoro to p-Cyano modification on **3B4** lead to the synthesis of **145A** (figure 2.5D). Additionally, given the increased potency on PYL8, 9, and 10, a modification of **6E5** involving a single carbon removal of the bicyclic ring lead to **141B**. Two other analogs were evaluated for the relevance of this oxygen linker (**3-43A**) and whether the substitution of the carboxylic acid with an amide (**5-43A**) could boost potency, resulting in a total of four analogs nitrile-containing analogs of the **3B4/6E5** scaffold (figure 2.5D).

145A has only a single modification of replacing the fluorine of **3B4** for the intended nitrile group, however this change surprisingly lowered affinity on all receptors except PYL4. The general loss of activity indicated that the addition of the nitrile to this scaffold did not allow for the intended interaction to occur without significant deleterious effects regarding other interactions. Given that the nitrile-group requires an ∠CNH in X-C≡N•••H-O-Y of approximately 180° to properly hydrogen-bond (54), we reasoned that the scaffold of **145A** may be too rigid to adopt this conformational requirement. The addition of a carbon, or oxygen linker observed in **6E5**, could add an increased flexibility of the molecule.

The two compounds **141B** and **3-43A** both showed encouraging enhancements in activity on the monomeric receptors, but were also observed to increase potency on PYL2. While **3-43A** was able to increase potency on monomeric receptors of PYL5, PYL6, and slightly PYL9, it lost substantial activity on PYL10 and PYL11. **141B**, on the other hand, was either the most potent analog or retained similar potency on most of the monomeric receptors tested, additionally, given it’s still relatively low activity on the dimeric receptors, its selectivity made it an excellent candidate to probe *in vivo* functions of the monomeric receptors. Lastly, the modification replacing the carboxylic acid of **3-43A** with an amide (**5-**

43A) was totally detrimental to activity of the parent carboxylic acid, but does indicate the preference of acids for this particular scaffold in the monomeric receptor pocket.

Activation of monomeric receptors is sufficient to inhibit seed germination

Given the monomeric specificity of these agonists, it would be interesting to observe whether this activation of this clade of receptors can mimic the inhibitory effects on germination and hypocotyl emergence seen with ABA or quinabactin. Further, testing these compounds on receptor knock-out mutants can reveal, with greater clarity, which receptors are responsible for any physiological responses observed. Seven of the strongest hits (**1G8**, **3B4**, **3E8**, **6E5**, **10H4**, **13D9**, **18D3**) and the four strongest analogs (**3-43A**, **5-43A**, **141B**, **145A**) were assayed for radicle and cotyledon emergence on WT (Col-0), the receptor mutants *pyr1/pyl1/pyl2* (*012*), *pyl4*, and *pyl8/pyl9* (*89*), and *abi1*. ABA is able to inhibit germination completely in WT at concentrations greater than 1 μM, however the ABA-insensitive mutant *abi1* is less sensitive to ABA and can be used to differentiate between ABA pathway-dependent activity, and ABA-independent inhibition that could be the result of off-target effects and general toxicity. These mutant backgrounds were included to verify that the inhibitory effects are indeed the result of ABA signaling, and probe the importance of these receptors in each of the agonist responses.

In a preliminary screen, three of the 10 original strong hits, **13F9**, **17G3**, and **19B2** were unable to inhibit germination or cotyledon emergence at 25 μM in WT, which was in agreement with their relatively weak potency in comparison to the other hits, and they were not characterized further.

Of all the synthetic compounds tested, only **141B** was able to inhibit germination (defined by radicle emergence) at 20 μM, but not all seeds were inhibited. While this likely

indicates the relatively weakened contribution towards germination inhibition of the monomeric receptors in comparison to the dimeric, there was still strong inhibition of cotyledon greening by most compounds (figure 2.6, table 2.2). **3B4**, **3E8**, **6E5**, **10H4**, **3-43A**, and **141B** all showed greater than 50% cotyledon greening inhibition as low as 5 μM on WT. In agreement with the greatest potency in IC_{50} values observed in the phosphatase assay, **141B** showed the strongest inhibition on WT with greater than 80% of cotyledons still inhibited at 1 μM.

10H4 and **18D3** both showed some activation with the dimeric receptors (albeit 18D3 did not show sub-micromolar IC_{50} values) and given the slight activity on PYL1 and PYL2 from some of the small acids, these compounds were tested on the *012* mutant. Both **10H4** and **18D3**, which were able to inhibit cotyledons on WT at 20 μM, could not on the *012* mutants, supporting these compound's mechanism of action proceeds through the dimeric receptors (Figure 2.7, table 2.2).

The retained inhibition observed with the small acids on *012* potentially indicates that this response is signaled through the monomeric receptors. Thus, screening against the *89* mutant was essential to understand the importance of these receptors in inhibition of germination and cotyledon emergence. Results indicated that the *89* mutant was resistant to nearly all of the monomeric specific hits (Figure 2.8, table 2.2), elucidating a role of these two receptors in mediating germination and cotyledon greening inhibition. Alternatively, **10H4** was the only compound able to provide some germination inhibition in this background, but this was restricted to the higher concentration of 20 μM. There was some observed effects in the seeds treated with **3-43A** which may be a result from its agonist activity on PYL2.

To differentiate the contributions that PYL8 or PYL9 had towards the inhibitory effects observed with the most potent agonist, **141B**, this compound was further evaluated on the single mutants in *pyl8* and *pyl9* in comparison to the double mutant *pyl8/pyl9*. A very clear difference was observed, revealing that PYL8 was playing an important role, and showed monomeric-specificity with this inhibitory response.

To evaluate whether PYL4 had any involvement in these seed responses, the compound **145A** was a valuable tool as it gave some moderate activity on this receptor. Revealing little involvement of this receptor, **141B** showed no inhibitory effects on WT at 20 μM. However, at a slightly higher concentration (25 μM), and early on in this assay (36 hours post-stratification), **145A**-treated seeds developed green cotyledons that did not emerge from the seed coat, while at the same concentration on WT, this effect was largely absent (Figure 2.11). This might indicate that activating PYL4 produces a weak inhibition of cotyledon greening, but that this effect is somewhat removed from seed germination.

The *abi1* mutant is highly insensitive to ABA treatments, able to germinate on higher concentrations of ABA than that of WT (55, 56). This mutant was observed to be insensitive to all compounds tested up to 20 μM, further validating that these compounds are all operating through the core ABA signaling pathway with regards to inhibition of cotyledon greening.

Activation of monomeric receptors is not sufficient to activate transcription of the

MAPKKK18 promoter

It has previously been shown that pan-activation of dimeric ABA receptors using multiple agonists induces an ABA-like transcriptional response. My new probes provide a means to test the role of monomeric receptors in ABA-mediated transcriptional responses. As a first step towards this goal, I tested their activity on transgenic ABA-reporter line in which an ABA-regulated promoter (pMAPKKK18) drives expression of an enhanced firefly luciferase, constructed by another lab member. MAPKKK18 was chosen because unlike other ABA-induced transcripts, MAPKKK18 has a very low basal transcript level. Interestingly, at 20 μM treatment, none of the analogs had discernable activation, with higher concentrations were required, with 100 μM inducing some luminescence. The greatest effect being observed with the dimeric-specific ligand **10H4** (figure 2.12A-B), but no ligands were able to replicate the luciferase activity observed with ABA or quinabactin.

10H4 gave the highest luciferase activity, followed by the weakly activating PYL2 agonist **3-43A**, suggesting that the monomeric receptors are less involved in the upstream signaling that that leads to the transcriptional response on pMAPKKK18. Even **141B**, which was observed to have the most potent effect in germination and cotyledon inhibition, had about half the luciferase intensity as that seen in **10H4**, or 1/4th that in ABA or quinabactin.

Activation of monomeric receptors inhibits root elongation

ABA displays a hormetic effect on primary root growth; enhancing, or maintaining growth at low concentrations (57–60), but inhibiting at higher concentrations (61). Some of these responses to the signaling pathway have been shown to be non-redundantly regulated by the monomeric receptor PYL8. For instance, genetic knock-outs of this receptor indicate its role in lateral and primary root growth (48, 49, 62). To evaluate

whether my strongest monomeric-specific compound in context of germination inhibition, **141B**, could also display this effect, 2-day old seedlings were transferred on agar media containing various concentrations of this agonist. After approximately 36 hours, the results of root growth indicated that there was growth promotion at 1, 0.5, and 0.25 μM, but an inhibitory effect above 5 μM on WT plants (figure 2.14A). To confirm this observation was derived from activating the ABA pathway, the same compound was tested on the *pyl8*, *pyl9*, and *pyl8/pyl9* mutants. While growth promotion was observed in the *pyl9* mutant (figure 2.14A), both the *pyl8* and *pyl89* mutant blocked this (figure 2.14B, C), indicating that, similar to the germination inhibition, PYL8 is the principal receptor for this response given the chemical's receptor selectivity. It is important to note that while the *pyl8* and *pyl8/pyl9* mutants blocked growth promotion effects, the inhibition of root growth at higher concentrations was still clearly observed and comparable to that of observed on the WT (figure 2.14C).

Discussion

Virtual screening has shown many successes in the past decade and has made major improvements in that time as well (63). While some studies have shown that ligand-based computational approaches often have superior or equivalent outcomes (often with less computational cost) (64, 65), others have shown clear superiority to structure-based efforts (66). Here we show supporting evidence that structure-based screening provides acceptable results, with a novel small amino-acid scaffold being discovered as an active ABA-receptor agonist. Only 1,724 compounds were purchased with six of these

compounds showing sub-micromolar IC_{50} values on any receptor and cotyledon emergence inhibition at 20 μM, representing a .35% hit rate.

While the virtual screening effort had some bias towards selecting ligands active on PYR1, due to a docking constraint used that involved this receptor, the most potent hits identified were largely monomeric specific. Given the lack of selective agonists for this subgroup of the PYL receptor family, these molecules proved excellent probes for evaluating their biological relevance *in vivo*. Further, with the availability of the crystal structures, and some SAR previously made available, optimizing these compounds by the addition of a hydrogen bond acceptor that could interact with the conserved trp-lock water increased the potency observed in multiple *in vivo* assays for the lead hit scaffolds.

The monomeric selective hits **1G8**, **3B4**, **3E8**, and **6E5**, as well as their respective analogs **141B**, **145A**, **3-43A**, and **5-43A** all inhibited cotyledon greening in emerging seedlings in a PYL8-dependent manner. This finding provides insight into the roles that this monomeric receptor partakes in, building on this receptor's non-redundant effects previously described (48–50). Surprisingly the lack of responses resultant of activating other monomeric receptors (PYL5, 6, 9, 10, and 11) in seedlings implies their absence in controlling relevant processes in early development such as germination inhibition, hypocotyl emergence, and primary root growth.

Surprisingly, the application of these monomeric-specific agonists to the pMAPKKK18::LUC reporter line, indicates a divergence between the activation of this downstream transcriptional response and the mechanisms controlling seed germination inhibition and primary root elongation induced that is induced by the ABA signaling pathway. Further, given that only the dimeric-specific screening hit **10H4** was able to

moderately activate this promoter expression, the involvement of this response seems to be dimeric specific, at least in young seedlings.

It is worth noting that, given the virtual screening protocol targeting PYR1, none of the small acids were able to activate this dimeric receptor with substantial potency. This could possibly indicate that the pocket of PYR1 is slightly larger, with potent binding requiring bulkier molecules to interact with crucial residues, as do the larger sulfonamides quinabactin and pyrabactin. Support for this is also highlighted by the PYR1 and PYL1 activity observed in the larger **10H4** compound (figure 2.3, table 2.2). Similarly, none of the small acids or their nitrile-analogs had sub-micromolar IC_{50} values on PYL1. The marginal activity on PYL2 by some of the acids and their respective analogs highlights a >10-fold specificity obtainable between this receptor and PYR1.

Finally, the ability for **145A** to display a sub-micromolar IC_{50} value on PYL4 was intriguing. No synthetic agonists for PYL4 have been described, and thus proved a difficult target to characterize *in vivo*. The reasoning for this is unclear, since the PYL4 binding pocket is not dramatically different from PYL2, containing only two differential positions. PYL4 however is unique in binding pocket sequence with the existence of L84 (analogous to PYR1 I62) which is the only homologous position of the *Arabidopsis* receptors to contain a leucine. Currently, no crystal structure of PYL4 exists, compounding the difficulty in interpreting the differential selectivity of this receptor.

Here, virtual screening efforts resulted in compounds with novel, monomeric-specific activity on the PYL receptors, offering tools to further differentiate PYL-receptor responses. Future work could utilize these probes in conjunction with other agonists, such as pyrabactin and quinabactin, to deconvolute receptor relevance in other important biological processes such as flowering and seed set. Additionally, as will be discussed in

the next chapter, these molecules can benefit our understanding of metabolomic control as regulated through the ABA signaling cascade.

References

1. Battisti DS, Naylor RL (2009) Historical warnings of future food insecurity with unprecedented seasonal heat. *Science* 323(5911):240–244.

2. Lobell DB, et al. (2008) Prioritizing climate change adaptation needs for food security in 2030. *Science* 319(5863):607–610.

3. Park S-Y, et al. (2009) Abscisic acid inhibits type 2C protein phosphatases via the PYR/PYL family of START proteins. *Science* 324(5930):1068–1071.

4. Ma Y, et al. (2009) Regulators of PP2C phosphatase activity function as abscisic acid sensors. *Science* 324(5930):1064–1068.

5. Melcher K, et al. (2009) A gate-latch-lock mechanism for hormone signalling by abscisic acid receptors. *Nature* 462(7273):602–608.

6. Yin P, et al. (2009) Structural insights into the mechanism of abscisic acid signaling by PYL proteins. *Nat Struct Mol Biol* 16(12):1230–1236.

7. Miyazono K-I, et al. (2009) Structural basis of abscisic acid signalling. *Nature* 462(7273):609–614.

8. Fujii H, et al. (2009) In vitro reconstitution of an abscisic acid signalling pathway. *Nature* 462(7273):660–664.

9. Kobayashi Y, et al. (2005) Abscisic acid-activated SNRK2 protein kinases function in the gene-regulation pathway of ABA signal transduction by phosphorylating ABA response element-binding factors. *Plant J* 44(6):939–949.

10. Johnson RR, Wagner RL, Verhey SD, Walker-Simmons MK (2002) The abscisic acid-responsive kinase PKABA1 interacts with a seed-specific abscisic acid response element-binding factor, TaABF, and phosphorylates TaABF peptide sequences. *Plant Physiol* 130(2):837–846.

11. Geiger D, et al. (2009) Activity of guard cell anion channel SLAC1 is controlled by drought-stress signaling kinase-phosphatase pair. *Proc Natl Acad Sci U S A* 106(50):21425–21430.

12. Lee SC, Lan W, Buchanan BB, Luan S (2009) A protein kinase-phosphatase pair interacts with an ion channel to regulate ABA signaling in plant guard cells. *Proc Natl Acad Sci U S A* 106(50):21419–21424.

13. Smirnoff N, Cumbes QJ (1989) Hydroxyl radical scavenging activity of compatible solutes. *Phytochemistry* 28(4):1057–1060.

14. Wang W, Vinocur B, Altman A (2003) Plant responses to drought, salinity and

extreme temperatures: towards genetic engineering for stress tolerance. *Planta* 218(1):1–14.

15. Spollen WG, Sharp RE, Saab IN, Wu Y (1993) Regulation of cell expansion in roots and shoots at low water potentials. *Water deficits: plant responses from cell to community*:37–52.

16. Sharp RE, Davies WJ (1989) A restricted supply of water. *Plants under stress: biochemistry, physiology and ecology and their application to plant improvement* 39:71.

17. De Smet I, Signora L, Beeckman T, Inzé D (2003) An abscisic acid- sensitive checkpoint in lateral root development of Arabidopsis. *The Plant*. Available at: http://onlinelibrary.wiley.com/doi/10.1046/j.1365-313X.2003.01652.x/full.

18. Mustilli A-C, Merlot S, Vavasseur A, Fenzi F, Giraudat J (2002) Arabidopsis OST1 protein kinase mediates the regulation of stomatal aperture by abscisic acid and acts upstream of reactive oxygen species production. *Plant Cell* 14(12):3089–3099.

19. Belin C, et al. (2006) Identification of features regulating OST1 kinase activity and OST1 function in guard cells. *Plant Physiol* 141(4):1316–1327.

20. Okamoto M, et al. (2013) Activation of dimeric ABA receptors elicits guard cell closure, ABA-regulated gene expression, and drought tolerance. *Proc Natl Acad Sci U S A* 110(29):12132–12137.

21. Bajorath J (2001) Selected Concepts and Investigations in Compound Classification, Molecular Descriptor Analysis, and Virtual Screening. *J Chem Inf Comput Sci* 41(2):233–245.

22. Shoichet BK (2004) Virtual screening of chemical libraries. *Nature* 432(7019):862–865.

23. Mysinger MM, Carchia M, Irwin JJ, Shoichet BK (2012) Directory of useful decoys, enhanced (DUD-E): better ligands and decoys for better benchmarking. *J Med Chem* 55(14):6582–6594.

24. Bender A, Glen RC (2005) A discussion of measures of enrichment in virtual screening: comparing the information content of descriptors with increasing levels of sophistication. *J Chem Inf Model* 45(5):1369–1375.

25. Blum LC, Reymond J-L (2009) 970 million druglike small molecules for virtual screening in the chemical universe database GDB-13. *J Am Chem Soc* 131(25):8732–8733.

26. Irwin JJ, Shoichet BK (2005) ZINC − A Free Database of Commercially Available Compounds for Virtual Screening. *J Chem Inf Model* 45(1):177–182.

27. Leeson P (2012) Drug discovery: Chemical beauty contest. *Nature* 481(7382):455–456.

28. Lipinski CA, Lombardo F, Dominy BW, Feeney PJ (2001) Experimental and computational approaches to estimate solubility and permeability in drug discovery and development settings. *Adv Drug Deliv Rev* 46(1-3):3–26.

29. Niu Huang, Brian K. Shoichet *., Irwin* JJ (2006) Benchmarking Sets for Molecular Docking. *J Med Chem* 49(23):6789–6801.

30. Berman HM, et al. (2000) The Protein Data Bank. *Nucleic Acids Res* 28(1):235–242.

31. Melcher K, et al. (2010) Identification and mechanism of ABA receptor antagonism. *Nat Struct Mol Biol* 17(9):1102–1108.

32. Nishimura N, et al. (2009) Structural mechanism of abscisic acid binding and signaling by dimeric PYR1. *Science* 326(5958):1373–1379.

33. Hao Q, et al. (2011) The molecular basis of ABA-independent inhibition of PP2Cs by a subclass of PYL proteins. *Mol Cell* 42(5):662–672.

34. Nakagawa M, Kagiyama M, Shibata N, Hirano Y, Hakoshima T (2014) Mechanism of high-affinity abscisic acid binding to PYL9/RCAR1. *Genes Cells* 19(5):386–404.

35. Li W, et al. (2013) Molecular basis for the selective and ABA-independent inhibition of PP2CA by PYL13. *Cell Res* 23(12):1369–1379.

36. Yuan X, et al. (2010) Single amino acid alteration between valine and isoleucine determines the distinct pyrabactin selectivity by PYL1 and PYL2. *J Biol Chem* 285(37):28953–28958.

37. Zhang X, et al. (2012) Complex structures of the abscisic acid receptor PYL3/RCAR13 reveal a unique regulatory mechanism. *Structure* 20(5):780–790.

38. Sastry GM, Adzhigirey M, Day T, Annabhimoju R, Sherman W (2013) Protein and ligand preparation: parameters, protocols, and influence on virtual screening enrichments. *J Comput Aided Mol Des* 27(3):221–234.

39. Irwin JJ, Shoichet BK (2005) ZINC--a free database of commercially available compounds for virtual screening. *J Chem Inf Model* 45(1):177–182.

40. Greenwood JR, Calkins D, Sullivan AP, Shelley JC (2010) Towards the comprehensive, rapid, and accurate prediction of the favorable tautomeric states of drug-like molecules in aqueous solution. *J Comput Aided Mol Des* 24(6-7):591–604.

41. Friesner RA, et al. (2006) Extra precision glide: docking and scoring incorporating a model of hydrophobic enclosure for protein-ligand complexes. *J Med Chem* 49(21):6177–6196.

42. Pettersen EF, et al. (2004) UCSF Chimera--a visualization system for exploratory research and analysis. *J Comput Chem* 25(13):1605–1612.

43. Peterson FC, et al. (2010) Structural basis for selective activation of ABA receptors. *Nat Struct Mol Biol* 17(9):1109–1113.

44. Hao Q, et al. (2010) Functional mechanism of the abscisic acid agonist pyrabactin. *J Biol Chem* 285(37):28946–28952.

45. Cao M, et al. (2013) An ABA-mimicking ligand that reduces water loss and promotes drought resistance in plants. *Cell Res* 23(8):1043–1054.

46. Park S-Y, et al. (2015) Agrochemical control of plant water use using engineered abscisic acid receptors. *Nature* 520(7548):545–548.

47. Mosquna A, et al. (2011) Potent and selective activation of abscisic acid receptors in vivo by mutational stabilization of their agonist-bound conformation. *Proc Natl Acad Sci U S A* 108(51):20838–20843.

48. Zhao Y, et al. (2014) The ABA receptor PYL8 promotes lateral root growth by enhancing MYB77-dependent transcription of auxin-responsive genes. *Sci Signal* 7(328):ra53.

49. Antoni R, et al. (2012) PYL8 plays an important role for regulation of ABA signaling in root. *Plant Physiol*. doi:10.1104/pp.112.208678.

50. Lee H-N, Lee K-H, Kim CS (2015) Abscisic acid receptor PYRABACTIN RESISTANCE-LIKE 8, PYL8, is involved in glucose response and dark-induced leaf senescence in Arabidopsis. *Biochem Biophys Res Commun* 463(1-2):24–28.

51. Naumann K (1999) Influence of chlorine substituents on biological activity of chemicals. *J Prakt Chem* 341(5):417–435.

52. Takahashi S, Oritani T, Yamashita K (1986) Synthesis and Biological Activities of (±)-Deoxy-abscisic Acid Isomers. *Agric Biol Chem* 50(12):3205–3206.

53. Helander JDM, Vaidya AS, Cutler SR (2016) Chemical manipulation of plant water use. *Bioorg Med Chem* 24(3):493–500.

54. Le Questel J-Y, Berthelot M, Laurence C (2000) Hydrogen-bond acceptor properties of nitriles: a combined crystallographic and ab initio theoretical investigation. *J Phys Org Chem* 13(6):347–358.

55. Gosti F, et al. (1999) ABI1 protein phosphatase 2C is a negative regulator of abscisic acid signaling. *Plant Cell* 11(10):1897–1910.

56. Rodriguez PL, Benning G, Grill E (1998) ABI2, a second protein phosphatase 2C involved in abscisic acid signal transduction in Arabidopsis. *FEBS Lett* 421(3):185–190.

57. Spollen WG, LeNoble ME, Samuels TD, Bernstein N, Sharp RE (2000) Abscisic acid accumulation maintains maize primary root elongation at low water potentials by restricting ethylene production. *Plant Physiol* 122(3):967–976.

58. Sharp RE, Wu Y, Voetberg GS, Saab IN, LeNoble ME (1994) Confirmation that abscisic acid accumulation is required for maize primary root elongation at low water potentials. *J Exp Bot* 45(Special_Issue):1743–1751.

59. Fujii H, Zhu J-K (2009) Arabidopsis mutant deficient in 3 abscisic acid-activated protein kinases reveals critical roles in growth, reproduction, and stress. *Proc Natl Acad Sci U S A* 106(20):8380–8385.

60. Geng Y, et al. (2013) A spatio-temporal understanding of growth regulation during the salt stress response in Arabidopsis. *Plant Cell* 25(6):2132–2154.

61. Davies WJ, Zhang J (1991) Root Signals and the Regulation of Growth and Development of Plants in Drying Soil. *Annu Rev Plant Physiol Plant Mol Biol* 42(1):55–76.

62. Xing L, Zhao Y, Gao J, Xiang C, Zhu J-K (2016) The ABA receptor PYL9 together with PYL8 plays an important role in regulating lateral root growth. *Sci Rep* 6:27177.

63. Forli S (2015) Charting a Path to Success in Virtual Screening. *Molecules* 20(10):18732–18758.

64. Evers A, Hessler G, Matter H, Klabunde T (2005) Virtual screening of biogenic amine-binding G-protein coupled receptors: comparative evaluation of protein- and ligand-based virtual screening protocols. *J Med Chem* 48(17):5448–5465.

65. McGaughey GB, et al. (2007) Comparison of Topological, Shape, and Docking Methods in Virtual Screening. *J Chem Inf Model* 47(4):1504–1519.

66. Vidler LR, et al. (2013) Discovery of novel small-molecule inhibitors of BRD4 using structure-based virtual screening. *J Med Chem* 56(20):8073–8088.

Figures and Tables

Table 0.1

	halo-PYR1 3K3K	apo-PYR1 3K3K	PYL1 3NMN	PYL2 3NS2	PYL2 4LA7	PYL3 3OJI	PYL3 4DSC	PYL9 3W9R	PYL9 IDF1	PYL9 IDF2	PYL10 3RT2	PYL13 4N0G
Resolution (Å)	1.7	1.7	2.15	1.63	1.98	1.84	1.95	1.9	1.9	1.9	1.5	2.38
True Positives	29	0	24	12	10	11	17	20	16	15	14	1
E_f	14.6	0.0	12.1	6.0	5.0	5.5	8.6	10.0	8.1	7.5	7.0	0.5

Table 2.1 The 12 structures screened and their respective ångstom resolution (Å), the amount of true-positive hits in the top 0.1%, and the enrichment factors (Ef). Total decoys was approximately 131,900 and total known-active, positive controls was 173.

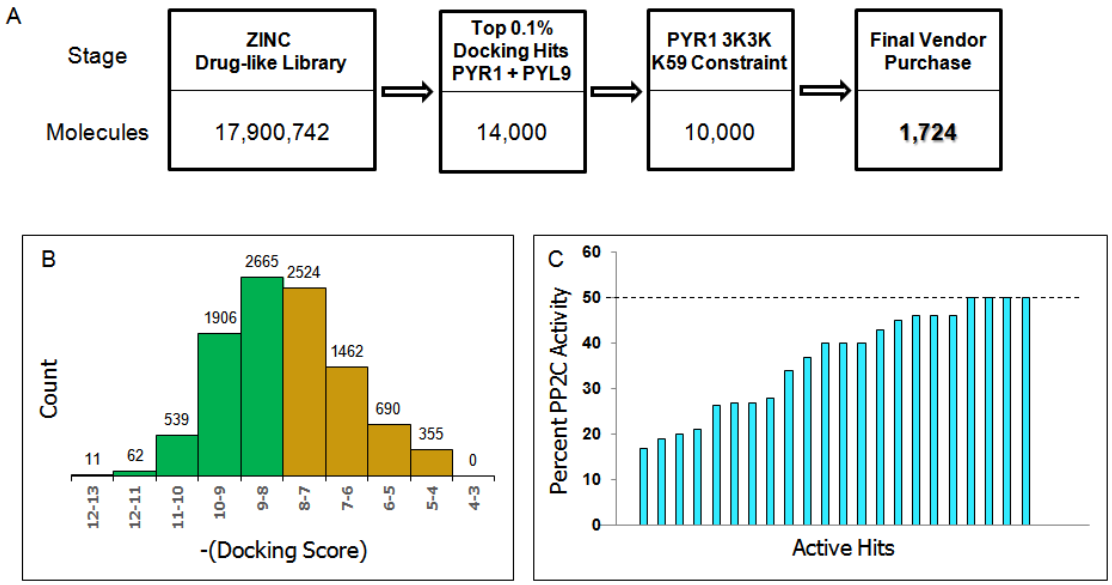

0.1

Figure 2.1 A) Virtual screening workflow, top indicates the stage and bottom indicates the resulting molecules. B) The docking scores of the 10,000 hits after the PYR1^{K59} constraint. All *in-vitro* active hits were scored in the green bins C) PP2C inhibition measured from fluorescence of HAB1 calculated from mean RFU/min compared to DMSO control

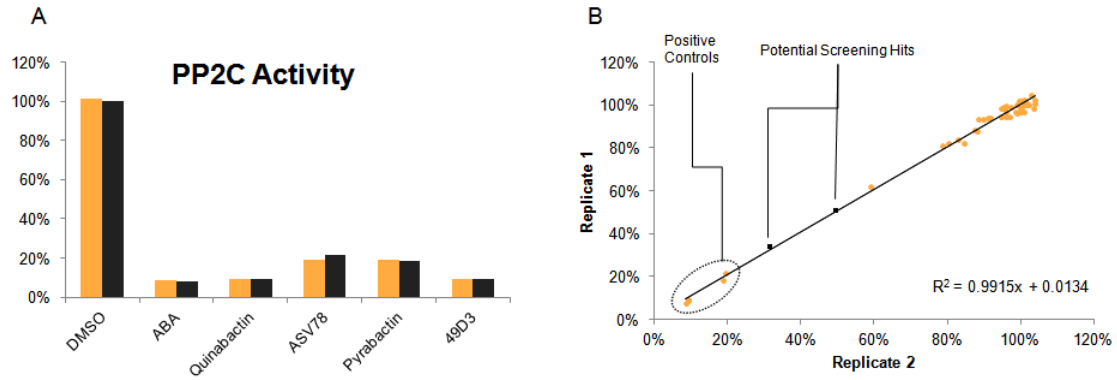

Figure 2.2 Validation of pooled receptor PP2C assay. A) The pan agonist ABA is compared alongside the PYL1/2-selectiv quinabactin, PYL1-selective pyrabactin, PYL2-selective quinabactin analog 49D3, and PYL8-selective hexabactin. All compounds were done in duplicate at 20 μM, and were able to inhibit PP2C activity to under 20%. B) Reproducibility of duplicate wells as measured by PP2C activity. Positive controls are indicated in the dotted ellipse and two potential agonist hits are indicated in black.

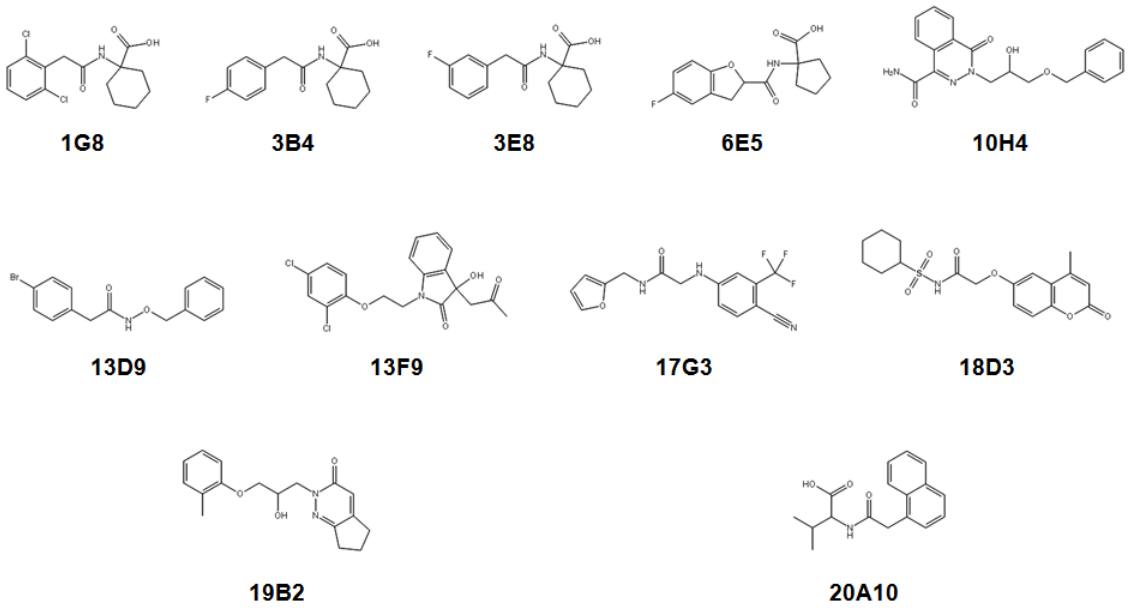

0.2

Figure 2.3 The 11 strongest hits from the library that showed an IC_{50} ≤ 25 μM in ABA receptor activation assays.

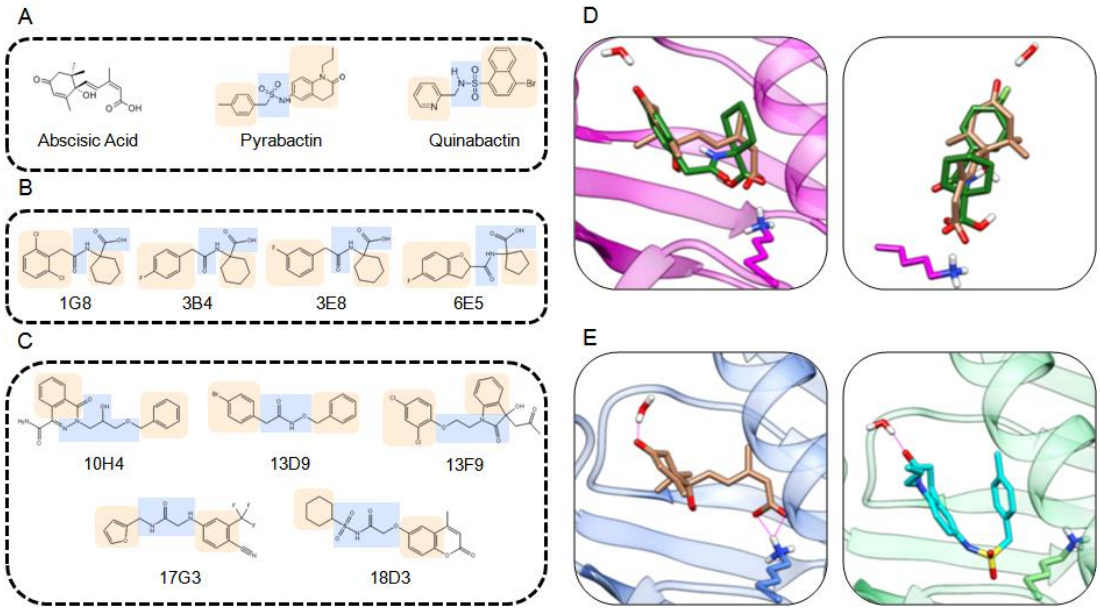

0.3

Figure 2.4 A) ABA and synthetic agonists pyrabactin and quinabactin. B) Lead hits from virtual screening C) Notable hits with relatively strong IC50 values, but were not fully characterized. D) Docking poses of ABA and 3B4 in PYR1 3K3K. K59 and gate-latch water are depicted. E) ABA from 3K3K and quinabactin from 4LA7 with hydrogen bonds highlighted in pink. Gate latch water and conserved Lysine depicted. In figures 1A-C, orange indicates hydrophobic region, and blue highlights hydrophilic linker region

IC_{50} Values (μM)

		ABA	10H4	1G8	3B4	3E8	6E5	3-43a	5-43a	141B	145A
Dimeric	PYR1	90	552	>10,000	>10,000	>10,000	>10,000	>10,000	>10,000	>10,000	>10,000
	PYL1	118	526	>10,000	2,200	4,500	>10,000	2,900	>10,000	>10,000	>10,000
	PYL2	21	>10,000	>10,000	1,600	3,200	>10,000	410	2,800	980	4,400
Monomeric	PYL3	ND	ND	ND	ND	ND	ND	ND	ND	ND	ND
	PYL4	24	>10,000	>10,000	>10,000	>10,000	>10,000	>10,000	>10,000	>10,000	420
	PYL5	10	5,000	1,500	73	115	222	17	104	31	412
	PYL6	9	>10,000	1,000	77	87	470	20	120	50	1,500
	PYL7	ND		ND	ND	ND	ND	ND	ND	ND	ND
	PYL8	18	>10,000	74	43	21	21	43	350	23	1,100
	PYL9	52	>10,000	810	400	145	200	326	>10,000	177	>10,000
	PYL10	140	>10,000	100	173	330	92	700	>10,000	36	4,800
	PYL11	33	ND	ND	341	1,750	4,870	5,270	>10,000	>10,000	>10,000
	PYL12	ND	ND	ND	ND	ND	ND	ND	ND	ND	ND

Table 0.2

Table 2.2 Table with IC_{50} values based on PP2C absorbance assay for HAB1 and the indicated PYL proteins. PYL3, 7, and 13 were not determined due to the proteins expressing poorly. Green and bold indicates an IC50 below 1000 μM. ND; not determined. The oligomer preference of each protein is indicated to the right of the table. PYL3 shows a monomer-dimer equilibrium.

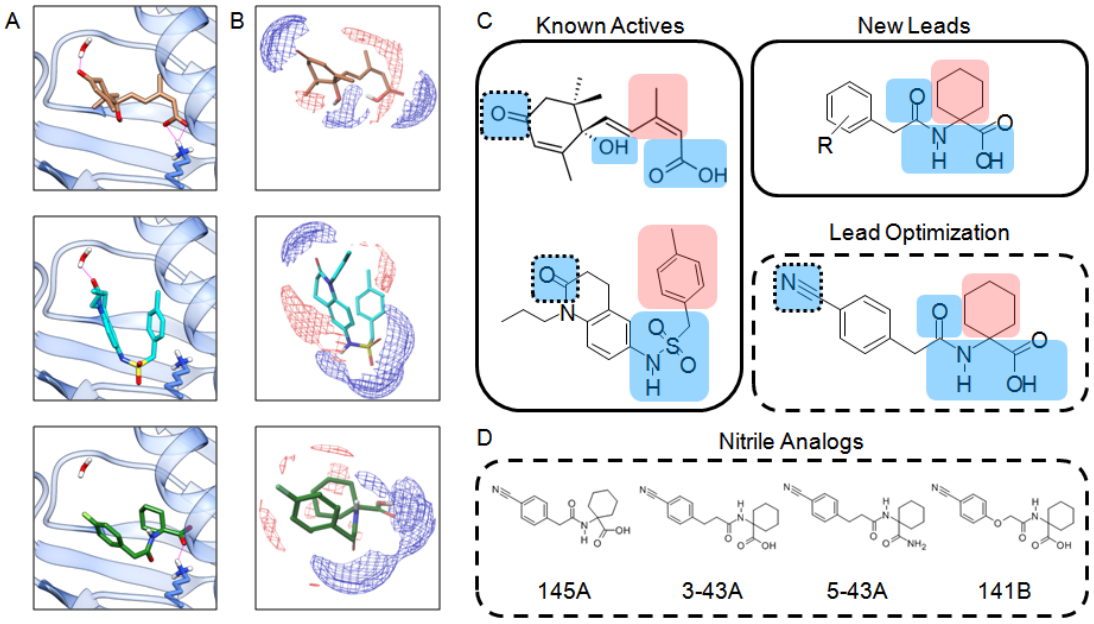

0.4

Figure 2.5 A) Chimera images, top; ABA, middle; quinabactin, and bottom; 3B4 redocked to PYR1 3K3K. Hydrogen bonds are indicated in pink. Gate-latch water and K59 are shown. B) Hydrophobic/hydrophilic surfaces shown as mesh as calculated by Maestro ABA redocked to 3K3K (top), quinabactin from 4LA7 (middle), and 3B4 redocked into 3K3K (bottom) C) Known actives, screening lead hits, and lead-optimization scaffolds with hydrophobic/hydrophilic regions highlighted; blue hydrophilic regions and red is hydrophobic. D) Synthesized nitrile analogs

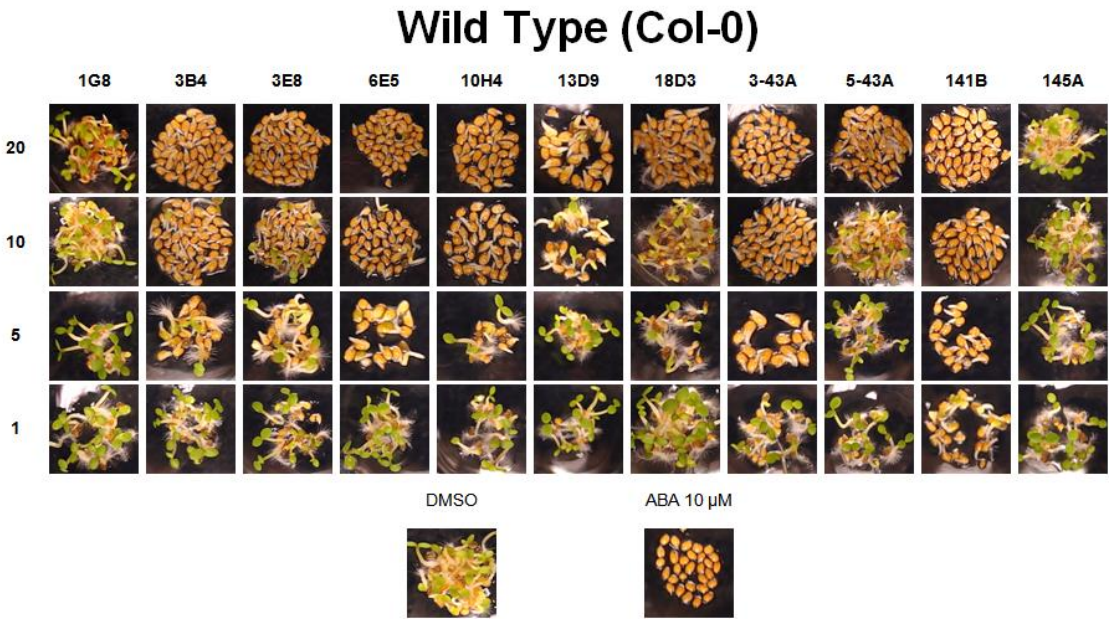

0.5

Figure 2.6 Germination inhibition of specified screening and nitrile-analogs on Col-0 plants at 1, 5, 10, and 20 µM. Positive (ABA) and vehicle controls are at the bottom.

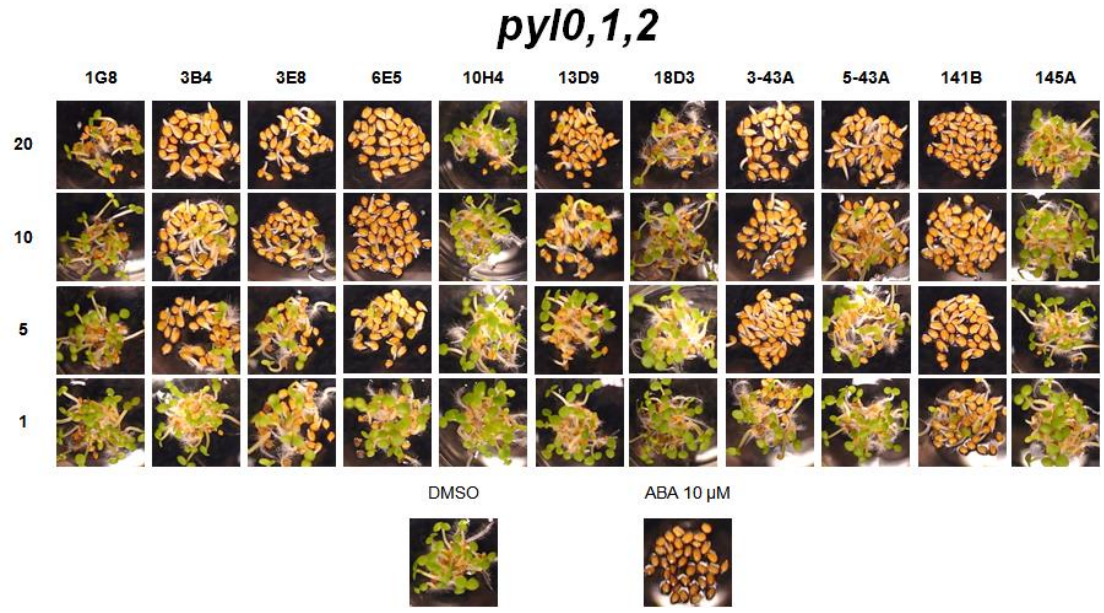

0.6

Figure 2.7 Germination inhibition of specified screening and nitrile-analogs on *pyr1/pyl1/pyl2* plants at 1, 5, 10, and 20 µM. Positive (ABA) and vehicle controls are at the bottom.

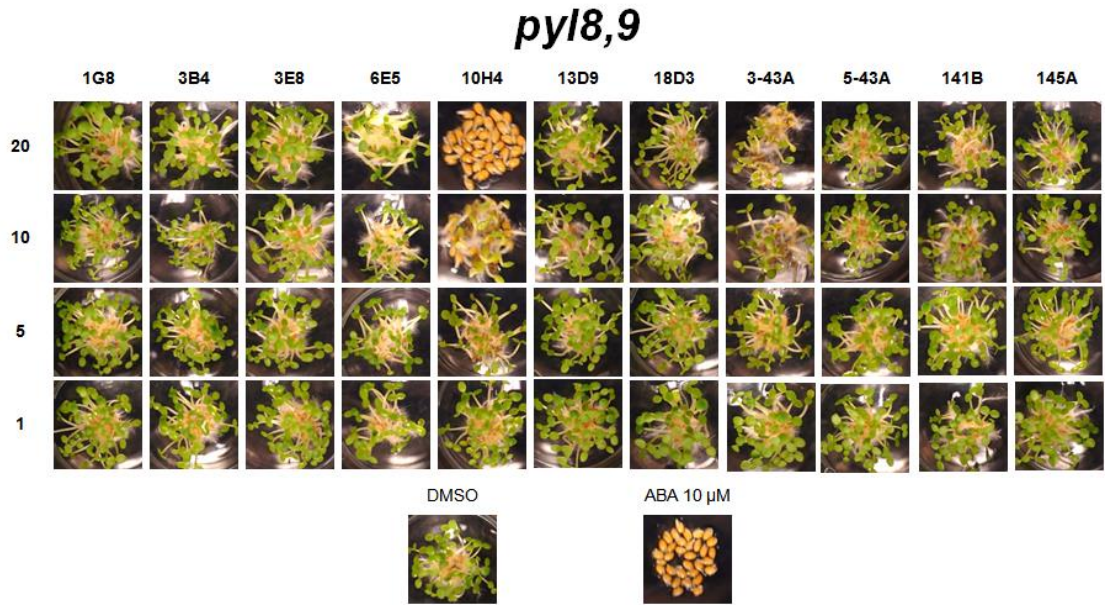

Figure 2.8 Germination inhibition of specified screening and nitrile-analogs on *pyl8/pyl9* plants at 1, 5, 10, and 20 µM. Positive (ABA) and vehicle controls are at the bottom.

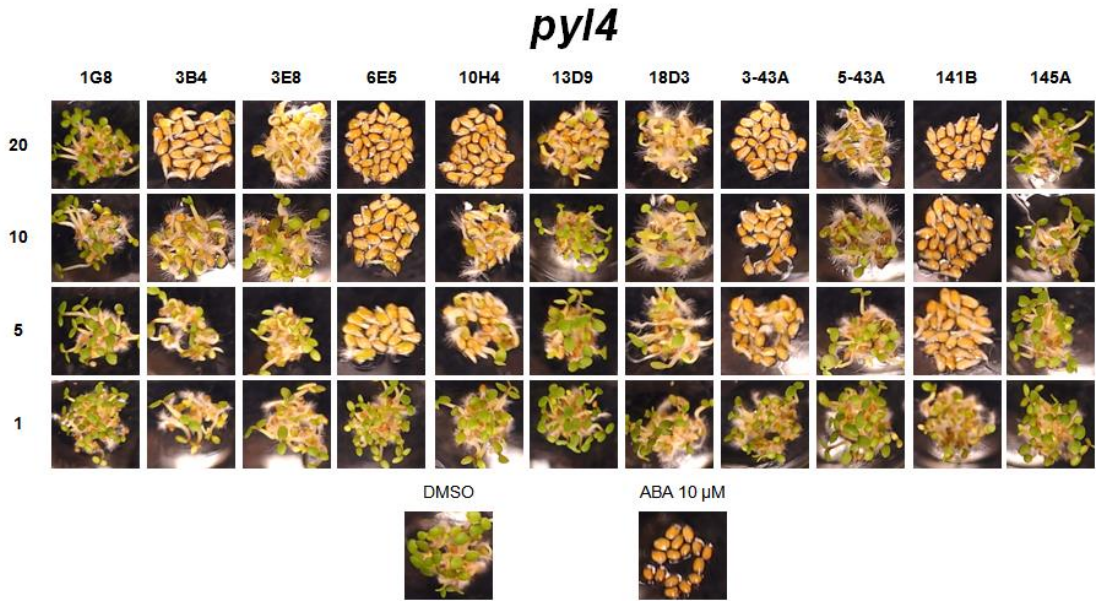

Figure 2.9 Germination inhibition of specified screening and nitrile-analogs on *pyl4* plants at 1, 5, 10, and 20 µM. Positive (ABA) and vehicle controls are at the bottom.

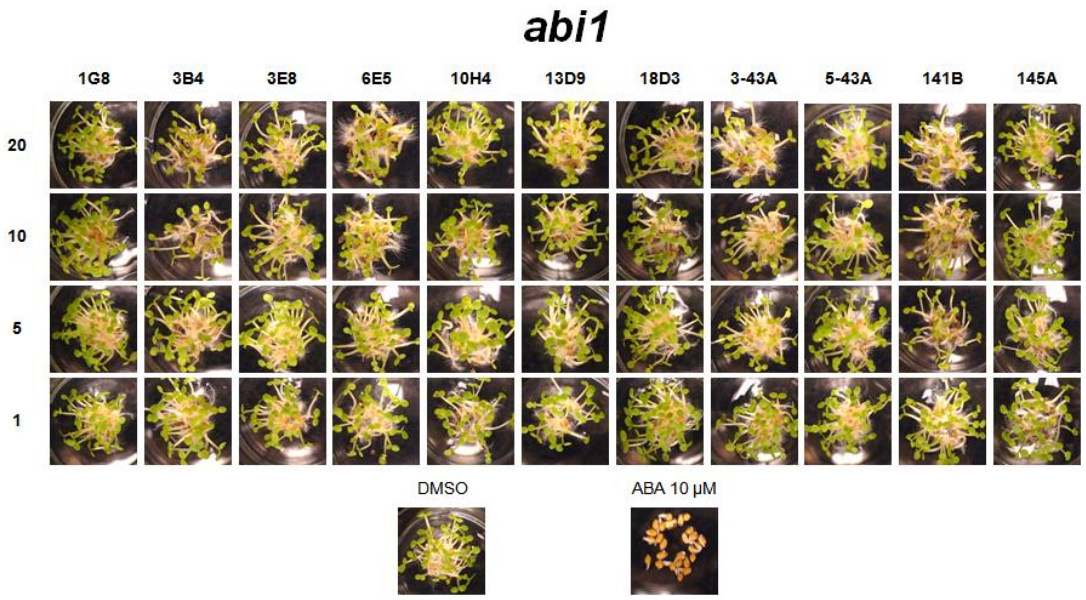

0.9

Figure 2.10 Germination inhibition of specified screening and nitrile-analogs on *abi1* plants at 1, 5, 10, and 20 µM. Positive (ABA) and vehicle controls are at the bottom.

	Wildtype										
	1G8	3B4	3E8	6E5	10H4	13D9	18D3	3-43A	5-43A	141B	145A
20 µM	0.30	0.00	0.00	0.00	0.00	0.04	0.00	0.00	0.02	0.00	1.00
10 µM	0.51	0.04	0.20	0.07	0.00	0.32	0.46	0.00	0.22	0.00	1.00
5 µM	1.00	0.17	0.29	0.00	0.31	0.69	0.75	0.00	1.00	0.00	1.00
1 µM	1.00	1.00	0.67	0.93	0.89	1.00	1.00	0.56	0.77	0.14	1.00

	0,1,2 triple mutant										
	1G8	3B4	3E8	6E5	10H4	13D9	18D3	3-43A	5-43A	141B	145A
20 µM	0.30	0.00	0.00	0.00	0.80	0.00	0.35	0.00	0.00	0.00	0.75
10 µM	0.81	0.11	0.12	0.00	0.80	0.21	0.43	0.00	0.23	0.00	0.81
5 µM	0.83	0.10	0.33	0.10	0.78	0.50	0.65	0.00	0.59	0.00	0.79
1 µM	0.95	0.80	0.47	0.67	0.80	0.85	0.90	0.48	0.76	0.08	0.82

	8,9 double mutant										
	1G8	3B4	3E8	6E5	10H4	13D9	18D3	3-43A	5-43A	141B	145A
20 µM	1.00	1.00	1.00	1.00	0.00	1.00	1.00	0.77	1.00	1.00	1.00
10 µM	1.00	1.00	1.00	1.00	0.59	1.00	1.00	1.00	1.00	1.00	1.00
5 µM	1.00	1.00	1.00	1.00	1.00	1.00	1.00	1.00	1.00	1.00	1.00
1 µM	1.00	1.00	1.00	1.00	1.00	1.00	1.00	1.00	1.00	1.00	1.00

	pyl4 mutant										
	1G8	3B4	3E8	6E5	10H4	13D9	18D3	3-43A	5-43A	141B	145A
20 µM	1.00	0.04	0.43	0.00	0.00	0.29	0.44	0.00	0.13	0.00	1.00
10 µM	1.00	0.13	0.65	0.00	0.14	0.94	0.43	0.00	0.50	0.00	1.00
5 µM	1.00	0.64	0.71	0.06	0.24	1.00	0.65	0.00	0.71	0.00	1.00
1 µM	1.00	0.73	0.93	1.00	1.00	1.00	1.00	1.00	1.00	0.71	1.00

	abi1 mutant										
	1G8	3B4	3E8	6E5	10H4	13D9	18D3	3-43A	5-43A	141B	145A
20 µM	1.00	1.00	1.00	1.00	1.00	1.00	1.00	1.00	1.00	1.00	1.00
10 µM	1.00	1.00	1.00	1.00	1.00	1.00	1.00	1.00	1.00	1.00	1.00
5 µM	1.00	1.00	1.00	1.00	1.00	1.00	1.00	1.00	1.00	1.00	1.00
1 µM	1.00	1.00	1.00	1.00	1.00	1.00	1.00	1.00	1.00	1.00	1.00

Table 0.3

Table 2.3 Ratio of emerged green cotyledons, color is based on ratio with higher ratio of emergence darker green.

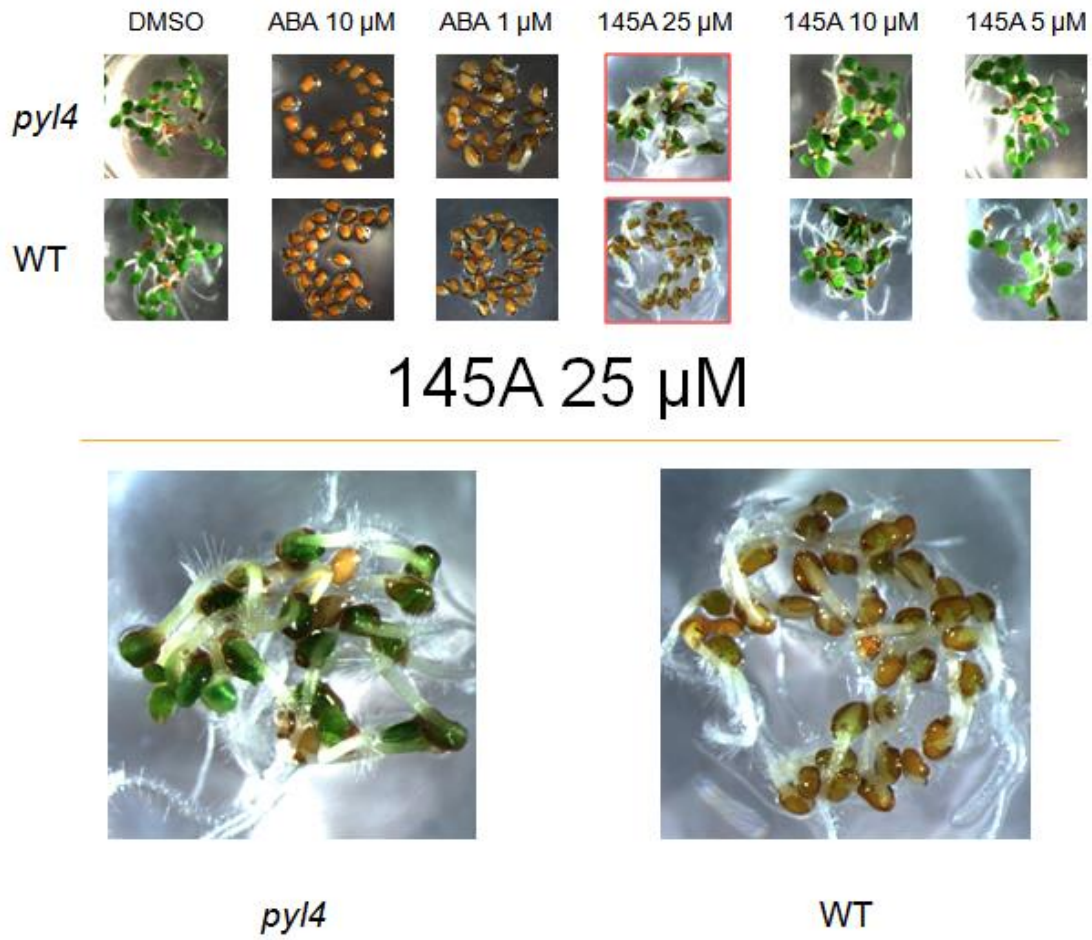

0.10

Figure 2.11 Seed germination and cotyledon greening inhibition with ABA and 145A on WT and *pyl4*. Lower is a close up of 145A at 25 µM on *pyl4* and WT.

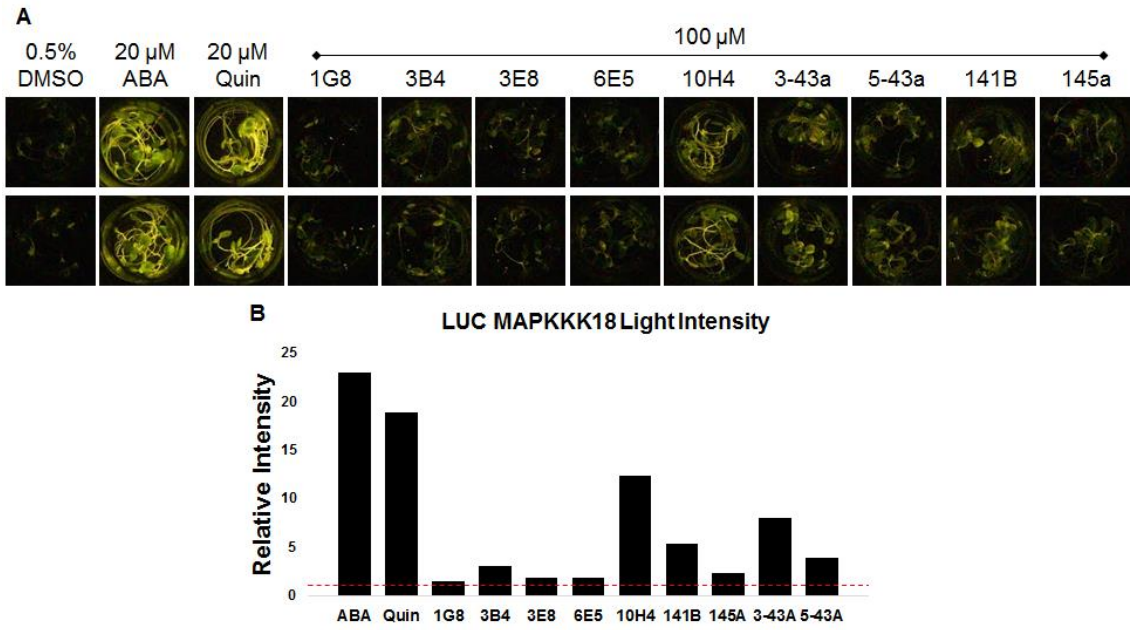

0.11

Figure 2.12 A) Relative luciferase expression from pMAPKKK18::LUC lines treated with indicated chemicals and concentrations. Upper and lower images are replicate wells. B) Average of light intensity from two replicates, relative to control. Red line indicates average of DMSO control.

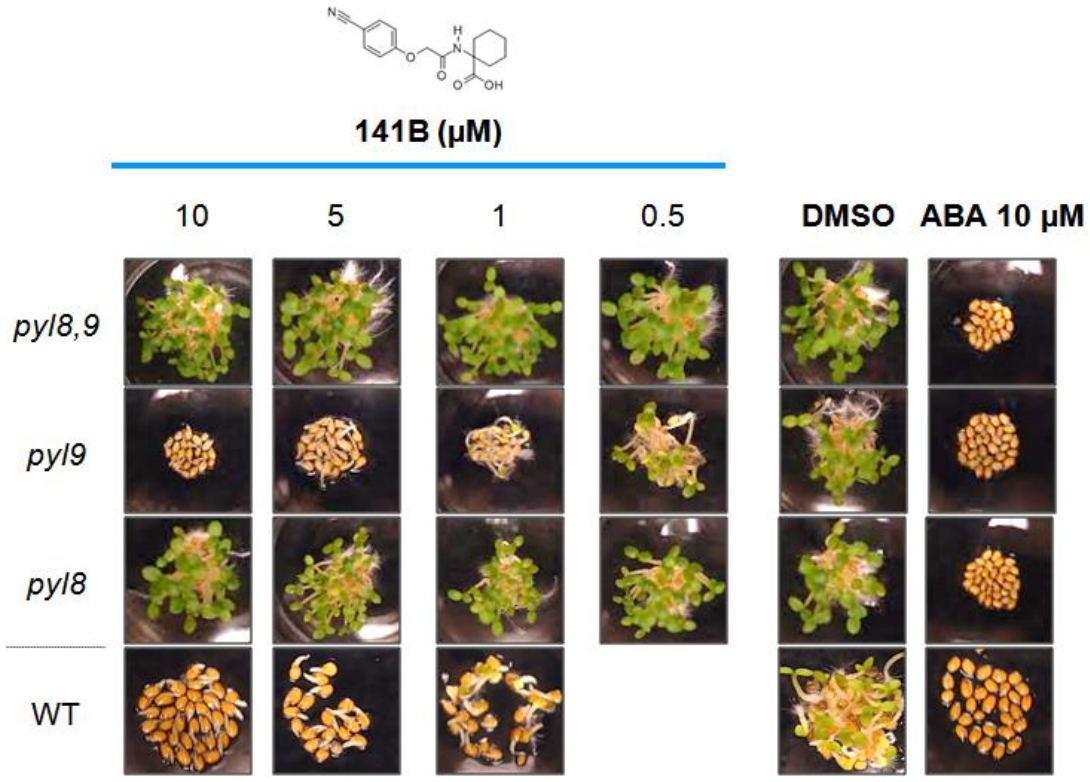

0.12

Figure 2.13 Germination inhibition of 141B on different genetic backgrounds in *Arabidopsis*. Note: WT was done on a different date, and extrapolated from figure 2.5.

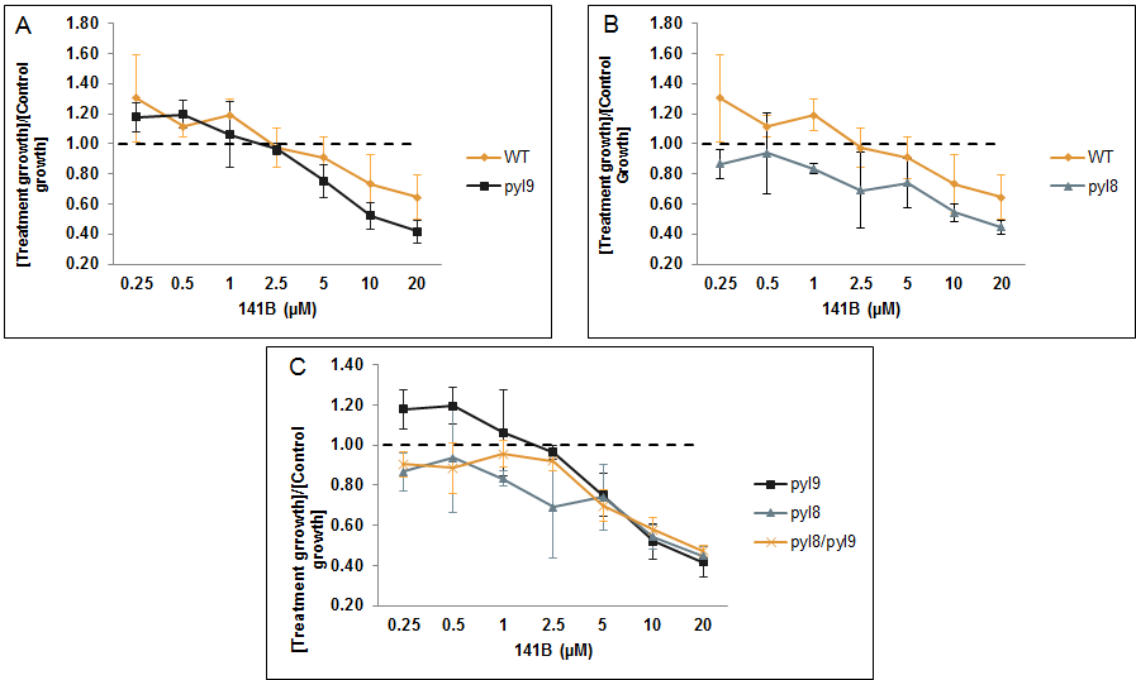

0.13

Figure 2.14 Root growth regulation in dose response to 141B on A) WT and *pyl9* mutant and B) WT and *pyl8* mutant and C) *pyl9*, *pyl8*, *pyl8/pyl9*. Error bars are standard deviation of 4 to 5 biological replicate seedlings.

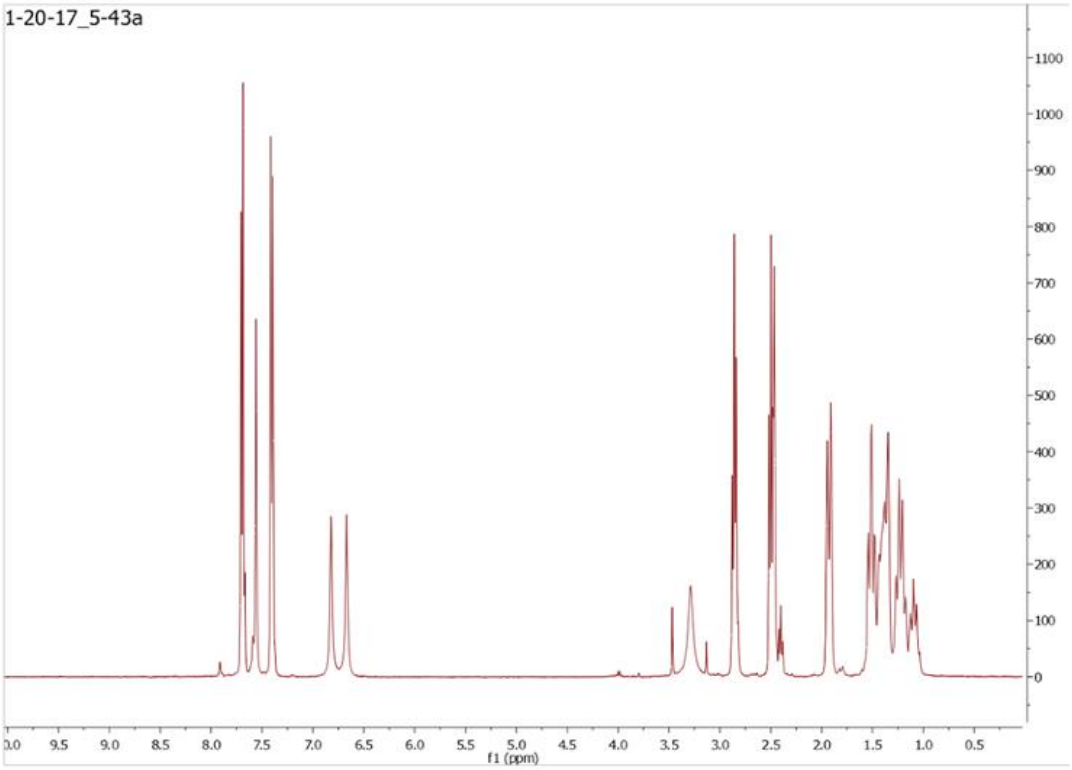

0.14

Figure 2.15 NMR spectrum of 5-43a, in d_6-DMSO, 400 mHz.

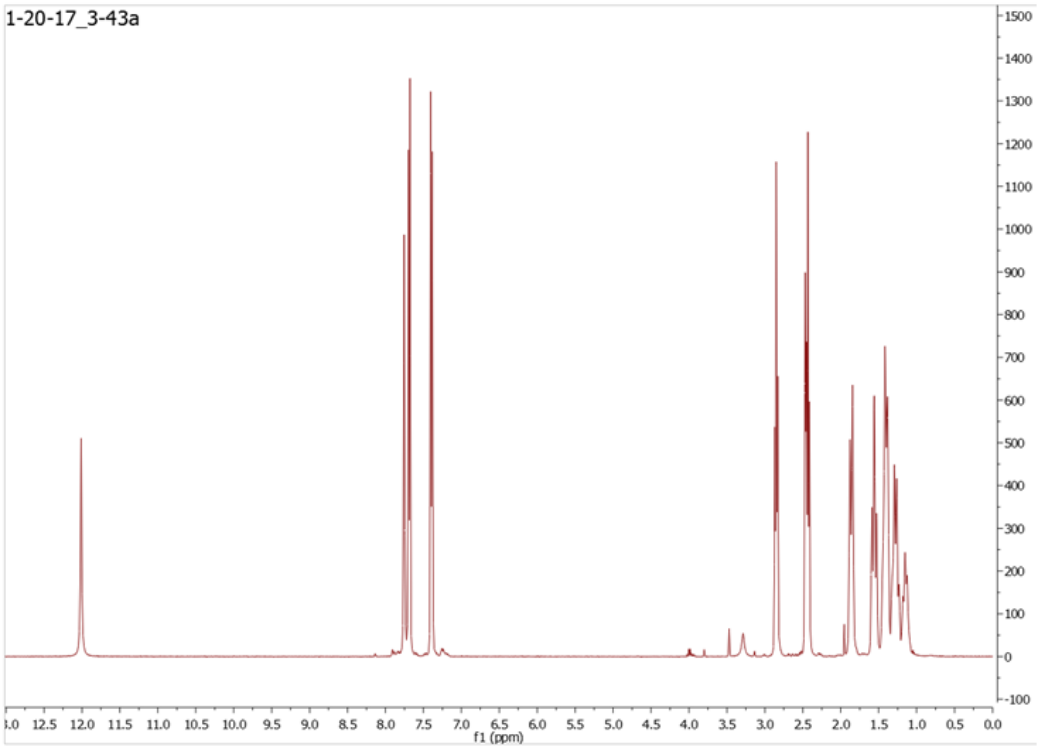

0.15

Figure 2.16 NMR spectrum of 3-43a, in d_6-DMSO, 400 mHz.

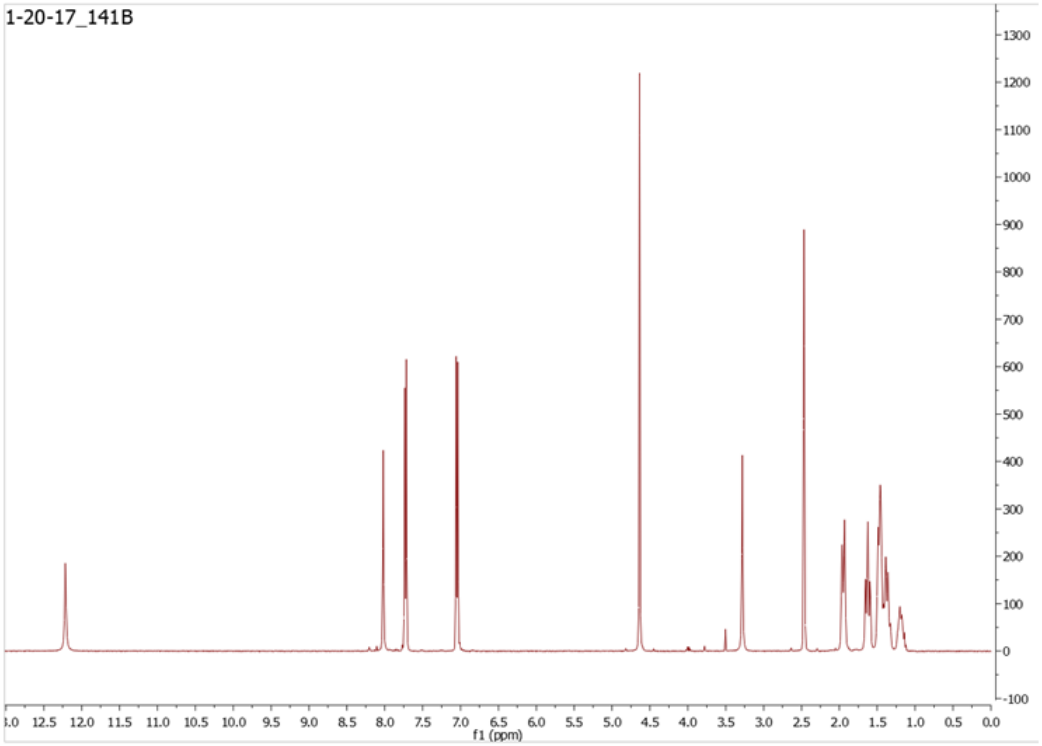

0.16

Figure 2.17 NMR spectrum of 141B in d_6-DMSO, 400 mHz.

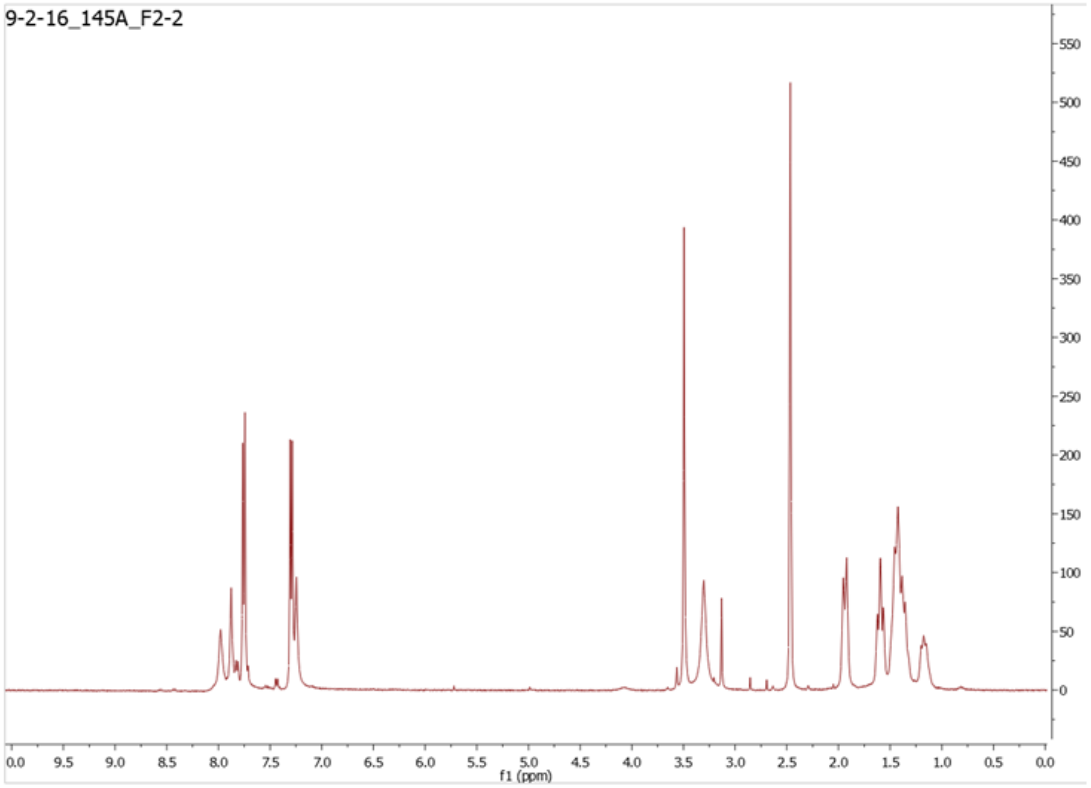

0.17

Figure 2.18 NMR spectrum of 141B in d_6-DMSO, 400 mHz.

Chapter Two: The Dimeric Receptors are the Major Contributors to Metabolic Regulation by ABA in *Arabidopsis* Seedlings

Abstract

Plants respond to drought with extensive metabolic changes that enhance their survival and reduce growth. These responses are controlled in part by the phytohormone abscisic acid. Previous metabolomic studies have described multiple metabolites regulated by drought stress and/or ABA (1–3), but it is unclear which ABA receptors are required for the widespread metabolic reprogramming that occurs during drought. Here, I use multiple selective agonists in combination with ABA receptor mutants to address this question. Untargeted LC-MS metabolomics of ABA and agonist treated seedlings was used to define a set of robust markers of ABA-mediated responses. These experiments confirmed previous reports of multiple amino acids increasing as well as increases in specific glucosinolates. Using these metabolic markers, my results show that the dimeric ABA receptors are primarily responsible for controlling the observed amino acid and glucosinolate responses in Arabidopsis seedlings. Additionally, I report that ABA and quinabactin treatments increase levels of sulfinylglucosinolates and decrease levels of their thionylglucosinolate precursors. Thus, my data demonstrate functional specialization of dimeric and monomeric ABA receptors in controlling metabolomic responses to ABA.

Introduction

Genetic and Agrichemical Manipulation of the ABA Pathway

Plants undergo extensive transcriptomic, proteomic, and metabolomic changes when subjected to drought stress conditions (1, 4–6). These changes can ultimately lead to stomatal closure, inhibition of plant growth, accumulation of protein- and membrane-protecting molecules, and increased free-radical scavenging systems (7, 8). A ubiquitous drought responses is the accumulation of osmo-compatible solutes (osmolytes, compatible solutes), for example proline, that offer protective properties (9–13). Abscisic acid (ABA) is required for many responses during water deficit (14, 15). ABA is perceived by a large and evolutionarily conserved family of receptors collectively known as the PYRABACTIN-RESISTANT LIKE PROTEINS (PYLs) (16–19). PYL receptor mutant strains are useful tools for characterizing receptor-mediated responses, but can be complicated by extensive redundancy that exists within the receptor family. Still, multiple non-redundant, or partially-redundant, functions of the PYL receptors have been described in *Arabidopsis*. For instance, PYL8 plays an important role in ABA-mediated inhibition root growth (20, 21); the *pyl8* single mutant has reduced sensitivity to ABA-mediated inhibition of primary root growth (20) and increased sensitivity to ABA-induced inhibition of lateral root growth (21). Additionally, *pyl4* and *pyl5* mutants are hypersensitive to methyl-jasmonate mediated inhibition of shoot growth and less sensitive to methyl-jasmonate induced anthocyanin accumulation (22). Examples of other single mutants within the ABA receptors producing differentiated phenotypes are limited, indicating most receptors function redundantly, with the strongest phenotypes requiring higher-order mutants in order to be observed.

Complementary to the PYL-mutant genetic tools are the recently characterized synthetic agonists, pyrabactin (3), quinabactin (2) and tetralone-ABA (11), which are selective on subsets of the ABA receptors (18, 23, 24), as well as the rationally designed antagonist compounds such as AS6 (15) (Figure 1.2B) (25). In the cases of pyrabactin and quinabactin, these compounds offer selective activation of subsets of receptors, which can aide in functional characterization, particularly when coupled to quantitative biochemical approaches. Pyrabactin was one of the first developed synthetic ABA-receptor agonists, and shows preferential activation of the dimeric receptors, and highest potency (sub-micromolar) on PYR1 receptor (figure 3.1B) (18). Quinabactin was discovered in a screen for it's ability to cause an interaction between the PYL receptors and HAB1 and displayed increased potency *in vitro* and *in vivo* compared to pyrabactin while still retaining a dimeric-receptor selectivity (23). A new agonist, hexabactin, was synthesized by the postdoctoral researcher Aditya Vaidya in the Cutler lab. This compound was synthesized using medicinal chemistry approaches on a monomeric-specific scaffold identified in the same assay as quinabactin, and preferentially activates the monomeric receptors (figure 3.1B). Thus, these three compounds, which have activity on multiple receptor subtypes, provide tools to probe receptor subtype functions. The power of this approach is improved by combining agonist studies with examination of phenotypes in loss-of-function mutant receptor strains.

As described in Chapter 1, I discovered and optimized a new monomeric receptor selective agonist called **141B** (figure 2.4D). This was identified in a virtual screening effort and has high potency and selectivity for the monomeric receptors. This new probe offers advantages over hexabactin due to its increased potency, but in this chapter I describe experiments with hexabactin because of its availability when I initiated my metabolomics

experiment. Conceptually, my conclusions using **141B** and hexabactin in both chapters are complementary.

In addition to receptor-selective agonists, an orthogonal approach is to study responses induced using engineered receptors. PYR1^{MANDI} is a modified ABA receptor engineered to bind the non-endogenous agrochemical mandipropamid and elicits down-stream signaling once bound (26). Importantly,PYR1^{MANDI} does not respond or bind to ABA, allowing transgenic plants expressing this engineered protein to activate PYR1-mediated responses with spatial and temporal level resolution using promoter-specific expression. In this chapter I used the PYR1^{MANDI} system to confirm that activation of PYR1, a key dimeric receptor, is sufficient to recapitulate ABA's effects on multiple metabolites. I also use this system to examine cell-type specific ABA-metabolic responses.

The Role of ABA in Metabolic Regulation

There are many agriculturally relevant metabolites that respond to ABA treatment in a broad variety of crop plants. For example anthocyanin-based coloration of grape (*Vitis vinifera*) berries and strawberry (*Fragaria* × *ananassa*) fruits can be improved by application of ABA (27–30) and ABA plays an important role in their ripening processes (31). The hardwood tree of peaches (*Prunus persica*) shows increased sugar accumulation in fruits when treated with exogenous ABA (32). These representative examples give applications that could benefit from using ABA for metabolic manipulation, but additionally, while some biological responses of ABA give clear phenotypes, metabolomic shifts could be hidden from visible changes. Thus, analysis of ABA-regulated metabolites could benefit agriculture directly, but also result in assays with increased sensitivity into novel regulatory roles of ABA in regards to metabolism. Further, dissection

of the specific roles of the individual ABA-receptors in these metabolic responses may reveal differential regulatory controls attributable to each receptor.

Proline and other Amino acids regulation by ABA and Drought

The amino acid proline is an ABA- and drought-regulated osmolyte in plants (33–35). Two independent studies have indicated that other amino acids are regulated by dehydration in both an ABA and ABA-independent manner. Leucine, tryptophan, and phenylalanine were observed to increase with drought in one set of experiments (1) with the other work identifying the branched chain amino acids (BCAAs) leucine, isoleucine and valine as significantly increased in both wild type and *aba-2* mutant (which is deficient in ABA-biosynthesis) plants withheld from water (36). However the fold-change increase was lower in the ABA-deficient mutant, indicating that some portion of the response is controlled by ABA. Interestingly, both research groups observed aspartic acid decreasing during the osmotic stress. In contrast to the major findings of upregulated metabolites, other similar studies done on the effects of metabolite levels in response to drought have shown no effect on leucine or isoleucine, but an increase in valine, alanine, proline and tyrosine (37). It is now well established that proline levels are elevated by water deficit and ABA in many plant species, however the results for other amino acids are conflicting between various studies and may be dependent on small changes between the study conditions or the methods of detection.

Glucosinolates are Regulated by the ABA Signaling Pathway

The model plant organism *Arabidopsis thaliana* belongs to the Brassicaceae family of plants which are known to have relatively high concentrations of glucosinolates, a major component of their flavor profile. Glucosinolates are a class of sulfur and nitrogen-containing compounds most notably associated with their prevalence in the Brassicaceae family, but have been identified in others (38). They are important for anti-bacterial (39), anti-fungal (40), and anti-herbivory (41) roles in plants, but also facilitate sulfur and nitrogen storage (42, 43). Glucosinolates have gained more attention recently due to their suggested efficacy in anti-cancer activity (44), however the mechanism for this is still under scrutiny. Multiple research efforts have since been employed to better understand the expression profiles of these sulfur-containing compounds across the cruciferous family of plants (45–48).

The glucosinolate family of compounds have seen some emerging connections in relation to ABA signaling. ABA- and H_2O_2-induced stomatal closure has been shown to be dependent on two myrosinases TGG1 and TGG2 in *Arabidopsis thaliana*, which are involved in glucosinolate breakdown and metabolism (49). Other proteins involved in glucosinolate biosynthesis, NITRILE SPECIFIER PROTEIN 5 (NSP5), NITRILASE 1 (NIT1) and NITRILASE 2 (NIT2), which are also involved in glucosinolate degradation, are upregulated by ABA in *Arabidopsis* suspension cells (50). In multiple Brassica species, a clear regulation of the glucosinolate levels themselves has been observed with the phytohormone ABA, as well as jasmonic acid, salicylic acid, and ethylene (51–53). More specifically, treatment of cabbage (*Brassica oleracea*) with ABA significantly increased aliphatic and aromatic glucosinolate levels (54). These studies indicate an involvement in the transcriptional and metabolomic regulation and crosstalk between glucosinolate metabolism with that of ABA perception and signaling. However, this connection has not

been extensively studied and warrants more research into the mechanisms that produce this response.

The biosynthesis of aliphatic glucosinolates starts from methionine and progresses through side-chain elongation which can result in multiple chemical species containing distinct aliphatic chain lengths. These products offer substrates for the aglycone addition, which results in the first defined glucosinolate, the methyl-thioglucosinolates. Side-chain modification of the methyl-thioglucosinolates proceeds by an iterative process of oxidation to the respective sulfinyl species, capable of undergoing desaturation (loss of CH_3-SO_2-) producing the terminal alkenyl products (55). Other modifications of the side chain are possible, such as hydroxylation and methoxylation, which proceed from the alkenyl derivatives (56). These variations to the side chain can have substantial effects on the flavor profile, the anti-herbivory and chemoprotective properties, and in the context of their medicinal properties in human health (55–57). The ability to manipulate this pathway agrichemically could prove beneficial with regards to these properties. To our knowledge, no studies have shown a clear distinction between the regulation of thioglucosinolates and sulfinyl glucosinolates on *Arabidopsis* using exogenous application of ABA, nor the deconvolution of receptor specificity in this response.

While both the glucosinolates and amino acids appear to be regulated to some degree by drought in both an ABA-dependent and ABA-independent manner, this regulatory control has not been studied in the context of ABA receptor-specificity. Additionally, unbiased studies of metabolomic responses at the receptor-specific level have not yet been conducted. For instance, activation of the dimeric receptors has been shown to be sufficient for a robust ABA response with respect to survival in low water conditions (23), however it is unclear if this activation is sufficient to mimic the metabolomic

profile of ABA treatment. Addressing these questions may be able to improve crop metabolite profiles or optimize the plant's response to drought with respect to water use efficiency.

The availability of selective agonists produced in our lab present tools that could potentially reveal novel metabolic regulations as well as deconvolution of differential receptor function. By transferring 11-day old *Arabidopsis* seedlings to media containing ABA and subsequent metabolite analysis, I provide new evidence supporting the connections between the phytohormone's signaling pathway with glucosinolates and multiple amino acids. Additionally, seedlings similarly subjected to the other selective agonists pyrabactin, quinabactin, hexabactin, and **141B** provide insights into the selectivity between the receptor's regulation of these metabolic responses. Combining agonist treatments with receptor mutant strains produces a valuable toolset for dissecting the receptor functions with good resolution. Specifically, the results from my studies indicate that multiple ABA-mediated metabolic changes can be mimicked by synthetic ABA-receptor agonists and are largely dependent on the dimeric ABA-receptors. The responses in the glucosinolates reflect a down-regulation of the aliphatic thionylglucosinolates and upregulation of the respective sulfinylglucosinolates, suggesting an activation of enzymes involved in their oxidation. Finally, I use the mandipropamid-responsive receptor system to identify some tissue-specific metabolomic controls of ABA signalling.

Methods

Chemicals and Reagents

Mobile phase solvents for liquid chromatography were purchased from Fisher scientific (LC/MS grade water, Morris Plains, NJ, USA), J.T. Baker (LC/MS grade water, Center Valley, PA USA), or Honeywell (LC/MS grade acetonitrile, Muskegon, MI, USA) and used as is. Ammonium hydroxide and ammonium acetate along with all standards were purchased from Sigma-Aldrich (St. Louis, MO, USA). ABA was sourced from (Itasca, IL, USA) and chemical agonists were synthesized as outlined in chapter 1.

Seedling growth and plate preparation

To 3.5 x 3.5 inch polypropylene plates there was dispensed 20 mL of agar solution consisting of 1% sucrose, 1% Gelzan DM, and 2.15 g/L MS media in 3.5x3.5 inch square plastic plates for plant growth phase. Chemical treatment plates were made by adding 20 µL of 20mM stock solution (or DMSO for control plates) of compound. For mannitol treatment, mannitol was added directly to the agar medium for a final concentration of 400 mM. Once the solution was semi-solid, a polypropylene mesh was placed on top, and the plates were used immediately once the media reached room temperature.

Plant sample preparation

To prepare 9 plates, approximately 75 µL of *Arabidopsis thaliana* seeds were sterilized using 1 mL of 1% bleach solution and soap for 12 minutes, followed by treatment with 1 mL of 70% ethanol for 7 minutes. The seeds were then washed 2 x 1 mL DI water, and placed in a 1 mL solution of 17% agar. The seeds were then pipetted on top of the polypropylene mesh. Seeds were placed in two rows per plate, with a total of approximately 80 seeds per plate. The plates were stratified for 2 days at 4°C, and then placed in a growth chamber for 11 days. On the 11^{th} day, the mesh sheets were transferred to the treatment or control plates and replaced in the growth chamber for another 24 hours.

After the treatment incubation period, plants were removed from the mesh, lightly dried using dry tissue-wipes (VWR), weighed, and placed in 2 mL reinforced tubes (XXTuff microvials, BioSpec Products, Inc.), which contained approximately 100 µL of zirconium beads (1.0 mm diameter, BioSpec Products, Inc.) followed immediately by suspending in liquid nitrogen. To the cold tubes, there was added 2 µL of LC/MS grade methanol per mg of plant material. While still cold, the tubes were placed in a Precellys 24 (Bertin Instruments) and homogenized at 6500 RPM for 20 seconds x 2. The samples were then centrifuged at 13,000 RPM for 10 minutes at 4° C and the supernatant filtered through 2 µm filters (Agilent) and filtrate kept on ice. 20 µL of filtrate from each sample was added to each of five separate pooled sample vials. All samples were stored at -80° C for longer term storage.

Desulfo-glucosinolate Extraction

For quantifying the differences and presence of desulfo-glucosinolates, the above methodology was employed to obtain a filtrate from each plant. The filtrate was heated to 90° C for 30 minutes to inactivate myrosinase. This filtrate was added to columns containing 1.5 mL of 1:5 sephadex/water (Sephadex A-25, Pharmacia, Uppsala, Sweden) , which had been washed once with 1 mL of LC/MS grade water. 20 µL of aryl sulfatase (0.77 mg/mL in water, Sigma-Aldrich) and 80 µL of LC/MS grade water was added, and the columns were incubated in the dark for 12 hours at room temperature. To elute the desulfoglucosinolates, 400 µL of 30% MeOH were added to the columns and collected. Sinigrin was added to each sample relative to the total MeOH added in the initial extraction to produce a final concentration injected of approximately 1.25 µM. This solution was detected using the reversed phase method described below.

Liquid Chromatography Mass Spectrometry

Samples were run on an HPLC system (1200 series, Agilent Technologies), coupled with a 6224 TOF (Agilent Technologies). For HILIC analyses, a Luna Aminopropyl, 3 µm NH_2, 100 mm × 2.0 mm I.D. column (Phenomenex) was used. Mobile phase solvent A consisted of 10 mM ammonium hydroxide and 10 mM ammonium acetate in water and solvent B 100% acetonitrile. The mobile phase gradient elution was 95% B (0-3 minutes, .6 mL/min), 95% B to 45% B (3-16 minutes, 0.5 mL/min), 45% B to 25% B (16-20 minutes, 0.45 mL/min), 25% B (20-26.5 minutes, 0.45 mL/min), 25% B to 95% B (26.5-27 minutes, 0.5 mL/min), and 95% B (27-29 minutes, 0.6 mL/min). ESI was set to negative mode.

For reversed phase (RP), a Poroshell 120 EC-C18, 2.7 µm, 3.0 x 50 mm column (Agilent) was used. Mobile phase solvent A was 0.1% formic acid in water (Honeywell) and solvent B was 0.1% formic acid in acetonitrile (Honeywell). The mobile phase gradient was 2% B (0-2 minutes), 2% to 15% B (2-3 minutes), 15% B to 25% B (3-5 minutes), 25% B to 40% B (5-10 minutes), 40% B to 70% B (10-12 minutes), 70% B to 90% B (12-17 minutes), 90% B (17-22.5 minutes), 90% B to 2% B (22.5-23 minutes), and 2% B (23-25.5 minutes). ESI was set to positive mode.

The sample injection volume was 5 µM and samples were kept at 4° C in the autoinjector. ESI source conditions were as follows: 325° C gas temperature, 11 L/minute drying gas, nebulizer 35 psig, capillary voltage +3,500 V or -4,000 V (for positive and negative ESI, respectively), skimmer 65 V, fragmentor 120 V, and OCT 1 RF Vpp 750 V in negative mode. The acquisition range was 70-1050 m/z, with an acquisition rate of 1.31 spectra/sec.

Data analysis

Raw data was converted to mzData file formats using Agilent Qualitative Analysis software version B.06.00 with export cut-off values of minimum peak height = 1000 and all other settings to default. Data analysis was initiated using XCMSonline (58, 59), using multigroup analysis. Treatment groups were compared to controls (DMSO). Pooled samples were used as Quality Control (QC) samples. The parameters in XCMS were set as follows: For HILIC: centWave settings for feature detection (Δ *m/z* = 25 ppm, minimum peak width = 20 seconds and maximum peak width = 140 seconds); obiwarp settings for retention time correction (profStep = 0.5); and other parameters including mzwid = 0.025, minfrac = 1 and bw = 5 for chromatogram alignment. Overlap between different chromatographic modes was performed by using exact mass value defined by Δ *m/z* = 0.015 Da. For RP: centWave settings for feature detection (Δ *m/z* = 30 ppm, minimum peak width = 10 seconds and maximum peak width = 60 seconds); obiwarp settings for retention time correction (profStep = 1); and other parameters including mzwid = 0.025, minfrac = .5 and bw = 5 for chromatogram alignment. Overlap between different chromatographic modes was performed by using exact mass value defined by Δ *m/z* = 0.015 Da. The relative quantification of metabolite features was based on the integrated EIC peak areas.

XCMS results were downloaded as a .csv file and analyzed manually. Generally, cut-off values were assigned of p-value ≤.02, and fold change ≥1.2 or ≤0.83. The number of peaks detected had to be greater than or equal to the number of treatment (or control)

samples plus the number of pooled samples, (i.e. the number of peaks detected had to be present in all pooled samples and all of either the control *or* the treatment samples).

Peaks were then sorted via retention time (RT), with the first minute being omitted from RP, as this contained a large number of saturating peaks with a large matrix effect. Peaks were then clustered that had similar RT which were likely adducts or fragments of the same parent compound. From each cluster, the features with the smallest p-value and/or the largest integration area were then assigned as the 'feature of interest', and assumed as the parent peak. Features identified from original runs were then compared to future runs to confirm reproducibility.

Peak Identification

For putative chemical identification of m/z species peaks, Agilent's MassHunter was used to generate formula from spectrum peaks based on isotopic distribution and m/z. This was used in combination with using the METLIN database to align the possible m/z metabolites in the database with the isotopic distribution to characterize likely metabolite species. The glucosinolate molecules were identified by occurrence of multiple sulfur-containing formulas predicted from MassHunter, in addition to the Metlin database results that displayed a matching m/z for glucosinolate species. The glucosinolate identities were further supported by the retention time differences which matched the varying hydrophobicity of the varying chain lengths of the aliphatic glucosinolates. Amino acids were verified with standards by alignment with retention time and m/z.

Results

Identification of ABA-regulated metabolites

Untargeted metabolomic analyses were performed on *Arabidopsis* seedlings to identify ABA-regulated metabolites. 11 day old seedlings were transferred to media containing 20 μM chemical or a vehicle control (DMSO) and metabolites extracted in methanol 24 hours after treatment using eight biological replicates and analyzed by LC-MS utilizing a HILIC column, borrowing from previous work aimed at covering a significant portion of the polar metabolome of bacteria (60). Peaks were identified and quantified using XCMSonline (58, 59). Using a p-value < 0.01 we observed that ABA regulates the levels of approximately 850 peaks in our experimental condition. A previous report examined ABA-dependent and ABA-independent metabolites regulated by drought stress and identified ABA-dependent changes in the levels of nine free amino acids and multiple sugars (1). Using these nine amino acids as starting validation targets, I was able to confirm, using commercially available standards, we could detect these nine metabolites using our method. Expansion of this set to probe all the amino acids allowed me to observe an additional seven amino acids (lysine, glycine, alanine and cysteine were not observed). Examination of mock control and ABA treated seedlings confirmed that most (14/16) of these are ABA-regulated in our experimental conditions (using a p<0.01 cutoff; Table 3.1). We used a set of 16 amino acids that responded as markers to quantify the responses induced by agonists in multiple genetic backgrounds to probe receptor function.

Dimeric receptors preferentially control metabolic responses to ABA

To probe the functions of the various receptors, the effects of ABA were compared to quinabactin, pyrabactin, and hexabactin (a monomeric receptor-selective compound)

(Figure 3.1B). ABA regulated 14 of the 16 amino acids in WT (Table 3.2, figure 3.3, Appendix table 1) . The levels of four amino acids (proline, serine, isoleucine/leucine, and tyrosine) responded to pyrabactin, indicating a weak response (figure 3.3, appendix table 4), consistent with previous reports of its weak activity in seedling tissues (18). Quinabactin, a broader spectrum agonist with greater potency, induced a strong response similar to that induced by ABA, increasing levels for 12 of the amino acids profiled (Figure 3.3, appendix table 8). Together these results suggest that activation of dimeric receptors is sufficient to mimic the ABA-induced increase in amino acid levels. In contrast, hexabactin treatments induced a weak amino acid response, with only four amino acids significantly responding with reduced fold-changes relative to ABA and quinabactin (figure 3.3, appendix table 12). Thus, hexabactin treatments are not sufficient to induce a strong ABA-like response, which is consistent with the hypothesis that dimeric receptors preferential control ABA-mediated changes in amino acid levels. To evaluate whether dimeric and monomeric receptor targets are required for ABA- and agonist-mediated responses, we examined metabolite changes using a *pyr1/pyl1/pyl2* (*012*) mutant strain, which lacks 3 key dimeric receptor targets and has reduced sensitivity to ABA, quinabactin and pyrabactin, but not hexabactin. We also examined responses of a *pyl8/pyl9* (*89*) mutant strain, which has greatly reduced sensitivity to hexabactin. The *012* mutant shows a dramatically reduced response to ABA, with only five amino acids regulated, versus the 14 observed in the WT (figure 3.3, appendix table 2) indicating their necessity for ABA-mediated changes in amino acid levels. Neither pyrabactin (appendix table 6) nor quinabactin (appendix table 9) treatments altered amino acid levels in the *012* mutant, demonstrating that these targets mediated their effects (figure 3.3). Thus, ABA's effects on amino acid levels are largely mediated by PYR1, PYL1, and PYL2. Consistent with this

conclusion, we observed that the *89* double mutant has an essentially wild type like amino acid response to ABA (appendix table 3) and quinabactin (appendix table 10, figure 3.3) supporting the hypothesis that the dimeric receptors preferentially control ABA-mediated changes in amino acid levels. Using proline as a specific marker for the ABA-response in amino acid regulation, figure 3.2 illustrates activation of the dimeric receptors is sufficient for this response and the primary mediators, with a weaker response attributed to the monomeric receptors.

Dimeric Receptors Control Aliphatic Glucosinolates levels

840 peaks were identified by XCMSonline as significantly different between ABA and control treatments. Inspection of the data revealed a set of peaks with predicted formulae suggesting the presence of sulfur. This group of putative sulfur containing compounds differed consecutively in m/z by ~14.01, which corresponded to -CH2-. The prevalence of the multiple sulfur groups, indicated by isotopic ratios, and the varying -$(CH_2)_n$-, suggested these peaks likely represented glucosinolates, a large family of specialized metabolites in the Brassicaceae. Based on METLIN matches by mass, the metabolites were predicted to include the aromatic glucobrassicin (GBR), and several aliphatic glucosinolates including: glucoerucin (GER), glucoberteroin (GBE), glucolesquerellin (GLE), 7-Methylthioheptyl glucosinolate (7MTG), 8-Methylthiooctyl (8MTG), and the aliphatic sulfinyls, glucoraphanin (GRA), glucohesperin (GHE), glucoibarin (GIB), and glucohirsutin (GHI) (Figure 3.5). To verify that these peaks were, in fact, derived from aliphatic glucosinolates, I utilized established RP LC-MS methods developed for desulfated glucosinolates (61) and purchased a commercially available standard for glucoerucin (GER) (Appendix figure 1). The desulfonation shift of m/z

([Glucosinolate-SO_4]$^+$) provides an orthogonal validation method to commercial standards. In these analyses comparing ABA and mock treated seedlings, only one of the desulfo-(ds)-thioglucosinolates (ds8MTG) responded to ABA (Figure 3.5, 3.6), however one outlier sample within the ABA-treated plants may have affected p-values. Together, the desulfonation ability of these compounds and their varied alkyl chain length as correlated to retention time (Figures 3.5, 3.6, and 3.7), my data suggest that aliphatic glucosinolates are regulated by ABA, consistent with published studies (50, 54).

One interesting observation is the likely inverse regulation of thio- and sulfinylglucosinolates levels. ABA and quinabactin treatments reduced the levels of several thionyl compounds and increased sulfinyl compounds (Figure 3.8, appendix tables 21, 28). These findings suggest that ABA regulates the oxidation of the thionyl glucosinolates, converting them into their respective sulfinyl groups. Consistent with this, two key enzymes in this transformation, GS-OX2 and GS-OX4 (62, 63), are ABA regulated as depicted in public microarray database. To interrogate the receptor selectivity of these changes, I examined the responses of the *012* and *89* mutant strains, which yielded results were similar to those observed with the amino acid regulation; the *012* mutant lowered intensity of the glucosinolate responses to ABA, pyrabactin, and quinabactin, demonstrating dependence on dimeric receptors. Interestingly quinabactin induced a modest responses (changes in GIB and GHI levels) in the *012* mutant, perhaps mediated by PYL3 or PYL5, which are also sensitive to quinabctin.

Hexabactin's effects were modest on wild type seedlings, with the amino acids, only a single glucosinolate (8MTG) was regulated. The *89* mutant responds to quinabactin and ABA, with each regulating statistically significant responses in five and six of the glucosinolates identified, respectively. In the *89* mutant, hexabactin's effects were largely

abrogated, but it did elicit an 8MTG response, however this was weaker in FC than that in hexabactin-treated WT plants, possibly due to activity through PYL10 and PYL11.

Activation of PYR1^{MANDI} is sufficient to alter amino acid and glucosinolate levels

A parallel strategy to verify that these metabolite classes are under control of dimeric receptors, we used the orthogonal PYR1^{MANDI} system, which employs a receptor that is selectively activated by the agrochemical mandipropamid (26). 35S::PYR1^{MANDI} plants were treated with 5 μM mandipropamid, which mimicked ABA's effect on glucosinolates and amino acids, and was strikingly much stronger than that induced by ABA treatment (Figure 3.9, 3.10). This is likely due to mandipropamid's greater metabolic stability and high level receptor expression in the transgenic line. The thionyl glucosinolates GER, GBE, GLE, 7MTG, and 8MTG were all observed to be at least below 33% of the concentration observed in the control. As previously observed, the most extreme fold-change was in the 8-methylthiooctyl glucosinolate, the longest chain thioglucosinolate detected. The sulfinyl GHE was increased ~4.5-fold in the mandipropamid treatment, versus a 3-fold increase in response to ABA. Similarly, the amino acids were also significantly regulated, and to a greater degree than ABA, by the activated 35S::PYR1^{MANDI}. Collectively, these observations show that selective activation of PYR1^{MANDI} recapitulates the effects of ABA and quinabactin and supports the conclusion that the dimeric receptors preferentially control amino acid and glucosinolate levels.

Cell type specific metabolite changes

To explore the tissue- or cell type-specificity, I used a CYP86A2::PYR1^{MANDI} transgenic, constructed by a Cutler lab member, Sang Park, which strongly expresses PYR1^{MANDI} in guard cells and, to a lesser extent, throughout the epidermis. Guard cells have high levels of myrosinases (49), the enzymes responsible for glucosinolate hydrolysis during herbivory and wounding. The 35S::PYR1^{MANDI} and CYP86A2::PYR1^{MANDI} transgenic lines were both able to regulate at least six glucosinolates (nine and six, respectively) compared to six regulated by ABA in the WT, indicating alterations in glucosinolate levels in responses to mandipropamid (Figure 3.10, appendix figures 38 and 39), while the amount of responding amino acids was greatly reduced in the CYP86A2::PYR1^{MANDI} line (Figure 3.10, appendix tables 18 and 20). This suggests that ABA's effect on glucosinolate levels is likely to occur largely in guard cells.

ABA-induced alterations in glucosinolate and amino acid levels occur during osmotic stress

To further interrogate these metabolic responses, I compared the effects of osmotic stress (400 mM mannitol) and ABA treatment on metabolite profiles. The profiled ABA-regulated metabolites were also regulated by mannitol treatment, but the intensity of their response was quantitatively higher (Figure 3.9 and 3.10). For example, both methionine and tryptophan increased ~50-fold in response to mannitol but only 2.5- and 6.3-fold in response to ABA, respectively. The differences between the two treatments with respect to glucosinolates were reduced less. Still, the thionyl down-regulation of 8MTG and sulfinyl up-regulation trend for GHE and GHI was observed in both mannitol and ABA treatment.

Discussion

We were able to verify multiple amino acids as being regulated by ABA with our method, and showed that the monomeric and dimeric receptors play differential roles in their regulation. The PYR1, PYL1, and PYL2 receptors are critical regulators of these responses, as agonist treatments have dramatically reduced responses in the *012*, but not *89,* mutant in comparison to WT. Consistent with this, neither of the monomeric-selective agonists hexabactin or 141B had effects as strong as ABA. Collectively these data demonstrate that the dimeric receptors preferentially control ABA-mediated regulation of the levels of several, but not all, amino acids and aliphatic glucosinolates. Although the underlying basis for this selective control is currently unclear, it may involve transcriptional regulation of amino acid biosynthetic genes with promoters that are differentially regulated by different receptor subclasses. Given the highly overlapping expression patterns for ABA receptor mRNAs and the shared core response pathway that converges on SnRK2 kinase activation, it is unclear how activating a specific receptor would differentially regulate a downstream output. One hypothesis is that there may be specific scaffolding proteins that compartmentalize the core signaling components into different complexes that contain different receptor subtypes and different downstream regulatory factors. This would allow dimeric receptor agonist like quinabactin to activate a different set of transcription factors than a monomeric selective agonist like hexabactin.

The aliphatic glucosinolates represent a class of methionine-derived compounds within the Brassicales that are known for their anti-herbivory properties. Some genes of the glucosinolate biosynthesis pathway have been previously linked to ABA treatment, for example mRNAs for the oxidation enzymes GS-OX1 and 5 are increased by ABA (64), and GS-OX1 catalyzes the *S*-oxidation of the aliphatic glucosinolates (62, 63). These

studies suggest transcriptional regulation of GS-OX mRNAs may underlie my observed decrease in thionyl- and respective increase in sulfinylglucosinolates. Moreover, our data have differentiated the receptor-selective control of regulation of these and other metabolites. This response appears stronger for longer chain glucosinolates (C7, C8) and apparently is mostly regulated through the dimeric receptors. Given that mandipropamid treatments of CYP86A::PYR1^{MANDI} mimic the glucosinolate response of ABA-treated WT plants, this strongly suggests that the oxidation of these metabolites occurs in guard cells.

The importance of this accumulation of aliphatic sulfinyl glucosinolates (and subsequent lowering of the thionyl counterparts) response by ABA signaling is not understood, but could potentially have some purpose in dealing with oxidative stress. Plants subjected to drought have increased oxidative stress, and require mechanisms to deal with the emergence of ROS (65). The aliphatic glucosinolates have sequential side chain modifications that primarily occur through oxidation (55) and may offer substrates for antioxidant potential. It is also clear from my data that these responses can be enhanced using 35S::PYR1^{MANDI}. Additionally, the finding that the guard cell localization of the ABA-response through use of the CYP86A::PYR1^{MANDI} nearly constitutes the full ABA response with respect to the glucosinolates provides a mechanism to probe the ABA signaling pathway with spatio- and temporal-specificity. Physiological controls, such as primary and lateral root growth, stomatal conductance, and seed germination could be differentially activated by different promoter systems using the modified receptor, as well as metabolomic changes, like the glucosinolates and amino acids, as outlined here. Differentially regulating these various down-stream signalling effects could prove useful in the context of drought mitigation methodologies.

References

1. Urano K, et al. (2009) Characterization of the ABA-regulated global responses to dehydration in Arabidopsis by metabolomics. *Plant J* 57(6):1065–1078.

2. Zhang J-Y, et al. (2014) Global reprogramming of transcription and metabolism in Medicago truncatula during progressive drought and after rewatering. *Plant Cell Environ* 37(11):2553–2576.

3. Alvarez S, Marsh EL, Schroeder SG, Schachtman DP (2008) Metabolomic and proteomic changes in the xylem sap of maize under drought. *Plant Cell Environ* 31(3):325–340.

4. Xie H, et al. iTRAQ-based quantitative proteomic analysis reveals proteomic changes in leaves of cultivated tobacco (Nicotiana tabacum) in response to drought stress. *Biochem Biophys Res Commun*. doi:10.1016/j.bbrc.2015.11.133.

5. Hajheidari M, et al. (2005) Proteome analysis of sugar beet leaves under drought stress. *Proteomics* 5(4):950–960.

6. Bechtold U, et al. (2016) Time-series transcriptomics reveals that AGAMOUS-LIKE22 links primary metabolism to developmental processes in drought-stressed Arabidopsis. *Plant Cell*. doi:10.1105/tpc.15.00910.

7. Wang W, Vinocur B, Altman A (2003) Plant responses to drought, salinity and extreme temperatures: towards genetic engineering for stress tolerance. *Planta* 218(1):1–14.

8. Chaves MM, Maroco JP, Pereira JS (2003) Understanding plant responses to drought — from genes to the whole plant. *Funct Plant Biol* 30(3):239–264.

9. Bohnert HJ, Sheveleva E (1998) Plant stress adaptations--making metabolism move. *Curr Opin Plant Biol* 1(3):267–274.

10. Bashir A, et al. (2014) Plant-derived compatible solutes proline betaine and betonicine confer enhanced osmotic and temperature stress tolerance to Bacillus subtilis. *Microbiology* 160(Pt 10):2283–2294.

11. Kempf B, Bremer E (1998) Uptake and synthesis of compatible solutes as microbial stress responses to high-osmolality environments. *Arch Microbiol* 170(5):319–330.

12. Street TO, Bolen DW, Rose GD (2006) A molecular mechanism for osmolyte-induced protein stability. *Proc Natl Acad Sci U S A* 103(38):13997–14002.

13. Smirnoff N, Cumbes QJ (1989) Hydroxyl radical scavenging activity of compatible solutes. *Phytochemistry* 28(4):1057–1060.

14. McAinsh MR, Brownlee C, Hetherington AM, Others (1990) Abscisic acid-induced elevation of guard cell cytosolic Ca2+ precedes stomatal closure. *Nature* 343(6254):186–188.

15. Skriver K, Mundy J (1990) Gene expression in response to abscisic acid and osmotic stress. *Plant Cell* 2(6):503–512.

16. Hauser F, Waadt R, Schroeder JI (2011) Evolution of abscisic acid synthesis and signaling mechanisms. *Curr Biol* 21(9):R346–55.

17. Tougane K, et al. (2010) Evolutionarily conserved regulatory mechanisms of abscisic acid signaling in land plants: characterization of ABSCISIC ACID INSENSITIVE1-like type 2C protein phosphatase in the liverwort Marchantia polymorpha. *Plant Physiol* 152(3):1529–1543.

18. Park S-Y, et al. (2009) Abscisic acid inhibits type 2C protein phosphatases via the PYR/PYL family of START proteins. *Science* 324(5930):1068–1071.

19. Ma Y, et al. (2009) Regulators of PP2C phosphatase activity function as abscisic acid sensors. *Science* 324(5930):1064–1068.

20. Antoni R, et al. (2012) PYL8 plays an important role for regulation of ABA signaling in root. *Plant Physiol*. doi:10.1104/pp.112.208678.

21. Zhao Y, et al. (2014) The ABA receptor PYL8 promotes lateral root growth by enhancing MYB77-dependent transcription of auxin-responsive genes. *Sci Signal* 7(328):ra53.

22. Lackman P, et al. (2011) Jasmonate signaling involves the abscisic acid receptor PYL4 to regulate metabolic reprogramming in Arabidopsis and tobacco. *Proc Natl Acad Sci U S A* 108(14):5891–5896.

23. Okamoto M, et al. (2013) Activation of dimeric ABA receptors elicits guard cell closure, ABA-regulated gene expression, and drought tolerance. *Proc Natl Acad Sci U S A* 110(29):12132–12137.

24. Nyangulu JM, et al. (2006) Synthesis and biological activity of tetralone abscisic acid analogues. *Org Biomol Chem* 4(7):1400–1412.

25. Takeuchi J, Ohnishi T, Okamoto M, Todoroki Y (2015) Conformationally restricted 3′-modified ABA analogs for controlling ABA receptors. *Org Biomol Chem* 13(14):4278–4288.

26. Park S-Y, et al. (2015) Agrochemical control of plant water use using engineered abscisic acid receptors. *Nature* 520(7548):545–548.

27. Cantín CM, Fidelibus MW, Crisosto CH (2007) Application of abscisic acid (ABA) at veraison advanced red color development and maintained postharvest quality of “Crimson Seedless” grapes. *Postharvest Biol Technol* 46(3):237–241.

28. Cecilia Peppi M, Fidelibus MW, Dokoozlian N (2006) Abscisic Acid Application Timing and Concentration Affect Firmness, Pigmentation, and Color of `Flame Seedless' Grapes. *HortScience* 41(6):1440–1445.

29. Mori K, et al. (2015) Effects of abscisic acid treatment and night temperatures on anthocyanin composition in Pinot noir grapes. *VITIS - Journal of Grapevine Research* 44(4):161.

30. Jiang Y, Joyce DC (2003) ABA effects on ethylene production, PAL activity, anthocyanin and phenolic contents of strawberry fruit. *Plant Growth Regul* 39(2):171–174.

31. Jia H-F, et al. (2011) Abscisic acid plays an important role in the regulation of strawberry fruit ripening. *Plant Physiol* 157(1):188–199.

32. Kobashi K, Gemma H, Iwahori S (1999) Sugar accumulation in peach [Prunus persica] fruit as affected by abscisic acid (ABA) treatment in relation to some sugar metabolizing enzymes. *Engei Gakkai zasshi* 68. Available at: http://agris.fao.org/agris-search/search.do?recordID=JP1999004699.

33. Verslues PE, Bray EA (2006) Role of abscisic acid (ABA) and Arabidopsis thaliana ABA-insensitive loci in low water potential-induced ABA and proline accumulation. *J Exp Bot* 57(1):201–212.

34. Delauney AJ, Verma DPS (1993) Proline biosynthesis and osmoregulation in plants. *Plant J* 4(2):215–223.

35. Hayat S, et al. (2012) Role of proline under changing environments: a review. *Plant Signal Behav* 7(11):1456–1466.

36. Nambara E, Kawaide H, Kamiya Y, Naito S (1998) Characterization of an Arabidopsis thaliana mutant that has a defect in ABA accumulation: ABA-dependent and ABA-independent accumulation of free amino acids during dehydration. *Plant Cell Physiol* 39(8):853–858.

37. Rizhsky L, et al. (2004) When defense pathways collide. The response of Arabidopsis to a combination of drought and heat stress. *Plant Physiol* 134(4):1683–1696.

38. Fahey JW, Zalcmann AT, Talalay P (2001) The chemical diversity and distribution of glucosinolates and isothiocyanates among plants. *Phytochemistry* 56(1):5–51.

39. Dufour V, Stahl M, Baysse C (2015) The antibacterial properties of isothiocyanates. *Microbiology* 161(Pt 2):229–243.

40. Bednarek P, et al. (2009) A glucosinolate metabolism pathway in living plant cells mediates broad-spectrum antifungal defense. *Science* 323(5910):101–106.

41. Hopkins RJ, van Dam NM, van Loon JJA (2009) Role of glucosinolates in insect-plant relationships and multitrophic interactions. *Annu Rev Entomol* 54:57–83.

42. Rausch T, Wachter A (2005) Sulfur metabolism: a versatile platform for launching defence operations. *Trends Plant Sci* 10(10):503–509.

43. Aghajanzadeh T, Hawkesford MJ, De Kok LJ (2014) The significance of glucosinolates for sulfur storage in Brassicaceae seedlings. *Front Plant Sci* 5:704.

44. Higdon JV, Delage B, Williams DE, Dashwood RH (2007) Cruciferous vegetables and human cancer risk: epidemiologic evidence and mechanistic basis. *Pharmacol Res* 55(3):224–236.

45. Kushad MM, et al. (1999) Variation of glucosinolates in vegetable crops of Brassica oleracea. *J Agric Food Chem* 47(4):1541–1548.

46. Kissen R, et al. (2016) Effect of growth temperature on glucosinolate profiles in Arabidopsis thaliana accessions. *Phytochemistry*. doi:10.1016/j.phytochem.2016.06.003.

47. Bhandari SR, Jo JS, Lee JG (2015) Comparison of Glucosinolate Profiles in Different Tissues of Nine Brassica Crops. *Molecules* 20(9):15827–15841.

48. Velasco P, Soengas P, Vilar M, Cartea ME, del Rio M (2008) Comparison of Glucosinolate Profiles in Leaf and Seed Tissues of Different Brassica napus Crops. *J Am Soc Hortic Sci* 133(4):551–558.

49. Islam MM, et al. (2009) Myrosinases, TGG1 and TGG2, redundantly function in ABA and MeJA signaling in Arabidopsis guard cells. *Plant Cell Physiol* 50(6):1171–1175.

50. Böhmer M, Schroeder JI (2011) Quantitative transcriptomic analysis of abscisic acid-induced and reactive oxygen species-dependent expression changes and proteomic profiling in Arabidopsis suspension cells. *Plant J* 67(1):105–118.

51. Thiruvengadam M, Baskar V, Kim S-H, Chung I-M (2016) Effects of abscisic acid, jasmonic acid and salicylic acid on the content of phytochemicals and their gene expression profiles and biological activity in turnip (Brassica rapa. *Plant Growth Regul*:1–14.

52. Thiruvengadam M, Kim S-H, Chung I-M (2015) Exogenous phytohormones increase the accumulation of health-promoting metabolites, and influence the expression patterns of biosynthesis related genes and biological activity in Chinese cabbage (Brassica rapa spp. pekinensis). *Sci Hortic* 193:136–146.

53. Wang Z, et al. (2015) Effects of abscisic acid on glucosinolate content, isothiocyanate formation and myrosinase activity in cabbage sprouts. *Int J Food Sci Technol* 50(8):1839–1846.

54. Wang Z, et al. (2015) Effects of abscisic acid on glucosinolate content, isothiocyanate formation and myrosinase activity in cabbage sprouts. *Int J Food Sci Technol* 50(8):1839–1846.

55. Giamoustaris A, Mithen R (1996) Genetics of aliphatic glucosinolates. IV. Side-chain

modification in Brassica oleracea. *Theor Appl Genet* 93(5-6):1006–1010.

56. Mikkelsen MD, Petersen BL, Olsen CE, Halkier BA (2002) Biosynthesis and metabolic engineering of glucosinolates. *Amino Acids* 22(3):279–295.

57. Beekwilder J, et al. (2008) The Impact of the Absence of Aliphatic Glucosinolates on Insect Herbivory in Arabidopsis. *PLoS One* 3(4):e2068.

58. Smith CA, Want EJ, O'Maille G, Abagyan R, Siuzdak G (2006) XCMS: processing mass spectrometry data for metabolite profiling using nonlinear peak alignment, matching, and identification. *Anal Chem* 78(3):779–787.

59. Tautenhahn R, Patti GJ, Rinehart D, Siuzdak G (2012) XCMS Online: a web-based platform to process untargeted metabolomic data. *Anal Chem* 84(11):5035–5039.

60. Ivanisevic J, et al. (2013) Toward 'Omic Scale Metabolite Profiling: A Dual Separation–Mass Spectrometry Approach for Coverage of Lipid and Central Carbon Metabolism. *Anal Chem* 85(14):6876–6884.

61. Barth C, Jander G (2006) Arabidopsis myrosinases TGG1 and TGG2 have redundant function in glucosinolate breakdown and insect defense. *Plant J* 46(4):549–562.

62. Li J, Hansen BG, Ober JA, Kliebenstein DJ, Halkier BA (2008) Subclade of flavin-monooxygenases involved in aliphatic glucosinolate biosynthesis. *Plant Physiol* 148(3):1721–1733.

63. Hansen BG, Kliebenstein DJ, Halkier BA (2007) Identification of a flavin-monooxygenase as the S-oxygenating enzyme in aliphatic glucosinolate biosynthesis in Arabidopsis. *Plant J* 50(5):902–910.

64. Kong W, et al. (2016) Two Novel Flavin-Containing Monooxygenases Involved in Biosynthesis of Aliphatic Glucosinolates. *Front Plant Sci* 7:1292.

65. Mittler R (2002) Oxidative stress, antioxidants and stress tolerance. Trends Plant Sci 7(9):405–410.

Tables and Figures

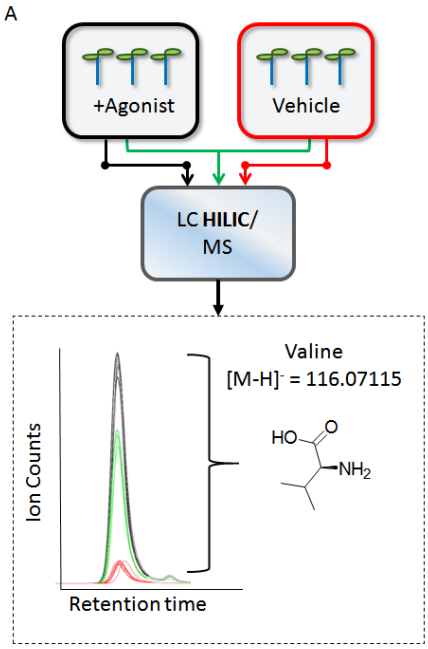

	Pyrabactin	Quinabactin	Hexabactin	ABA
PYR1	656	103	>10,000	307
PYL1	1,197	250	>10,000	301
PYL2	>10,000	267	>10,000	151
PYL3	>10,000	724	>10,000	70
PYL4	>10,000	>10,000	>10,000	68
PYL5	5,174	649	>10,000	27
PYL6	>10,000	>10,000	>10,000	29
PYL11	>10,000	>10,000	190	64
PYL12	nd	nd	nd	nd
PYL7	nd	nd	nd	nd
PYL9	>10,000	>10,000	38	60
PYL8	>10,000	>10,000	78	57
PYL10	1,892	>10,000	250	121

0.1

Figure 3.1. A) Diagram illustrating basic workflow of metabolomics approach. Black indicates agonist treatment, green indicates pooled, and red indicates vehicle control B) chemical structures of major agonists tested and phylogenetic tree of the ABA receptors along with each agonist's IC_{50} values. Green letters indicate an IC_{50} below 1,000 µM.

	ABA	Urano Drought	Quinabactin	Hexabactin
Proline	S	S	S	NS
Glutamic Acid	S	-	S	NS
Histidine	S	S	S	S
Valine	S	S	S	S
Asparagine	S	-	S	NS
Serine	S	-	S	NS
Arginine	NS	-	NS	NP
Methionine	S	S	S	NP
Phenylalanine	S	S	S	NS
Threonine	S	-	S	NS
Isoleucine/Leucine	S	S	S	S
Tryptophan	S	S	S	NP
Aspartic Acid	S	-	NS	S
Tyrosine	S	S	S	NP
GABA	NS	-	NS	S
Glutamine	S	S	S	NS

Table 0.1

Table 3.1 Verification of amino acids being regulated by ABA treatment in our method compared to Urano et al. Dark green/S = significantly regulated, defined by fold change ±20%, and a p-value ≤ 0.01. NS = not statistically significant, NP = not present or not identified by XCMSonline. Quinabactin and hexabactin are added for comparison.

	ABA on WT		ABA on *89*	
	Mean FC	-log(p-value)	Mean FC	-LOG(p-value)
Proline	**2.35**	**8.22**	**5.54**	**4.04**
Glutamic Acid	**1.21**	**3.62**	1.08	**0.21**
Histidine	**2.86**	**8.71**	**1.60**	**5.54**
Valine	**2.90**	**7.49**	**1.67**	**6.05**
Asparagine	**2.03**	**7.51**	**1.28**	**2.93**
Serine	**1.67**	**6.99**	**1.54**	**4.70**
Arginine	0.74	**0.80**	**0.61**	**3.44**
Methionine	**2.52**	**6.30**	**1.58**	**3.01**
Phenylalanine	**4.71**	**7.84**	**2.43**	**6.11**
Threonine	**2.44**	**9.98**	**1.69**	**2.90**
Isoleucine/Leucine	**3.73**	**7.69**	**2.55**	**4.79**
Tryptophan	**6.26**	**5.69**	**1.96**	**7.11**
Aspartic Acid	**1.54**	**7.31**	0.98	**0.06**
Tyrosine	**3.97**	**10.56**	**1.65**	**4.25**
GABA	0.93	**0.15**	**0.63**	**3.10**
Glutamine	**2.35**	**8.22**	**1.37**	**5.74**

Table 0.2

Table 3.2 Representative fold changes (FC) and –log(p-value) of the observed amino acids in ABA-treated WT and *89* plants. Dark green -log(p-values) indicate a significant difference defined by fold change ±20%, and a p-value ≤ 0.01. Mean fold changes are green if significantly upregulated, no color if no significance, or blue is down-regulated. The four differentially regulated metabolites between samples are highlighted in red. Notice that these are all special cases of amino acids. **Please see full Table 3.3**.

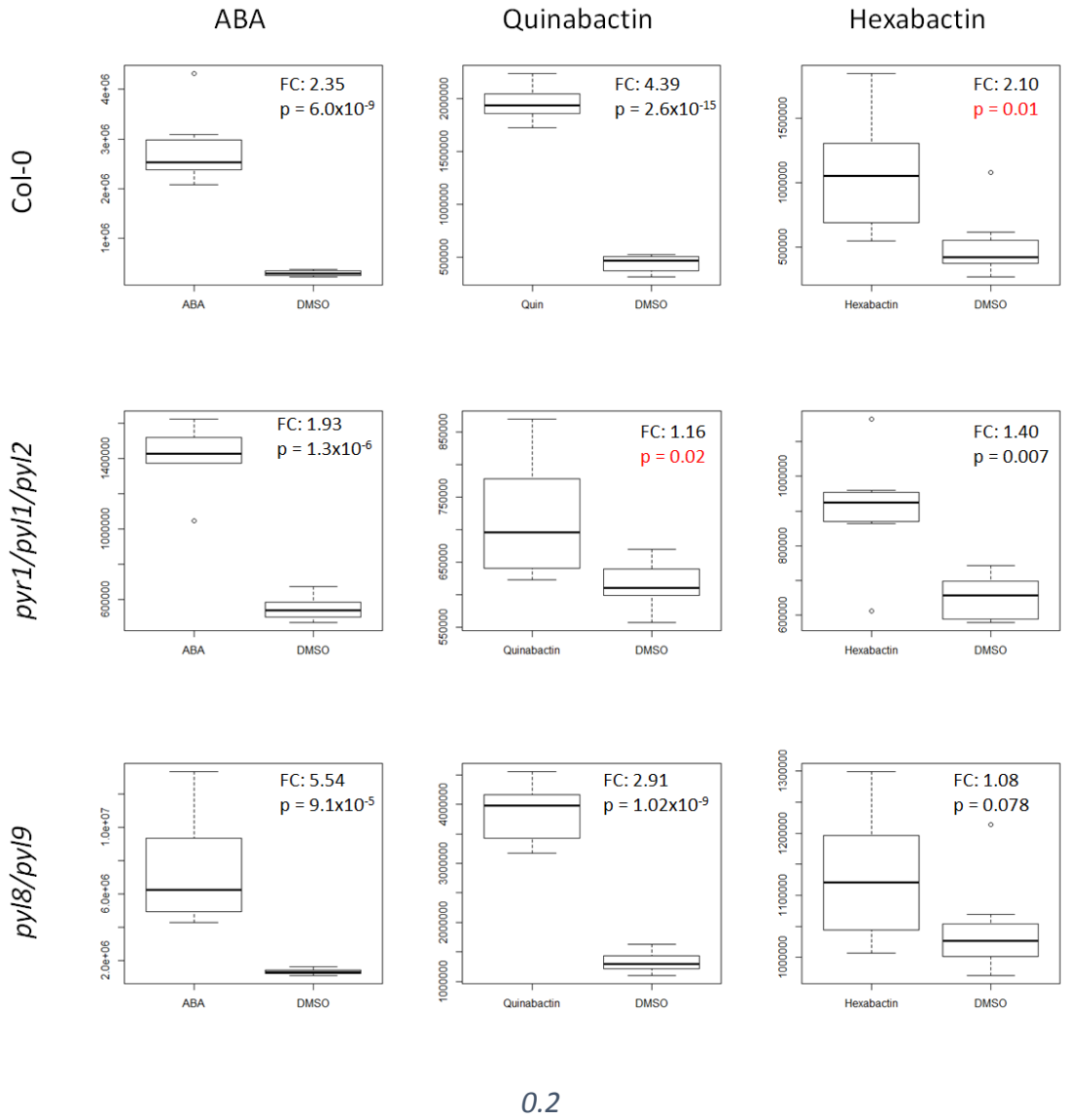

0.2

Figure 3.2 Boxplots of integrated peak area respective to proline in the indicated genetic backgrounds Col-0 (WT, top row), *012* mutant (middle row), *89* (bottom row) with ABA (left column), Quinabactin (middle column), and Hexabactin (Right column). FC = Fold change, red indicates not significantly different using our specified cutoff of $p < 0.01$.

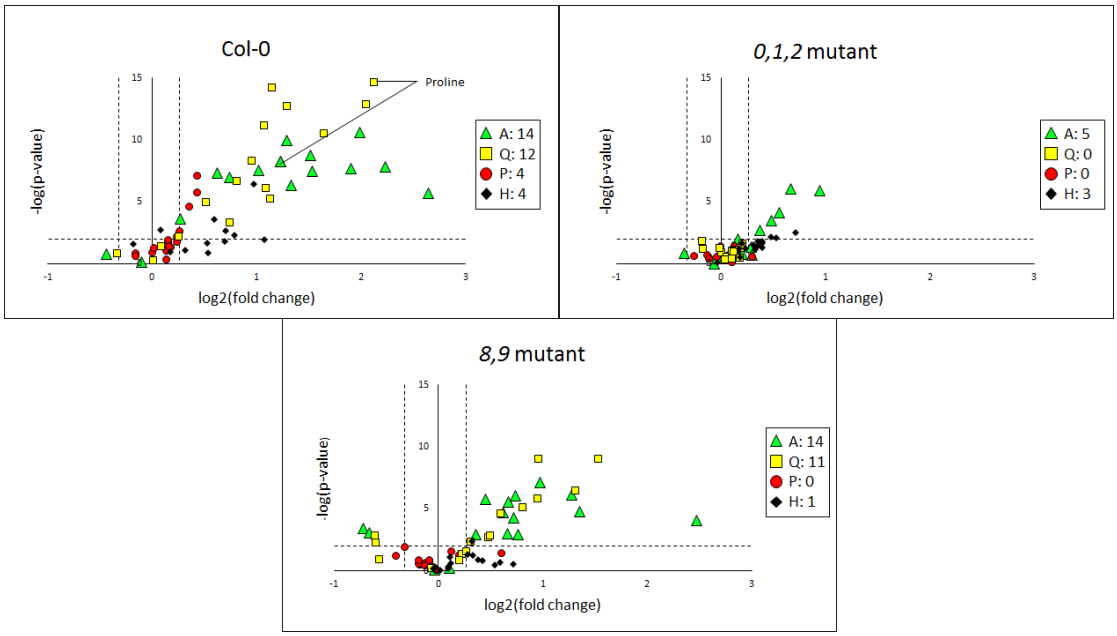

0.3

Figure 3.3 Volcano plots of identified amino acids (proline, glutamic acid, histidine, valine, asparagine, serine, arginine, methionine, phenylalanine, threonine, isoleucine/leucine, tryptophan, aspartic acid, tyrosine, GABA, glutamine) in LC/MS analysis of different genetic backgrounds following 24 hours of incubation on agar plates containing 20 µM of specified chemical. ABA ("A", green triangles), quinabactin ("Q", yellow squares), pyrabactin ("P", red circles), and hexabactin ("H", black diamonds) on Col-0 (WT, top left), *012* (top right), and *89* (bottom). Dotted lines indicate a fold change of = ±20%, and a p-value ≤ 0.01. Legend indicates number of significantly regulated amino acids from the 16 evaluated.

A

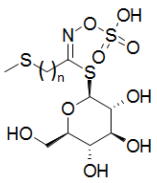

n = 4, Glucoerucin, GER
n = 5, Glucoberteroin, GBE
n = 6, Glucolesquerellin*, GLE
n = 7, 7-methylthioheptyl glucosinolate, 7MTG
n = 8, 8-methylthiooctyl glucosinolate, 8MTG

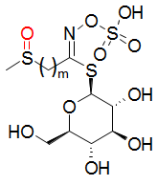

m = 4, Glucoraphanin, GRA
m = 5, Glucoalyssin*, GAL
m = 6, Glucohesperin*, GHE
m = 7, Glucoibarin*, GIB
m = 8, Glucohirsutin, GHI

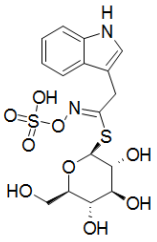

Glucobrassicin, GBR

0.4

Figure 3.4 Chemical structures of the aliphatic glucosinolates and the aromatic glucosinolate, glucobrassicin. Asterisks indicate low abundance, and were observed in all samples; glucoalyssin was never observed in my methodology.

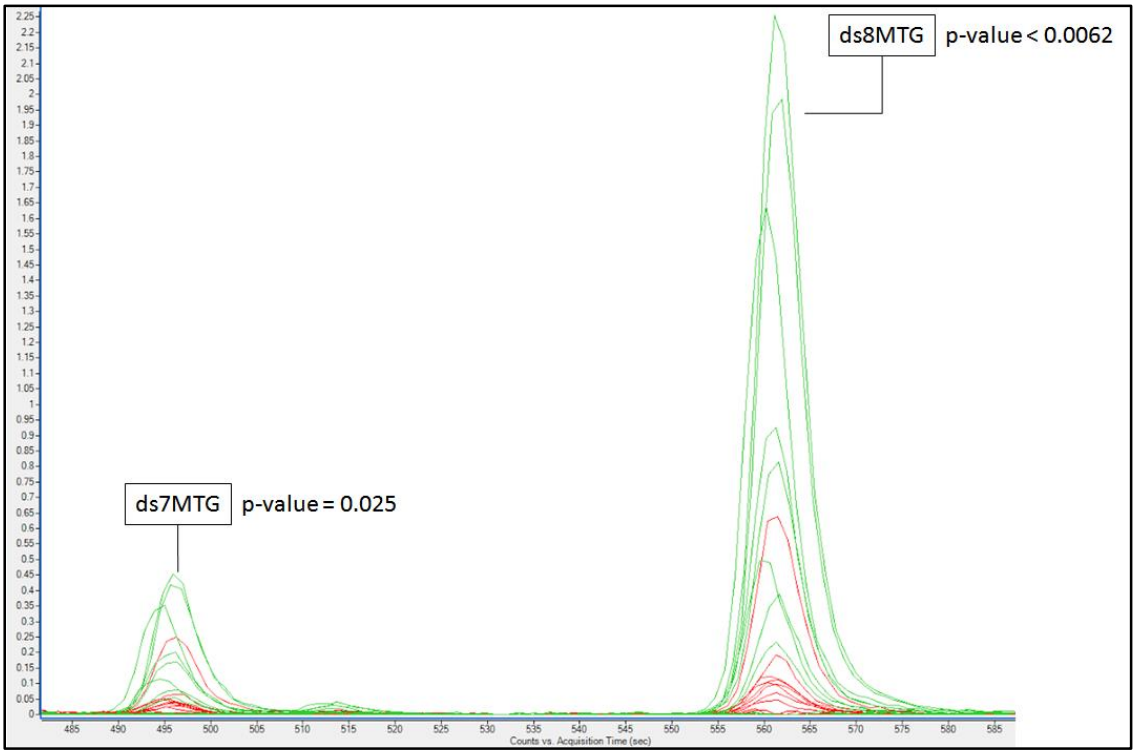

0.5

Figure 3.5 Extracted masses pertaining to desulfo-7-methylthioglucosinolate (ds7MTG) and desulfo-8-methylthioglucosinolate (ds8MTG). Green represents control-treatment and red indicates ABA treatment.

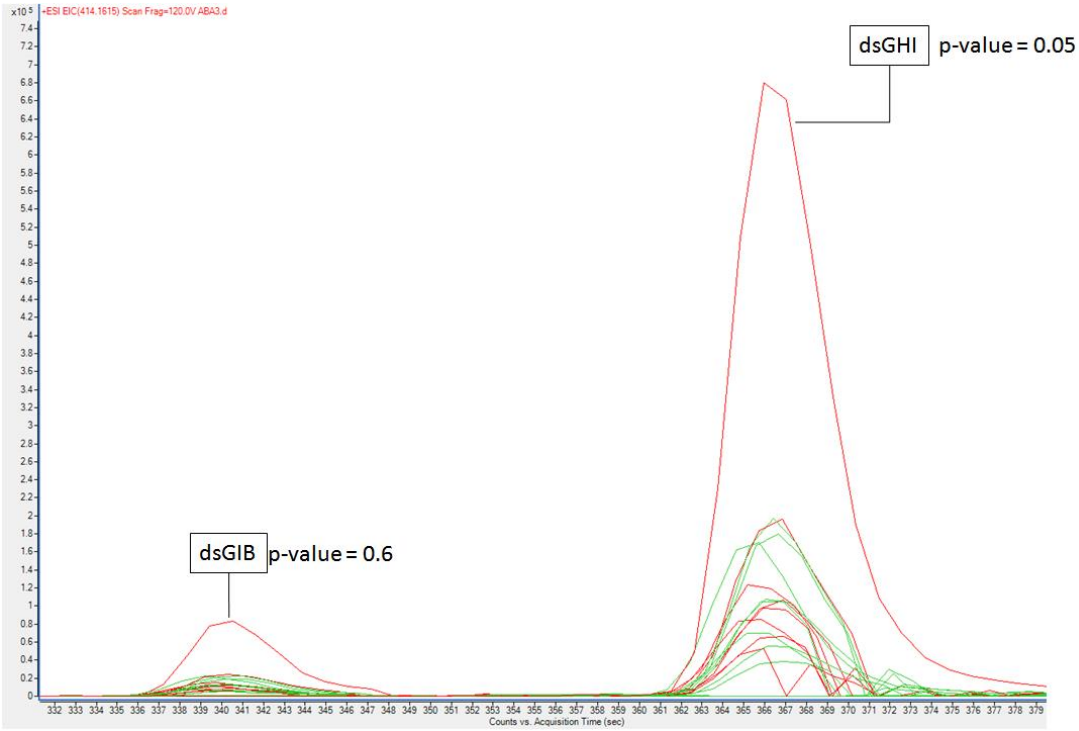

0.6

Figure 3.6 Extracted masses pertaining to desulfo-glucoibarin (dsGIB) and desulfo-glucohirsutin (dsGHI). Green represents control-treatment and red indicates ABA treatment.

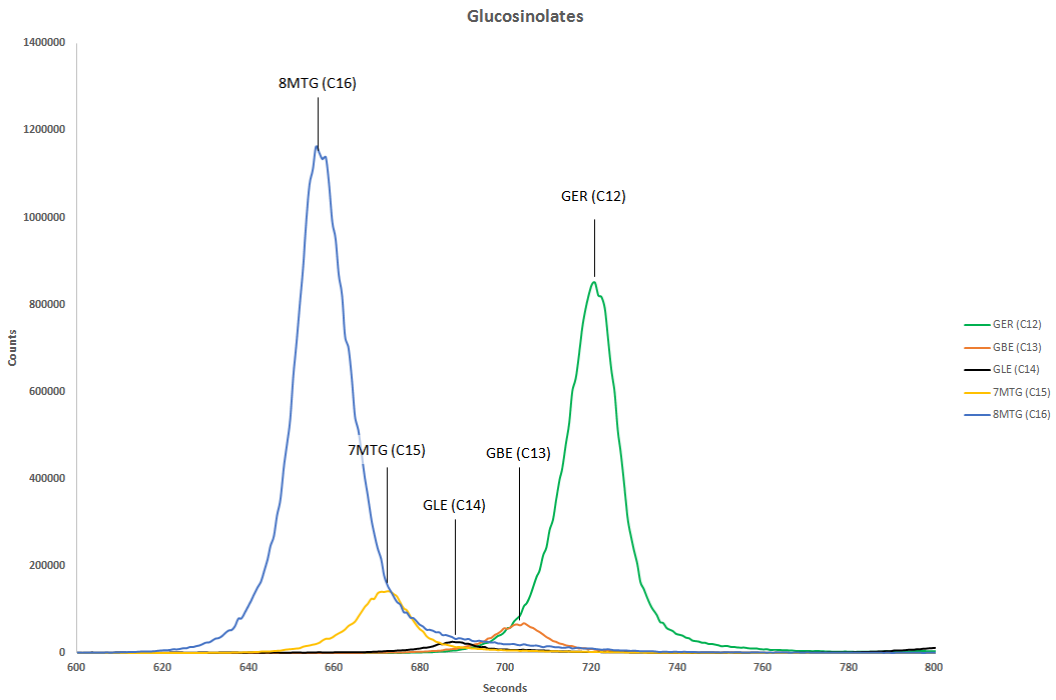

0.7

Figure 3.7 Retention time shifts of the iterative changes of carbon length observed with the thionyl glucosinolates. Carbon length is indicated in parentheses.

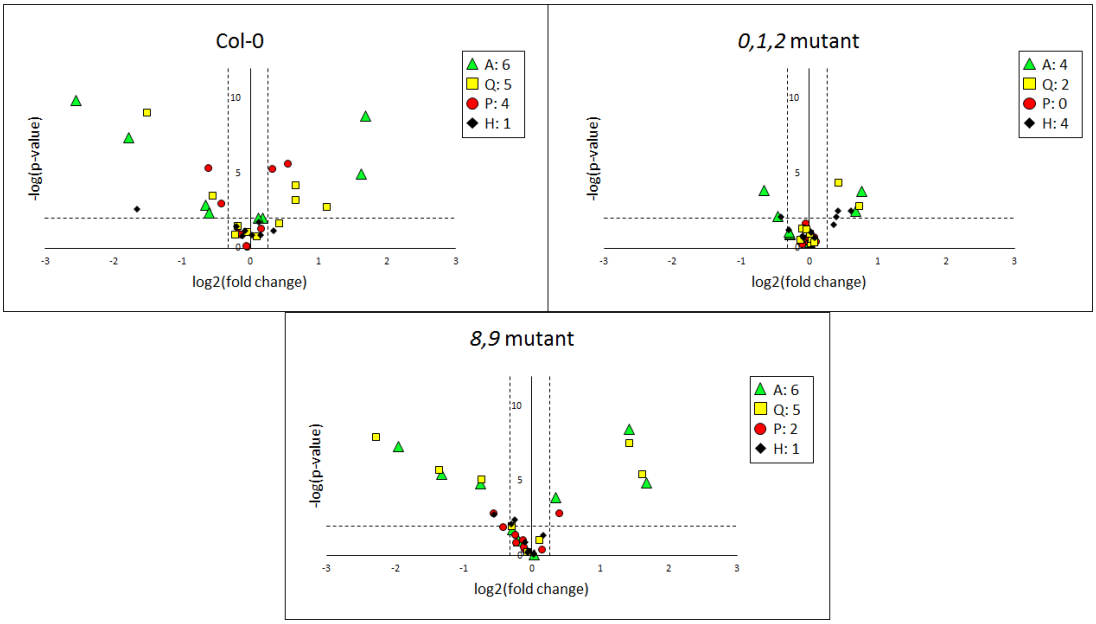

0.8

Figure 3.8 Volcano plots of identified glucosinolates in different genetic backgrounds following 24 hours of incubation on agar plates containing 20 µM of ABA on WT ("A", green triangles), quinabactin ("Q", yellow squares), pyrabactin ("P", red circles), or hexabactin ("H", black diamonds). Dotted lines indicate a fold change of = ±20%, and a p-value ≤ 0.01. Legend indicates the number of significantly regulated amino acids from the 16 evaluated.

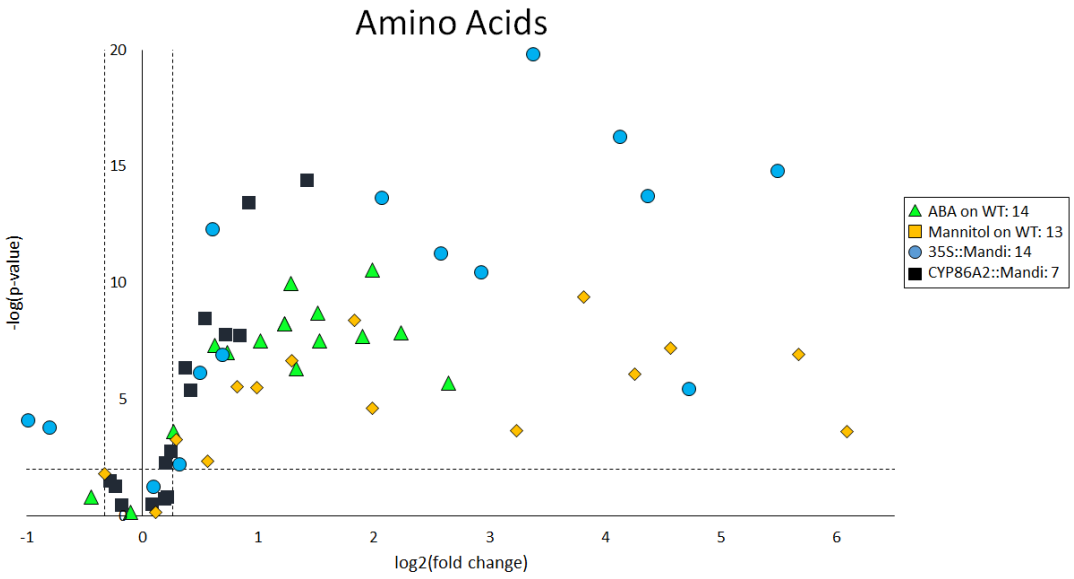

0.9

Figure 3.9 Volcano plot of amino acids as regulated by ABA on WT (green triangles), mannitol on WT (yellow diamonds), Mandipropamid on 35S::PYR1^{MANDI} (blue circles), Mandipropamid on pCYP86A2::Mandi (black squares). Dotted lines indicate a p value = 0.01 [-log(p-value) = 2], and fold changes either >1.20 or <0.80.

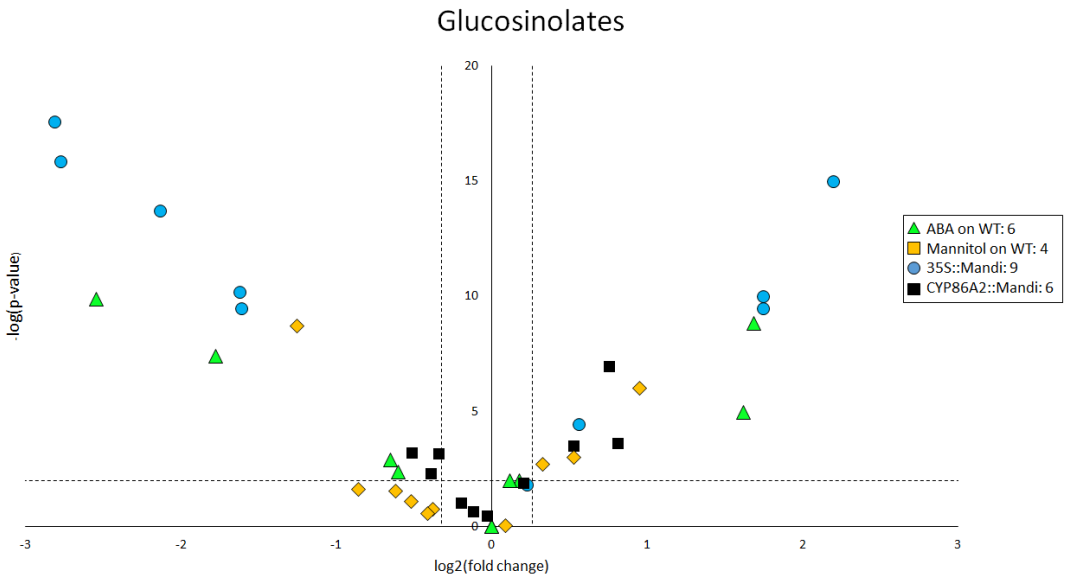

0.10

Figure 3.10 Volcano plot of glucosinolates as regulated by ABA on WT (green triangles), mannitol on WT (yellow diamonds), Mandipropamid on 35S::PYR1^{MANDI} (blue circles), Mandipropamid on pCYP86A2::PYR1^{MANDI} (black squares). Dotted lines indicate a p value = 0.01 [-log(p-value) = 2], and fold changes either >1.20 or <0.80.

Appendix

Appendix Tables 1-20

Treatment and genetic background indicated in top row. Dark green -log(p-values) indicate a significant difference defined by fold change ±20%, and a p-value ≤ 0.01. Mean fold changes are green if significantly upregulated, no color if no significance, or blue is down-regulated.

			ABA on WT					
	Formula	MW	Average RT	log2(fc)	Mean FC	log(p-value)	p-value	q-value
Proline	C5H9NO2	114.0561	788.905	1.23	**2.35**	8.22	**6.02E-09**	6.82E-08
Glutamic Acid	C5H9NO4	146.0459	1167.295	0.27	**1.21**	3.62	**0.000238494**	0.000348446
Histidine	C6H9N3O2	154.0622	829.56	1.51	**2.86**	8.71	**1.95E-09**	2.91E-08
Valine	C5H11NO2	116.0717	668.24	1.54	**2.90**	7.49	**3.23E-08**	2.22E-07
Asparagine	C4H8N2O3	131.0462	815.525	1.02	**2.03**	7.51	**3.06E-08**	2.14E-07
Serine	C3 H7 N O3	104.0353	811.6	0.74	**1.67**	6.99	**1.03E-07**	5.36E-07
Arginine	C6H14N4O2	173.1044	869.225	-0.44	0.74	0.80	0.158120599	0.059976467
Methionine	C5H11NO2S	148.0438	688.93	1.33	**2.52**	6.30	**4.99E-07**	1.92E-06
Phenylalanine	C9H11NO2	164.0717	679.37	2.24	**4.71**	7.84	**1.46E-08**	1.22E-07
Threonine	C4H9NO3	118.051	774.495	1.29	**2.44**	9.98	**1.06E-10**	3.63E-09
Isoleucine/Leucine	C6H13NO2	130.0874	621.07	1.90	**3.73**	7.69	**2.03E-08**	1.54E-07
Tryptophan	C11H12N2O2	203.0826	Low	2.65	**6.26**	5.69	**2.05E-06**	6.29E-06
Aspartic Acid	C4H7NO4	132.0302	1165.03	0.63	**1.54**	7.31	**4.91E-08**	2.99E-07
Tyrosine	C9H11NO3	180.0666	NP	1.99	**3.97**	10.56	**2.74E-11**	1.29E-09
GABA	C4H9NO2	102.0561	797.395	-0.10	0.93	0.15	0.712207384	0.184290035
Glutamine	C5H10N2O3	145.0619	794.02	1.20	**2.30**	8.59	**2.57E-09**	6.82E-08

Appendix Table 1

			ABA on 012					
	Formula	MW	Average RT	log2(fc)	Mean FC	log(p-value)	p-value	q-value
Proline	C5H9NO2	114.0561	699.24	0.95	1.93	5.88	1.32E-06	3.81E-05
Glutamic Acid	C5H9NO4	146.0459	938.035	-0.07	0.96	0.02	0.947227571	0.523798619
Histidine	C6H9N3O2	154.0622	865.46	0.37	1.29	2.69	0.002034402	0.014314828
Valine	C5H11NO2	116.0717	667.56	0.16	1.12	2.01	0.009733989	0.04421431
Asparagine	C4H8N2O3	131.0462	816.79	0.48	1.39	3.45	0.000356033	0.003585266
Serine	C3 H7 N O3	104.0353	813.58	0.11	1.08	1.37	0.042264173	0.112114931
Arginine	C6H14N4O2	173.1044	872.82	0.20	1.15	0.76	0.175062314	0.216950179
Methionine	C5H11NO2S	148.0438	Low	#NUM!		#NUM!		
Phenylalanine	C9H11NO2	164.0717	676.05	0.67	1.59	6.05	8.90E-07	2.90E-05
Threonine	C4H9NO3	118.051	777.6	0.14	1.10	1.33	0.047272948	0.11900999
Isoleucine/Leucine	C6H13NO2	130.0874	error	#NUM!		#NUM!		
Tryptophan	C11H12N2O2	203.0826	684.485	0.29	1.22	1.32	0.047601784	0.119480113
Aspartic Acid	C4H7NO4	132.0302	1177.38	0.30	1.23	0.72	0.191511016	0.227321145
Tyrosine	C9H11NO3	180.0666	751.535	-0.04	0.97	0.41	0.388437973	0.340804855
GABA	C4H9NO2	102.0561	798.71	-0.35	0.79	0.87	0.13569969	0.19521426
Glutamine	C5H10N2O3	145.0619	788.44	0.56	1.48	4.14	7.27E-05	0.001091414

Appendix Table 2

			ABA on 89					
	Formula	MW	Average RT	log2(fc)	Mean FC	log(p-value)	p-value	q-value
Proline	C5H9NO2	114.0561	610.33	2.47	5.54	4.04	0.0000916	0.156141264
Glutamic Acid	C5H9NO4	146.0459	1061.59	0.11	1.08	0.21	0.617050862	0.77843344
Histidine	C6H9N3O2	154.0622	771.71	0.67	1.60	5.54	0.00000288	0.787430025
Valine	C5H11NO2	116.0717	591.71	0.74	1.67	6.05	0.000000899	0.830836881
Asparagine	C4H8N2O3	131.0462	762.83	0.36	1.28	2.93	0.001164843	0.805238251
Serine	C3 H7 N O3	104.0353	758.82	0.62	1.54	4.70	0.0000201	0.808273199
Arginine	C6H14N4O2	173.1044	795.045	-0.72	0.61	3.44	0.000359108	0.828412538
Methionine	C5H11NO2S	148.0438	613.88	0.66	1.58	3.01	0.000988361	0.830895423
Phenylalanine	C9H11NO2	164.0717	605.63	1.28	2.43	6.11	0.000000776	0.80179055
Threonine	C4H9NO3	118.051	717.96	0.76	1.69	2.90	0.001272977	0.830894172
Isoleucine/Leucine	C6H13NO2	130.0874	541.94	1.35	2.55	4.79	0.0000163	0.312101357
Tryptophan	C11H12N2O2	203.0826	622.14	0.97	1.96	7.11	7.85E-08	0.11280087
Aspartic Acid	C4H7NO4	132.0302	1060.81	-0.03	0.98	0.06	0.876767511	0.830890822
Tyrosine	C9H11NO3	180.0666	695.21	0.72	1.65	4.25	0.0000557	0.382880258
GABA	C4H9NO2	102.0561	739.92	-0.66	0.63	3.10	0.000796285	0.570557593
Glutamine	C5H10N2O3	145.0619	736.11	0.45	1.37	5.74	0.00000181	0.826075179

Appendix Table 3

			ABA on abi1					
	Formula	MW	Average RT	log2(fc)	Mean FC	log(p-value)	p-value	q-value
Proline	C5H9NO2	114.0561	630.87	1.49	**2.81**	12.06	**8.66E-13**	0.844480873
Glutamic Acid	C5H9NO4	146.0459	890.39	0.40	**1.32**	4.71	**0.0000196**	0.844474534
Histidine	C6H9N3O2	154.0622	799.03	0.70	**1.62**	7.38	**4.19E-08**	0.844480859
Valine	C5H11NO2	116.0717	605.82	0.58	**1.49**	6.63	**0.000000235**	0.844480797
Asparagine	C4H8N2O3	131.0462	769.84	0.62	**1.54**	8.35	**4.5E-09**	0.844480871
Serine	C3 H7 N O3	104.0353	858.19	0.73	**1.65**	10.43	**3.75E-11**	0.844480873
Arginine	C6H14N4O2	173.1044	806.73	-0.36	**0.78**	2.24	**0.005707969**	0.842613538
Methionine	C5H11NO2S	148.0438	630.6	0.63	**1.55**	5.97	**0.00000108**	0.844480525
Phenylalanine	C9H11NO2	164.0717	624.2	0.93	**1.90**	8.40	**3.94E-09**	0.844480872
Threonine	C4H9NO3	118.051	726.05	0.51	**1.43**	4.30	**0.0000497**	0.844464794
Isoleucine/Leucine	C6H13NO2	130.0874	564.51	0.80	**1.75**	2.03	**0.009276081**	0.841423562
Tryptophan	C11H12N2O2	203.0826	640.24	0.53	**1.44**	6.87	**0.000000134**	0.844480829
Aspartic Acid	C4H7NO4	132.0302	1082.1	0.16	1.12	0.25	0.56520678	0.306027405
Tyrosine	C9H11NO3	180.0666	706.835	0.00	1.00	0.00	0.993799995	0.082333666
GABA	C4H9NO2	102.0561	752.76	-0.33	0.80	1.10	0.080011464	0.813828117
Glutamine	C5H10N2O3	145.0619	742.26	0.52	**1.43**	8.32	**4.79E-09**	0.844480871

Appendix Table 4

			Pyrabactin on WT					
	Formula	MW	Average RT	log2(fc)	Mean FC	log(p-value)	p-value	q-value
Proline	C5H9NO2	114.0561	645.59	0.36	**1.29**	4.51	**3.07E-05**	0.847344583
Glutamic Acid	C5H9NO4	146.0459	1095.11	0.01	1.01	0.82	0.152236861	0.750465369
Histidine	C6H9N3O2	154.0622	796.19	0.19	1.14	1.25	0.056158655	0.820230313
Valine	C5H11NO2	116.0717	625.18	0.16	1.12	1.67	0.021424554	0.837961826
Asparagine	C4H8N2O3	131.0462	788.30	0.25	1.19	1.71	0.019319431	0.838933894
Serine	C3 H7 N O3	104.0353	785.08	0.27	**1.21**	2.53	**0.002968701**	0.846119462
Arginine	C6H14N4O2	173.1044	811.80	0.14	1.10	0.28	0.523505683	0.166140028
Methionine	C5H11NO2S	148.0438	645.66	-0.15	0.90	0.80	0.157445505	0.745624274
Phenylalanine	C9H11NO2	164.0717	638.47	0.14	1.11	0.99	0.10160631	0.79150031
Threonine	C4H9NO3	118.051	744.09	0.02	1.02	1.20	0.06291073	0.816384987
Isoleucine/Leucine	C6H13NO2	130.0874	569.55	0.44	**1.36**	7.05	**8.98E-08**	0.84735726
Tryptophan	C11H12N2O2	203.0826	653.25	0.16	1.12	1.86	0.013883991	0.84139334
Aspartic Acid	C4H7NO4	132.0302	1094.40	0.24	**1.18**	2.16	**0.006926132**	0.844438116
Tyrosine	C9H11NO3	180.0666	722.82	0.44	**1.36**	5.66	**2.19E-06**	0.847356392
GABA	C4H9NO2	102.0561	765.22	-0.15	0.90	0.59	0.257064048	0.627052057
Glutamine	C5H10N2O3	145.0619	761.40	0.17	1.12	1.37	0.042499656	0.827598869

Appendix Table 5

			Pyrabactin on 012					
	Formula	MW	Average RT	log2(fc)	Mean FC	log(p-value)	p-value	q-value
Proline	C5H9NO2	114.0561	683.67	0.06	1.04	0.42	0.377230369	0.197108204
Glutamic Acid	C5H9NO4	146.0459	1127.95	0.12	1.09	1.01	0.097741175	0.118303872
Histidine	C6H9N3O2	154.0622	827.815	-0.03	0.98	0.47	0.33861852	0.191580458
Valine	C5H11NO2	116.0717	657.655	0.07	1.05	0.58	0.26326801	0.178724068
Asparagine	C4H8N2O3	131.0462	804.94	0.06	1.04	0.45	0.351312191	0.193336177
Serine	C3 H7 N O3	104.0353	800.845	0.10	1.07	0.60	0.250026699	0.175914507
Arginine	C6H14N4O2	173.1044	830.765	-0.25	0.84	0.59	0.255090321	0.177012739
Methionine	C5H11NO2S	148.0438	674.18	-0.10	0.93	0.40	0.401841041	0.201756239
Phenylalanine	C9H11NO2	164.0717	662.475	-0.12	0.92	0.65	0.222407247	0.169341673
Threonine	C4H9NO3	118.051	744.965	0.14	1.10	1.32	0.04795252	0.075919793
Isoleucine/Leucine	C6H13NO2	130.0874	605.4	0.11	1.08	0.09	0.821109537	0.286674057
Tryptophan	C11H12N2O2	203.0826	674.595	-0.10	0.93	0.33	0.470556553	0.215490995
Aspartic Acid	C4H7NO4	132.0302	1127.22	0.00	1.00	1.37	0.042450036	0.069576775
Tyrosine	C9H11NO3	180.0666	737.91	0.07	1.05	0.57	0.270273864	0.180132192
GABA	C4H9NO2	102.0561	786.49	0.31	1.24	0.50	0.314071606	0.18788967
Glutamine	C5H10N2O3	145.0619	782.04	0.14	1.10	0.76	0.174529274	0.154963032

Appendix Table 6

			Pyrabactin on 89					
	Formula	MW	Average RT	log2(fc)	Mean FC	log(p-value)	p-value	q-value
Proline	C5H9NO2	114.0561	611.79	-0.01	0.99	0.03	0.93511692	0.01422344
Glutamic Acid	C5H9NO4	146.0459	1061.49	-0.17	0.89	0.41	0.388865385	0.675400527
Histidine	C6H9N3O2	154.0622	771.71	-0.08	0.95	0.56	0.275990634	0.552007755
Valine	C5H11NO2	116.0717	591.61	-0.01	1.00	0.03	0.937606036	0.686741575
Asparagine	C4H8N2O3	131.0462	762.66	-0.04	0.98	0.20	0.632301218	0.111324577
Serine	C3 H7 N O3	104.0353	758.82	0.21	1.15	1.23	0.058639739	0.686786677
Arginine	C6H14N4O2	173.1044	795.01	-0.18	0.88	0.54	0.289137446	0.629019199
Methionine	C5H11NO2S	148.0438	614.19	-0.31	0.81	1.86	0.013757035	0.025105306
Phenylalanine	C9H11NO2	164.0717	605.93	-0.12	0.92	0.58	0.261083188	0.030005458
Threonine	C4H9NO3	118.051	718.06	-0.18	0.89	0.77	0.169869906	0.686720032
Isoleucine/Leucine	C6H13NO2	130.0874	541.585	0.61	1.53	1.34	0.046022838	0.686284686
Tryptophan	C11H12N2O2	203.0826	623.33	-0.02	0.99	0.11	0.774563307	0.01422344
Aspartic Acid	C4H7NO4	132.0302	1060.55	-0.40	0.76	1.12	0.075700521	0.685190625
Tyrosine	C9H11NO3	180.0666	695.32	0.14	1.10	1.50	0.031435934	0.256839423
GABA	C4H9NO2	102.0561	739.91	-0.12	0.92	0.38	0.41268224	0.669223271
Glutamine	C5H10N2O3	145.0619	736.13	-0.08	0.94	0.78	0.164808599	0.678660991

Appendix Table 7

			Quinabactin on WT					
	Formula	MW	Average RT	log2(fc)	Mean FC	log(p-value)	p-value	q-value
Proline	C5H9NO2	114.0561	692.43	2.13	4.39	14.58	2.63E-15	1.33E-12
Glutamic Acid	C5H9NO4	146.0459	941.44	0.26	1.20	2.14	0.007246036	0.009373577
Histidine	C6H9N3O2	154.0622	826.69	1.10	2.14	6.03	0.000000944	0.00000511
Valine	C5H11NO2	116.0717	670.22	0.96	1.95	8.27	5.37E-09	6.65E-08
Asparagine	C4H8N2O3	131.0462	818.5	0.75	1.68	3.29	0.000513932	0.001189051
Serine	C3 H7 N O3	104.0353	816.52	0.52	1.44	4.91	1.23E-05	4.81E-05
Arginine	C6H14N4O2	173.1044	867.54	0.02	1.01	0.22	0.608573139	0.233239738
Methionine	C5H11NO2S	148.0438	686.63	1.15	2.23	14.17	6.75E-15	2.26E-12
Phenylalanine	C9H11NO2	164.0717	675.73	1.29	2.45	12.62	2.38E-13	1.84E-11
Threonine	C4H9NO3	118.051	779.22	1.08	2.11	11.12	7.62E-12	2.64E-10
Isoleucine/Leucine	C6H13NO2	130.0874	622.86	1.14	2.20	5.17	6.78E-06	2.82E-05
Tryptophan	C11H12N2O2	203.0826	682.73	1.65	3.14	10.48	3.33E-11	9.32E-10
Aspartic Acid	C4H7NO4	132.0302	1162.85	0.10	1.07	1.35	0.044622987	0.037739502
Tyrosine	C9H11NO3	180.0666	571.54	2.06	4.16	12.80	1.57E-13	1.58E-11
GABA	C4H9NO2	102.0561	800.16	-0.33	0.80	0.78	0.167290604	0.097547298
Glutamine	C5H10N2O3	145.0619	793.77	0.81	1.76	6.58	2.66E-07	1.68E-06

Appendix Table 8

			Quinabactin on 012					
	Formula	MW	Average RT	log2(fc)	Mean FC	log(p-value)	p-value	q-value
Proline	C5H9NO2	114.0561	666.85	0.22	1.16	1.58	0.026398301	0.091527566
Glutamic Acid	C5H9NO4	146.0459	914.86	-0.16	0.89	1.11	0.07774693	0.127110916
Histidine	C6H9N3O2	154.0622	841.05	0.15	1.11	0.56	0.272988653	0.205953795
Valine	C5H11NO2	116.0717	642.82	0.13	1.10	0.81	0.155434164	0.158600823
Asparagine	C4H8N2O3	131.0462	811.43	0.14	1.10	0.71	0.196485064	0.17424912
Serine	C3 H7 N O3	104.0353	806.98	0.19	1.14	1.18	0.066375732	0.122584483
Arginine	C6H14N4O2	173.1044	831.3	0.19	1.14	0.45	0.354395419	0.238834708
Methionine	C5H11NO2S	148.0438	658.64	0.01	1.01	0.86	0.136997879	0.15289957
Phenylalanine	C9H11NO2	164.0717	642.01	0.14	1.10	1.03	0.092609509	0.135280541
Threonine	C4H9NO3	118.051	771.67	0.06	1.04	0.47	0.338127488	0.232753307
Isoleucine/Leucine	C6H13NO2	130.0874	582.08	0.11	1.08	0.96	0.110682758	0.143621094
Tryptophan	C11H12N2O2	203.0826	655.77	0.13	1.09	0.91	0.122778896	0.148234823
Aspartic Acid	C4H7NO4	132.0302	1112.17	-0.17	0.89	1.77	0.016982713	0.081901042
Tyrosine	C9H11NO3	180.0666	861.6	-0.01	1.00	1.20	0.063497166	0.121246223
GABA	C4H9NO2	102.0561	786.65	0.12	1.08	0.36	0.440027058	0.27498112
Glutamine	C5H10N2O3	145.0619	785.86	0.04	1.03	0.30	0.506865341	0.300624021

Appendix Table 9

			Quinabactin on 89					
	Formula	MW	Average RT	log2(fc)	Mean FC	log(p-value)	p-value	q-value
Proline	C5H9NO2	114.0561	609.51	1.54	**2.91**	8.99	**1.02E-09**	0.089402904
Glutamic Acid	C5H9NO4	146.0459	1061.65	-0.07	0.96	0.14	0.728887476	0.824726588
Histidine	C6H9N3O2	154.0622	771.67	0.48	**1.40**	2.65	**0.002254582**	0.178784122
Valine	C5H11NO2	116.0717	591.49	0.81	**1.76**	5.09	**0.00000811**	0.836255997
Asparagine	C4H8N2O3	131.0462	762.66	0.23	1.18	1.29	0.051393928	0.108014808
Serine	C3 H7 N O3	104.0353	758.82	0.61	**1.52**	4.58	**0.0000266**	0.551402411
Arginine	C6H14N4O2	173.1044	795.01	-0.59	**0.66**	2.18	**0.006552786**	0.063892755
Methionine	C5H11NO2S	148.0438	613.34	0.27	1.21	1.51	0.030649811	0.836250787
Phenylalanine	C9H11NO2	164.0717	605.12	0.95	**1.94**	5.76	**0.00000173**	0.824368579
Threonine	C4H9NO3	118.051	717.96	0.50	**1.42**	2.82	**0.001530759**	0.836255988
Isoleucine/Leucine	C6H13NO2	130.0874	1243.98	0.21	1.15	0.81	0.156232086	0.754246275
Tryptophan	C11H12N2O2	203.0826	621.8	1.32	**2.50**	6.42	**0.000000383**	0.662441243
Aspartic Acid	C4H7NO4	132.0302	1216.74	-0.56	**0.68**	0.84	0.143385619	0.835941192
Tyrosine	C9H11NO3	180.0666	695.22	0.97	**1.96**	8.97	**1.08E-09**	0.040289584
GABA	C4H9NO2	102.0561	739.92	-0.60	**0.66**	2.79	**0.001623393**	0.836255822
Glutamine	C5H10N2O3	145.0619	736.13	0.31	**1.24**	2.31	**0.004874102**	0.058327936

Appendix Table 10

			Quinabactin on abi1					
	Formula	MW	Average RT	log2(fc)	Mean FC	log(p-value)	p-value	q-value
Proline	C5H9NO2	114.0561	640.12	0.98	**1.97**	5.59	**0.00000258**	0.832654478
Glutamic Acid	C5H9NO4	146.0459	1071.12	0.28	1.22	1.95	0.011231902	0.828568578
Histidine	C6H9N3O2	154.0622	786.585	0.53	**1.44**	3.31	**0.000488299**	0.832481741
Valine	C5H11NO2	116.0717	608.7	0.54	**1.45**	4.12	**0.0000752**	0.83262867
Asparagine	C4H8N2O3	131.0462	773.63	0.47	**1.39**	2.99	**0.001017597**	0.832293101
Serine	C3 H7 N O3	104.0353	771.42	0.72	**1.65**	5.62	**0.00000239**	0.832654547
Arginine	C6H14N4O2	173.1044	813.77	0.14	1.10	0.26	0.55044591	0.281119854
Methionine	C5H11NO2S	148.0438	628.33	0.17	1.12	0.77	0.17049636	0.744584081
Phenylalanine	C9H11NO2	164.0717	620.31	0.55	**1.46**	3.69	**0.000206187**	0.832582113
Threonine	C4H9NO3	118.051	730.49	0.83	**1.78**	5.89	**0.00000128**	0.832654939
Isoleucine/Leucine	C6H13NO2	130.0874	548.05	0.49	**1.40**	3.79	**0.000160842**	0.832598234
Tryptophan	C11H12N2O2	203.0826	636.68	0.64	**1.55**	4.23	**0.0000591**	0.832634398
Aspartic Acid	C4H7NO4	132.0302	1070.44	0.37	**1.30**	2.37	**0.004238194**	0.831136111
Tyrosine	C9H11NO3	180.0666	706.68	0.58	**1.49**	4.87	**0.0000135**	0.832650591
GABA	C4H9NO2	102.0561	1071.13	0.29	**1.22**	2.07	**0.008552495**	0.829561241
Glutamine	C5H10N2O3	145.0619	747.18	0.45	**1.36**	3.45	**0.000353548**	0.832529699

Appendix Table 11

			ASV78 on WT					
	Formula	MW	Average RT	log2(fc)	Mean FC	log(p-value)	p-value	q-value
Proline	C5H9NO2	114.0561	705.03	1.07	2.10	1.97	0.010763166	0.0169364
Glutamic Acid	C5H9NO4	146.0459	1205.23	-0.18	0.88	1.62	0.024225878	0.03073097
Histidine	C6H9N3O2	154.0622	841.54	0.60	**1.51**	3.59	**0.000254448**	0.000928589
Valine	C5H11NO2	116.0717	676.7	0.71	**1.63**	2.68	**0.002072297**	0.004977982
Asparagine	C4H8N2O3	131.0462	830.64	0.31	1.24	1.09	0.081453471	0.072981366
Serine	C3 H7 N O3	104.0353	852.34	0.54	1.45	0.90	0.125268443	0.098886171
Arginine	C6H14N4O2	173.1044	low	#NUM!		#NUM!		
Methionine	C5H11NO2S	148.0438	low	#NUM!		#NUM!		
Phenylalanine	C9H11NO2	164.0717	680.33	0.70	1.62	1.82	0.015203047	0.021923157
Threonine	C4H9NO3	118.051	790.86	0.52	1.44	1.68	0.020678868	0.027138561
Isoleucine/Leucine	C6H13NO2	130.0874	639.24	0.97	**1.96**	6.43	**3.74E-07**	4.93E-06
Tryptophan	C11H12N2O2	203.0826		#NUM!		#NUM!		
Aspartic Acid	C4H7NO4	132.0302	1162.955	0.08	1.06	2.73	**0.001862568**	0.004566668
Tyrosine	C9H11NO3	180.0666		#NUM!		#NUM!		
GABA	C4H9NO2	102.0561	815.07	0.79	**1.73**	2.29	**0.005133402**	0.00992024
Glutamine	C5H10N2O3	145.0619	806.22	0.18	1.13	0.97	0.106433224	0.087615916

Appendix Table 12

			ASV78 on 012					
	Formula	MW	Average RT	log2(fc)	Mean FC	log(p-value)	p-value	q-value
Proline	C5H9NO2	114.0561	677	0.48	**1.40**	2.17	**0.006767182**	0.009548508
Glutamic Acid	C5H9NO4	146.0459	1129.84	0.40	1.32	1.79	0.016095167	0.013567704
Histidine	C6H9N3O2	154.0622	829.4	0.36	1.28	1.42	0.037850688	0.019314617
Valine	C5H11NO2	116.0717	656.04	0.31	1.24	1.51	0.03101505	0.017944483
Asparagine	C4H8N2O3	131.0462	808.85	0.40	1.32	1.65	0.02237194	0.015693673
Serine	C3 H7 N O3	104.0353	804.42	0.53	**1.45**	2.11	**0.007780135**	0.010076812
Arginine	C6H14N4O2	173.1044	826.21	-0.03	0.98	0.11	0.772990994	0.117847401
Methionine	C5H11NO2S	148.0438	673.44	0.39	1.31	1.30	0.050094487	0.021445425
Phenylalanine	C9H11NO2	164.0717	659.82	0.71	**1.64**	2.50	**0.003133967**	0.006981863
Threonine	C4H9NO3	118.051	Low	#NUM!		#NUM!		
Isoleucine/Leucine	C6H13NO2	130.0874	604.55	0.23	1.18	1.24	0.057953805	0.022500447
Tryptophan	C11H12N2O2	203.0826	672.66	0.33	1.25	1.20	0.062824122	0.023166141
Aspartic Acid	C4H7NO4	132.0302	1128.35	0.20	1.15	1.69	0.02050161	0.01509644
Tyrosine	C9H11NO3	180.0666	739.32	0.17	1.13	1.21	0.062294228	0.023081816
GABA	C4H9NO2	102.0561	786.225	0.18	1.13	0.51	0.310048286	0.057018503
Glutamine	C5H10N2O3	145.0619	784.13	0.36	1.28	1.79	0.016236684	0.013615442

Appendix Table 13

			ASV78 on 89					
	Formula	MW	Average RT	log2(fc)	Mean FC	log(p-value)	p-value	q-value
Proline	C5H9NO2	114.0561	636.61	0.11	1.08	1.10	0.078727357	0.796804239
Glutamic Acid	C5H9NO4	146.0459	1069.48	-0.03	0.98	0.29	0.516523273	0.101183131
Histidine	C6H9N3O2	154.0622	784.03	0.59	1.51	0.66	0.218939334	0.639072546
Valine	C5H11NO2	116.0717	607.11	0.09	1.07	0.31	0.485714005	0.138588118
Asparagine	C4H8N2O3	131.0462	771.37	0.28	1.22	1.34	0.045352474	0.819539659
Serine	C3 H7 N O3	104.0353	769.25	0.32	1.25	2.42	**0.003822582**	0.842219858
Arginine	C6H14N4O2	173.1044	812.03	0.09	1.07	0.21	0.61883743	0.032329555
Methionine	C5H11NO2S	148.0438	627.26	0.12	1.09	0.60	0.251964502	0.584077761
Phenylalanine	C9H11NO2	164.0717	619.12	0.38	1.30	0.91	0.122792349	0.759219218
Threonine	C4H9NO3	118.051	Low	#NUM!		#NUM!		
Isoleucine/Leucine	C6H13NO2	130.0874	544.815	0.54	1.45	0.48	0.331146865	0.428154192
Tryptophan	C11H12N2O2	203.0826	635.76	0.42	1.34	0.85	0.14225117	0.739436581
Aspartic Acid	C4H7NO4	132.0302	1068.75	0.02	1.01	0.06	0.863033765	0.001770103
Tyrosine	C9H11NO3	180.0666	703.725	0.72	1.64	0.54	0.291648447	0.509351933
GABA	C4H9NO2	102.0561	756.9	-0.05	0.97	0.23	0.592801594	0.042734605
Glutamine	C5H10N2O3	145.0619	746.31	0.33	1.25	1.29	0.051633972	0.815594389

Appendix Table 14

			ASV78 on abi1					
	Formula	MW	Average RT	log2(fc)	Mean FC	log(p-value)	p-value	q-value
Proline	C5H9NO2	114.0561	623.77	0.31	1.24	1.07	0.085310496	0.111782453
Glutamic Acid	C5H9NO4	146.0459	1026.64	-0.07	0.95	0.60	0.24983188	0.191773168
Histidine	C6H9N3O2	154.0622	763.32	0.20	1.15	0.75	0.177310816	0.165194683
Valine	C5H11NO2	116.0717	596.08	0.11	1.08	0.61	0.248134818	0.191248427
Asparagine	C4H8N2O3	131.0462	730.72	0.25	1.19	0.64	0.230628953	0.185659858
Serine	C3 H7 N O3	104.0353	728.15	0.26	1.20	1.10	0.07887961	0.106538003
Arginine	C6H14N4O2	173.1044	765.97	-0.38	0.77	0.82	0.152086755	0.153327584
Methionine	C5H11NO2S	148.0438	611.78	0.07	1.05	0.21	0.619032445	0.313396122
Phenylalanine	C9H11NO2	164.0717	599.82	0.23	1.17	0.78	0.167667471	0.16087678
Threonine	C4H9NO3	118.051	NP	#NUM!		#NUM!		
Isoleucine/Leucine	C6H13NO2	130.0874	552.125	0.28	1.21	1.21	0.062225909	0.091936177
Tryptophan	C11H12N2O2	203.0826	612.66	0.35	1.27	0.97	0.106778778	0.127227236
Aspartic Acid	C4H7NO4	132.0302	1026.44	0.40	1.32	2.60	**0.002529605**	0.010647077
Tyrosine	C9H11NO3	180.0666	668.12	0.17	1.13	0.57	0.269418992	0.197534486
GABA	C4H9NO2	102.0561	717.44	0.02	1.01	0.17	0.669240646	0.330416134
Glutamine	C5H10N2O3	145.0619	709.165	0.58	1.50	1.17	0.067236194	0.096567099

Appendix Table 15

			Mannitol					
	Formula	MW	Average RT	log2(fc)	Mean FC	log(p-value)	p-value	q-value
Proline	C5H9NO2	114.0561	674.175	4.56	23.62	7.19	6.45E-08	1.71E-07
Glutamic Acid	C5H9NO4	146.0459	1120.54	0.30	1.23	3.27	0.000540603	0.000438112
Histidine	C6H9N3O2	154.0622	909.57	1.84	3.57	8.38	4.19E-09	2.07E-08
Valine	C5H11NO2	116.0717	677.39	3.23	9.41	3.66	0.000220878	0.000189862
Asparagine	C4H8N2O3	131.0462	789.83	0.82	1.77	5.56	2.75E-06	3.66E-06
Serine	C3 H7 N O3	104.0353	785.94	0.99	1.99	5.49	3.24E-06	4.21E-06
Arginine	C6H14N4O2	173.1044	837.425	0.11	1.08	0.14	0.719844617	0.208220038
Methionine	C5H11NO2S	148.0438	662.68	5.67	50.96	6.92	1.20E-07	2.77E-07
Phenylalanine	C9H11NO2	164.0717	682.85	4.25	19.05	6.08	8.24E-07	1.29E-06
Threonine	C4H9NO3	118.051	785.39	1.99	3.96	4.62	2.39E-05	2.43E-05
Isoleucine/Leucine	C6H13NO2	130.0874	606.84	3.82	14.09	9.39	4.03E-10	3.10E-09
Tryptophan	C11H12N2O2	203.0826	689.88	6.09	68.04	3.62	0.000242198	0.000207149
Aspartic Acid	C4H7NO4	132.0302	1120.4	-0.32	0.80	1.81	0.015427495	0.008656728
Tyrosine	C9H11NO3	180.0666	LOW	#NUM!		#NUM!		
GABA	C4H9NO2	102.0561	773.18	0.57	1.48	2.33	0.004686576	0.003006696
Glutamine	C5H10N2O3	145.0619	797.97	1.30	2.45	6.67	2.13E-07	4.31E-07

Appendix Table 16

			141B on WT					
	Formula	MW		log2(fc)	Mean FC	log(p-value)		
Proline	C5H9NO2	114.0561	608.55	0.088	1.06	0.36	4.35E-01	0.848168537
Glutamic Acid	C5H9NO4	146.0459	1000.98	0.363	1.29	1.90	1.27E-02	0.186736399
Histidine	C6H9N3O2	154.0622	737.28	0.398	1.32	1.88	1.32E-02	0.191703976
Valine	C5H11NO2	116.0717	575.26	0.352	1.28	1.02	9.45E-02	0.548216959
Asparagine	C4H8N2O3	131.0462	714.12	0.240	1.18	0.75	1.77E-01	0.694774398
Serine	C3 H7 N O3	104.0353	712.62	0.431	1.35	1.58	2.65E-02	0.294798131
Arginine	C6H14N4O2	173.1044	740.56	0.218	1.16	0.48	3.33E-01	0.810187249
Methionine	C5H11NO2S	148.0438	587.93	**0.590**	**1.51**	2.60	**2.51E-03**	0.05277092
Phenylalanine	C9H11NO2	164.0717	578.77	**0.642**	**1.56**	3.76	**1.72E-04**	0.005593943
Threonine	C4H9NO3	118.051	NP	#NUM!		#NUM!		
Isoleucine/Leucine	C6H13NO2	130.0874	537.46	0.413	1.33	1.12	7.55E-02	0.492106097
Tryptophan	C11H12N2O2	203.0826	589.33	0.303	1.23	0.80	1.60E-01	0.672612015
Aspartic Acid	C4H7NO4	132.0302	1000.26	-0.078	0.95	0.05	8.88E-01	0.919339084
Tyrosine	C9H11NO3	180.0666	650.675	0.391	1.31	1.77	1.68E-02	0.224154459
GABA	C4H9NO2	102.0561	704.08	0.029	1.02	0.02	9.55E-01	0.92459993
Glutamine	C5H10N2O3	145.0619	693.72	0.347	1.27	1.69	2.02E-02	0.250683342

Appendix Table 17

			Mandi 5 uM on 35S:MANDI					
	Formula	MW	Average RT	log2(fc)	Mean FC	log(p-value)	p-value	q-value
Proline	C5H9NO2	114.0561	646.92	4.13	17.56	16.23	5.92E-17	1.97E-15
Glutamic Acid	C5H9NO4	146.0459	1116.83	0.61	1.53	12.29	5.18E-13	1.76E-12
Histidine	C6H9N3O2	154.0622	855.31	2.07	4.20	13.62	2.40E-14	1.36E-13
Valine	C5H11NO2	116.0717	633.34	3.38	10.40	19.78	1.68E-20	6.97E-18
Asparagine	C4H8N2O3	131.0462	795.24	0.70	1.62	6.87	1.35E-07	1.16E-07
Serine	C3 H7 N O3	104.0353	855.17	0.50	1.42	6.13	7.40E-07	5.54E-07
Arginine	C6H14N4O2	173.1044	813.93	-0.80	0.58	3.77	0.00016879	8.49E-05
Methionine	C5H11NO2S	148.0438	658.91	2.93	7.63	10.44	3.62E-11	6.73E-11
Phenylalanine	C9H11NO2	164.0717	653.77	4.37	20.71	13.72	1.93E-14	1.18E-13
Threonine	C4H9NO3	118.051	NP	#NUM!		#NUM!		
Isoleucine/Leucine	C6H13NO2	130.0874	577.215	4.73	26.49	5.44	3.64E-06	2.40E-06
Tryptophan	C11H12N2O2	203.0826	668.1	5.49	45.08	14.79	1.63E-15	1.84E-14
Aspartic Acid	C4H7NO4	132.0302	1116.12	0.10	1.07	1.24	0.056897219	0.017771484
Tyrosine	C9H11NO3	180.0666	734.25	2.59	6.00	11.25	5.58E-12	1.30E-11
GABA	C4H9NO2	102.0561	768.9	-0.98	0.51	4.07	8.56E-05	4.51E-05
Glutamine	C5H10N2O3	145.0619	767.62	0.33	1.26	2.21	0.006231576	0.002386749

Appendix Table 18

			Mandi 20 uM on 35S:MANDI					
	Formula	MW	Average RT	log2(fc)	Mean FC	log(p-value)	p-value	q-value
Proline	C5H9NO2	114.0561	680.22	5.21	36.98	11.88	1.32E-12	8E-12
Glutamic Acid	C5H9NO4	146.0459	1205.69	0.44	1.36	3.91	0.000122959	0.00009
Histidine	C6H9N3O2	154.0622	896.365	3.21	9.26	11.16	6.93E-12	2.92E-11
Valine	C5H11NO2	116.0717	656.92	4.00	15.95	13.58	2.62E-14	6.67E-13
Asparagine	C4H8N2O3	131.0462	808.04	0.92	1.89	7.04	9.03E-08	0.000000111
Serine	C3 H7 N O3	104.0353	800.2	0.42	1.34	3.32	0.000482738	0.000318035
Arginine	C6H14N4O2	173.1044	828.25	-1.25	0.42	6.59	0.000000259	0.000000296
Methionine	C5H11NO2S	148.0438	679.45	4.28	19.48	11.15	7.04E-12	2.94E-11
Phenylalanine	C9H11NO2	164.0717	715.52	4.83	28.46	11.84	1.46E-12	8.64E-12
Threonine	C4H9NO3	118.051	766.17	1.94	3.84	16.92	1.19E-17	6.99E-15
Isoleucine/Leucine	C6H13NO2	130.0874	619.67	5.10	34.19	11.66	2.19E-12	1.2E-11
Tryptophan	C11H12N2O2	203.0826	674.51	6.16	71.75	13.73	1.87E-14	5.55E-13
Aspartic Acid	C4H7NO4	132.0302	1139.855	-1.06	0.48	2.59	0.002566367	0.001464996
Tyrosine	C9H11NO3	180.0666	740.92	2.57	5.95	14.27	5.37E-15	2.62E-13
GABA	C4H9NO2	102.0561	781.785	-0.98	0.51	2.56	0.00276102	0.001568469
Glutamine	C5H10N2O3	145.0619	830.56	1.51	2.85	9.97	1.08E-10	2.91E-10

Appendix Table 19

			Mandi 5 uM on Cyp86a:MANDI					
	Formula	MW	Average RT	log2(fc)	Mean FC	log(p-value)	p-value	q-value
Proline	C5H9NO2	114.0561	650.94	1.42	**2.67**	14.43	**3.75E-15**	4.84E-13
Glutamic Acid	C5H9NO4	146.0459	1111.57	0.20	**1.15**	2.28	**0.005291392**	0.006824694
Histidine	C6H9N3O2	154.0622	802.49	0.71	**1.64**	7.79	**1.62E-08**	0.000000388
Valine	C5H11NO2	116.0717	630.3	0.36	**1.29**	6.38	**0.000000419**	0.00000583
Asparagine	C4H8N2O3	131.0462	791.51	0.19	1.14	0.73	0.186398286	0.086060999
Serine	C3 H7 N O3	104.0353	850.68	0.41	**1.33**	5.40	**0.00000395**	0.0000311
Arginine	C6H14N4O2	173.1044	812.5	-0.28	0.82	1.52	0.030454406	0.023526342
Methionine	C5H11NO2S	148.0438	655.82	0.54	**1.45**	8.48	**3.32E-09**	0.000000118
Phenylalanine	C9H11NO2	164.0717	650.2	0.92	**1.89**	13.44	**3.63E-14**	3.74E-12
Threonine	C4H9NO3	118.051	NP	#NUM!		#NUM!		
Isoleucine/Leucine	C6H13NO2	130.0874	572.94	0.25	**1.19**	2.80	**0.001580343**	0.002645554
Tryptophan	C11H12N2O2	203.0826	665.01	0.84	**1.79**	7.75	**1.77E-08**	0.000000413
Aspartic Acid	C4H7NO4	132.0302	1110.84	-0.24	0.85	1.28	0.052020751	0.035176428
Tyrosine	C9H11NO3	180.0666	730.295	0.21	1.16	0.81	0.154289248	0.075651372
GABA	C4H9NO2	102.0561	767.92	-0.18	0.88	0.47	0.337598625	0.12809465
Glutamine	C5H10N2O3	145.0619	763.92	0.08	1.06	0.53	0.296680001	0.117454682

Appendix Table 20

Appendix Tables 21-39

Treatment and genetic background indicated in top row. Dark green -log(p-values) indicate a significant difference defined by fold change ±20%, and a p-value ≤ 0.01. Mean fold changes are green if significantly upregulated, no color if no significance, or blue is down-regulated.

				ABA on WT					
	Common Name	Chemical Formula	[M-H]-	Average RT	log2(fc)	Mean FC	-log10(p-value)	p-value	q-value
Aromatic	Sinalbin	C14H19NO10S2	424.0378	Low abundance		Low abundance			
	Gluconasturtiin	C15H21NO9S2	422.0585	Low abundance		Low abundance			
	Glucobrassicin	C16H20N2O9S2	447.0537	843	0.176322773	**1.13**	**1.99**	**1.03E-02**	0.003991295
Thionyl	Glucoerucin	C12H23NO9S3	420.0462	770	-0.651137014	**0.64**	**2.89**	**1.30E-03**	0.000905482
	Glucoberteroin	C13H25NO9S3	434.0619	750	-0.602095146	**0.66**	**2.36**	**4.38E-03**	0.002242938
	Glucolesquerellin	C14H27NO9S3	448.0787	748	#VALUE!	Low abundance	**#NUM!**		
	7-Methylthioheptyl glucosinolate	C15H29NO9S3	462.0941623	717	-1.77725637	**0.29**	**7.40**	**3.94E-08**	0.000000177
	8-Methylthiooctyl glucosinolate	C16H31NO9S3	476.1105759	704	-2.546406963	**0.17**	**9.87**	**1.35E-10**	2.27E-09
Sulfinyl	Glucoraphanin	C12H23NO10S3	436.04059	949	0.116985903	**1.08**	**2.00**	**1.00E-02**	0.003922647
	Glucoalyssin	C13H25NO10S3	450.0568	N/P	#VALUE!	N/P	**#NUM!**		
	Glucohesperin	C14H27NO10S3	464.0719	892	1.619513167	**3.07**	**4.95**	**1.12E-05**	0.0000205
	Glucoibarin	C15H29NO10S3	478.0879	859	#VALUE!	Low abundance	**#NUM!**		
	Glucohirsutin	C16H31NO10S3	492.1048	826	1.690415552	**3.23**	**8.82**	**1.51E-09**	1.62E-08

Appendix Table 21

				ABA on *8,9*					
				Average RT	log2(fc)	Mean FC	-log10(p-value)	p-value	q-value
Aromatic	Sinalbin	C14H19NO10S2	424.0378	Low Abundance					
	Gluconasturtiin	C15H21NO9S2	422.0585	Low Abundance					
	Glucobrassicin	C16H20N2O9S2	447.0537	807.19	0.35308034	**1.28**	**3.89**	**0.000127402**	0.230898158
Thionyl	Glucoerucin	C12H23NO9S3	420.0462	721.09	-0.195803817	**0.87**	**0.98**	**0.104615276**	0.829718634
	Glucoberteroin	C13H25NO9S3	434.0619	703.28	-0.279134477	**0.82**	**1.71**	**0.019324561**	0.379656079
	Glucolesquerellin	C14H27NO9S3	448.0787	687.66	-0.752783017	**0.59**	**4.80**	**1.59305E-05**	0.038715481
	7-Methylthioheptyl glucosinolate	C15H29NO9S3	462.0941623	671.04	-1.311509069	**0.40**	**5.46**	**3.47E-06**	0.801724402
	8-Methylthiooctyl glucosinolate	C16H31NO9S3	476.1105759	657.42	-1.941439102	**0.26**	**7.31**	**4.92273E-08**	0.15633622
Sulfinyl	Glucoraphanin	C12H23NO10S3	436.04059	913.92	0.030503772	**1.02**	**0.08**	**0.824150089**	0.830838274
	Glucoalyssin	C13H25NO10S3	450.0568	N/P	#NUM!		**#NUM!**		
	Glucohesperin	C14H27NO10S3	464.0719	859.35	1.673910249	**3.19**	**4.88**	**1.31259E-05**	0.826551319
	Glucoibarin	C15H29NO10S3	478.0879	Low Abundance	#NUM!		**#NUM!**		
	Glucohirsutin	C16H31NO10S3	492.1048	791.39	1.4298526	**2.69**	**8.43**	**3.677E-09**	0.830895287

Appendix Table 22

				ABA on *0,1,2*					
				Average RT	log2(fc)	Mean FC	-log10(p-value)	p-value	q-value
Aromatic	Sinalbin	C14H19NO10S2	424.0378						
	Gluconasturtiin	C15H21NO9S2	422.0585						
	Glucobrassicin	C16H20N2O9S2	447.0537	850.5	0.008180551	1.01	**0.41**	0.389413196	0.340804855
Thionyl	Glucoerucin	C12H23NO9S3	420.0462	764.98	-0.27938573	0.82	**0.92**	0.120632705	0.185606037
	Glucoberteroin	C13H25NO9S3	434.0619	745.34	-0.281300005	0.82	**0.96**	0.108469031	0.17650599
	Glucolesquerellin	C14H27NO9S3	448.0787	729.47	-0.295141795	0.81	**1.12**	0.076675237	0.152328719
	7-Methylthioheptyl glucosinolate	C15H29NO9S3	462.0941623	713.43	-0.456329321	**0.73**	**2.16**	**0.006997753**	0.035660866
	8-Methylthiooctyl glucosinolate	C16H31NO9S3	476.1105759	700.3	-0.662590487	**0.63**	**3.87**	**0.000134239**	0.001820551
Sulfinyl	Glucoraphanin	C12H23NO10S3	436.04059	956.22	0.025390402	1.02	**0.98**	0.103906421	0.173524224
	Glucoalyssin	C13H25NO10S3	450.0568	low abundance	#NUM!		**#NUM!**		
	Glucohesperin	C14H27NO10S3	464.0719	903.44	0.679169007	**1.60**	**2.50**	**0.003144984**	0.020033724
	Glucoibarin	C15H29NO10S3	478.0879	N/P	#NUM!		**#NUM!**		
	Glucohirsutin	C16H31NO10S3	492.1048	829.69	0.771020878	**1.71**	**3.78**	**0.000167036**	0.002136822

Appendix Table 23

				ABA on *abi1*					
				Average RT	log2(fc)	Mean FC	-log10(p-value)	p-value	q-value
Aromatic	Sinalbin	C14H19NO10S2	424.0378						
	Gluconasturtiin	C15H21NO9S2	422.0585						
	Glucobrassicin	C16H20N2O9S2	447.0537	828.58	0.366100482	1.29	**5.18**	0.00000663	0.844478731
Thionyl	Glucoerucin	C12H23NO9S3	420.0462	732.42	-0.101887635	0.93	**0.25**	0.566426197	0.304312429
	Glucoberteroin	C13H25NO9S3	434.0619	712.11	-0.386679641	**0.76**	**2.35**	**0.004419825**	0.843038826
	Glucolesquerellin	C14H27NO9S3	448.0787	694.42	-0.399615416	**0.76**	**4.41**	**0.0000393**	0.844468176
	7-Methylthioheptyl glucosinolate	C15H29NO9S3	462.0941623	677.3	-0.672308155	**0.63**	**5.54**	**0.00000286**	0.844479947
	8-Methylthiooctyl glucosinolate	C16H31NO9S3	476.1105759	664.39	-0.866971075	**0.55**	**7.71**	**1.94E-08**	0.844480867
Sulfinyl	Glucoraphanin	C12H23NO10S3	436.04059	922.39	0.032694719	1.02	**0.19**	0.647287134	0.199279902
	Glucoalyssin	C13H25NO10S3	450.0568	N/P	#NUM!		**#NUM!**		
	Glucohesperin	C14H27NO10S3	464.0719	Low abundance	#NUM!		**#NUM!**		
	Glucoibarin	C15H29NO10S3	478.0879	Low abundance	#NUM!		**#NUM!**		
	Glucohirsutin	C16H31NO10S3	492.1048	805.16	1.400328514	**2.64**	**5.74**	**0.00000184**	0.844480277

Appendix Table 24

				Pyrabactin on WT					
	Common Name	Chemical Formula	[M-H]-	**Average RT**	**log2(fc)**	**Mean FC**	**-log10(p-value)**	**p-value**	**q-value**
Aromatic	Sinalbin	C14H19NO10S2	424.0378	Low abundance					
	Gluconasturtiin	C15H21NO9S2	422.0585	Low abundance					
	Glucobrassicin	C16H20N2O9S2	447.0537	830	0.16851023	1.12	**1.24**	0.057148515	0.82
Thionyl	Glucoerucin	C12H23NO9S3	420.0462	738	-0.030146895	0.98	**0.04**	0.918121548	0.005744705
	Glucoberteroin	C13H25NO9S3	434.0619	717.59	-0.040534997	0.97	**0.09**	0.804572712	0.012757743
	Glucolesquerellin	C14H27NO9S3	448.0787	701.58	-0.169805739	0.89	**1.00**	0.100866846	0.792024552
	7-Methylthioheptyl glucosinolate	C15H29NO9S3	462.0941623	685	-0.416963214	**0.75**	**2.94**	**0.001140366**	0.846884161
	8-Methylthiooctyl glucosinolate	C16H31NO9S3	476.1105759	671.34	-0.606968791	**0.66**	**5.32**	**0.00000482**	0.847355302
Sulfinyl	Glucoraphanin	C12H23NO10S3	436.04059	937.02	-0.118234138	0.92	**0.83**	0.147652118	0.754625381
	Glucoalyssin	C13H25NO10S3	450.0568	N/P	#NUM!		**#NUM!**		
	Glucohesperin	C14H27NO10S3	464.0719	N/P	#NUM!		**#NUM!**		
	Glucoibarin	C15H29NO10S3	478.0879	842.435	0.33547233	**1.26**	**5.24**	**0.00000579**	0.847354902
	Glucohirsutin	C16H31NO10S3	492.1048	812.17	0.558177789	**1.47**	**5.62**	**0.00000238**	0.847356314

Appendix Table 25

				Pyrabactin on *8,9*					
				Average RT	**log2(fc)**	**Mean FC**	**-log10(p-value)**	**p-value**	**q-value**
Aromatic	Sinalbin	C14H19NO10S2	424.0378	Low Abundance					
	Gluconasturtiin	C15H21NO9S2	422.0585	Low Abundance					
	Glucobrassicin	C16H20N2O9S2	447.0537	807.19	-0.120257437	0.92	**0.98**	0.104304414	0.01750615
Thionyl	Glucoerucin	C12H23NO9S3	420.0462	721.09	-0.088520425	0.94	**0.34**	0.458342008	0.397047473
	Glucoberteroin	C13H25NO9S3	434.0619	703.3	-0.107103911	0.93	**0.53**	0.293360604	0.18802729
	Glucolesquerellin	C14H27NO9S3	448.0787	687.82	-0.233568561	0.85	**1.31**	0.04872761	0.015909718
	7-Methylthioheptyl glucosinolate	C15H29NO9S3	462.0941623	671.15	-0.412206054	0.75	**1.85**	0.013973859	0.173520057
	8-Methylthiooctyl glucosinolate	C16H31NO9S3	476.1105759	657.7	-0.539749292	0.69	**2.77**	**0.001681106**	0.68456105
Sulfinyl	Glucoraphanin	C12H23NO10S3	436.04059	913.26	-0.21370194	0.86	**0.81**	0.155664001	0.355579033
	Glucoalyssin	C13H25NO10S3	450.0568	N/P	#NUM!		**#NUM!**		
	Glucohesperin	C14H27NO10S3	464.0719	859.34	0.165756136	1.12	**0.35**	0.449003776	0.015313811
	Glucoibarin	C15H29NO10S3	478.0879	Low abundance	#NUM!		**#NUM!**		
	Glucohirsutin	C16H31NO10S3	492.1048	791.39	0.408366197	1.33	**2.79**	**0.001624541**	0.541756975

Appendix Table 26

				Pyrabactin on *0,1,2*					
				Average RT	log2(fc)	Mean FC	-log10(p-value)	p-value	q-value
Aromatic	Sinalbin	C14H19NO10S2	424.0378						
	Gluconasturtiin	C15H21NO9S2	422.0585						
	Glucobrassicin	C16H20N2O9S2	447.0537	849.96	0.084064265	1.06	**0.69**	0.202216585	0.163809508
Thionyl	Glucoerucin	C12H23NO9S3	420.0462	752.985	0.003486808	1.00	**0.41**	0.389652694	0.199500653
	Glucoberteroin	C13H25NO9S3	434.0619	733.735	0.046525444	1.03	**0.49**	0.327097475	0.189899386
	Glucolesquerellin	C14H27NO9S3	448.0787	718.69	0.110518788	1.08	**0.40**	0.399917473	0.201406086
	7-Methylthioheptyl glucosinolate	C15H29NO9S3	462.0941623	702.195	0.004003567	1.00	**0.32**	0.480198585	0.217567809
	8-Methylthiooctyl glucosinolate	C16H31NO9S3	476.1105759	689.805	-0.085080801	0.94	**0.23**	0.588671287	0.240393919
Sulfinyl	Glucoraphanin	C12H23NO10S3	436.04059	963.71	-0.008105129	0.99	**0.68**	0.210159747	0.166068216
	Glucoalyssin	C13H25NO10S3	450.0568	np	#NUM!		**#NUM!**		
	Glucohesperin	C14H27NO10S3	464.0719	low abundance	#NUM!		**#NUM!**		
	Glucoibarin	C15H29NO10S3	478.0879	863.85	-0.058415472	0.96	**1.23**	0.059435255	0.087857821
	Glucohirsutin	C16H31NO10S3	492.1048	825.23	-0.039982924	0.97	**1.60**	0.024978723	0.047546348

Appendix Table 27

				Quinabactin on WT					
	Common Name	Chemical Formula	[M-H]-	**Average RT**	**log2(fc)**	**Mean FC**	**-log10(p-value)**	**p-value**	**q-value**
Aromatic	Sinalbin	C14H19NO10S2	424.0378	Low abundance					
	Gluconasturtiin	C15H21NO9S2	422.0585	Low abundance					
	Glucobrassicin	C16H20N2O9S2	447.0537	842.91	0.43756719	1.35	**1.62**	0.023911417	0.023579807
Thionyl	Glucoerucin	C12H23NO9S3	420.0462	768.62	-0.174464289	0.89	**1.43**	0.037149546	0.032854566
	Glucoberteroin	C13H25NO9S3	434.0619	748.09	-0.028181079	0.98	**1.03**	0.092887184	0.064074466
	Glucolesquerellin	C14H27NO9S3	448.0787	730.49	-0.207494023	0.87	**0.88**	0.130489402	0.082733671
	7-Methylthioheptyl glucosinolate	C15H29NO9S3	462.0941623	713.92	-0.532656724	**0.69**	**3.45**	**0.000352672**	0.000880745
	8-Methylthiooctyl glucosinolate	C16H31NO9S3	476.1105759	699.49	-1.498168965	**0.35**	**8.98**	**1.04E-09**	1.78E-08
Sulfinyl	Glucoraphanin	C12H23NO10S3	436.04059	957.56	0.102836555	1.07	**0.73**	0.184953162	0.103990392
	Glucoalyssin	C13H25NO10S3	450.0568	N/P	#NUM!		**#NUM!**		
	Glucohesperin	C14H27NO10S3	464.0719	898.72	0.676529996	**1.60**	**4.14**	**0.0000732**	0.000225226
	Glucoibarin	C15H29NO10S3	478.0879	861.26	0.674628088	**1.60**	**3.18**	**0.00065731**	0.001447566
	Glucohirsutin	C16H31NO10S3	492.1048	829.18	1.125260607	**2.18**	**2.69**	**0.002052646**	0.003605322

Appendix Table 28

				Quinabactin on *8,9*					
				Average RT	**log2(fc)**	**Mean FC**	**-log10(p-value)**	**p-value**	**q-value**
Aromatic	Sinalbin	C14H19NO10S2	424.0378						
	Gluconasturtiin	C15H21NO9S2	422.0585						
	Glucobrassicin	C16H20N2O9S2	447.0537	807.06	0.127489018	1.09	**0.98**	0.103639681	0.614480496
Thionyl	Glucoerucin	C12H23NO9S3	420.0462	721.04	-0.053113794	0.96	**0.19**	0.649014509	0.832513467
	Glucoberteroin	C13H25NO9S3	434.0619	703.28	-0.277211544	0.83	**1.94**	0.011391532	0.81713637
	Glucolesquerellin	C14H27NO9S3	448.0787	687.97	-0.722826606	**0.61**	**5.01**	**9.79E-06**	**0.674419404**
	7-Methylthioheptyl glucosinolate	C15H29NO9S3	462.0941623	671.15	-1.34290431	**0.39**	**5.65**	**2.21369E-06**	**0.832843221**
	8-Methylthiooctyl glucosinolate	C16H31NO9S3	476.1105759	657.36	-2.26641726	**0.21**	**7.87**	**1.33438E-08**	**0.836248044**
Sulfinyl	Glucoraphanin	C12H23NO10S3	436.04059	913.21	-0.059690889	0.96	**0.16**	0.694735192	0.82491184
	Glucoalyssin	C13H25NO10S3	450.0568		#NUM!		**#NUM!**		
	Glucohesperin	C14H27NO10S3	464.0719	859.07	1.62988377	**3.09**	**5.40**	**3.96768E-06**	0.101777893
	Glucoibarin	C15H29NO10S3	478.0879	Low abundance	#NUM!		**#NUM!**		
	Glucohirsutin	C16H31NO10S3	492.1048	791.45	1.437725691	**2.71**	**7.47**	**3.38655E-08**	0.803428032

Appendix Table 29

				Quinabactin on *0,1,2*					
				Average RT	log2(fc)	Mean FC	-log10(p-value)	p-value	q-value
Aromatic	Sinalbin	C14H19NO10S2	424.0378	np					
	Gluconasturtiin	C15H21NO9S2	422.0585						
	Glucobrassicin	C16H20N2O9S2	447.0537	788.98	-0.097006302	0.93	**1.25**	0.056857656	0.117783873
Thionyl	Glucoerucin	C12H23NO9S3	420.0462	712.46	0.030608568	1.02	**0.31**	0.49542928	0.296423284
	Glucoberteroin	C13H25NO9S3	434.0619	694.28	0.047164771	1.03	**0.59**	0.259183325	0.20019094
	Glucolesquerellin	C14H27NO9S3	448.0787	680.2	0.089881305	1.06	**0.32**	0.473353192	0.288101801
	7-Methylthioheptyl glucosinolate	C15H29NO9S3	462.0941623	666.11	0.017835823	1.01	**0.90**	0.127281514	0.149792426
	8-Methylthiooctyl glucosinolate	C16H31NO9S3	476.1105759	653.81	-0.11834314	0.92	**0.52**	0.303783032	0.219135314
Sulfinyl	Glucoraphanin	C12H23NO10S3	436.04059	930.84	-0.030483675	0.98	**1.19**	0.063996509	0.12148484
	Glucoalyssin	C13H25NO10S3	450.0568	np	#NUM!		**#NUM!**		
	Glucohesperin	C14H27NO10S3	464.0719	low abundance	#NUM!		**#NUM!**		
	Glucoibarin	C15H29NO10S3	478.0879	818.74	0.443103875	**1.36**	**4.34**	**4.61E-05**	0.002242458
	Glucohirsutin	C16H31NO10S3	492.1048	785.82	0.739496827	**1.67**	**2.79**	**0.001632687**	0.0241081

Appendix Table 30

				Quinabactin on *abi1*					
				Average RT	log2(fc)	Mean FC	-log10(p-value)	p-value	q-value
Aromatic	Sinalbin	C14H19NO10S2	424.0378	np					
	Gluconasturtiin	C15H21NO9S2	422.0585	np					
	Glucobrassicin	C16H20N2O9S2	447.0537	809.22	0.099687402	1.07	**0.56**	0.275543081	0.653235048
Thionyl	Glucoerucin	C12H23NO9S3	420.0462	716.88	-0.167686217	0.89	**0.61**	0.243114032	0.685098567
	Glucoberteroin	C13H25NO9S3	434.0619	697.98	-0.132145278	0.91	**0.46**	0.343166949	0.575826194
	Glucolesquerellin	C14H27NO9S3	448.0787	683.74	-0.335531479	0.79	**1.58**	0.026319468	0.822764134
	7-Methylthioheptyl glucosinolate	C15H29NO9S3	462.0941623	667.36	-0.643699939	0.64	**3.20**	**0.000630482**	0.83243111
	8-Methylthiooctyl glucosinolate	C16H31NO9S3	476.1105759	655.08	-1.178522666	0.44	**5.36**	**4.32E-06**	0.832653861
Sulfinyl	Glucoraphanin	C12H23NO10S3	436.04059	916.68	-0.037374479	0.97	**0.23**	0.594103453	0.222881739
	Glucoalyssin	C13H25NO10S3	450.0568	N/P	#NUM!		**#NUM!**		
	Glucohesperin	C14H27NO10S3	464.0719	Low abundance	#NUM!		**#NUM!**		
	Glucoibarin	C15H29NO10S3	478.0879	822.81	0.811993466	1.76	**5.98**	**1.05E-06**	0.832655021
	Glucohirsutin	C16H31NO10S3	492.1048	794.1	1.27117901	2.41	**8.00**	**0.00000001**	0.832655391

Appendix Table 31

				ASV78 on WT					
	Common Name	Chemical Formula	[M-H]-	**Average RT**	**log2(fc)**	**Mean FC**	**-log10(p-value)**	**p-value**	**q-value**
Aromatic	Sinalbin	C14H19NO10S2	424.0378						
	Gluconasturtiin	C15H21NO9S2	422.0585						
	Glucobrassicin	C16H20N2O9S2	447.0537	845.97	0.333876758	1.26	**1.15**	0.070598324	0.064722069
Thionyl	Glucoerucin	C12H23NO9S3	420.0462	773.66	0.12895194	1.09	**1.75**	0.017626271	0.024378783
	Glucoberteroin	C13H25NO9S3	434.0619	754.49	0.029573366	1.02	**0.87**	0.134712658	0.104174685
	Glucolesquerellin	C14H27NO9S3	448.0787	Low Abundance	#NUM!		**#NUM!**		
	7-Methylthioheptyl glucosinolate	C15H29NO9S3	462.0941623	747.09	-0.073911515	0.95	**1.20**	0.0637139	0.061052247
	8-Methylthiooctyl glucosinolate	C16H31NO9S3	476.1105759	704.22	-1.658786421	**0.32**	**2.60**	**0.002484909**	0.005693586
Sulfinyl	Glucoraphanin	C12H23NO10S3	436.04059	959.69	-0.121168503	0.92	**0.80**	0.158321456	0.116774037
	Glucoalyssin	C13H25NO10S3	450.0568	N/P	#NUM!		**#NUM!**		
	Glucohesperin	C14H27NO10S3	464.0719	904.205	-0.205335862	0.87	**1.47**	0.034107744	0.039389249
	Glucoibarin	C15H29NO10S3	478.0879	N/P	#NUM!		**#NUM!**		
	Glucohirsutin	C16H31NO10S3	492.1048	833.48	0.144620962	1.11	**0.86**	0.137076572	0.105230859

Appendix Table 32

				ASV78 on *8,9*					
				Average RT	**log2(fc)**	**Mean FC**	**-log10(p-value)**	**p-value**	**q-value**
Aromatic	Sinalbin	C14H19NO10S2	424.0378	Low abundance					
	Gluconasturtiin	C15H21NO9S2	422.0585	Low Abundance					
	Glucobrassicin	C16H20N2O9S2	447.0537	811.25	0.167198637	1.12	**1.35**	0.045165126	0.81965509
Thionyl	Glucoerucin	C12H23NO9S3	420.0462	718.36	-0.101010901	0.93	**0.89**	0.128057269	0.75407291
	Glucoberteroin	C13H25NO9S3	434.0619	699.85	0.033391624	1.02	**0.14**	0.71881898	0.00968715
	Glucolesquerellin	C14H27NO9S3	448.0787	685.42	-0.049031766	0.97	**0.30**	0.499556451	0.120745762
	7-Methylthioheptyl glucosinolate	C15H29NO9S3	462.0941623	668.23	-0.30220049	**0.81**	**2.12**	**0.007670841**	0.84034727
	8-Methylthiooctyl glucosinolate	C16H31NO9S3	476.1105759	656.21	-0.557843955	**0.68**	**2.75**	**0.001782118**	0.843195303
Sulfinyl	Glucoraphanin	C12H23NO10S3	436.04059	917.63	-0.245095625	**0.84**	**2.40**	**0.003949978**	0.842158558
	Glucoalyssin	C13H25NO10S3	450.0568	N/P	#NUM!		**#NUM!**		
	Glucohesperin	C14H27NO10S3	464.0719	N/P	#NUM!		**#NUM!**		
	Glucoibarin	C15H29NO10S3	478.0879	824.23	-0.055665452	0.96	**0.22**	0.605734884	0.037257225
	Glucohirsutin	C16H31NO10S3	492.1048	795.44	0.027139513	1.02	**0.09**	0.812147987	0.003068974

Appendix Table 33

				ASV78 on *0,1,2*					
				Average RT	log2(fc)	Mean FC	-log10(p-value)	p-value	q-value
Aromatic	Sinalbin	C14H19NO10S2	424.0378						
	Gluconasturtiin	C15H21NO9S2	422.0585						
	Glucobrassicin	C16H20N2O9S2	447.0537	839.94	0.362481953	1.29	**1.56**	0.027795114	0.017192497
Thionyl	Glucoerucin	C12H23NO9S3	420.0462	747.6	-0.079129085	0.95	**0.70**	0.1990206	0.041929788
	Glucoberteroin	C13H25NO9S3	434.0619	725.75	0.083641623	1.06	**0.70**	0.201185933	0.042231046
	Glucolesquerellin	C14H27NO9S3	448.0787	710.62	-0.094530039	0.94	**0.83**	0.148571339	0.034762231
	7-Methylthioheptyl glucosinolate	C15H29NO9S3	462.0941623	694.66	-0.293418432	0.82	**1.24**	0.057270981	0.022408234
	8-Methylthiooctyl glucosinolate	C16H31NO9S3	476.1105759	681.78	-0.416818898	**0.75**	**2.11**	**0.007689942**	0.010033314
Sulfinyl	Glucoraphanin	C12H23NO10S3	436.04059	960.93	0.027312473	1.02	**1.04**	0.091803702	0.026940391
	Glucoalyssin	C13H25NO10S3	450.0568	LOW	#NUM!		**#NUM!**		
	Glucohesperin	C14H27NO10S3	464.0719	897.72	0.606191506	**1.52**	**2.51**	**0.003066453**	0.006918266
	Glucoibarin	C15H29NO10S3	478.0879	855.98	0.424110824	**1.34**	**2.53**	**0.002945089**	0.006799783
	Glucohirsutin	C16H31NO10S3	492.1048	820.7	0.399310757	1.32	**2.10**	0.007939275	0.010152029

Appendix Table 34

				ASV78 on *abi1*					
				Average RT	log2(fc)	Mean FC	-log10(p-value)	p-value	q-value
Aromatic	Sinalbin	C14H19NO10S2	424.0378	np					
	Gluconasturtiin	C15H21NO9S2	422.0585	np					
	Glucobrassicin	C16H20N2O9S2	447.0537	770	0.056268433	1.04	**0.21**	0.615019095	0.31199822
Thionyl	Glucoerucin	C12H23NO9S3	420.0462	684.67	-0.022097542	0.98	**0.30**	0.503653952	0.273219318
	Glucoberteroin	C13H25NO9S3	434.0619	666.7	0.042128259	1.03	**0.22**	0.60070391	0.306965354
	Glucolesquerellin	C14H27NO9S3	448.0787	653.54	-0.12624273	0.92	**0.28**	0.527574996	0.281837695
	7-Methylthioheptyl glucosinolate	C15H29NO9S3	462.0941623	639.59	-0.427366668	0.74	**1.38**	0.041926725	0.072037738
	8-Methylthiooctyl glucosinolate	C16H31NO9S3	476.1105759	628.54	-0.775374906	**0.58**	**2.80**	**0.00160315**	0.007803219
Sulfinyl	Glucoraphanin	C12H23NO10S3	436.04059	878.34	-0.462597063	**0.73**	**2.49**	**0.003234529**	0.012659641
	Glucoalyssin	C13H25NO10S3	450.0568	NP	#NUM!		**#NUM!**		
	Glucohesperin	C14H27NO10S3	464.0719	Low abundance	#NUM!		**#NUM!**		
	Glucoibarin	C15H29NO10S3	478.0879	786.08	-0.061564649	0.96	**0.69**	0.205548208	0.176770008
	Glucohirsutin	C16H31NO10S3	492.1048	752.01	-0.001443943	1.00	**0.33**	0.471290655	0.26301531

Appendix Table 35

				Mannitol on WT					
				Average RT	log2(fc)	Mean FC	-log10(p-value)	p-value	q-value
Aromatic	Sinalbin	C14H19NO10S2	424.0378	Low abundance					Low abundance
	Gluconasturtiin	C15H21NO9S2	422.0585	Low abundance					Low abundance
	Glucobrassicin	C16H20N2O9S2	447.0537	824.03	-0.377615428	0.76970876	**0.74**	0.180536913	**0.068203791**
Thionyl	Glucoerucin	C12H23NO9S3	420.0462	745.11	-0.409328374	0.752973828	**0.57**	**0.268796792**	**0.093440476**
	Glucoberteroin	C13H25NO9S3	434.0619	725.57	-0.615338028	0.652776928	**1.53**	0.029209831	**0.014808398**
	Glucolesquerellin	C14H27NO9S3	448.0787	710.365	-0.519038527	0.697836746	**1.08**	0.082556297	0.035186061
	7-Methylthioheptyl glucosinolate	C15H29NO9S3	462.0941623	722.175	-0.855378145	0.552720434	**1.60**	0.024841746	**0.012884763**
	8-Methylthiooctyl glucosinolate	C16H31NO9S3	476.1105759	680.92	-1.253192923	0.419518715	**8.71**	1.97E-09	**1.13E-08**
Sulfinyl	Glucoraphanin	C12H23NO10S3	436.04059	931.51	0.328279144	1.255514894	**2.71**	0.001932104	**0.001380088**
	Glucoalyssin	C13H25NO10S3	450.0568	N/P	#NUM!		**#NUM!**		
	Glucohesperin	C14H27NO10S3	464.0719	874.68	0.952277083	1.934924243	**6.01**	9.87E-07	**1.49E-06**
	Glucoibarin	C15H29NO10S3	478.0879	726.73	0.091181641	1.065242313	**0.05**	0.894832143	0.246366231
	Glucohirsutin	C16H31NO10S3	492.1048	808.56	0.528636765	1.442565439	**2.99**	0.001019959	**0.000779472**

Appendix table 36

				141B on WT					
	Common Name	Chemical Formula	[M-H]-	Average RT	log2(FC)	Mean FC	-LOG(p-value)	p-value	q-value
Aromatic	Sinalbin	C14H19NO10S2	424.0378						
	Gluconasturtiin	C15H21NO9S2	422.0585						
	Glucobrassicin	C16H20N2O9S2	447.0537	744.56	-0.015568513	0.989266746	**0.00**	0.990110514	0.927058946
Thionyl	Glucoerucin	C12H23NO9S3	420.0462	655.42	-0.14764027	0.90272579	**0.58**	0.263524156	0.771833634
	Glucoberteroin	C13H25NO9S3	434.0619	638.47	-0.063789369	0.956747831	**0.13**	0.734305371	0.904086121
	Glucolesquerellin	C14H27NO9S3	448.0787	625.11	-0.19889641	0.871216746	**1.49**	0.032573627	0.330250788
	7-Methylthioheptyl glucosinolate	C15H29NO9S3	462.0941623	612.07	-0.331328661	**0.794804166**	**2.88**	**0.00133227**	0.032330244
	8-Methylthiooctyl glucosinolate	C16H31NO9S3	476.1105759	602.14	-0.624854794	**0.648485044**	**5.38**	**4.15E-06**	0.000172373
Sulfinyl	Glucoraphanin	C12H23NO10S3	436.04059	851.89	0.131473679	1.095412067	**0.84**	0.146105814	0.652235476
	Glucoalyssin	C13H25NO10S3	450.0568	NP	#NUM!		**#NUM!**		
	Glucohesperin	C14H27NO10S3	464.0719	NP	#NUM!		**#NUM!**		
	Glucoibarin	C15H29NO10S3	478.0879	763.35	0.711668163	**1.637696663**	**7.03**	**9.32E-08**	5.49E-06
	Glucohirsutin	C16H31NO10S3	492.1048	732.03	0.86384099	**1.819877055**	**6.70**	**2.01E-07**	1.09E-05

Appendix Table 37

				Mandi 5 uM on 35S:MANDI					
				Average RT	log2(fc)	Mean FC	-log10(p-value)	p-value	q-value
Aromatic	Sinalbin	C14H19NO10S2	424.0378						
	Gluconasturtiin	C15H21NO9S2	422.0585						
	Glucobrassicin	C16H20N2O9S2	447.0537	870.09	0.5612274	**1.48**	**4.44**	**3.63E-05**	2.01E-05
Thionyl	Glucoerucin	C12H23NO9S3	420.0462	763.76	-1.620905805	**0.33**	**10.16**	**6.92E-11**	1.2E-10
	Glucoberteroin	C13H25NO9S3	434.0619	745.51	-1.610066491	**0.33**	**9.45**	**3.54E-10**	5.31E-10
	Glucolesquerellin	C14H27NO9S3	448.0787	727.92	-2.132212752	**0.23**	**13.71**	**1.94E-14**	1.18E-13
	7-Methylthioheptyl glucosinolate	C15H29NO9S3	462.0941623	710.46	-2.772376395	**0.15**	**15.86**	**1.38E-16**	3.34E-15
	8-Methylthiooctyl glucosinolate	C16H31NO9S3	476.1105759	696.06	-2.813050548	**0.14**	**17.58**	**2.66E-18**	2.66E-16
Sulfinyl	Glucoraphanin	C12H23NO10S3	436.04059	955.65	0.227811079	**1.17**	**1.81**	**0.015653276**	0.005568291
	Glucoalyssin	C13H25NO10S3	450.0568	LOW	#NUM!		**#NUM!**		
	Glucohesperin	C14H27NO10S3	464.0719	901.19	2.201411142	**4.60**	**14.98**	**1.04E-15**	1.32E-14
	Glucoibarin	C15H29NO10S3	478.0879	866.48	1.749953124	**3.36**	**10.00**	**1.01E-10**	1.68E-10
	Glucohirsutin	C16H31NO10S3	492.1048	837.61	1.750826699	**3.37**	**9.48**	**3.34E-10**	5.04E-10

Appendix Table 38

				Mandi 5 uM on Cyp86a:MANDI					
				Average RT	log2(fc)	Mean FC	-log10(p-value)	p-value	q-value
Aromatic	Sinalbin	C14H19NO10S2	424.0378						
	Gluconasturtiin	C15H21NO9S2	422.0585						
	Glucobrassicin	C16H20N2O9S2	447.0537	862.42	-0.114658869	0.92	**0.60**	0.251121927	0.105201687
Thionyl	Glucoerucin	C12H23NO9S3	420.0462	754.78	-0.338889097	**0.79**	**3.14**	**0.000727154**	0.001446628
	Glucoberteroin	C13H25NO9S3	434.0619	736.43	-0.50745762	**0.70**	**3.19**	**0.000645958**	0.001302697
	Glucolesquerellin	C14H27NO9S3	448.0787	719.43	-0.384459344	**0.77**	**2.25**	**0.005560711**	0.007044801
	7-Methylthioheptyl glucosinolate	C15H29NO9S3	462.0941623	702.7	-0.190580984	0.88	**0.98**	0.104502128	0.057851025
	8-Methylthiooctyl glucosinolate	C16H31NO9S3	476.1105759	690.03	-0.023040101	0.98	**0.42**	0.382817327	0.139447486
Sulfinyl	Glucoraphanin	C12H23NO10S3	436.04059	952.35	0.210240673	1.16	**1.85**	0.014158812	0.013264602
	Glucoalyssin	C13H25NO10S3	450.0568	LOW	#NUM!		**#NUM!**		
	Glucohesperin	C14H27NO10S3	464.0719	897.515	0.762132629	**1.70**	**6.92**	**0.000000121**	0.00000208
	Glucoibarin	C15H29NO10S3	478.0879	861.395	0.534203127	**1.45**	**3.48**	**0.000331222**	0.000726242
	Glucohirsutin	C16H31NO10S3	492.1048	831.81	0.817048165	**1.76**	**3.59**	**0.000259537**	0.000597706

Appendix Table 39

Appendix Figures

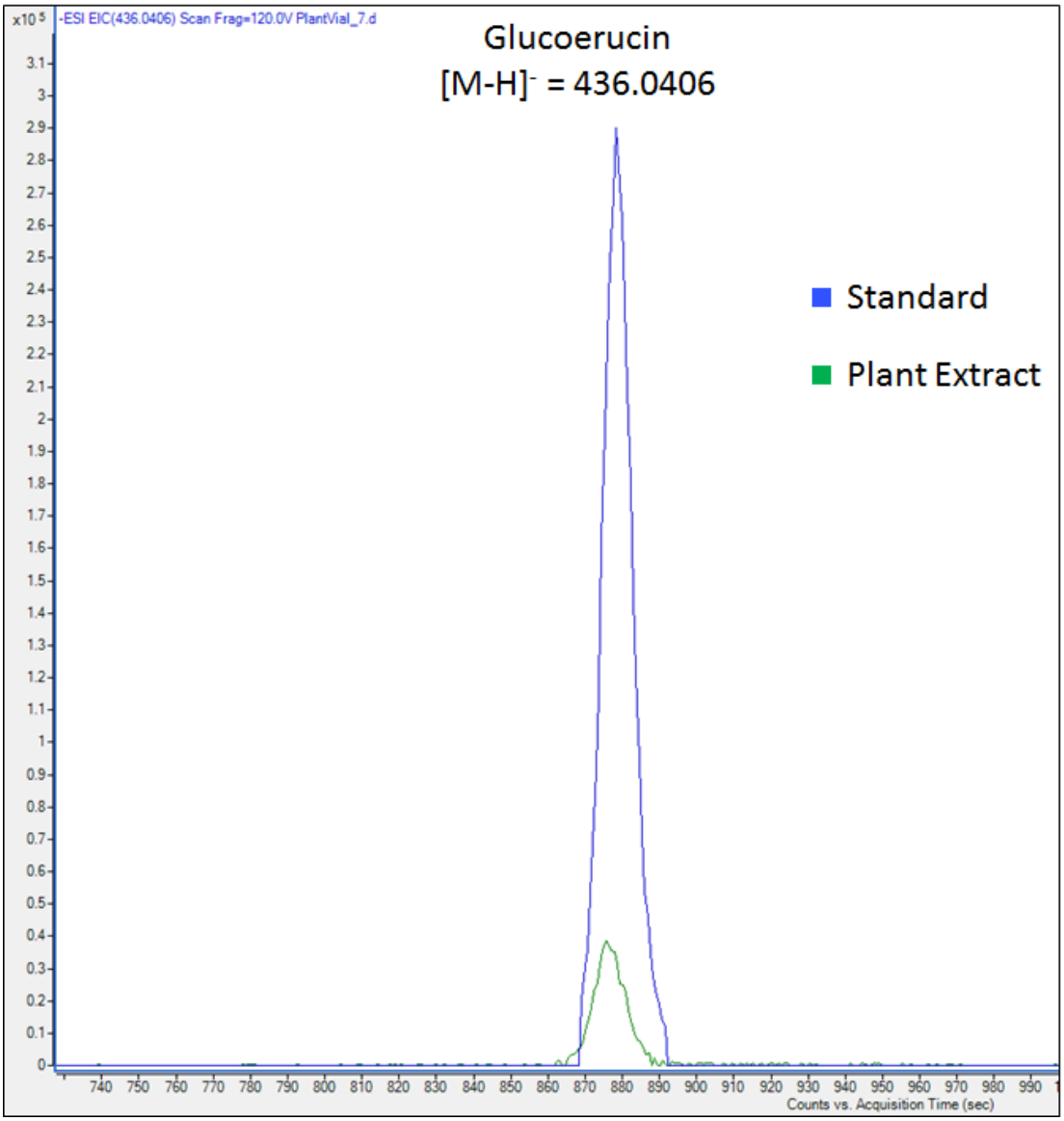

Appendix Figure 1 The extracted ion chromatogram pertaining to the mass of the negative ion from glucoerucin. Commercial standard of glucoerucin (blue) and plant extract treated with ABA (green) showing similar retention times and m/z when injected into the LC/MS HILIC method.

Appendix: Publications

Chemical manipulation of plant water use

Jonathan DM Helander [a1], Aditya S Vaidya [a1] and Sean R Cutler [a*]

[a] Institute for Integrative Genome Biology, Center for Plant Cell Biology, and Department of Botany and Plant Sciences, University of California, Riverside, California 92521, USA.

[1] these authors contributed equally

sean.cutler@ucr.edu

951-827-6990

Abstract

Agricultural productivity is dictated by water availability and consequently drought is the major source of crop losses worldwide. The phytohormone abscisic acid (ABA) is elevated in response to water deficit and modulates drought tolerance by reducing water consumption and inducing other drought-protective responses. The recent identification of ABA receptors, elucidation of their structures and understanding of the core ABA signaling network has created new opportunities for agrochemical development. An unusually large gene family encodes ABA receptors and, until recently, it was unclear if selective or pan-agonists would be necessary for modulating water use. The recent identification of the selective agonist quinabactin has resolved this issue and defined *Pyrabactin Resistance 1* (PYR1) and its close relatives as key targets for water use control. This review provides an overview of the structure and function of ABA receptors,

progress in the development of synthetic agonists, and the use of orthogonal receptors to enable agrochemical control in transgenic plants.

Introduction

Drought is the major source of crop losses worldwide and major improvements to agricultural productivity may be realized by improving water use and drought tolerance [1]. There are many strategies for mitigating the effects of drought on yield, including the development of drought tolerant crops through breeding or transgenic approaches [2–4]; here we focus on abscisic acid (ABA **1, Figure 1**) receptor agonists, which afford direct control of plant transpiration by targeting a highly conserved family of receptors that control a negative regulatory response pathway (**Figure 1**). ABA controls plant water use primarily through modulating ion transport in guard cells, pairs of specialized epidermal cells that form a stomatal pore that opens and closes in response to environmental signals (**Figure 1**). The accumulation of new biomass through photosynthesis depends on entry of atmospheric CO_2 to inner leaf mesophyll cells through stomata, but this comes at the cost of H_2O escape driven by the large difference in water vapor pressure between the inner leaf and atmosphere. Plants therefore face an intrinsic tradeoff between water conservation and growth, and consequently perturbations that reduce water consumption typically come at the cost of reduced growth. Conversely, selection for high yielding crop varieties has been associated with increased stomatal conductance in some crops [5,6].

Although the water / growth tradeoff may appear to create an insurmountable dilemma from the perspective of increasing yields during drought, the effects of drought vary throughout a plant's life cycle. In maize for example, drought during the early juvenile growth phases or late growth phases is less detrimental to final grain yield than during

flowering, where drought can cause reproductive failure [7]. Monsanto's recently introduced DroughtGard™ trait achieves ~6% yield increases under conditions of moderate drought by overexpression of a *B. subtilis* cold-stress induced RNA chaperone protein [4]. This trait selectively reduces the water consumption of juvenile plants during water deficit, which in turn increases soil water content at flowering relative to non-GMO controls [4]. The molecular mechanism of the trait's physiological action is unclear, but it nonetheless illustrates the potential of "water banking" to improve yield during drought. Synthetic ABA agonists, such as quinabactin (**2**) and pyrabactin (**3**) [8,9], are attractive because agonists can, in principle, enable an agrochemical strategy for water banking in any crop of interest.

Molecular aspects of ABA perception and action

S-(+)-ABA is a chiral sesquiterpenoid, with a decorated cyclohexenone ring appended to a dienoic acid sidechain. ABA is derived from β-carotene and was discovered in the 1960s by activity guided identification of plant growth regulators [10–12]. In addition to its role in guard cell physiology, ABA mediates other abiotic stress responses (for example freezing tolerance) and plays a central role in inducing seed

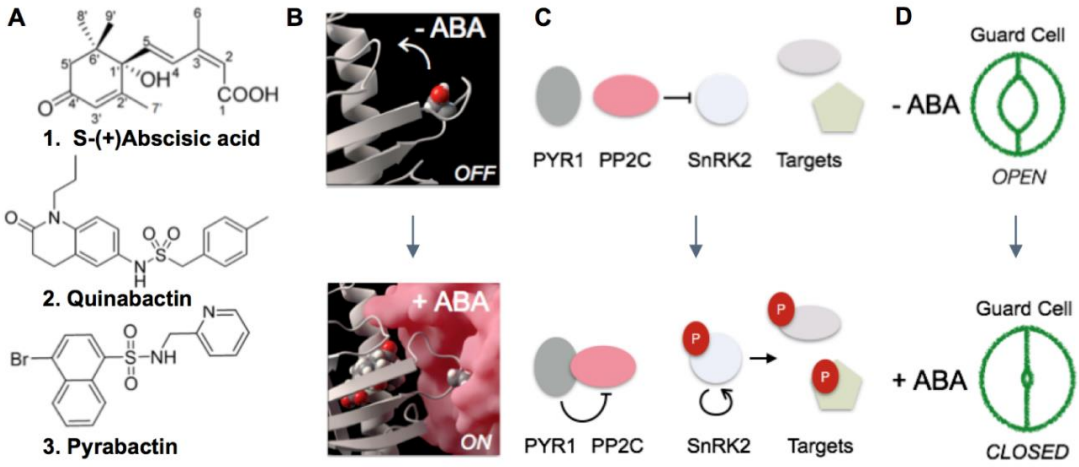

Figure 1. (a) Structures of *S*-(+) abscisic acid (**1**), quinabactin (**2**) and pyrabactin (**3**) (b) The gate-latch-lock structural mechanism for ABA recognition and biochemical activation. The receptor is depicted as a gray cartoon, ABA is depicted in a gray CPK model, and the PP2C is depicted as a pink surface. c) Biochemical pathway downstream of activation of ABA receptors. d) The physiological response of guard cell closure in the presence of ABA or other receptor agonists.

dormancy, controlling root architecture, and influences several biotic interactions [10]. ABA biosynthesis is tied to water status and cellular osmotic pressure; reductions in osmotic pressure lead to rapid transcriptional induction of ABA biosynthetic enzymes, in particular nine-cis epoxycarotenoid dioxygenases (NCEDs), which act at the first committed step in ABA biosynthesis [12]. ABA levels rise greater than 25-fold under mild drought conditions due to *de novo* ABA biosynthesis and hydrolysis of inactive glucose-esters [12,13]. Mutants deficient in NCEDs or other biosynthetic enzymes lose leaf turgor (i.e. wilt) more rapidly than wild type plants [12,14]. Conversely, treatment of plants with exogenous ABA or synthetic agonists causes guard cell closure, reduces transpiration, and prolongs the time before wilting occurs relative to untreated plants [8,9,13,15]. ABA also induces the transcription of genes encoding enzymes that increase cellular osmolytes levels, and has other drought-protective effects [16].

ABA responses are mediated by a negative regulatory signaling module that involves soluble *Pyrabactin Resistance 1* / *PYR1-Like* / *Regulatory Component of ABA Receptor (*PYR/PYL/RCAR) ABA receptors, clade A type 2C protein phosphatases (PP2Cs) and subfamily 3 Snf1-related kinases (SnRK2s; **Figure 1**). The SnRK2s directly phosphorylate and control the activity of several downstream effectors such as transcription factors, and anion channels that are required for guard cell closure [17]. The SnRK2s autoactivate by cis- and trans-autophosphorylation, but their activity is suppressed by the PP2Cs, which dephosphorylate and inactivate the kinases [18,19]. When ABA binds to soluble PYR/PYL/RCAR ABA receptors, the receptors bind stably within PP2C active sites and inhibit PP2C activity, this in turn enables accumulation of activated SnRK2 kinases, which regulate downstream factors by direct phosphorylation [20–22].

ABA receptors are members of the START / Bet v 1 superfamily [5], an ancient family characterized by an α - β - α_2- β_6- α topology that forms a helix-grip fold in which 7 anti-parallel beta-sheets (and intervening short loops and helices) enclose a long C-terminal helix to form a central ligand binding pocket [23–25]. The structures of several ligand-receptor complexes have been elucidated by X-ray crystallography and depict the conformation of receptor-bound ABA as a half-chair with a pseudoaxial sidechain [26–32] (**Figure 2**). ABA binding induces a conformational change that enables the receptors to dock into and inhibit PP2C activity. The largest conformational change occurs in a “gate”-loop that flanks the ligand binding pocket, which adopts a closed conformation via direct hydrophobic contacts to ABA [26,27,29,30,33]. A second “latch”-loop also changes conformation and encloses the bound ligand (**Figure 1**). The sidechain of an invariant serine in the -SGLPA-gate-loop points in towards the ligand binding pocket in apo-receptor structures but becomes solvent exposed after agonist binding / gate closure, which enables the closed

conformer to bind and competitively inhibit PP2C enzymatic activity. The majority of ABA recognition occurs inside the receptors and involves 25 highly conserved residues that make direct or water-mediated contacts to ABA. Additionally, a critical PP2C tryptophan located in a recognition loop that is specific to ABA regulated PP2Cs, called the “lock”, inserts into a small pore directly above ABA’s 4’-carbon and makes a water mediated contact to ABA’s ketone [29,30,33,34]. ABA binding is stabilized by both direct and water-mediated hydrogen bonds, in addition to multiple hydrophobic interactions. Notably, a conserved lysine in the PYL protein family (K59 in PYR1) forms a direct hydrogen bond to the carboxylate of ABA. A water-mediated H-bond network interacts with both carboxylate oxygen atoms of ABA to produce hydrogen bonding to residues homologous to PYR1’s *Y120*, *S122*, and *E141*, which are part of a hydrophilic region located deep within the pocket [26]. The gate-latch interface facilitates hydrophobic interactions with the cyclohexenone ring and the 7’-, 8’- and 9’-methyl constituents of ABA [26,30], forming a hydrophobic region of the top of the pocket.

The ABA receptor gene family is unusually large, for example there are 14 members in *Arabidopsis thaliana,* 15 members in tomato, and 21 members in soybean [35,36]. The receptors form three phylogenetically distinct subfamilies that can be found in all flowering plant genomes sequenced (**Figure 3**) [37–39]. The biological roles of the different subfamilies are still being established, but as we describe below, activation of the PYR1-subfamily of dimeric receptors is sufficient to elicit guard cell closure, reduce water consumption and induce ABA-transcriptional responses in many species, which demonstrates its centrality in plant water relations [8].

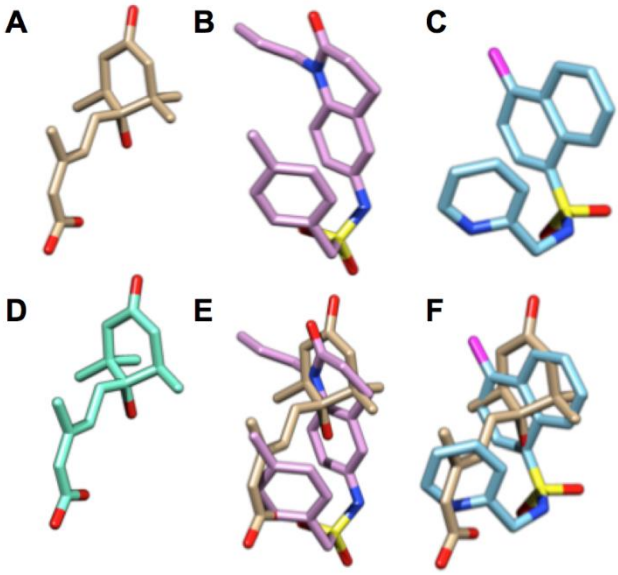

Figure 2. 3-D aligned structures of receptor-bound agonists. (a) ABA (3QN1), (b) quinabactin (4LA7), (c) pyrabactin (3NMN), (d) R-(–)-ABA, and overlays of ABA with quinabactin (e) or pyrabactin (f) The PDB accessions used for each ligand in parentheses.

In Arabidopsis, there are nine clade A PP2Cs [40]. One of the nine PP2Cs (*ABA Hypersensitive Germination 1*, AHG1) is recalcitrant to PP2C mediated inhibition due to a naturally occurring mutation of the Trp lock residue [41]. Genetic evidence indicates redundant / overlapping functions for the PP2Cs [42], but biochemical evidence demonstrates differences in ABA sensitivity for different PP2C-receptor complexes [41,43], and at least one receptor (PYL13/RCAR7) selectively interacts with a subset of clade A PP2Cs [44]. The values measured in receptor-mediated PP2C inactivation assays are thus influenced by the specific PP2C utilized, and direct biophysical measurements, such as isothermal titration calorimetry (ITC), have obvious value for inferring intrinsic agonist-receptor binding affinities. ITC measurements have shown low micromolar K_d values [21,33,43,45,46], and that the inclusion of PP2Cs in binding reactions lowers apparent K_d*s* by ~10- to 25-fold [21,45], presumably by reducing K_{off}. For example, PYL5 displays an apparent K_d of 1 µM for ABA binding, which is lowered to 38 nM by the addition of HAB1 to binding reactions [45]. *In vivo* potency, receptor-agonist K_d, and PP2C-inhibitory activity generally

correlate and IC_{50} values can be used to rank compound potency and selectivity relative to ABA [8]. Typical IC_{50} values for ABA-mediated PP2C inhibition range from ~20 - 300 nM (**Figure 3**) when assayed using the PP2Cs ABA Insensitive 1 (ABI1), ABA Insensitive 2 (ABI2) or Homolog of ABI1 (HAB1) [8,20,21,45].

Members of the PYR1 subfamily (PYR1, PYL1 - 3) form homodimers in solution, while the members of the other subfamilies are monomeric and display higher ABA affinity [26,27,33, 31]. The PYR1 homodimerization interface overlaps substantially with the PP2C binding interface of the ligand-bound complex, which necessitates dimer dissociation prior to ligand-induced PP2C inhibition [33,47]. ABA shifts dimeric PYR1 towards a monomeric state *in vitro*, as measured using size exclusion chromatography [47] and analytical ultracentrifugation, the latter of which has shown that ABA increases the homodimerization K_d*s* of PYL2 and PYL3 ~3 - 6-fold [46]. The decreased ABA affinity of dimeric receptors has been proposed to result from a thermodynamic penalty imposed by dimer dissociation [47], however it is also likely that an additional hydrogen bond to ABA in monomeric receptors, as observed with PYL9 [32], contributes to differences in sensitivity as well. PYL10 was initially described as a constitutively active receptor [31], however this erroneous conclusion was due to an *in vitro* artifact caused by the spurious ability of BSA (utilized in PP2C assays) to weakly activate PYL10 [48]. Additionally, backbone dynamics measurements indicate that PYL10's conformational entropy increases upon ABA binding, which may function to stimulate receptor-PP2C interactions [48].

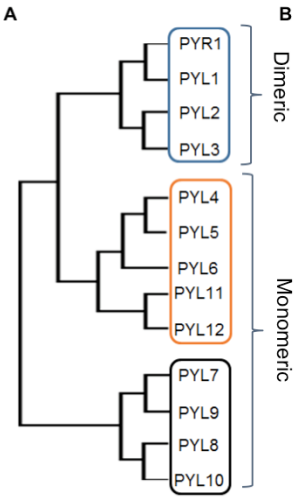

Receptor	ABA(nM)	Pyrabactin(nM)	Quinabactin(nM)
PYR1	307	656	103
PYL1	301	1197	250
PYL2	151	>10000	267
PYL3	70	>10000	724
PYL4	68	>10000	>10000
PYL5	27	5174	649
PYL6	29	>10000	>10000
PYL11	64	>10000	>10000
PYL12	ND	ND	ND
PYL7	ND	ND	ND
PYL9	60	>10000	>10000
PYL8	57	>10000	>10000
PYL10	121	1892	>10000

Figure 3. Arabidopsis ABA receptor sub-families. The left panel shows a phylogeny of the Arabidposis thaliana PYR/PYL/RCAR receptors and the right panel shows IC_{50} values for receptor-mediated inhibition of HAB1 by ABA, pyrabactin and quinabactin. (adapted from reference 8). PYL13 has been omitted, but it is a member of the PYL5 subfamily.

Thus extensive biochemical analyses of Arabidopsis receptors show that the PYR1 subfamily encodes dimeric receptors of lower intrinsic affinity and sensitivity to ABA, while the PYL5- and PYL8-subfamilies (**Figure 3**) are monomeric, higher affinity receptors, a pattern conserved in tomato and rice receptor subfamilies as well [36,49]. It has been hypothesized that the different subfamilies function in different regions of the ABA dose response curve, with the PYR1-subfamily being activated by the high ABA levels produced during abiotic stress [47]. Genetic studies, however, have shown additive contributions of several Arabidopsis receptors for the control of stomatal conductance, implying overlapping functions within guard cells [50]. The PYL8 subfamily may contribute differentially to root responses to ABA, as Arabidopsis the roots of plants harboring *pyl8* mutations are less sensitive to ABA in multiple assays [51,52]. Given the extensive genetic

redundancy observed for ABA receptors, selective agonists will undoubtedly help probe receptor function *in vivo*.

Synthetic ABA Receptor Agonists

The identification of ABA receptors and elucidation of their structures has created new opportunities for discovering and designing modulators of receptor function. Although ABA could, in principle, be used directly as an agrochemical, it has been limited by its molecular complexity, photolability [53–55], moderate chemical stability,[20,21] and rapid catabolic inactivation [56,57] by plant cytochrome P450s in the CYP707A subfamily [57]. Synthetic agonists with improved properties are therefore of interest and multiple synthetic agonists have been described and characterized, as have numerous ABA analogs (see below). These compounds have revealed functional differences between receptors and defined the dimeric ABA receptors as targets that can be used to chemically control transpiration.

The identification and characterization of the selective agonist pyrabactin (**3**) played a critical role in the identification of ABA receptors. Pyrabactin was identified as a molecule that phenocopies ABA's inhibitory effect on seed germination using a phenotype-based screen of a small molecule diversity library [20,58]. Molecular and physiological characterization demonstrated that pyrabactin activates seed ABA responses without strongly activating vegetative tissue ABA responses [20]. Genetic mechanism-of-action studies established that *PYR1* is required for pyrabactin's bioactivity, that pyrabactin and ABA both directly bind to PYR1, and that the key biochemical function of ABA agonists is to promote the formation of a receptor / PP2C complex that inhibits PP2C activity [20]. This

work converged with the identification of RCAR1 (PYL9), which was identified by characterization of PP2C binding proteins and subsequent determination that RCARs bind ABA to mediate PP2C inhibition [21]. Additional studies identified multiple members of the receptor family as binding partners of ABI1 and HAB1 [45,59]. Collectively, these studies defined the PYR/PYL/RCAR gene family as encoding ABA receptors. Numerous groups had previously attempted to identify ABA receptors using genetic approaches in Arabidopsis and in hindsight these attempts failed because of the extensive genetic redundancy between the 14-members of the receptor gene family. PYR1 loss-of-function mutants do not show pronounced defects in ABA responses, and higher-order mutants are required to observe strong reductions of ABA responses. Pyrabactin's selective effects on seeds is a result of both its preferential activation of PYR1 and the high level expression of *PYR1* mRNA in seeds; features which allowed a single loss of function mutation to reveal *PYR1*'s role in ABA signaling. Thus, the selectivity of pyrabactin enabled it to bypass the functional redundancy that had hampered discovery of ABA receptors by forward genetic approaches.

Pyrabactin is a selective agonist that can activate PYR1, PYL1, PYL5, and PYL10 (IC_{50} values of 660, 1200, 5200, and 1900 nM respectively, ~2 – 60x that of ABA measured on the same receptors). Since mutations in *PYR1* block pyrabactin's bioactivity, it is likely that PYR1 is pyrabactin's key cellular target. Why does pyrabactin not activate all ABA receptors, like ABA does? This has been addressed with genetic and structural studies dissecting the differential pyrabactin sensitivity of PYR1 and PYL2 [60–62], which pinpointed two residues, PYR1 *I110* and to a lesser degree *I62*, as determinants of pyrabactin selectivity. PYL2 possesses a smaller valine residue at its corresponding residues (*V67* and *V114*). Swapping these residues to create the mutants PYR1^{I62V,I110V} and PYL2^{V67I,V114I}

converts PYL2 into a pyrabactin responsive receptor and removes responsiveness from PYR1 [60–62]. X-ray crystallographic and HSQC-binding studies unexpectedly revealed that pyrabactin can bind to, but not activate, PYL2 because it binds in an unproductive orientation that prevents gate closure [60–63]. This property makes pyrabactin an antagonist of PYL2, however it is too weak to measurably antagonize ABA action *in vivo* [60,64]. Thus, PYR1 and PYL2 contain subtle sequence differences in ligand contacting residues (**Figure 4**) that can be exploited to tune agonist selectivity.

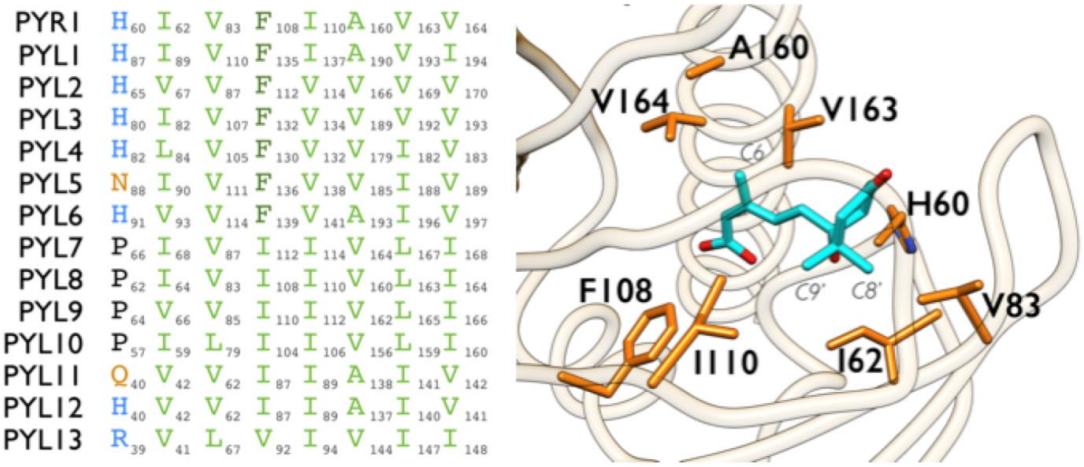

Figure 4 . Variable amino acid residues within the ligand-binding pockets of *Arabidopsis thaliana* PYR/PYL/RCAR receptors.

Several analogs of pyrabactin (**Figure 5**) have been characterized and provide insight into structure-activity relationships. Apyrabactin (**4**), a biologically inactive analog lacking the pyridyl nitrogen, is unable to form a water-mediated hydrogen bond to the highly conserved lysine (*K59* in PYR1) that normally forms a hydrogen bond to ABA's carboxylate [60,62]. Changing the positioning of the nitrogen on the pyridyl ring (compound **5**) or replacement of the bromine atom on the napthyl ring with hydrogen or a methyl group (compound **6** and **7**) reduce activity. Non-polar alterations to the napthyl moiety are also

detrimental, but to a lesser effect (compounds **8** and **9**) [20], suggesting that the gate-latch-agonist interface can tolerate subtle modifications in this region of the pyrabactin scaffold [62]. Replacement of pyrabactin's pyridyl methylamino substructure with a methionine-derivative (**10**), a modification suggested from virtual screening experiments, yields an equipotent compound in PYR1 / PP2C inhibition assays [60]. Bioisosteres of pyrabactin's sulfonamide moiety have recently been described: phosphonamide (**11**) and phosphonate substitutions of the sulfonamide linker have yielded compounds with similar or stronger effects than pyrabactin, however these analogs have not been characterized biochemically [65]. Pyrabactin's napthyl ring can be replaced by a naptholactam moiety (**12**), which can likely form a hydrogen bond to the conserved gate-latch water, however the activity of **12** is reduced in comparison to pyrabactin. Other naptholactams that replace the pyridyl ring with a tetrahydrofuranyl moiety (**13**) or an ethyl ester (**14**) display modest *in vitro* activity [60]. Arylsulfonamides related to pyrabactin have been described in the patent literature as compounds for controlling abiotic stress tolerance [66], however pyrabactin's limited activity in vegetative ABA responses will likely need to be circumvented in order to develop agriculturally useful agents from this scaffold. Nonetheless, pyrabactin has proven a valuable probe molecule for both genetic and functional dissection of receptor function.

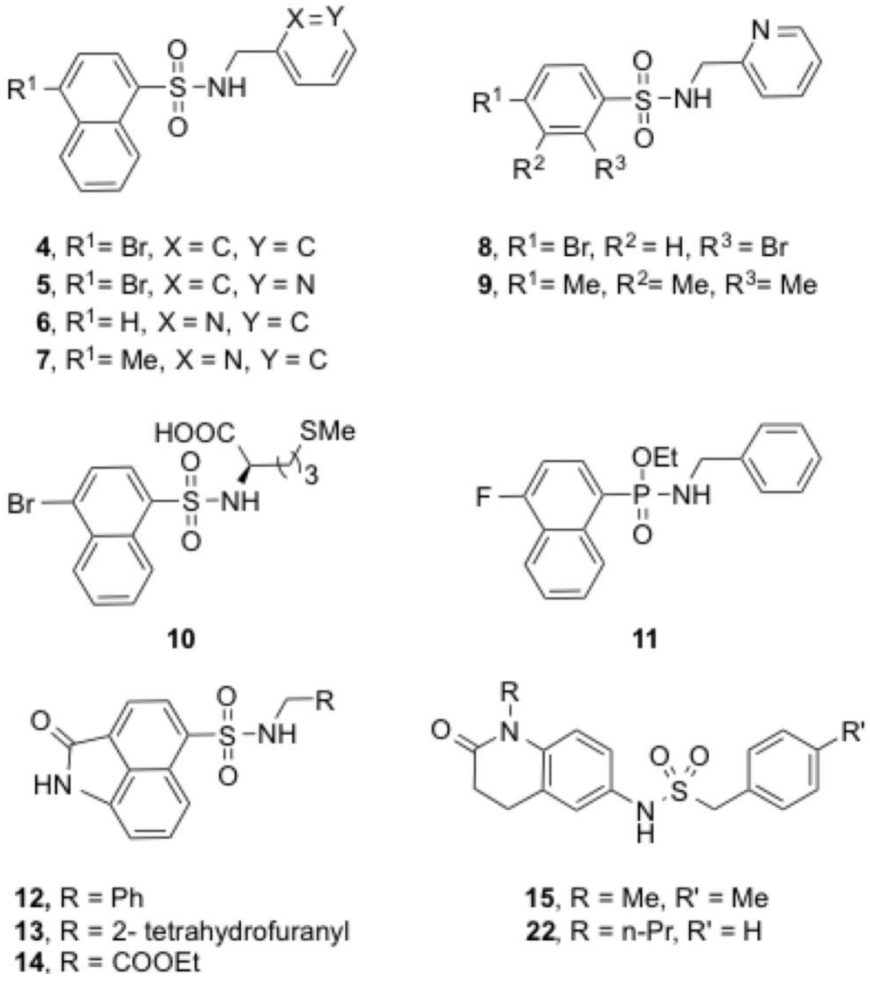

Figure 5. Structures of pyrabactin and quinabactin analogs.

Given pyrabactin's limitations, Okamoto et al. conducted small molecule screens for compounds capable of activating multiple receptors (PYR1 - PYL4) using heterologous yeast two hybrid reporter strains, which report agonist activity by the ligand-induced physical interaction between receptors and PP2C [8,20,61]. This screening effort identified quinabactin (**2**), a dihydroquinolinone sulfonamide that, like pyrabactin, contains two aromatic rings separated by a sulfonamide-containing linker. Remarkably, quinabactin (also named AM1) was independently isolated in a screen for small molecules that induce PYR1-HAB1 binding using a direct biophysical assay [9]. Quinabactin possesses activity on

PYR1, PYL1, PYL2, PYL3 and PYL5 in phosphatase inhibition assays, although its IC_{50} values for PYL3 and PYL5 are >10-fold higher than ABA's [8,9]. Quinabactin also preferentially activates tomato dimeric subfamily receptors[36].

The biological effects of quinabactin are highly similar to those of ABA, despite its inability to activate the full complement of ABA receptors. Quinabactin inhibits Arabidopsis seed germination and induces a genome-wide ABA-like transcriptional response in seedlings [8,9]. Quinabactin also induces guard cell closure and reduces transpiration in multiple species and, like ABA, increases survival after extended water deficit in Arabidopsis [8]. Collectively, these observations demonstrate that a pan-agonist is not necessary for controlling guard cell and other vegetative ABA responses.

Although quinabactin most strongly activates the dimeric subfamily of receptors, it also weakly activates PYL5. Mutational analyses using a *pyr1/pyl1/pyl2/pyl4* quadruple mutant genotype have shown that PYL5 does not make a substantial contribution to quinabactin action. The *pyr1/pyl1/pyl2/pyl4* quadruple mutant is ABA hyposensitive in many assays, but still retains some ABA sensitivity due to redundancy between receptors. For example, ABA-induced transcription of marker genes is reduced by only ~80% in the quadruple mutant strain. Subsequent genetic removal of *PYL5* and *PYL8* strongly enhances the ABA insensitivity of the quadruple mutant, indicating that the residual ABA-response in the quadruple is mediated by other PYL receptors [8,50]. Unlike ABA however, quinabactin does not induce a residual transcriptional response in the quadruple mutant, which is also highly insensitive to quinabactin's inhibition of seed germination [8]. Collectively, these data show that the dimeric receptors are targets that can be used to chemically control transpiration, however the relative importance of specific subfamily members is unclear. Quinabactin and pyrabactin differ in that

pyrabactin is unable to activate PYL2. This could imply that PYL2 activation or co-activation is important for quinabactin's unique bioactivity. The development of agonists with greater selectivity will help resolve this point. Additionally, the development of agonists selective for the other subfamilies will help establish if the other receptor subfamilies can be used to control transpiration.

Figure 6. The 3'-tunnel (A) and C6-cleft (B) are variable regions of the receptors' ligand-binding pockets. Amino acids that are variable between receptors are labeled with an asterisk. V163 andF159, which are also part of the C6-cleft have been omitted for clarity. Made from PDB 3QN1.

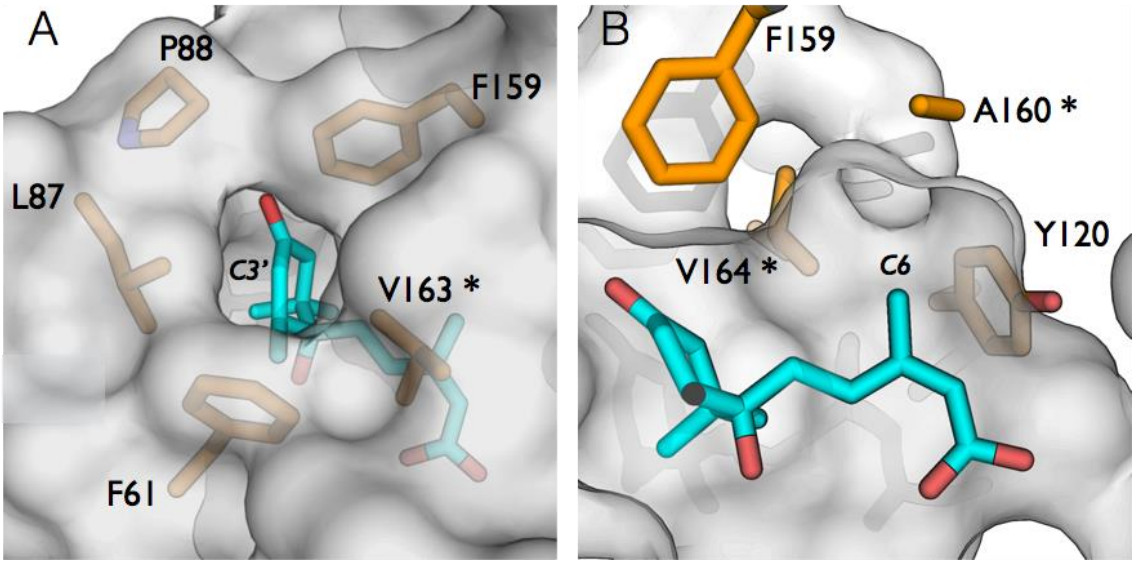

Shortening quinabactin's *N*-alkyl chain from *N*-propyl to *N*-methyl substantially (**15**) reduces *in vitro* activity [9], which can be rationalized by reduced hydrophobic interactions with the 3'-tunnel, a small hydrophobic pore directly above ABA's 3'-carbon that forms after gate closure (**Figure 6a**) [64]. The importance of this region for modulating agonist interactions is supported by the improved activity of ABA analogs (**Figure 7**) that expand into this pocket. For example, a series of 3'-alkylsulfanyl ABA analogs (**16** & **17**) were synthesized to probe this region [64]. The analog AS2 (ethylsulfanyl-ABA, **16**) possesses

increased agonist activity both *in vitro* and *in vivo* and shows increased selectivity for the dimeric subfamily receptors relative to ABA. AS2, like quinabactin, activates vegetative ABA responses, which provides independent support for the conclusion that activating the dimeric receptors is sufficient to reduce water use [64]. The analog AS6 (hexylsulfanyl-ABA, **17**), which has a sufficiently long carbon chain to protrude through the 3'-tunnel, blocks PYR1-PP2C interactions and antagonizes endogenous ABA responses in multiple species [64].

Manipulating hydrophobic interactions with the vicinity of the 3'-tunnel and gate is likely to provide a general strategy for improving dimeric receptor agonist activity, as hydrophobic expansion into the 3'-tunnel improves activity of other ABA analogs. For example, bicyclic tetralone ABAs (**18**), which incorporate ABA's 3', 4' and 7' carbons into a phenyl ring, have improved activity *in vitro* and *in vivo* [67–69]. Tetralone-ABA derivatives with 11'-alkyl ether chains (**19**) that are predicted to extend into the 3'-tunnel gain favorable activity with short alkyl chains (n=1), but sufficiently long alkyl-chains (n=4) yield antagonists [70]. 7'-nor-ABA (**20**), which replaces the 7'-methyl with an H, which should reduce hydrophobic interactions with the gate, has greatly reduced *in vitro* and *in vivo* activity, indicating interactions in this region are necessary with the ABA scaffold [71]. Thus, modifications of ligands in positions proximal to the 3' tunnel and gate can be used to improve agonist activity or to engineer antagonists [64].

Gate closure creates a second pore above ABA's 4'-carbonyl that enables a water mediated contact between ABA's ketone oxygen and the Trp lock that is located on the PP2Cs. Quinabactin's quinolinone carbonyl oxygen, which can be superimposed on ABA's cyclohexenone oxygen when comparing receptor-ligand complexes (**Figure 2f**), participates in a water mediated contact to the Trp lock [8,9]. Quinabactin's ability to H-bond

to the Trp lock likely underlies its improved activity relative to pyrabactin, as pyrabactin does not possess a hydrogen bond acceptor positioned to interact with the Trp lock. Consistent with the general importance of this interaction, 4'-deoxo-ABA (**21**) displays greatly reduced bioactivity [72].

Quinabactin's 4-methylbenzyl methyl substituent occupies a small cleft that is normally occupied by ABA's C6-methyl (**Figure 6b)**. An analog of quinabactin that replaces the 4-methyl substituent with a hydrogen atom (**22**) has greatly reduced activity *in vitro* and *in vivo* [9,73], implying that hydrophobic contacts inside the cleft are critical for activity. Consistent with this hypothesis, the ABA analog 6-nor-ABA (**23**), which converts ABA's C6 methyl to an H, also shows greatly reduced activity [71]. These studies demonstrate the importance of agonist interactions with the C6-cleft for activity. In addition, three of the 6 residues that form the C6-cleft are variable between receptors (**Figures 4 & 6b**), suggesting that the C6-cleft might be exploited for tuning agonist selectivity.

Pyrabactin and quinabactin are both constructed from two aromatic ring systems connected by a short sulfonamide linker and both compounds adopt a similar U-shaped conformation (**Figure 2**) in the ligand binding pocket, positioning their hydrophobic rings adjacent to the hydrophobic gate (3'-and 4'-tunnels) and C6-cleft, which normally contact ABA's hydrophobic cyclohexenone head group and its C6-methyl, respectively. The sulfonamide linkage in both molecules is positioned towards the bottom of the ligand binding pocket and interacts with residues that would normally contact ABA's carboxylate and ring hydroxyl. In both agonists, their sulfonamide NH forms a direct hydrogen bond to *E94* (*E98* in PYL2), which normally participates in water-mediated H-bonds to ABA's carboxylate and ring hydroxyl groups. The *pyr1-6* allele, which encodes *E94K*, disrupts

this residue and possesses strong pyrabactin insensitivity *in vivo*, consistent with the critical importance of this interaction to agonist activity [20]. Across published ABA structures, ABA binding is stabilized by 4 water molecules that form an H-bond network, quinabactin binding displaces 3 of these waters, which may contribute favorably to the thermodynamics of quinabactin binding.

Stereoselectivity, ABA affinity and ABA Metabolism

S-(+)-ABA is the naturally occurring ABA, however some ABA receptors can accommodate the *R*-(–)-isomer (**24**) if its ring rotates 180º [11,26,28]; *R*-(–)-ABA therefore possesses varying degrees of bioactivity [74]. The 180° rotation of the cyclohexenone ring needed for (–)-ABA binding causes the 8'- and 9'-methyl substituents to occupy the space normally occupied by ABA's 7'-methyl. Not all receptors can accommodate (–)-ABA due to sequence variation in residues homologous to *I62* and *I110* in PYR1 (which also influence pyrabactin sensitivity, as described above) [28]. For example, wild type Arabidopsis PYL9 does not efficiently bind (–)-ABA, but PYL5 does. The PYL9 mutants *V66I* and *I112V* make their ligand binding pockets more PYL5-like and imbue partial *R*-(–)-ABA responsiveness on the mutant receptors [28]. In addition to stereoselectivity, ABA receptors also display differences in their intrinsic ABA binding affinities due to variable ligand-binding pocket architectures. For example, sequence variation in residues lining the C6-cleft (**Figure 6**) orient ABA in the monomeric receptor PYL9 so that an additional H-bond between ABA's carboxylate and *N169* can form. This H-bond is not observed in dimeric receptor/ABA complexes and contributes to PYL9's higher intrinsic ABA affinity [32]. These data further illustrate the impact of relatively subtle sequence variation between receptors on agonist selectivity and affinity.

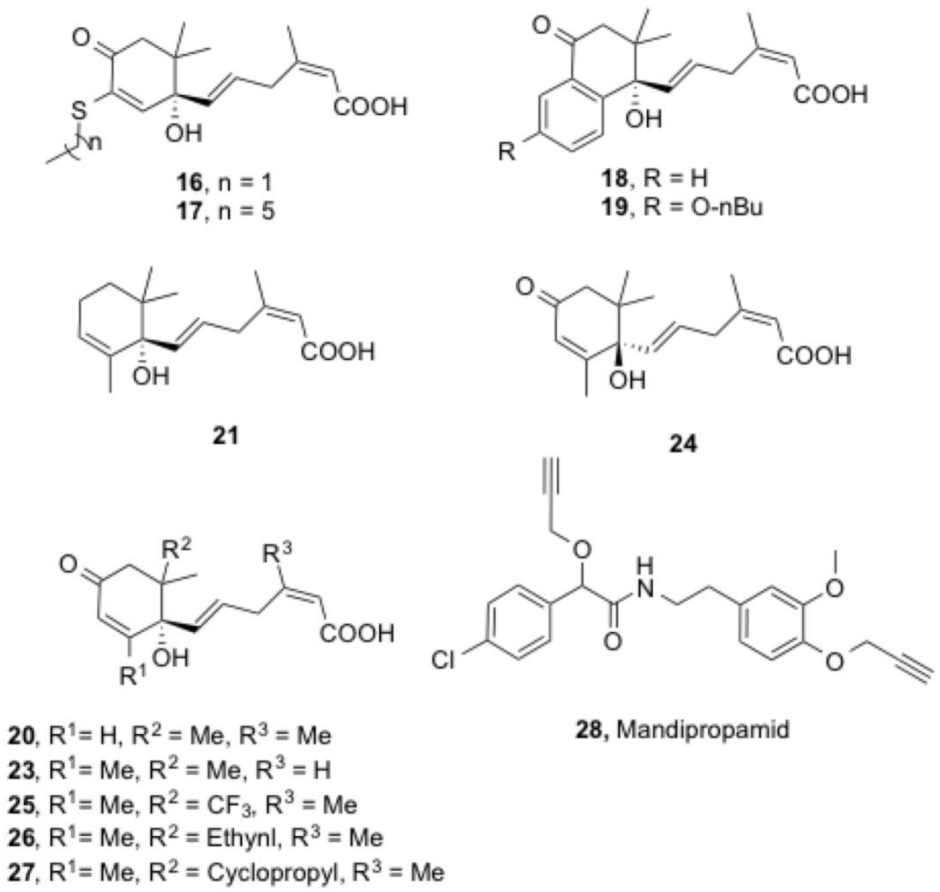

Figure 7. Structures of ABA analogs.

Manipulation of endogenous ABA levels provides an alternate path to controlling plant water relations. The concentration of free ABA is determined by rates of biosynthesis and catabolism and perturbations of either can change ABA levels [12]. ABA is catabolized primarily by oxidation of its ring methyl groups and glucosylation of its carboxylate. The CYP707A subfamily of cytochrome P450 enzymes catalyze the formation of 8'- and 9'-OH ABA, which spontaneously cyclize to form phaseic acid (PA) and neo-phaseic acid (neoPA) respectively [12,75]. PA can be subsequently reduced to dihydroPA (DPA). The major ABA metabolites are unlikely to activate ABA receptors *in vivo* as PA, neoPA,, 7'-OH ABA, and ABA-glucoside display IC_{50} values much lower than (+)-ABA when tested

with representative members of each receptor subfamily [68]. Alteration of the 8'-methyl group to yield 8',8'-difluoroabscisic acid and 8',8',8'-trifluoroabscisic acid (**25**) yields analogs that show delayed metabolism *in vivo* and increased bioactivity [76]. Similarly, alkynyl derivatives at the 8' (**26**) and 9' position have yielded CYP707A suicide inhibitors that are of interest because they have more persistent biological effects than ABA [77]. Both 8'- and 9'-acetylene ABA analogs display agonist activity comparable to that of ABA in *in vitro* PP2C assays with multiple receptors, but a bulkier 8'-cyclopropyl analog (**27**) shows reduced activity [78] consistent with the limited space available adjacent to the 8'/9' methyls.

Engineered Agrochemical Control of Transpiration

ABA agonists hold potential as future agrochemicals for controlling plant water consumption and improving yield under drought conditions. A parallel strategy to gaining agrochemical control is to engineer ABA receptors so that they can respond to an existing agrochemical, a strategy based on orthogonal ligand / receptor systems, which have enabled selective chemical control of diverse targets [79,80]. For example, several kinases have been engineered to respond to kinase inhibitor analogs that are too bulky to inhibit wild type kinases, but can inhibit mutant kinases with enlarged ATP-binding pockets [80]. The orthogonal / ligand receptor strategy has been widely employed in chemical biology and used, for example, to engineer receptors activated by "near drugs", inactive drug metabolites and other agonist / antagonist relatives [81–84].

The orthogonal receptor/ligand design strategy commonly involves the modification of existing ligands concomitant with mutations to their receptors, however repurposing an existing agrochemical is a different task. To identifying suitable ligands, Park et al. used site-saturation mutagenesis to create a collection of mutant PYR1

receptors that contain all possible 475 single amino acid substitution mutations in the receptor's 25 ligand-contacting residues [85]. This library of receptor variants was constructed in combination with the PYR1-K59R mutation, which removes intrinsic ABA responsiveness by disrupting a highly conserved H-bond to ABA's carboxylate [85,86]. Park et al. screened a panel of commonly used non-herbicidal agrochemical for agonists of any of the 475 receptors using the yeast-two hybrid assay described earlier. These screens were conducted at high concentrations (100 μM) so that weakly interacting ligands could be identified and subsequently optimized. Four weakly activating ligands were identified and subsequent mutageneses and selections were utilized to improve the sensitivity of each ligand-receptor pair identified. This process worked most successfully with mandipropamid (**28**), sold as Revus™, which is used to control *Phytophthora infestans* (late blight) in vegetable crops. Multiple rounds of mutagenesis and functional selections yielded a hextuple mutant receptor, PYR1^{MANDI}, with nanomolar sensitivity to mandipropamid. X-ray crystallographic data show that two key mutations that replace bulky residues (*F108A* and *F159L*) are crucial for preventing steric clashes between mandipropamid's two O-propargyl substituents that would otherwise occur with the native receptor, and that mandipropamid's amide forms direct and water mediated H-bonds to polar residues in the mutant's binding pocket, functioning analogous to the interactions of sulfonamides with wild type receptors[85].

Constitutive expression of PYR1^{MANDI} in transgenic Arabidopsis and tomato enables mandipropamid triggered activation of multiple ABA responses, such as reduced transpiration and genome-wide ABA-like transcriptional responses. Importantly, overexpression of the mutant receptor, which does not possess intrinsic ABA responsiveness, is not associated with growth defects or substantial alterations of basal

transcriptomes in the absence of mandipropamid treatment. Mandipropamid applications are able to improve Arabidopsis survival after water deficit with efficacy similar to that of ABA, suggesting that mandipropamid could be used as an agrochemical agent to control transpiration when used in combination with PYR1$^{MANDI\ 85}$. Additionally, the data demonstrate that selectively activating a single receptor (when expressed at high enough levels) is sufficient to elicit guard cell closure and other important ABA responses. Thus, although ABA normally co-activates multiple ABA receptors *in vivo*, co-activation is not a prerequisite for ABA action.

Looking forward

Growing demands on the freshwater needs of agriculture, due to population growth and increasing weather extremes, are motivating efforts to improve crop yields under conditions of drought. Important improvements have already been achieved through classical breeding and new transgenes, and these strategies will likely continue to deliver improvements. Agrochemical modulators of stress tolerance and water use have the advantage that they can, in principle, be used with any genotype across multiple species. ABA receptors are validated targets and it is anticipated that agonists suitable for agriculture can be developed from existing scaffolds. The isolation and characterization of quinabactin has demonstrated the importance of dimeric ABA receptors as targets for controlling transpiration, but our understanding of the underlying biological functions of the multiple receptor subfamilies is still incomplete. Structure-activity relationships of ABA-receptor agonists will facilitate agonist and antagonist design efforts, which will undoubtedly help probe receptor function and facilitate agrochemical development efforts.

Ultimately, field studies will be required to establish the efficacy of ABA agonists for improving yield during drought.

The development of PYR1^{MANDI} has demonstrated that an existing agrochemical can be repurposed to control a defined trait (transpiration via the ABA response pathway). The future of plant biotechnology will undoubtedly involve greater use of engineered proteins and pathways to specifically modulate defined traits. Orthogonal control systems using agrochemical ligands offer the advantage that the traits can remain silent in the absence of chemical intervention.

Acknowledgements

This review was supported by the NSF (IOS1258175, MCB1022378) and NIFA HATCH funds to SRC.

References Cited

1. Battisti, D. S.; Naylor, R. L. *Science* **2009**, *323*, 240–244.

2. Campos, H.; Cooper, M.; Edmeades, G. O.; Loffler, C.; Schussler, J. R.; Ibanez, M. *Maydica* **2006**, *51*, 369.

3. Campos, H.; Cooper, M.; Habben, J. E.; Edmeades, G. O.; Schussler, J. R. *Field Crops Res.* **2004**, *90*, 19–34.

4. Nemali, K. S.; Bonin, C.; Dohleman, F. G.; Stephens, M.; Reeves, W. R.; Nelson, D. E.; Castiglioni, P.; Whitsel, J. E.; Sammons, B.; Silady, R. A.; Anstrom, D.; Sharp, R. E.; Patharkar, O. R.; Clay, D.; Coffin, M.; Nemeth, M. A.; Leibman, M. E.; Luethy, M.; Lawson, M. *Plant Cell Environ.* **2015**, *38*, 1866–1880.

5. Fischer, R. A.; Rees, D.; Sayre, K. D.; Lu, Z.-M.; Condon, A. G.; Saavedra, A. L. *Crop Sci.* **1998**, *38*, 1467.

6. Fischer, R. A.; Edmeades, G. O. *Crop Sci.* **2010**, *50*, S–85–S–98.

7. Boyer, J. S.; Westgate, M. E. *J. Exp. Bot.* **2004**, *55*, 2385–2394.

8. Okamoto, M.; Peterson, F. C.; Defries, A.; Park, S.-Y.; Endo, A.; Nambara, E.; Volkman, B. F.; Cutler, S. R. *Proc. Natl. Acad. Sci. U. S. A.* **2013**, *110*, 12132–12137.

9. Cao, M.; Liu, X.; Zhang, Y.; Xue, X.; Zhou, X. E.; Melcher, K.; Gao, P.; Wang, F.; Zeng, L.; Zhao, Y.; Zhao, Y.; Deng, P.; Zhong, D.; Zhu, J.-K.; Xu, H. E.; Xu, Y. *Cell Res.* **2013**, *23*, 1043–1054.

10. Cutler, S. R.; Rodriguez, P. L.; Finkelstein, R. R.; Abrams, S. R. *Annu. Rev. Plant Biol.* **2010**, *61*, 651–679.

11. Milborrow, B. V. *Annu. Rev. Plant Physiol.* **1974**, *25*, 259–307.

12. Nambara, E.; Marion-Poll, A. *Annu. Rev. Plant Biol.* **2005**, *56*, 165–185.

13. Wilkinson, S.; Davies, W. J. *Plant Cell Environ.* **2002**, *25*, 195–210.

14. Frey, A.; Effroy, D.; Lefebvre, V.; Seo, M.; Perreau, F.; Berger, A.; Sechet, J.; To, A.; North, H. M.; Marion-Poll, A. *Plant J.* **2012**, *70*, 501–512.

15. Jones, R. J.; Mansfield, T. A. *J. Exp. Bot.* **1970**, *21*, 714–719.

16. Verslues, P. E.; Sharma, S. *Arabidopsis Book* **2010**, *8*, e0140.

17. Kulik, A.; Wawer, I.; Krzywińska, E.; Bucholc, M.; Dobrowolska, G. *OMICS* **2011**, *15*, 859–872.

18. Soon, F.-F.; Ng, L.-M.; Zhou, X. E.; West, G. M.; Kovach, A.; Tan, M. H. E.; Suino-Powell, K. M.; He, Y.; Xu, Y.; Chalmers, M. J.; Brunzelle, J. S.; Zhang, H.; Yang, H.; Jiang, H.; Li, J.; Yong, E.-L.; Cutler, S.; Zhu, J.-K.; Griffin, P. R.; Melcher, K.; Xu, H. E. *Science* **2012**, *335*, 85–88.

19. Ng, L.-M.; Soon, F.-F.; Zhou, X. E.; West, G. M.; Kovach, A.; Suino-Powell, K. M.; Chalmers, M. J.; Li, J.; Yong, E.-L.; Zhu, J.-K.; Griffin, P. R.; Melcher, K.; Xu, H. E. *Proc. Natl. Acad. Sci. U. S. A.* **2011**, *108*, 21259–21264.

20. Park, S.-Y.; Fung, P.; Nishimura, N.; Jensen, D. R.; Fujii, H.; Zhao, Y.; Lumba, S.; Santiago, J.; Rodrigues, A.; Chow, T.-F. F.; Alfred, S. E.; Bonetta, D.; Finkelstein, R.; Provart, N. J.; Desveaux, D.; Rodriguez, P. L.; McCourt, P.; Zhu, J.-K.; Schroeder, J. I.; Volkman, B. F.; Cutler, S. R. *Science* **2009**, *324*, 1068–1071.

21. Ma, Y.; Szostkiewicz, I.; Korte, A.; Moes, D.; Yang, Y.; Christmann, A.; Grill, E. *Science Signalling* **2009**, *324*, 1064.

22. Fujii, H.; Chinnusamy, V.; Rodrigues, A.; Rubio, S.; Antoni, R.; Park, S. Y.; Cutler, S. R.; Sheen, J.; Rodriguez, P. L.; Zhu, J. K. *Nature* **2009**, *462*, 660–664.

23. Iyer, L. M.; Koonin, E. V.; Aravind, L. *Proteins: Struct. Funct. Bioinf.* **2001**, *43*, 134–144.

24. Ponting, C. P.; Aravind, L. *Trends Biochem. Sci.* **1999**, *24*, 130–132.

25. Radauer, C.; Lackner, P.; Breiteneder, H. *BMC Evol. Biol.* **2008**, *8*, 286.

26. Nishimura, N.; Hitomi, K.; Arvai, A. S.; Rambo, R. P.; Hitomi, C.; Cutler, S. R.; Schroeder, J. I.; Getzoff, E. D. *Science* **2009**, *326*, 1373.

27. Santiago, J.; Dupeux, F.; Round, A.; Antoni, R.; Park, S.-Y.; Jamin, M.; Cutler, S. R.; Rodriguez, P. L.; Márquez, J. A. *Nature* **2009**, *462*, 665–668.

28. Zhang, X.; Jiang, L.; Wang, G.; Yu, L.; Zhang, Q.; Xin, Q.; Wu, W.; Gong, Z.; Chen, Z. *PLoS One* **2013**, *8*, e67477.

29. Melcher, K.; Ng, L. M.; Zhou, X. E.; Soon, F. F.; Xu, Y.; Suino-Powell, K. M.; Park, S. Y.; Weiner, J. J.; Fujii, H.; Chinnusamy, V.; Others *Nature* **2009**, *462*, 602–608.

30. Miyazono, K.-I.; Miyakawa, T.; Sawano, Y.; Kubota, K.; Kang, H.-J.; Asano, A.; Miyauchi, Y.; Takahashi, M.; Zhi, Y.; Fujita, Y.; Yoshida, T.; Kodaira, K.-S.; Yamaguchi-Shinozaki, K.; Tanokura, M. *Nature* **2009**, *462*, 609–614.

31. Hao, Q.; Yin, P.; Li, W.; Wang, L.; Yan, C.; Lin, Z.; Wu, J. Z.; Wang, J.; Yan, S. F.; Yan, N. *Mol. Cell* **2011**, *42*, 662–672.

32. Nakagawa, M.; Kagiyama, M.; Shibata, N.; Hirano, Y.; Hakoshima, T. *Genes Cells* **2014**, *19*, 386–404.

33. Yin, P.; Fan, H.; Hao, Q.; Yuan, X.; Wu, D.; Pang, Y.; Yan, C.; Li, W.; Wang, J.; Yan, N. *Nat. Struct. Mol. Biol.* **2009**, *16*, 1230–1236.

34. Weiner, J. J.; Peterson, F. C.; Volkman, B. F.; Cutler, S. R. *Curr. Opin. Plant Biol.* **2010**, *13*, 495–502.

35. Bai, G.; Yang, D.-H.; Zhao, Y.; Ha, S.; Yang, F.; Ma, J.; Gao, X.-S.; Wang, Z.-M.; Zhu, J.-K. *Plant Mol. Biol.* **2013**, *83*, 651–664.

36. Gonzalez-Guzman, M.; Rodriguez, L.; Lorenzo-Orts, L.; Pons, C.; Sarrion-Perdigones, A.; Fernandez, M. A.; Peirats-Llobet, M.; Forment, J.; Moreno-Alvero, M.; Cutler, S. R.; Albert, A.; Granell, A.; Rodriguez, P. L. *J. Exp. Bot.* **2014**, eru219.

37. Hauser, F.; Waadt, R.; Schroeder, J. I. *Curr. Biol.* **2011**, *21*, R346–55.

38. Umezawa, T.; Nakashima, K.; Miyakawa, T.; Kuromori, T.; Tanokura, M.; Shinozaki, K.; Yamaguchi-Shinozaki, K. *Plant Cell Physiol.* **2010**, *51*, 1821–1839.

39. Raghavendra, A. S.; Gonugunta, V. K.; Christmann, A.; Grill, E. *Trends Plant Sci.* **2010**, *15*, 395–401.

40. Fuchs, S.; Grill, E.; Meskiene, I.; Schweighofer, A. *FEBS J.* **2012**, no–no.

41. Antoni, R.; Gonzalez-Guzman, M.; Rodriguez, L.; Rodrigues, A.; Pizzio, G. A.; Rodriguez, P. L. *Plant Physiol.* **2012**, *158*, 970–980.

42. Rubio, S.; Rodrigues, A.; Saez, A.; Dizon, M. B.; Galle, A.; Kim, T.-H.; Santiago, J.; Flexas, J.; Schroeder, J. I.; Rodriguez, P. L. *Plant Physiol.* **2009**, *150*, 1345–1355.

43. Szostkiewicz, I.; Richter, K.; Kepka, M.; Demmel, S.; Ma, Y.; Korte, A.; Assaad, F. F.; Christmann, A.; Grill, E. *Plant J.* **2009**, *61*, 25–35.

44. Fuchs, S.; Tischer, S. V.; Wunschel, C.; Christmann, A.; Grill, E. *Proceedings of the National Academy of Sciences* **2014**, *111*, 5741–5746.

45. Santiago, J.; Rodrigues, A.; Saez, A.; Rubio, S.; Antoni, R.; Dupeux, F.; Park, S. Y.; Márquez, J. A.; Cutler, S. R.; Rodriguez, P. L. *Plant J.* **2009**, *60*, 575–588.

46. Zhang, X.; Zhang, Q.; Xin, Q.; Yu, L.; Wang, Z.; Wu, W.; Jiang, L.; Wang, G.; Tian, W.; Deng, Z.; Wang, Y.; Liu, Z.; Long, J.; Gong, Z.; Chen, Z. *Structure* **2012**, *20*, 780–790.

47. Dupeux, F.; Santiago, J.; Betz, K.; Twycross, J.; Park, S.-Y.; Rodriguez, L.; Gonzalez-Guzman, M.; Jensen, M. R.; Krasnogor, N.; Blackledge, M.; Holdsworth, M.; Cutler, S. R.; Rodriguez, P. L.; Márquez, J. A. *EMBO J.* **2011**, *30*, 4171–4184.

48. Li, J.; Shi, C.; Sun, D.; He, Y.; Lai, C.; Lv, P.; Xiong, Y.; Zhang, L.; Wu, F.; Tian, C. *Sci. Rep.* **2015**, *5*, 10890.

49. He, Y.; Hao, Q.; Li, W.; Yan, C.; Yan, N.; Yin, P. *PLoS One* **2014**, *9*, e95246.

50. Gonzalez-Guzman, M.; Pizzio, G. A.; Antoni, R.; Vera-Sirera, F.; Merilo, E.; Bassel, G. W.; Fernández, M. A.; Holdsworth, M. J.; Perez-Amador, M. A.; Kollist, H.; Rodriguez, P. L. *Plant Cell* **2012**, *24*, 2483–2496.

51. Antoni, R.; Gonzalez-Guzman, M.; Rodriguez, L.; Peirats-Llobet, M.; Pizzio, G. A.; Fernandez, M.; Winne, N. D.; Jaeger, G. D.; Dietrich, D.; Bennett, M. J.; Rodriguez, P. L. *Plant Physiol.* **2012**.

52. Zhao, Y.; Xing, L.; Wang, X.; Hou, Y.-J.; Gao, J.; Wang, P.; Duan, C.-G.; Zhu, X.; Zhu, J.-K. *Sci. Signal.* **2014**, *7*, ra53.

53. Todoroki, Y.; Tanaka, T.; Kisamori, M.; Hirai, N. *Bioorg. Med. Chem. Lett.* **2001**, *11*, 2381–2384.

54. Plancher, B. **1979**.

55. Wenjian, L.; Xiaoqiang, H.; Yumei, X.; Jinlong, F.; Yuanzhi, Z.; Huizhe, L.; Mingan, W.; Zhaohai, Q. *Phytochemistry* **2013**, *96*, 72–80.

56. Abrams, S. R.; Rose, P. A.; Cutler, A. J.; Balsevich, J. J.; Lei, B.; Walker-Simmons, M. K. *Plant Physiol.* **1997**, *114*, 89–97.

57. Kushiro, T.; Okamoto, M.; Nakabayashi, K.; Yamagishi, K.; Kitamura, S.; Asami, T.; Hirai, N.; Koshiba, T.; Kamiya, Y.; Nambara, E. *EMBO J.* **2004**, *23*, 1647–1656.

58. Zhao, Y.; Chow, T. F.; Puckrin, R. S.; Alfred, S. E.; Korir, A. K.; Larive, C. K.; Cutler, S. R. *Nat. Chem. Biol.* **2007**, *3*, 716–721.

59. Nishimura, N.; Sarkeshik, A.; Nito, K.; Park, S. Y.; Wang, A.; Carvalho, P. C.; Lee, S.; Caddell, D. F.; Cutler, S. R.; Chory, J.; Others *Plant J.* **2009**, *61*, 290–299.

60. Melcher, K.; Xu, Y.; Ng, L.-M.; Zhou, X. E.; Soon, F.-F.; Chinnusamy, V.; Suino-Powell, K. M.; Kovach, A.; Tham, F. S.; Cutler, S. R.; Li, J.; Yong, E.-L.; Zhu, J.-K.; Xu, H. E. *Nat. Struct. Mol. Biol.* **2010**, *17*, 1102–1108.

61. Peterson, F. C.; Burgie, E. S.; Park, S. Y.; Jensen, D. R.; Weiner, J. J.; Bingman, C. A.; Chang, C. E. A.; Cutler, S. R.; Phillips, G. N., Jr; Volkman, B. F. *Nat. Struct. Mol. Biol.* **2010**, *17*, 1109–1113.

62. Hao, Q.; Yin, P.; Yan, C.; Yuan, X.; Li, W.; Zhang, Z.; Liu, L.; Wang, J.; Yan, N. *J. Biol. Chem.* **2010**, *285*, 28946–28952.

63. Yuan, X.; Yin, P.; Hao, Q.; Yan, C.; Wang, J.; Yan, N. *J. Biol. Chem.* **2010**, *285*, 28953–28958.

64. Takeuchi, J.; Okamoto, M.; Akiyama, T.; Muto, T.; Yajima, S.; Sue, M.; Seo, M.; Kanno, Y.; Kamo, T.; Endo, A.; Nambara, E.; Hirai, N.; Ohnishi, T.; Cutler, S. R.; Todoroki, Y. *Nat. Chem. Biol.* **2014**, *10*, 477–482.

65. Van Overtveldt, M.; Heugebaert, T. S. A.; Verstraeten, I.; Geelen, D.; Stevens, C. V. *Org. Biomol. Chem.* **2015**, *13*, 5260–5264.

66. Frackenpohl, J.; Heinemann, I.; Müller, T.; Von Koskull-Döring, P.; Dittgen, J.; Schmutzler, D.; Rosinger, C. H.; Häuser-Hahn, I.; Hills, M. J. Aryl-and hetarylsulfonamides as active ingredients against abiotic plant stress. *US Patent* **2011**.

67. Nyangulu, J. M.; Nelson, K. M.; Rose, P. A.; Gai, Y.; Loewen, M.; Lougheed, B.; Quail, J. W.; Cutler, A. J.; Abrams, S. R. *Org. Biomol. Chem.* **2006**, *4*, 1400–1412.

68. Kepka, M.; Benson, C. L.; Gonugunta, V. K.; Nelson, K. M.; Christmann, A.; Grill, E.; Abrams, S. R. *Plant Physiol.* **2011**, *157*, 2108–2119.

69. Han, X.; Wan, C.; Li, X.; Li, H.; Yang, D.; Du, S.; Xiao, Y.; Qin, Z. *Bioorg. Med. Chem. Lett.* **2015**, *25*, 2438–2441.

70. Takeuchi, J.; Ohnishi, T.; Okamoto, M.; Todoroki, Y. *Org. Biomol. Chem.* **2015**, *13*, 4278–4288.

71. Takeuchi, J.; Ohnishi, T.; Okamoto, M.; Todoroki, Y. *Bioorg. Med. Chem. Lett.* **2015**, *25*, 3507–3510.

72. Takahashi, S.; Oritani, T.; Yamashita, K. *Agric. Biol. Chem.* **1986**, *50*, 3205–3206.

73. Culter, S. R.; Okamoto, M. Synthetic compounds for vegetative aba responses. *International Patent* **2013**.

74. Lin, B.-L.; Wang, H.-J.; Wang, J.-S.; Zaharia, L. I.; Abrams, S. R. *J. Exp. Bot.* **2005**, *56*, 2935–2948.

75. Okamoto, M.; Kushiro, T.; Jikumaru, Y.; Abrams, S. R.; Kamiya, Y.; Seki, M.; Nambara, E. *Phytochemistry* **2011**, *72*, 717–722.

76. Todoroki Y, Hirai N, Koshimizu K. Phytochemistry **2005** 38, 561-568

77. Rose, P. A.; Cutler, A. J.; Irvine, N. M.; Shaw, A. C.; Squires, T. M.; Loewen, M. K.; Abrams, S. R. *Bioorg. Med. Chem. Lett.* **1997**, *7*, 2543–2546.

78. Benson, C. L.; Kepka, M.; Wunschel, C.; Rajagopalan, N.; Nelson, K. M.; Christmann, A.; Abrams, S. R.; Grill, E.; Loewen, M. C. *Phytochemistry* **2015**, *113*, 96–107.

79. Belshaw, P. J.; Schoepfer, J. G.; Liu, K.-Q.; Morrison, K. L.; Schreiber, S. L. *Angew. Chem. Int. Ed Engl.* **1995**, *34*, 2129–2132.

80. Bishop, A. C.; Ubersax, J. A.; Petsch, D. T.; Matheos, D. P.; Gray, N. S.; Blethrow, J.; Shimizu, E.; Tsien, J. Z.; Schultz, P. G.; Rose, M. D.; Others *Nature* **2000**, *407*, 395–401.

81. Doyle, D. F.; Braasch, D. A.; Jackson, L. K.; Weiss, H. E.; Boehm, M. F.; Mangelsdorf, D. J.; Corey, D. R. *J. Am. Chem. Soc.* **2001**, *123*, 11367–11371.

82. Park, J. S.; Rhau, B.; Hermann, A.; McNally, K. A.; Zhou, C.; Gong, D.; Weiner, O. D.; Conklin, B. R.; Onuffer, J.; Lim, W. A. *Proc. Natl. Acad. Sci. U. S. A.* **2014**, *111*, 5896–5901.

83. Conklin, B. R.; Hsiao, E. C.; Claeysen, S.; Dumuis, A.; Srinivasan, S.; Forsayeth, J. R.; Guettier, J.-M.; Chang, W. C.; Pei, Y.; McCarthy, K. D.; Others *Nat. Methods* **2008**, *5*, 673–678.

84. Dong, S.; Rogan, S. C.; Roth, B. L. *Nat. Protoc. 5*, 561–573.

85. Park, S.-Y.; Peterson, F. C.; Mosquna, A.; Yao, J.; Volkman, B. F.; Cutler, S. R. *Nature* **2015**, *520*, 545–548.

86. Mosquna, A.; Peterson, F. C.; Park, S. Y.; Lozano-Juste, J.; Volkman, B. F.; Cutler, S. R. *Proceedings of the National Academy of Sciences* **2011**, *108*, 20838–20843.

Figure legends

Figure 1. (a) Structures of S-(+) abscisic acid (**1**), quinabactin (**2**) and pyrabactin (**3**) (b) The gate-latch-lock structural mechanism for ABA recognition and biochemical activation. The receptor is depicted as a gray cartoon, ABA is depicted in a gray CPK model, and the PP2C is depicted as a pink surface. c) Biochemical pathway downstream of activation of ABA receptors. d) The physiological response of guard cell closure in the presence of ABA or other receptor agonists.

Figure 2. 3-D aligned structures of receptor-bound agonists. (a) ABA (3QN1), (b) quinabactin (4LA7), (c) pyrabactin (3NMN), (d) R-(–)-ABA, and overlays of ABA with quinabactin (e) or pyrabactin (f) The PDB accessions used for each ligand in parentheses.

Figure 3. Arabidopsis ABA receptor sub-families. The left panel shows a phylogeny of the Arabidposis thaliana PYR/PYL/RCAR receptors and the right panel shows IC_{50} values for receptor-mediated inhibition of HAB1 by ABA, pyrabactin and quinabactin. (adapted from reference 8). PYL13 has been omitted, but it is a member of the PYL5 subfamily.

Figure 4 . Variable amino acid residues within the ligand-binding pockets of *Arabidopsis thaliana* PYR/PYL/RCAR receptors.

Figure 5. Structures of pyrabactin and quinabactin analogs.

Figure 6. The 3'-tunnel (A) and C6-cleft (B) are variable regions of the receptors' ligand-binding pockets. Amino acids that are variable between receptors are labeled with an asterisk. V163 andF159, which are also part of the C6-cleft have been omitted for clarity. Made from PDB 3QN1.

Figure 7. Structures of ABA analogs.